MAGNETISM AND LAWS OF BULK ELASTICITY

EDITORS
P.I. POLYAKOV
T.A. RYUMSHYNA

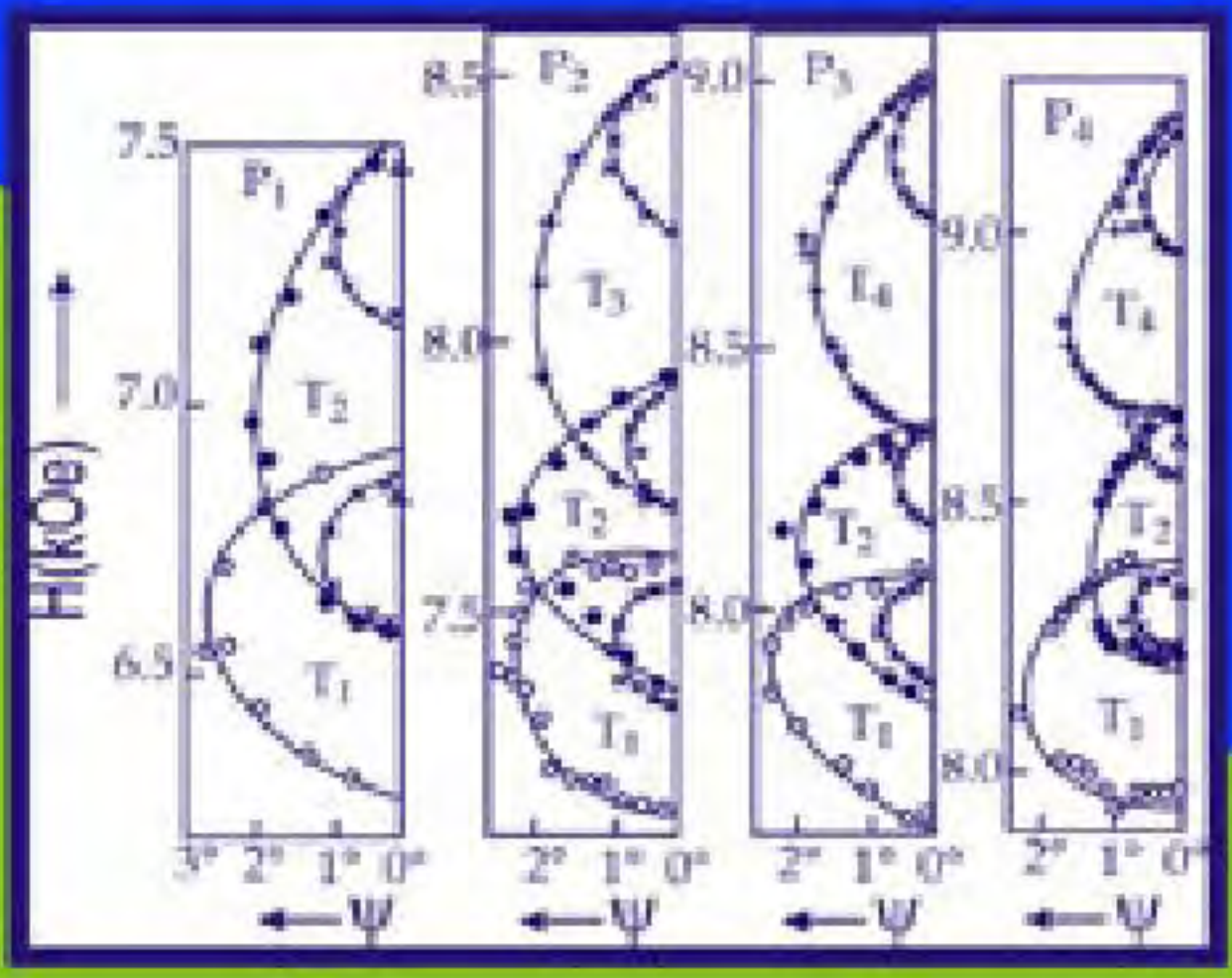

TRANSWORLD RESEARCH NETWORK

Magnetism and Laws of Bulk Elasticity

2009

Editors
P.I. Polyakov

Inst. for Phys. of Mining Processes
R. Luxembourg 72, Donetsk 83114
Ukraine

T.A. Ryumshyna

Institute for Physics and Engineering
named after O.O.Galkin R. Luxembourg 72
Donetsk 83114
Ukraine

Magnetism and Laws of Bulk Elasticity

2009

Published by Transworld Research Network

Transworld Research Network
T.C. 37/661(2), Fort P.O.,
Trivandrum-695 023, Kerala, India

ISBN: 978-81-7895-379-3

Preface

Physical processes in magnet-containing media determine the regularities of evolution of states, properties and phenomena. The development of the more sensitive methods of investigations led to the specialization of studies in the narrower areas, as a result the possibility to observe and to generalize laws of physical processes was lost. The analysis of the wide spectrum of results about well studied galvanomagnetic phenomena into magnetodielectrics, semiconductors and metals makes it possible to reveal the generality of the effects of temperature, magnetic field and pressure (T, H, P).

In the present work we consider the mechanism of elastic strains and stresses as the main controlling factor of structure change under the influence of temperature, magnetic field, hydrostatic pressure. We should take into account that the energy of elastic deformation is commensurate to the energy of electric interactions and that is much higher than the rest of the bonds of lower energy value. Besides, the energy elastic stresses are of long range, so it forms the linearity in magnetization and bulk change. These regularities requires a fundamental understanding of the laws of interaction with respect to accepted interpretation of quantum mechanical forces of short range that are attributes of magnetism formation.

From existing thermodynamic parameters the high pressure proved to be that most important parameter, which allowed us to establish the role of the elastic stresses. Allowance method for high pressure is described in a separate chapter. Developed devices permitted us to combine the studies under varied temperature, magnetic field and hydrostatic pressure.

The estimations of the parameters of the structure of a single-crystal magneto-dielectric under hydrostatic pressure were performed. The fact of irregular evolution of the structure parameters and anisotropy of elasticity was established.

Due to the high sensitivity of electronic and resonance properties with respect to small changes of the structure, we were able to define the direct relation between elastic stresses and field-frequency dependences, as well as to analyze the evolution of the dynamics of phase transitions and phase states. A cycle of studies of the influence of hydrostatic pressure on the resonance properties are presented also. The analysis of the effect of magnetic, magneto-elastic and elastic energy allowed us to define the combinations of magnetoelastic interactions.

The results of investigations of magnetic semiconductors and their electronic properties revealed the linear dependence of T-P-H influence that

confirmed the role of elastic stresses in the structure changes. The same regularity was established in magnetization and magnetostriction features in single crystals. The explanation of the heating and cooling effects of the pressure and magnetic field is presented. The secondary signs of the structural phase transition of the second order are singled out from the correspondences of the maxima of baric, magnetic and resistive effects.

The role of elastic stresses in the linear changes of the magnetostriction, magnetization, magnetoelasticity of single-crystal magnetic semiconductors is described in details. We suggest also the explanation of the colossal magnetoresistance as a consequence of the elasticity laws. Here we state the results of the causal action of the elastic stresses that control the evolution of the structure and the properties and form the phase transformations in magnetic dielectrics and metals.

Ideas about nature of the formation of internal stresses in the solid are presented in chapter 10, written by Dr. T.A.Ryumshyna. Several versions of the estimates of the stresses are proposed, which show the amount several GPa. The model of phase transformations was offered as rearrangement of internal structure of crystalline cristalline body when internal inlying stresses arrive at some critical value importance.

Authors express gratitude to N.Bojko, E.Sapego, T.Melnik, A.Masur for their help in the process of execution of work.

Italy

P.I. Polyakov
T.A. Ryumshyna

Contents

Transworld Research Network
37/661 (2), Fort P.O., Trivandrum-695 023, Kerala, India

Magnetism and Laws of Bulk Elasticity, 2009: 1-7 ISBN: 978-81-7895-379-3
Editors: P.I. Polyakov and T.A. Ryumshyna

1 Relationship between galvanomagnetic phenomena and bulk elasticity in magnet-containing structures of semiconductors, dielectrics and metals

P.I. Polyakov and T.A. Ryumshyna
Inst. for Phys. of Mining Processes, R. Luxembourg 72, Donetsk 83114, Ukraine

In 60-70ies of the last century, an opinion was formed that the principal electro-magnetic phenomena in metals, semiconductors and dielectrics had been well studied and understood on the base of model theoretical representations. Later on, the studies were devoted mainly to detailing. However, the revealed experimentally colossal magnetoresistance (CM) and properties of high-temperature superconductivity (HTSC) brought the attention of scientists to the

Correspondence/Reprint request: Dr. P.I. Polyakov, Inst. for Phys. of Mining Processes, R. Luxembourg 72 Donetsk 83114, Ukraine. E-mail: poljakov@mail.fti.ac.donetsk.ua

question of important corrections to the image of galvanomagnetic phenomena. No attention was given to the investigation of critical phenomena in magnet-containing systems from viewpoint of formation of structural phase transitions [1] and the laws of bulk elasticity in metals, semiconductors and dielectrics. And we have to analyze dissimilar experimental results (changes in symmetry, volume, structure instability, displacement of the lattice sites, jumps in properties, etc.) within the framework of structural phase transition when the dynamic rearrangement is due inner anisotropic elastic stresses. The principal aim of this study is the ascertaining of the relation between the bulk elasticity and magnetism through the physics of galvanomagnetic phenomena.

The correlation of changes of electrical conductivity and magnetism in transitional and rare-earth elements was studied in details first by Dutch scientists Jonkerom and van Santem [2]. In the course of extended studies, magnetic semiconductors were of high interest. This area of investigations touched upon single crystals and polycrystals of multi-component structures where the physical influence of magnetic field resulted in the absence of magnetic compensation. We accept the state of magnetic non-compensation as a property of the structure formed by sites bound by valent and free electrons. By definition, the sites are associated with atoms and molecules with non-compensated magnetic spins (small magnets). Magnetic factor reaches its maximum at $T=0^0K$ and vanishes at high structure-forming temperatures.

The studied phenomena have become ever more important after the colossal magnetoresistance was discovered in some structures in the region of phase transition (PT) [3,4] when the jump of electrical conductivity by several orders of the magnitude was noted. During the last 10-15 years, a lot of publication appeared in this field, but the problem has not been fundamentally solved yet on the base of existing models. We should note that these studies were directed at the estimation of the interrelation between structural changes caused by different substitutions and influences of T, P and H parameters and affecting magnetic and transport properties. From the other hand, these models did not take into account the mechanisms of bulk elasticity. That is the regularity that is revealed in linear and non-linear dependences of magnetostriction properties in monocrystal $LaMnO_3$ [5] at varied T and H (see Fig.1). The causing role is also played by elastically deforming stresses and elastic anisotropy at formation of the jump of the properties and hysteresis at the structural phase transition of the second type [6] where the temperature of the phase transition decreases with the rise of the magnetic field whereas magnetostriction dependences have the characteristic jump of properties near the phase transition observed on monocrystal $LaMnO_3$ [5] with selected direction in a wide range of magnetic fields at fixed temperatures. This result allowed us to establish the role of sign alteration of the effect of elastic stresses with H and T change for the evolution of striction properties. The shift of the

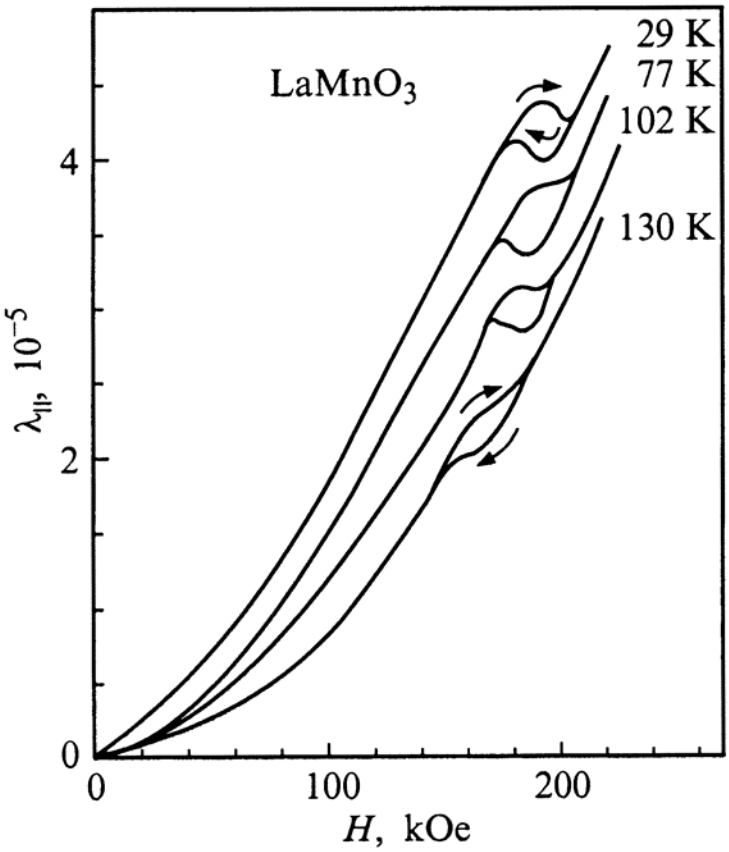

Figure 1.1. Field dependences of longitudinal magnetostriction of $LaMnO_3$.

priorities in the form of linear regularity of magnetic stresses at the initial parts of the selected dependences takes place due to the contribution of thermal elastic deforming stresses.

In the variety of papers and methods, we can note studies where high hydrostatic pressures were taken as a parameter. Under the uniform compression, the following physical process is modeled in the structure: the interatomic distances are changed under action of external mechanical stresses. But the pressure effect makes sense in these studies if pressure values correspond to coefficient of bulk compressibility which is low in the studied samples (about 10^{-5}-10^{-7}), by definition. As a result, it is very difficult to study physical processes at low temperatures under pressure of about 3GPa. At the same time, the results show that the application of such pressures help in the understanding of relationship between the energy of elasticity and magnetic, electronic and structural changes in the course of investigations of galvanomagnetic phenomena.

Numerous reviews and papers on investigations of combined compositions based on manganese perovskites drew our attention to interlacing small changes of parameters in compounds of one type and it became possible to distinguish the properties of metals, dielectrics, ionic and covalent crystals and

changeable character of phase transition. In this variety of investigations, there was an important regularity in changes of PT accompanied by considerable jump of the properties. This fact was a subject of thorough studies, individual model researches and search for analogies. It also determined the direction of model theoretical presentations. The problem of jump of properties remains the principal one. Thus, in papers by Landau [6], there is a detailed study of jumps of superconductivity properties in the neighborhood of phase transitions for the magnetic field strengths over than zero (Fig. 2). The model theoretical presentations based on quantum mechanics and the numerous applied methods have demonstrated this problem to be the casual basis of a property, magnetic-field orientation, sample shape and affecting the state of the phenomena. In the course of the experiment, they are accompanied by both the jump in properties and the important ascertained fact of the process, volume change and changes in symmetry of the structure. It should be noted that the multiple model presentations using the theories of exchange and anisotropy, the molecular field theory do not used the concept of elastic stresses to explain the physical processes [11]. Model presentations do not take into account the regularities of elasticity displayed by thermodynamic parameter affecting the structure, first of all. The causing role of mechanisms of elastic anisotropically deforming stresses has not been established at formation of the structural phase transitions.

Together with marking out the regularities of linearity in magnetostriction, magnetization, magnetoelasticity and magnetoresistivity, the role of elastic properties is noted, too. A direct method of such investigations needs the analogy to be drawn, i.e. combined influence of field H and pressure P. It is difficult in magnet-containing systems because of the high coefficient of compressibility in solids. It varies between 10^{-2}-10^{-8}. This fact is the casual basis for both the magnetism and structural phase transition.

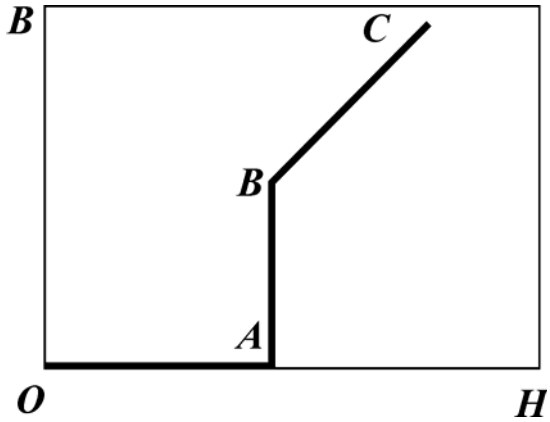

Figure 1.2. Dependence of induction from tension of the magnetic field in the first-order superconductor [8].

Considering the existing contradictions in the understanding of the nature of striction in superconductors and magnets, we see that the statement of the problem of structural phase transition eliminates uncertainty in the mechanisms of formation of jump of properties in the whole range of solids. By such analysis, we can explain discontinuity of properties of magnetization, heat capacity, resistivity, high frequency properties and show the regularities of elasticity for Hall and Lifshits effects. We can also explain peculiarities of the physical process of Meissner effect with specific changes of symmetry and volume affecting the intensity of magnetic factor (magnetic non-compensation) of the superconducting phase during semiconductor – metal transition with common regularities of magnetostriction. The results of studies of classical magneto-dielectrics are the most demonstrable with respect to the processes of establishment of relation of resonance properties and magnetization near structural phase transitions. The outskirts of a phase transition are characterized by the reaction of frequency spectrum with approaching the point of the structural phase transition under varied external thermodynamic parameter as T, P or H.

Intensive experimental studies of $CuCl_2 \cdot 2H_2O$ have shown first-order phase transition to be the structural one with the characteristic jump of properties near 0^0K and the succeeding regularity of growth of T at rising H.

As far back as in the first experimental work by Paulus [7], a regularity was revealed with respect to the jump of magnetization properties at temperature between 1.5-40 K (Fig.3) and that of linearity before and after the jump of PT properties. Multiple experimental results obtained with using high-frequency methods, hydrostatic pressure, by change of the sample shape, elastic and magnetoelastic properties enabled the authors to present regularities of the structural phase transition and to split the system to superconducting and metallic phases [8]. As a consequence, it can be stated, that numerous studies of the sublattice “flip-flop” is purposeful study of regularities of the structural phase transition with changes of properties in the region of PT under the influence of magnetic field through mechanisms of magnetic elastically deforming stresses.

Persistent interest in peculiarities of galvano-magnetic phenomena in metals in high magnetic fields at low temperatures has attracted the attention of researchers. Plentiful results can be found in first papers by Kapitsa [9] who has distinguished the linear law of resistance increase in some metals andnoted how changes in field direction with respect to orientation of the structure influence the properties. Those were the works where the author suggested the idea explaining the linear growth of the resistance under H effect. The influence of the magnetic field results in structural failure affecting the conductivity in the systems of impurities or lattice defects. The field H impacts

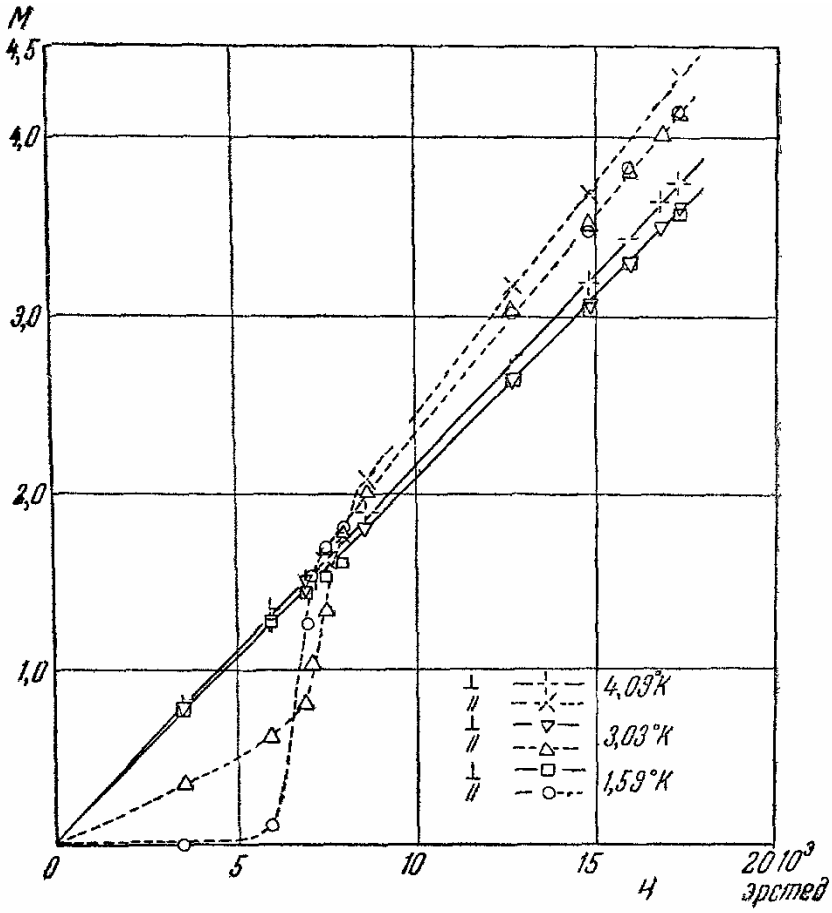

Figure 1.3. Magnetization along the a and b-axes as a function of field [6].

the motion of electrons and is a disrupting factor of the structure of location of atoms, sites and the lattice in whole that determines the electron mobility, in turn.

In succeeding papers of Lazarev [10], it was found that practically in the whole of investigated metals, the quadratic growth of the resistance with the magnetic field was followed by the linear dependence in high magnetic fields. The dynamics of current carriers because of the magnetic field strength and depending on orientation appears as the anisotropy of properties.

These regularities are grounded by theoretic diversity and universal topology of Fermi surface which are the basis of model presentations for the case of galvanomagnetic phenomena in pure metals. Unfortunately, there are no theoretical developments where the role of the energy of elastic deformation and regularities of the anisotropy of elasticity were taken into account for analysis of structural changes, phase transitions, magnetism and conductivity.

New approaches to investigation of dynamics of critical phenomena generalized the structural phase transitions to be universal on a microscopic level, which takes into consideration the defining contribution of the elastic

deformation and anisotropy of elasticity to the jump of the properties. Consideration of these specific mechanisms, more exactly of the energies, is not simple because of the lack of consecutively developed basis where the accounted laws of bulk elasticity would not contradict to the existing phenomenological theories.

In this analysis and generalizations, the attention is drawn to the fact that in methodology of the classical mechanisms, the common dynamic regularities coincide with those of simple processes. This is understood as mechanical determinism. But in the quantum mechanics, there is a dynamic which does not coincide with that of single processes by virtue of specific understanding of a “state” and nor grounds the mechanical determinism. As a consequence, the dynamic interpretation of quantum mechanical presentations with a definite degree of restrictions could not explain a real physical process satisfying the principles of the classical mechanical determinism. Is it not a neglection in the understanding of real physical processes and in the grounding of their model theoretical presentations?

CHAPTER 2

Non-magnetic high-pressure chambers for physical investigations

Fundamental researches by P. Bridgeman [12] initiated studying of the behavior of materials under pressure. Effects of such powerful thermodynamic parameters as temperature and pressure on changes of resistive, resonance, optical and magnetic properties of solids remain still of interest.

Unfortunately, the literature data are deficient, concerning the development of experimental procedures for investigations under pressure. In a number of monographs [12-17], various physical methods are described that are based on joint application of hydrostatic pressure, temperature and magnetic fields used for studying properties of materials.

Current level of research work requires new approaches to stimulate the development of methods and procedures. Utilization of new composite non-magnetic materials demands modernization and unification of the existing methods of pressure generation together with design of pressure vessels.

Here we generalize methods used to study properties of materials under hydrostatic compression up to 3 GPa (30 kbar). Several described HPC modifications are intended for different physical methods of investigation. High attention is paid to the technology of packing, optimization of geometric dimensions. We demonstrate methodic and practical developments of multifunctional nonmagnetic HPC for pressure up to 3.0 GPa in a wide temperature range (0.4-450 K).

The proposed designs and methods can be of interest for experimentalists working in the field of high-pressure physics and technology.

2.1. Non-magnetic HPC (up to 15 GPa) for resonance investigations

One-layer straight resonator-chamber (Fig. 2.1) is designed for experiments in a wide range of frequencies, magnetic fields and pressures. Dimensions of the chamber are optimal: D/d=3.65 (D is the external diameter, D=31 mm, d is the diameter of working channel, d=8.5 mm).

The design and procedure show that the force is transmitted from hydraulic press via plunger 16 made of beryllium bronze (БрБ2) after special thermomechanical processing. At plunger side, the chamber is sealed with rings 13,1 5 made of БрБ2 (HRC-33-36). Teflon ring 14 tightened with screw 12 is placed for the case of pentane use. Nut 17 serves for plunger location, nut 18 is for plunger removal for inspection or refilling the chamber. Radio-frequency shutter 3 is anchored by nut 1 and sealed by lead or PTFE ring 5

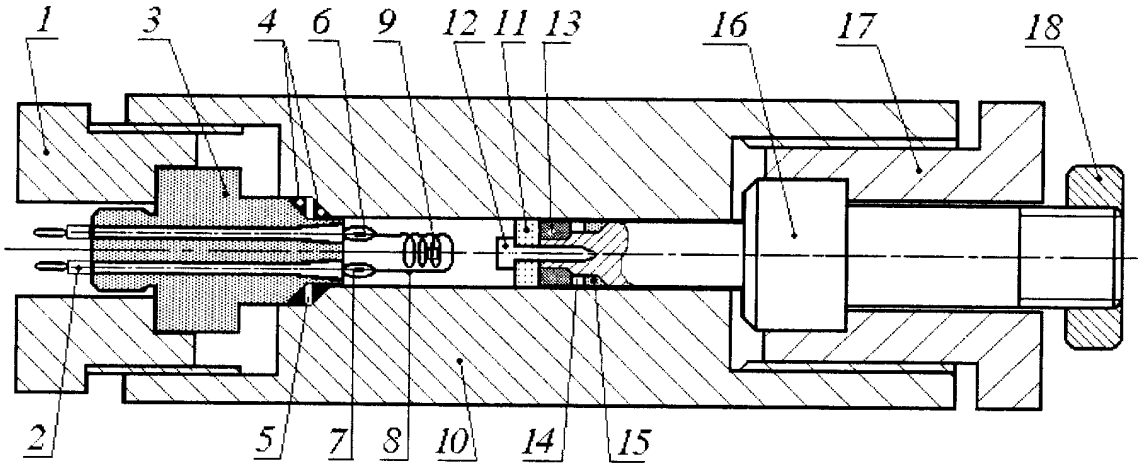

Figure 2.1. Non-magnetic HPC (up to 1.5 GPa) for resonance investigations.

together with anti-extrusion rings 4 made of БрБ2. The shutter has screw for remover. Coaxial bushings 6 and 7 are insulated with araldite rein AA-004.

Chamber casing 10, plunger and shutter were subjected to thermomechanical treatment for increase the pressure range where deformations remain elastic. During the treatment, the channel was autofretted by sequential pushing of high-strength cores-mandrels (steel ХВГ, HRC-60-62).

The chamber was used for observation of antiferromagnetic resonance (AFMR) under high hydrostatic pressure for $CuCl_2 \cdot 2H_2O$ crystal in decimeter wave band and inclined magnetic field at helium temperatures [18].

The resonator-chamber together with a sample was placed in a Dewar vessel filled with liquid helium at temperature varied from 1.68 to 4.2 K by pumping helium vapor out. The pressure was measured and the elasticity of transmitting medium (oil-kerosene mixture) was tested by a contactless method. A washer of pure tin 11, by 6 mm in diameter and 1mm in height was pasted to screw 12. The temperature of superconducting transition was estimated by vapor of the helium bath.

SHF-power was transmitted from generator to coaxial inlet 7. Sample 2 was placed in the center of spiral 8 on polystyrene holder. Power was transmitted from coaxial terminal 6 via joint 2 to the receiving section. Frequencies were checked by the signal of free radical of biphenyltecrylhydrasile placed in the resonator.

2.2. Two-layer non-magnetic HPC (up to 2.56 GPa)

Peculiar features of the HPC are two-layer embodiment (БрБ2 is used in the both layers), D/d ratio is 5-7 and pressure application is extended up to 2.56 GPa [19-21]. To provide the advantages of a two-layer chamber [19], the autofretting was done (prior to installation) to extend the range of elastic operation of the external layer.

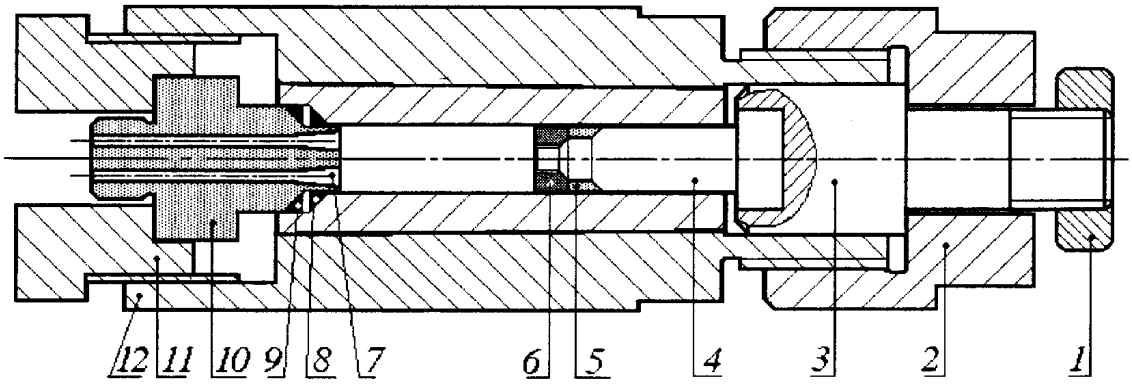

Figure 2.2. Two-layer non-magnetic chamber (up to 2.56 GPa).

The optimal HPC dimensions and the technology of treatment have given such parameters: d=8.5 mm, D=45 mm (D/d=5.29), the length of working cavity under pressure was 20 mm. The external layer of the chamber was autofretted by a steel hardened (HRC-60) mandrel (core angle was 2^o, the tension was 0.37 mm). The inner layer was pressed into the external one with tension of 0.15 mm.

Figure 2.2 shows the general view of the chamber. Shutter unit 10,11 and packing of БрБ2 (HRC-30-32) 5,6,8,9 were like those described in [18] and operated safely in the whole pressure range (up to 2.56 GPa).

The working part 4 of the plunger was made of ceramics and aligned with guide part 3 by clearance fit. Insert made of microlite provides normal loading upto 2.3-2.56 GPa at room temperature, that is why the HPC casing was tested by using inserts made of metal-ceramic alloy BK10. Cavity pressure was measured by a manganin manometer.

Inspection and control of HPC operation channel showed no residual deformations in the casing, shutter and loading plunger after multiple pressure tests.

2.3. Solenoid-chamber

To increase the strength of high-pressure container, different methods are used, in particular banding of container bushing by high-strength wire or tape (Fig. 2.3) [22].

Superconducting winding 1 of wire HT-50 was laid with tension of 25-30kg/mm^2 in circular cut of bushing 5 made of bronze БрБ2 with hardness HRC-40. Frame and superconductor have no extra isolation. Sample 2 is fixed in working space of bushing channel bounded by plungers with ferromagnetic poles 3 fixed by restraining nuts 6. Current leads are fixed to shutter 4.

At room temperature, the container is loaded up to prescribed pressure by a hydraulic press; plunger position is fixed by nuts. After cooling to the liquid

helium temperature, the material of bushing is hardened by a factor of 1.3 resulting in 10% compensation for the decrease of supporting force due to radial forces acting on the winding in the maximum magnetic field [23, 24].

Dimensions of the unit are as follows: d=8.5mm, the diameter of the external bushing is more than 22 mm, the total length is 46.2 mm, the lengths of upper and lower circular cuts are 35 mm and 25 mm, respectively. Winding with wire HT-50 (diameter of 0.33 mm) provided the magnetic field of 5.54 T for the current of 34 A, sectional winding with wire of diameter of 0.1 mm and 0.5 mm yields 7 T.

For a large solenoid, banding can be in the form of a separate sectional winding (Fig. 2.3, 6). Being banded with a superconductor (diameter of 0.7 mm) and having dimensions d=8.5 mm, diameter of inner bushing is 22 mm, external dimension is 41.3 mm, the structure (d=8.5mm) provides the total magnetic field of 9.2T [24]. After mounting the shutter and the piston made of steel with pole tips made of dysprosium, the container was tested at room temperature and pressure of 1.6 GPa. At 1.8 K and the working pressure of 10 GPa, the total magnetic field in the gap (2mm) between the tips was equal to

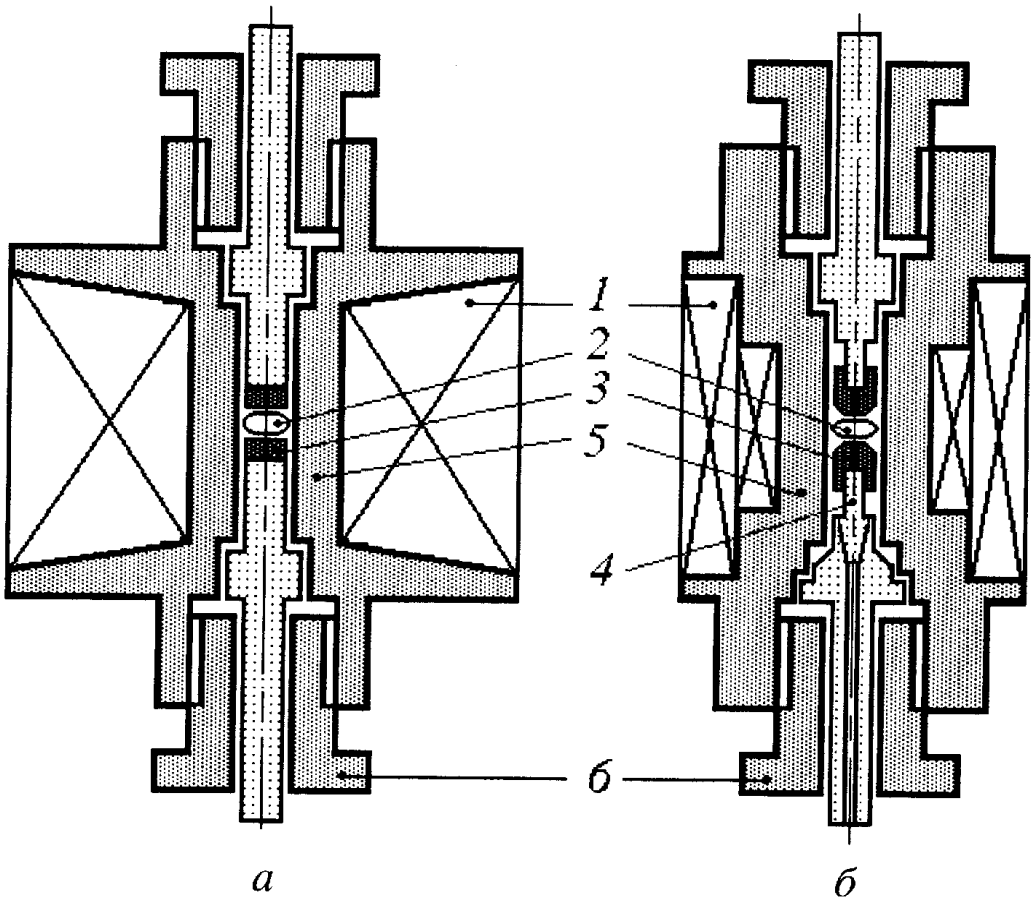

Figure 2.3. Solenoid-chamber with integral (a) and sectional (б) winding.

12 T. The pressure was estimated by initial loading of the container in the hydraulic press.

Thus, the solenoid-container is a promising structure for a complex use of high pressure, low temperature and strong magnetic field.

2.4. HPC (up to 3 GPa) for wide application

Figure 2.4 illustrates a two-layer non-magnetic HPC. It has been constructed by auto fastening of inner and external layers [19, 25] that has given container of smaller dimensions (D/d=4.3-4.8) and pressure increase by a factor of two.

Container with load – carrying parts made of БрБ2 has the overall dimensions of 30x130 mm, those of the active part are 7x30 mm. The piston is sectional. The packing is an antiextrusion ring of triangle section made of БрБ2 (HRC-35), teflon cone and a plug of benzo-oil resistant rubber. Pusher and rod are made of nickel alloy 38ХНЮ.

The shutter has two modifications depending on the measurement procedure. In the former case, it has two cone-like coaxial inlets for resonance investigations. In the latter case, current-carrying and measurement leads are taken off the zone of pressure by using cone insert as a sealing. These characteristics provide high technological quality of preparation and simple application.

The depicted container [26, 27] was used to investigate the influence of high hydrostatic pressure on the character of phase transitions in three-dimensional Heisenberg ferromagnets $CuM_2Cl_4 \cdot 2H_2O$ (M can be K, NH_4, Rb). For these crystals, the measurements of magnetic susceptibility were made under pressure up to 1.76 GPa in the temperature range of 0.4-4.2 K. The pressure dependence of the Curie temperature has been determined.

A modified container structure (with all load-carrying elements made of alloy of 38ХНЮ –type and rod of hard alloy ВК8, d=6.5 mm, D=31 mm, D/d=4.8) has made it possible to raise pressure in container working volume up to 2.7 GPa (2.1 GPa under helium temperatures). The container was used in

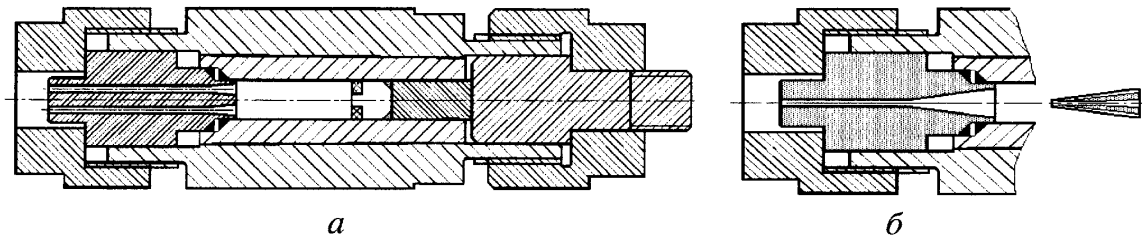

Figure 2.4. HPC (up to3 GPa) for wide application (a) (b is the modification of shutter).

studies of high hydrostatic pressure effect on the Neel temperature and H-T phase diagram of $GdBa_2Cu_3O_{7-\delta}$ (δ-1) [27].

Non-magnetic material with improved strength characteristics (40ХНЮ) permitted to extend the range of intra-chamber pressure up to 3.0 GPa with a 500-cycles loading-unloading process. Papers [28-32] contain the results of investigations on magnetic-field (to 8 kOe) effect on resistive properties of manganites for pressure to 1.8 GPa in 77-350 K temperature range.

2.5. Small-sized non-magnetic HPC (to 1.2 GPa)

Important features of HPC structure are the minimal length of 90 mm, that of operation space 23 mm, D=18 mm, d=8mm and 5.4 mm (D/d=2.2 and 3.3, respectively), see Figure 2.5 [33].

In this structure, the hydraulic-press force is transmitted via pusher made of alloy 40ХНЮ (HRC-45-47), rod is made of structural ceramics (HRC-68), proton-free fluorite fluid C_8F_{12} is used to transmit pressure. Casing and sleeve nut of the rod are made of 40ХНЮ (HRC-45-47), shutter support is made of БрБ2 (HRC-37).

The reduction of the dimensions (see figure 2.6) required the optimization of supporting area of check nut, to have larger supporting area and shorter length of the shutter.

The chamber [33] was used for NMR studies in proton-containing samples. Figure 2.7 illustrates the general view of all HPC described above.

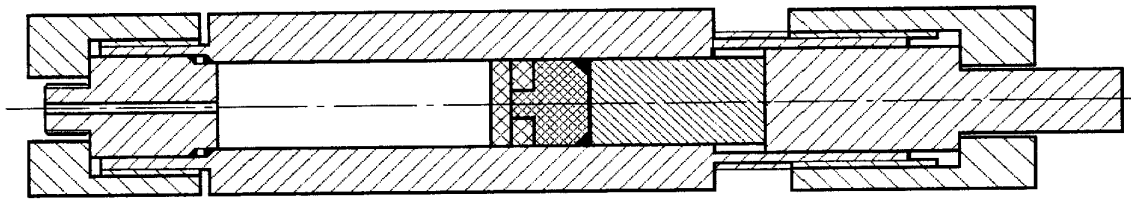

Figure 2.5. Small-sized nonmagnetic HPC (to1.2 GPa).

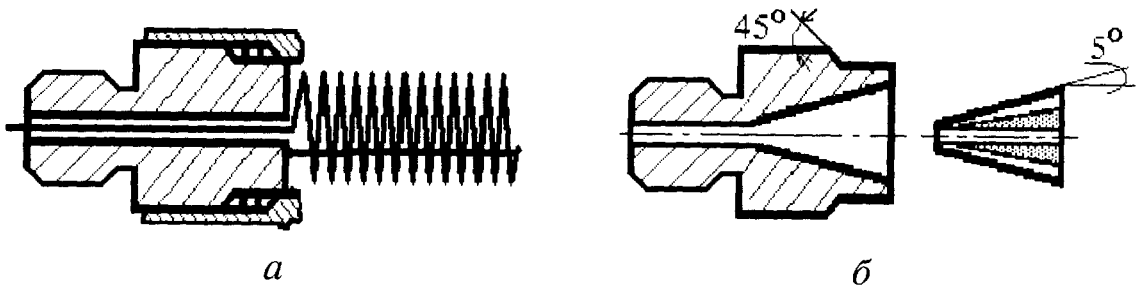

Figure 2.6. Modification of shutter for resonance (a) and resistivity (b) investigations.

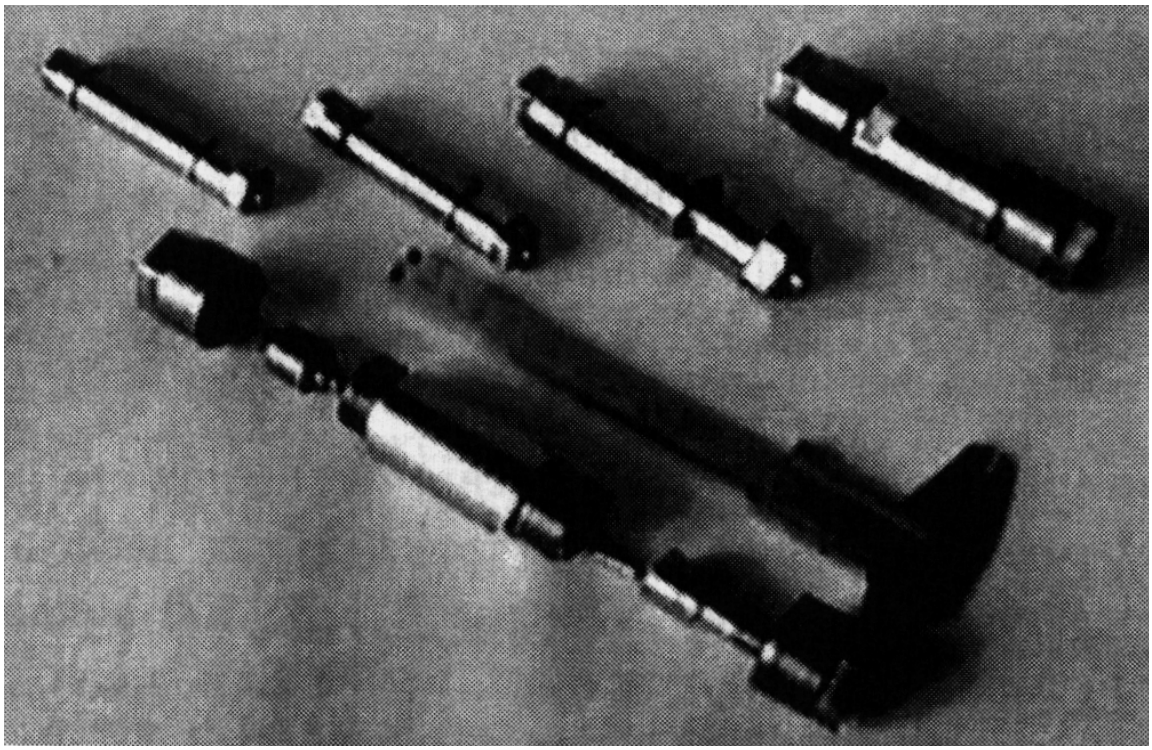

Figure 2.7. High-pressure chambers.

2.6. X-ray diffraction studies at high pressures

During X-ray diffraction studies, the compressibility factors are determined by the relative changes of the dimensions of the crystal lattice under the uniform compression. The advantages of the method of measurement of the compressibility are shown in [34].

It is especially suitable when the crystals of large enough linear dimensions are not available. This is the only method enabling the investigation of compressibility anisotropy in polycrystalline samples. Therefore, the application of X-ray diffraction method makes the problem of obtaining the test samples much simpler because the requirements as to the linear dimensions and state of the samples are reduced. The measurements can be made on single crystals, polycrystals and powders of any degree of dispersion.

The peculiarity of the X-ray diffraction method used to measure the compressibility is that there is no contribution to the diffraction pattern from those parts of the samples where the crystal structure is distorted on the account of the defects and cracks. Thus, the information is taken by the method from crystal parts of the perfect structure.

High accuracy is provided by the modern high-resolution X-ray equipment and design of the high-pressure chamber with which both the measured parameters and the experimental conditions (pressure, temperature) can be

controlled. The accuracy is also improved by the statistical methods of data processing. The measurements done on the single-crystalline samples are much more accurate than those on polycrystals.

The detailed description of the high-pressure chamber is given in [35]. In our case, the chamber is of cylinder-piston type. It is an attachment to the home-made DRON-1,5 type horizontal diffractometer.

The figure 2.8 consists of the high-pressure chamber and a thermal stabilization system (not shown). Inside the chamber casing 1, there are beryllium container 4, gripped by two punches 2 and 3. The container is a bilateral casing with an axial hole, 2.5 mm in diameter. The outer diameter in the medium section of the casing makes 10 mm, taper angle is 4^{o}. Nut 5 is for the container compression. Gaskets 6 made of annealed copper are between the container and the punches; they prevent the pressure-transmitting liquid from

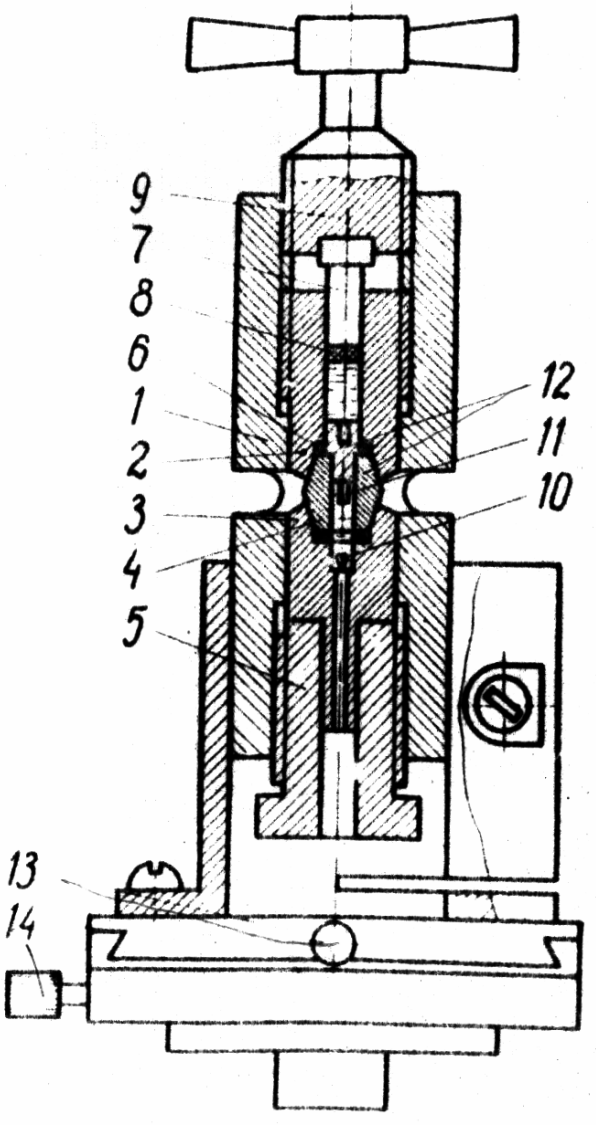

Figure 2.8. The high-pressure chamber for X-ray investigation.

the leakage. In the upper punch, there is a 3 mm diameter orifice where the pressure is generated with the help of piston 7. The piston diameter is 0.02-0.05 mm smaller than that of the channel. The piston is sealed by a two-layer plug 8 made of benzo-resistant rubber and paraffin. The benzene is a pressure transmitting liquid. Nut 9 is used to vary the pressure in the chamber. The pressure value is determined by a change of the resistance of manganite transducer 10. The resistance is measured by a direct-current bridge MO-62. With a microvoltammeter F18 Used as an external galvanometer for the bridge, it was possible to register the pressure changes in the chamber to within ±10 bars. The temperature was measured by a copper-constantan thermocouple. The transducer and the thermocouple leads go through the channel in the lower punch and are pasted with epoxy resin. The investigated sample 11 is introduced to the container by holder 12 through the channel in the upper punch (the sealing plug 8 is removed). The substitution of the sample needs on serious dismounting of the chamber. In the chamber casing, there are partition windows for the fixation of X-ray pictures; The position of the chamber windows is not symmetric, so the range of the measured angles can be extended with the stable cell strength. The chamber is mounted on the goniometer of X-ray diffractometer DRON-1,5 by means of an adjusting device 13 which ensures the chamber motion in two mutually perpendicular directions with respect to goniometer axis during the adjustment with two micrometer screws 14. The rigid enough adjusting device makes it possible to vary the pressure directly at the goniometer and to avoid sudden errors in the measurement of relative changes in the crystal-lattice parameters induced by the pressure and by the use of removable chambers as a result.

CHAPTER 3

Elastic and structural properties of hydrate-containing ferrites

Phase diagrams of ferrites with evident uniaxial anisotropy have been studied for a long time in the course of physics of magnetic phenomena [36-39].

By the mid-60ies, experimental and theoretical investigations were done, in which the idea of anisotropy presence in two planes was developed and elaborated on [39]. These studies resulted in fixing the plane where the phase transformation is formed. The investigation of $CuCl_2 \cdot 2H_2O$ [40-42] have shown that there is a phase transition on the phase diagram in inclined magnetic field below T~4.2 K. The phase diagram undergoes strong changes if the field is varied near the anisotropy axes [43]. There exist values of angles where magnetic properties are changed too, i.e. the phase transition disappears. Identical samples of $CuCl_2 \cdot 2H_2O$ and $CuCl_2 \cdot 2D_2O$ were taken for the analysis. They were the crystals of low-temperature ferrites of the same symmetry group D_{2h}^7 - P_{emn} without axes higher of the second order of symmetry. The analysis of structural and magnetic properties obtained by different methods gave us a possibility of both qualitative and quantitative control of the validity of our results.

The crystal structure of $CuCl_2 \cdot 2H_2O$ (Fig. 3.1) was considered in detail in [45-50]. The crystal had three binary axes and three planes of symmetry. The structure of $CuCl_2 \cdot 2D_2O$ was investigated in [44, 45, 51]. The values of the parameters are listed in Table 3.1. The crystalline field of approximately rhombic symmetry was acting on copper ions in $CuCl_2 \cdot 2D_2O$.

In $CuCl_2 \cdot 2H_2O$, the magnetic ordering determined by NMR method [45, 49] had shown that magnetic moments of copper ions lying in (ab) plane were ordered ferrimagnetically. The period of the magnetic unit cell 2x3.7 Å was twice larger of the crystal-chemical cell, the direction of the easiest magnetization was aligned with $\overline{a}$ axis. In the single crystal, the magnetic ordering was directly observed by magnetic neutron diffraction analysis at T=1.5 K [52, 53]. A model was proposed [26] where the local environment of the magnetic ion assumes non-zero anti-symmetric super-exchange interactions. Typical bevel of the spin moments in $\overline{ac}$ and $\overline{ab}$ planes is taken into account by renormalization of the fields of magnetic anisotropy in relativistic branches. The data of neutron diffraction [54] give the value of 0.353 K characterizing the bevel of spin moments in $\overline{ac}$ plane.

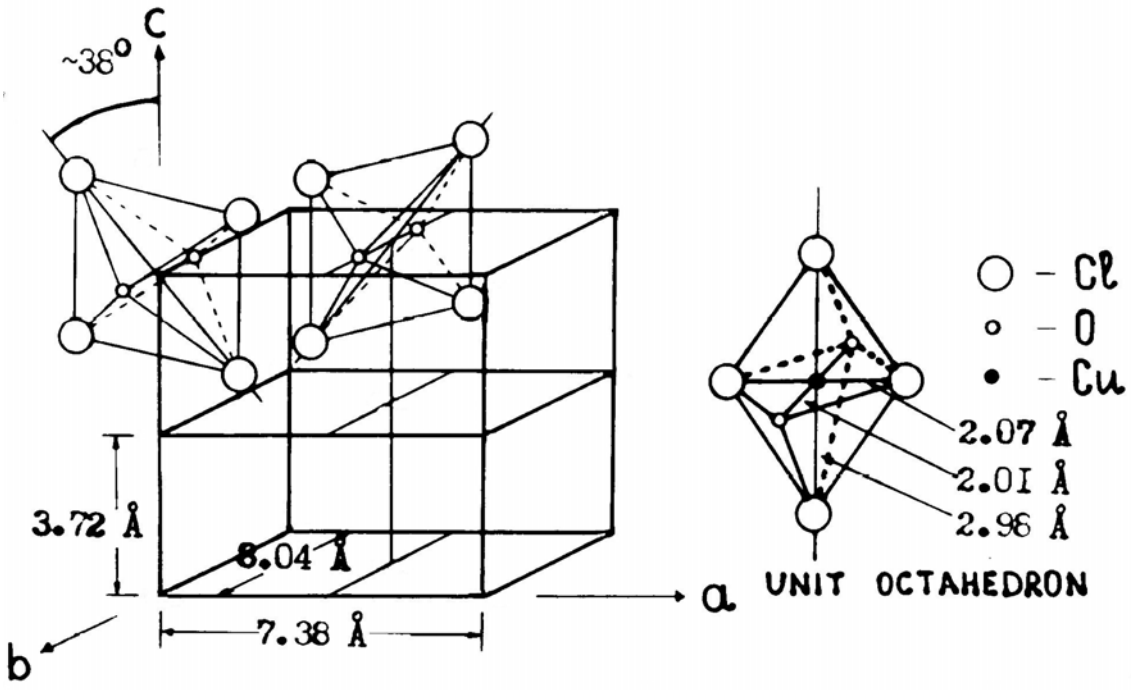

Figure 3.1. The crystal structure of $CuCl_2 \cdot 2H_2O$.

Table 3.1. The results of X-ray investigations.

	$CuCl_2 \cdot 2H_2O$		$CuCl_2 \cdot 2D_2O$	
	Data of [23]	Measurements	Data of [19]	Measurements
a	7.41(2) Å	7.436±0.003 Å	7.38 Å	7.436±0.003 Å
b	8.08(2) Å	8.148±0.001 Å	8.04 Å	8.027±0.001 Å
c	3.74(1) Å	3.756±0.006 Å	3.72 Å	3.751±0.006 Å
K_a		$(2.39\pm0.07)\cdot10^{-12}$ cm^2/dyn		$(2.49\pm0.07)\cdot10^{-12}$ cm^2/dyn
K_b		$(0.95\pm0.06)\cdot10^{-12}$ cm^2/dyn		$(1.02\pm0.06)\cdot10^{-12}$ cm^2/dyn
K_c		$(2.40\pm0.07)\cdot10^{-12}$ cm^2/dyn		$(2.53\pm0.07)\cdot10^{-12}$ cm^2/dyn
χ		$5.74\ 10^{-12}$ cm^2/dyn		$6.03\cdot10^{-12}$ cm^2/dyn

Both the neutron diffraction analysis and the spin – echo method [55] assume the existence of the structure of four sublattices splayed from $\overline{a}$ axis to $\overline{c}$ axis. The analysis of this model [54, 56] has shown that the bevel of magnetic spins in $\overline{ac}$ plane is possible but it is practically vanished in $\overline{ab}$ plane. In these systems, a weak ferromagnetism can develop according to the symmetry discussed in [57]. It can be accounted for by renormalizing of the number of constants of exchange and relativistic anisotropy in the first and the second approximations. The resonance properties are not affected in areas of

low frequencies and low fields and so, they are not the subjects of investigations in the low-frequency range.

Unfortunately, an attempt of revealing of weak ferromagnetism [44, 51] by neutron diffraction methods did not give a convincing result for $CuCl_2 \cdot 2D_2O$.

The studies of magnetization in the magnetic field in a wide temperature range by Faraday method [40] have resulted in a statement the in the paramagnetic region the susceptibility obeys Curie-Weiss law

$$\chi = \frac{\delta}{H} = \frac{c}{T - \theta} \quad \theta \simeq 5\,K$$

and for T=4.23, K M(T) dependence has a typical jump corresponding to a phase transition. For T=4.3 K, a jump in the heat capacity is accompanied by an anomaly.

While observe the character of changes of magnetization along three axes at T lower than 4.3 K, the authors of [40] stated that magnetization is of several hundreds Oe along $\overline{a}$ axis till H=6.5 kOe, then it increases rapidly and becomes proportional to the field in strong magnetic fields. The general pattern of magnetization in $\overline{ac}$ plane is similar to the behavior in $\overline{ab}$ plane for T<T. However, the comparison of $\delta = f(H)$ of both the planes shows that $\chi_a = 1.702 \cdot 10^{-4}$, $\chi_b = 1.48 \cdot 10^{-4}$, $\chi_c = 1.83 \cdot 10^{-4}$ at $\chi_b < \chi_a < \chi_c$. One of the most popular methods is the study of magnetization in the pulse field that enables the estimation of He exchange field and anisotropy field on the mentioned axis. Thus, $H_e = 7.4 \cdot 10^4\,Oe$, $H_A = 3.3 \cdot 10^2\,Oe$ [58] differ very much from $H=1.5 \cdot 10^5$ Oe [59].

Studies of magnetization in $CuCl_2 \cdot 2H_2O$ [60] gave the following values of the fields: $150 \pm 2\,kOe$, $161 \pm 2\,kOe$, $146 \pm 2\,kOe$ directed along $\overline{a}$, $\overline{b}$, $\overline{c}$ axis, respectively. The values of interaction between layers of ferromagnetic ordering of copper ions lying in the plane aligned with $\overline{c}$ axis were found to be $y = 5.51 \pm 0.07K$ and $y = 0.67 \pm 0.08\,K$ in $\overline{(ab)}$ plane.

The temperature of PT depended on the direction of applied magnetic field.

The temperature dependence of the field of phase transition was analyzed by the jump of heat capacity [62]. The method of nuclear magnetic resonance is the most informative one. It was used for the study of regularities of the first-order PT [63, 64] in $CuCl_2 \cdot 2H_2O$ where changes of Hp as a function of temperature and inclination to the easy axis were observed. The method enables us to analyze the phase diagram (HT) to determine parameters for the

existence of PT at ~150 Oe and to evaluate the critical region of phase transition $\psi_c \sim 11'$ for T=1.84K.

The changes of magnetization of a ferrite in the magnetic field result in deformation thereof (the magnetostriction is involved). The magnetostriction phenomenon relates to processes and interactions in the structure. The changes of the energy of interaction in view of deformation can be accounted for by additional magnetoelastic and elastic components introduced to free-energy density of magnet-containing crystals. The "free-energy" term implies a great number of phenomenological constants characterizing the magnetic, magnetoelastic and elastic energy. The parameters can be determined experimentally with arbitrary stress-tensor components, and by measurement of variable strains and components of vectors $\vec{l}$, $\vec{m}$. This data set would help in the determining and the control of experimental results and theoretical statements. We consider hydrostatic pressure as a convenient external parameter affecting properties of the sample, temperature changes of PT, frequencies of the critical-point resonance. So, we can determine combinations of magnetostriction constants by virtue of pressure-dependent parameters.

For single-crystalline hydrate-containing samples, the compressibility is one of important parameters. The changes of the interplanar spacings, determination of coefficients of anisotropy of compressibility for the principal crystallographic directions give us complete information about relative changes of lattice parameters which are an important factor for PT and ferrite properties.

3.1. Structural peculiarities and determination of compressibility parameters for hydrate-containing single crystals

Studies of $CuCl_2 \cdot 2H_2O$ and $CuCl_2 \cdot 2D_2O$ structures gave almost identical parameters [48, 50] that pointed to X-ray diffraction analysis application for testing.

X-ray diffractometer of DRON-1.5 type was used for estimation of coefficients of compressibility along principal crystallographic directions. The measurements were made at room temperature. The high-pressure chamber [34] was used. The chamber design made it possible to make measurements by X-ray diffractometer with scanning under pressure without the chamber removal from the goniometer. These arrangements excluded measurement errors because of multiple dismounting of the chamber from X-ray device, thus the accuracy was a increased. The pressure-transmitting medium was petrol. The pressure was varied within 0÷0,2 GPa and measured by a pressure pick-up.

The compressibility was determined during the investigations of interplanar spacings along (400), (040) and (003) directions. X-ray photography

was conducted in cobalt radiation. Fig. 3.1 illustrates experimental values of the intercrystalline spacings d_{400}, d_{040}, d_{003} in the 0÷0,2 GPa pressure range. Experimental points were processed by the least-square method with linear dependence taken into account. The results of the processing are solid lines (see Fig. 3.2). For the maximum accuracy of relative interplanar distance measurements in the course of pressure change, the profiles of diffraction lines were recorded automatically and fixed in the constant range of angles with X-ray tube and quantum counter operating continuously. The total experimental error consisting of the error of determining of lattice parameters and pressure error did not exceed 3%.

The coefficients of compressibility K_a, K_b, K_c along the corresponding crystallographic axis calculated for the orthorhombic structure of the investigated crystal are as follows:

$K_a=2.49\cdot10^{-12}$ cm^2/dyn,
$K_b=1.02\cdot10^{-12}$ cm^2/dyn,
$K_c=2.52\cdot10^{-12}$ cm^2/dyn.
The total compressibility $K=6.03\cdot10^{-12}$ cm^2/dyn.

As noted above, the experimental points were processed by the least-squares method with the linear dependence taken into account. The X-ray photography was made in cobalt radiation. The results are listed in Table 3.1. For comparison, there are crystal lattice parameters obtained by other authors. As for the compressibility, such studies have not been done beforehand, as we know.

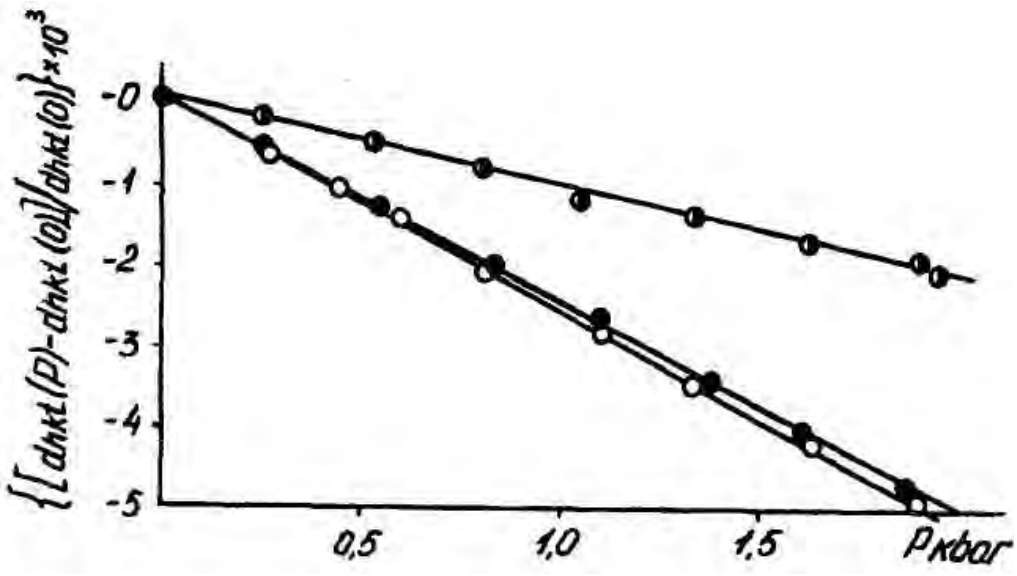

Figure 3.2. Dependence of interplanar spacings d_{400}, d_{040}, d_{003} on uniform compression in $CuCl_2\cdot2H_2O$ [64, 65].

Analogous experiments were done with $CuCl_2 \cdot 2D_2O$ [53]. In this case, the X-ray photography was done in copper radiation. The interplanar distances d_{800}, d_{010}, d_{003} were determined. The coefficient of compressibility were derived from pressure dependencies of interplanar distances d_{400}, d_{040} and d_{003} similar to $CuCl_2 \cdot 2H_2O$.

The data on compressibility for $CuCl_2 \cdot 2D_2O$ are listed in Table 3.1.

The testing of $CuCl_2 \cdot 2H_2O$ and $CuCl_2 \cdot 2D_2O$ is in a good conformity with the data obtained from other experiments. The results point to the difference of copper chloride dehydrate parameters from those of $CuCl_2 \cdot 2D_2O$ along $\overline{b}$ and $\overline{c}$ axis as well as to divergences in linear and bulk compressibility.

3.2. EPR investigations in $CuCl_2 \cdot 2H_2O$ and $CuCl_2 \cdot 2D_2O$ under pressure

In a broader temperature range, where AFMR frequencies could be observed under pressure, T_N was shifted toward higher temperatures.

To study this regularity, the EPR method was proposed. More exactly, it was EPR vanishing at the boundary of the transition [64]. The EPR lines broaden abruptly near T=4.5 K when Neel temperature is approached and practically disappear at $T\text{-}T_N$=0.01 K. $T_N(P)$ dependences give values of Neel temperature derivative with respect to pressure $dT_N/dp = 0.185\,K \cdot kbar^{-1}$. In the experimental study of EPR under pressure [64], the external magnetic field was oriented strictly along $\overline{a}$ axis. With the value of the field under which EPR was observed and the frequency, the value of g-factor for $CuCl_2 \cdot 2H_2O$ can be derived from the relation

$$h\nu = q\mu_B H \qquad (3.1)$$

where h is Dirac action constant, ν is the frequency, q is the factor, μ_B is Bohr magneton, H is the value of the external field.

For P=0, the frequency was ν=4.539 GHz, the field where EPR was observed was H=1.493 kOe. Thus, q-factor was evaluated as 2.173.

For P=3.1 kbar, the frequency ν=4.72 GHz, the corresponding field was 1.57 kOe. In this case, q=2.149. We note a good agreement between the obtained q-factor value for zero pressure and those from [66-68].

However, the data for dT_p/dp obtained by NMR method [50, 71] somewhat differ from the present data. We have dT_p/dp =0.18 $K \cdot kbar^{-1}$. This difference can be due to, first, different accuracy of pressure measurements, second, the difference in registration of the temperature by the both methods. Third, NMR measurements are made at higher values of external magnetic field as compared to EPR method.

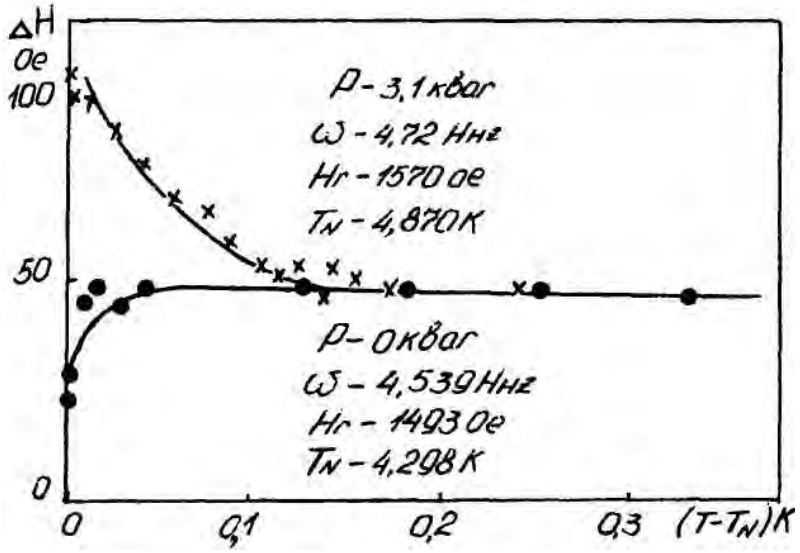

Figure 3.3. Dependence of half-width of EPR lines on (T-T_p) distance in $CuCl_2 \cdot 2H_2O$ at varied pressures [64].

Similar investigation of pressure dependence of T_p was done for $CuCl_2 \cdot 2D_2O$ single crystal [65]. For P=0, EPR study of $CuCl_2 \cdot 2D_2O$ gave T_p=4.148 K. The reduction of the temperature indicates that deuterium substitution for hydrogen results in the decrease of the value of intersublattice exchange interaction between copper ions. The reduction of the value of indirect exchange interaction can result from deuteration and expansion of $CuCl_2 \cdot 2D_2O$ lattice along $\bar{b}$ and $\bar{c}$ axis in comparison with $CuCl_2 \cdot 2H_2O$ case. Our result for relative T change in deuterated single crystal agrees well with results of [69] stating that deuteration gives 3-3.5 % decrease of T as compared with the case of the aqueous crystal.

EPR data can be used for evaluation of q-factor for $CuCl_2 \cdot 2H_2O$. In this case, the external field was oriented along $\bar{a}$ axis of the crystal, too. For the frequency ν=2.2054 GHz under zero pressure, EPR was observed at H=0.727 kOe. At these values, q-factor is equal to 2.167 which is close to that of $CuCl_2 \cdot 2H_2O$. For P=2.3 kbar, EPR was observed at ν=2.1036 GHz in the field H=0.698 kOe. Hence, q-factor equals 2.154. In such way, q-factor decreases with the rise of the pressure both in $CuCl_2 \cdot 2H_2O$ and $CuCl_2 \cdot 2D_2O$.

In both the crystals, at temperatures higher of T_p, the half-width of EPR lines was diminishing with pressure increase. EPR line half-widths for zero pressure are close to those of [66, 70].

Basing on T_p(P) dependence, the temperature derivative with respect to the pressure dT_p/dp =0.180 kbar for $CuCl_2 \cdot 2D_2O$. dT_p/dp of deutorated sample turned out to be lower than that of $CuCl_2 \cdot 2H_2O$. This result complies with NMR data [71] obtained under the measurement of T_p(P) dependence. In [71],

$CuCl_2 \cdot 2D_2O$ dT_p/dp was equal to 0.172 K·kbar and was lower than that obtained for copper chloride dehydrate by the same method.

The uniform compression affects, first of all, the interplanar spacings in the crystal and the value of magnetic exchange interaction as follows from $T_p(P)$ evolution and it influences also resonance properties, phase transitions and other parameters of AFM.

3.3. Conclusions

The current approach to the problem of low-temperature magnetism, resonance absorption, theory, first-order structural phase transition together with single-crystal symmetry has required the copper chloride dehydrate crystal to be taken as an object of investigations. It is a low-temperature magneto-dielectric with D_{12}^7 - P_{emn} symmetry group and the lowest rhombic system without axis of the order higher than the second one. It is a rhombic bipyramidal crystal with two H_2O molecules in the unit cell. Copper ions have orthorhombic symmetry in the crystal structure.

The studies of hydrostatic pressure effect on the changes of the structure made by X-ray diffraction method have shown that the uniform compression changes the elastic parameters of the structure and as a consequence, the energy of interactions through the mechanisms of elastic stresses with the symmetry remained unchanged. This fact is explained by the changes of thermodynamic parameters.

The compressibility of the hydrated single crystals was investigated by using X-ray diffractometer at room temperature. The linear pressure dependences of interplanar distances have been determined.

The compressibility factors have been determined for the corresponding crystallographic axes a, b, c of the orthorhombic structure. With the known compressibility factors, it is possible to use the energy of elastically deforming stresses in the expression presenting the interaction energies.

CHAPTER 4

First-order structural phase transition. Low-frequency properties of a low-temperature dielectric

In magnet-containing media, phase transitions are accompanied by changes of states and physical properties. The formation and evolution of the structural phase transitions of types 1 and 2 are initiated by temperature, pressure, magnetic field effect through the mechanisms of elastic stresses. The processes resulting in change of the phase state of a solid are accompanied by physical phenomena and effects able to explain the nature of inner interactions in the structure and evaluate their parameters.

The complex study of magnetic, elastic, magnetoelastic, high-frequency properties peculiar to the first order structural phase transition is an urgent problem from the viewpoint of both the object, i.e. the phase transition, and special properties.

$CuCl_2 \cdot 2H_2O$ crystal with isotopic modification $CuCl_2 \cdot 2D_2O$ are the classical objects of investigation of the physics of magnetism. They are associated with an important set of physical properties and phenomena studied at low frequencies, within centimetric and decimetric wave bands, in magnetic fields up to 12-15 kOe, at the temperature of 4.33 K and lower and under pressures up to12 kbar.

The studied physical processes and phenomena are inherent to multiple magnet-containing structures and as a consequence, the obtained results contribute a lot to the fundamental physics of magnetism.

The current approach to the problem of low-temperature magnetism is connected with investigations of phase transition neighborhood, i.e. the range of fields corresponds to the first order superconducting state.

By the example of secondary indications, this fact is confirmed by a peculiar jump of the properties of low-frequency resonance band and by magnetization [6, 7]. The separation of metal and superconducting phases occurs in the region of the first-order phase transition. The nature of magnetic properties of solids can be revealed due to investigations of the resonance absorption in inclined magnetic fields and changes of dependences of the low-temperature spectrum, explanation of the character of phase transition, characterization of different pre-critical and super-critical states.

4.1. Experimental investigation of the low-frequency resonance branch in $CuCl_2 \cdot 2H_2O$

First studies of the resonance were done by Nagamiya [73] and Kittel [74]. They studied an uniaxial magneto-dielectric and the absolute zero temperature

within the model of the molecular field. Next, the model theoretical representations were spread to rhombic single crystals studied at arbitrary temperatures. For rhombic $CuCl_2 \cdot 2H_2O$ structure, the resonance theory was developed in parallel with the accumulation of experimental results [75-86, 130]. The resonance absorption frequencies were calculated first for the rhombic single crystal at zero temperature in the magnetic field directed along the crystallographic axis [75] with the anisotropy of neighbor ions exchange interaction taken into account. The calculation of frequencies with Lande factor of anisotropy taken into consideration and for arbitrary orientation of the magnetic field with respect to crystal axis is given in [87]. The theory represented complete resonance properties at zero temperature. Otherwise, the proposed theories do not practically make it possible to determine phase-transition character and resonance features in inclined magnetic fields. The papers [88] give the most successive resonance spectra for all the possible phases in the external magnetic field and for the first-order phase transition. The developed theory of resonance in the inclined magnetic field [76-79, 87] does not explain resonance features (the existence of linearity). It still determines the sensitivity of field deviation from the easy axis in the region of phase transition.

In copper chloride dehydrate, the resonance has been experimentally detected by a group of Dutch researchers [89, 90] for frequencies of 9.4 GHz in magnetic fields up to 10 kOe and at the low-temperature range (Fig. 4.1).

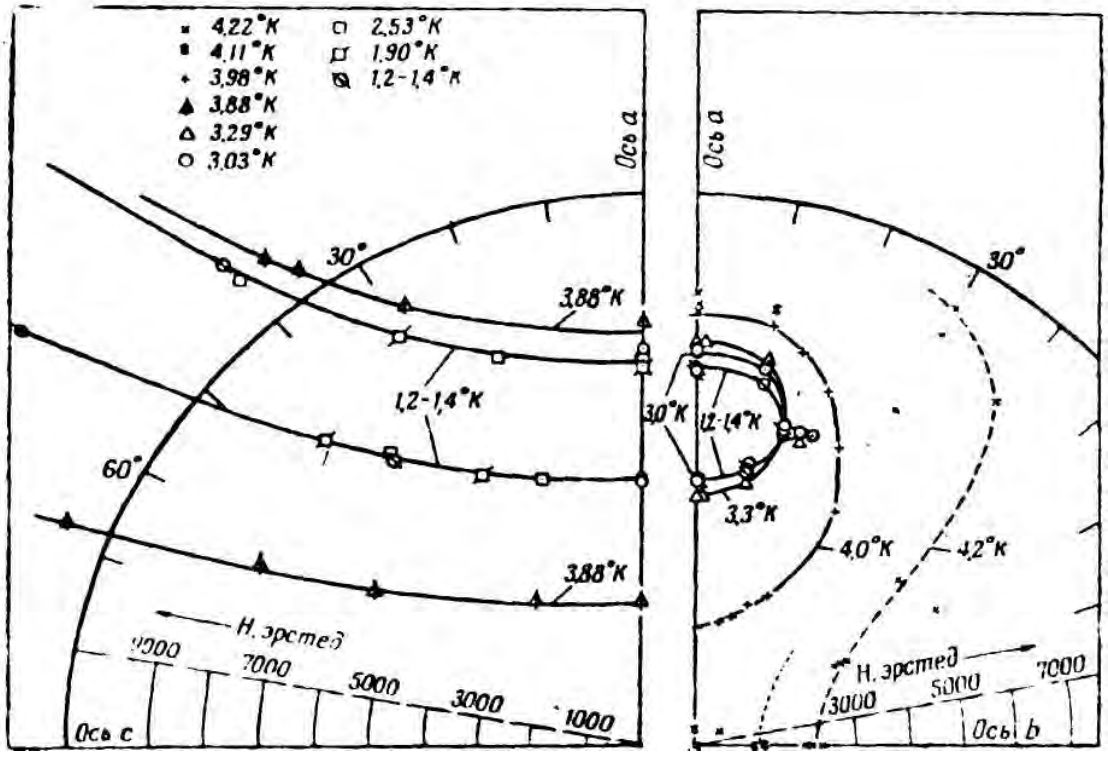

Figure 4.1. The polar diagrams of resonance field location at the frequency of 9.4 GHz in $CuCl_2 \cdot 2H_2O$ [90].

High-frequency power absorption was measured as a function of the magnitude and orientation of the external magnetic field relatively to crystallographic axes. The objects of studies were samples with a,b and a,c planes pre-oriented by means of X-ray methods. In ab plane, the values and the direction of resonance fields were found down to the lowest temperatures, on the dependences of closed curves near the critical field H of the corresponding region of the structural phase transition. With the temperature increase, the closed curves of the dependences (Fig. 4.1) shifted towards the rising field and the distance between the resonance fields was increasing, too.

The investigations of the resonance gave typical parameters for the relation of exchange energies and anisotropy in a- and c-directions at the frequencies of 323 GHz [91] and 3.5 MHz [92]. The frequency spectrum has been restored for rhombic crystal at $T=0^oK$ [90, 91]. It was noted that the values of resonance fields of the region of phase transition agreed well with those from NMR experiment and, as a consequence, the resonance field dependence coincided qualitatively with the estimates obtained by using the molecular field theory.

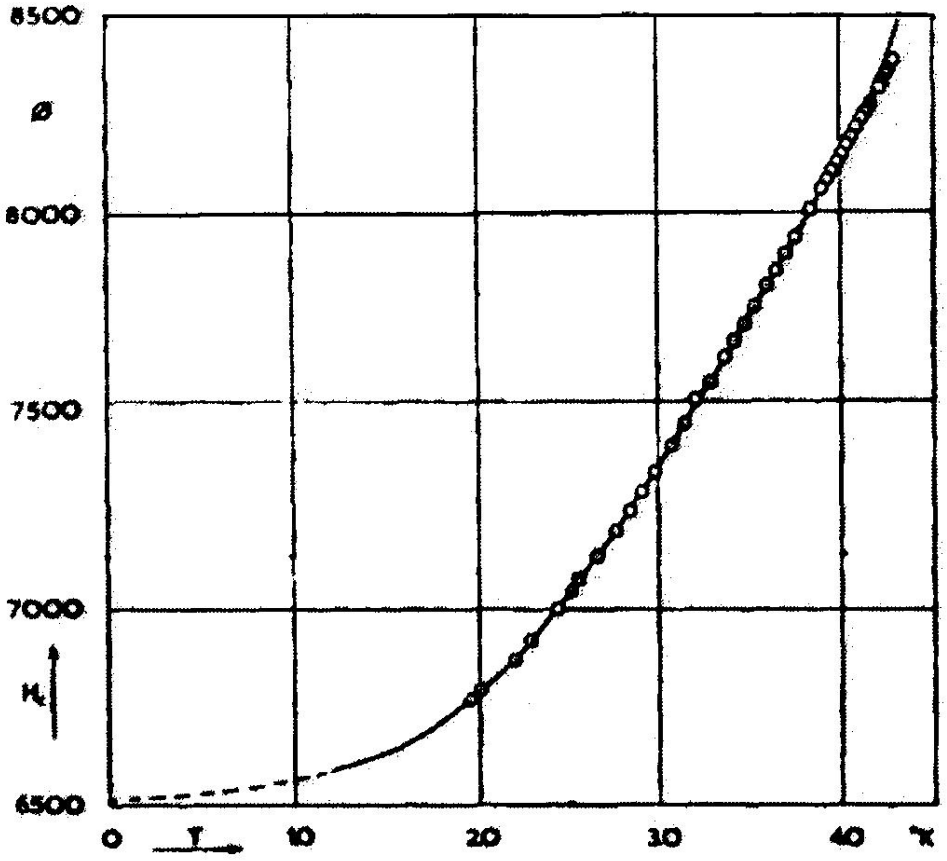

Figure 4.2. Temperature dependence of the critical field aligned with a-axis for $CuCl_2 \cdot 2H_2O$ [92].

The result obtained at frequencies of 3.5 MHz in *ab*-plane is the resonance in so-called heavy plane at HII-a, and it has the form of a single resonance line [92]. The value of the field corresponds to the region of PT realization. The results of PT studies through changes of the field H in ac-plane demonstrate the regularity as a hyperbolic dependence (Fig. 4.2).

Unfortunately, the variety of resonance frequencies [79, 89-93] could not explain the peculiarities of magnetodielectric behavior in the fields corresponding to the phase transition. The results obtained for the low-frequency resonance range [81] gave more information about the character of the phase transition. There, the measurements were made at four frequencies $\nu_1 = 5.2\ GHz$, $\nu_2 = 3.0\,GHz$, $\nu_3 = 1.1GHz$, $\nu_4 = 0.65\,GHz$ at 1.58 K. With the magnetic field H aligned with the a-axis, there were two lines of resonance absorption at each of three frequencies, and only one absorption line was present at ν_4 that corresponded in magnitude to both PT region and the value of resonance field H_{2p} in the region of the phase state for all frequencies mentioned above. This result allowed us to state that in $CuCl_2 \cdot 2H_2O$, the phase transition is of the first order (Fig. 4.3).

The peculiarities of the resonance fields were studied in [84] in the case of the inclined magnetic field if the easy *ab*-plane (Fig. 4.4). It has been revealed that the angles of coincidence of the resonance fields vary with the temperature increase. There was also a dip on the diagram position change with the angle. The dip depth decreases with the frequency and the temperature as well as with the width of the resonance line.

This region of the phase transition was studied by resonance methods in numerous papers [81, 94-99]. NMR method was used to determine the range of

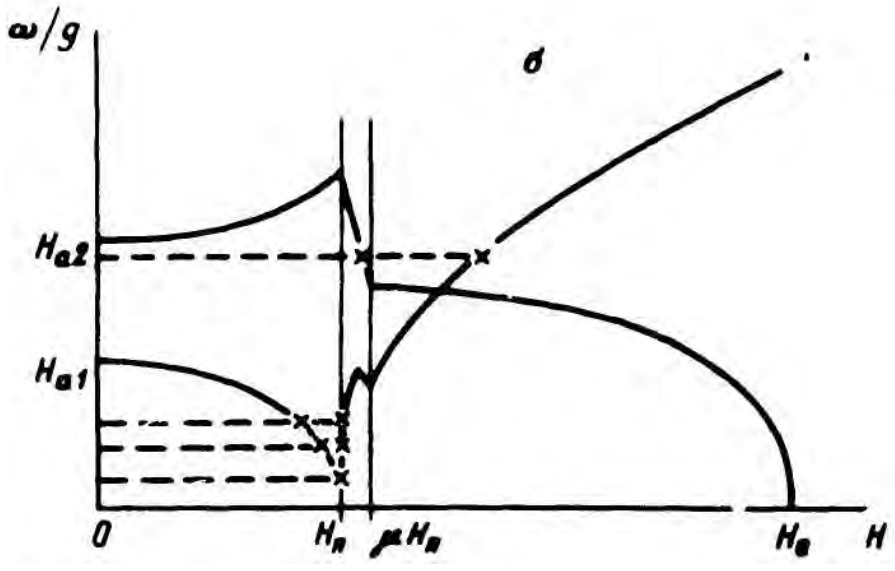

Figure 4.3. Resonance frequencies in magnetic field H||a [81].

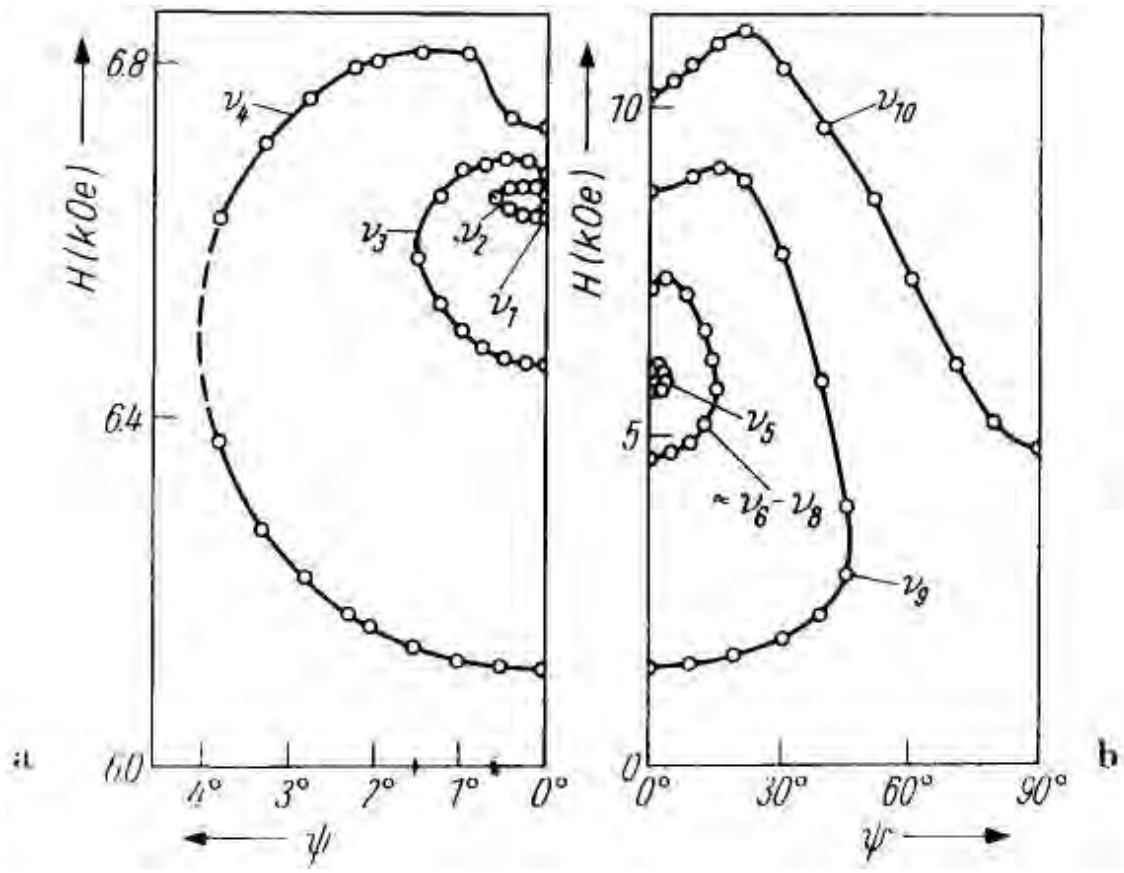

Figure 4.4. Angular dependences of resonance fields within the frequency range of (0.65 GHz-5.2 GHz) at T=1.57 K and (4.2 GHz-24.2 GHz)at T=1.4 K [84, 94].

existence of PT region for ellipsoidal sample at T=1.65 K and to confirm the typical features of the first-order transition [95]. The study of the low-temperature branch [81] has revealed regularity to state changes of phase states corresponding to different regions. A lower resonance field relates to the absorption in the region of one phase (the superconducting one). The position of a higher resonance field does not depend on the frequency. Moreover, it corresponds to the region of PT realization. A similar result was obtained for the high-frequency resonance branch [96], where $CuCl_2 \cdot 2H_2O$ was studied under pressure and temperature (T=1.65 K) within the frequency range of 25-36.5 GHz, see Fig. 4.5. This result demonstrates the resonance absorption in the region of PT to be regular with an enough exact orientation of the magnetic field with respect to the “easy” axis of the crystal. The deviation of the angle by 10-20 increases the values of the resonance field.

We should mention the results of [98, 99] where the high-frequency properties were studied in high magnetic fields. The experiment was done with plates of 3x0.3mm size. The accuracy of the orientation of magnetic field H was equal to 3. It appeared impossible to separate the resonance absorption that contradicted to [81, 96]. It is connected with an insufficient accuracy of

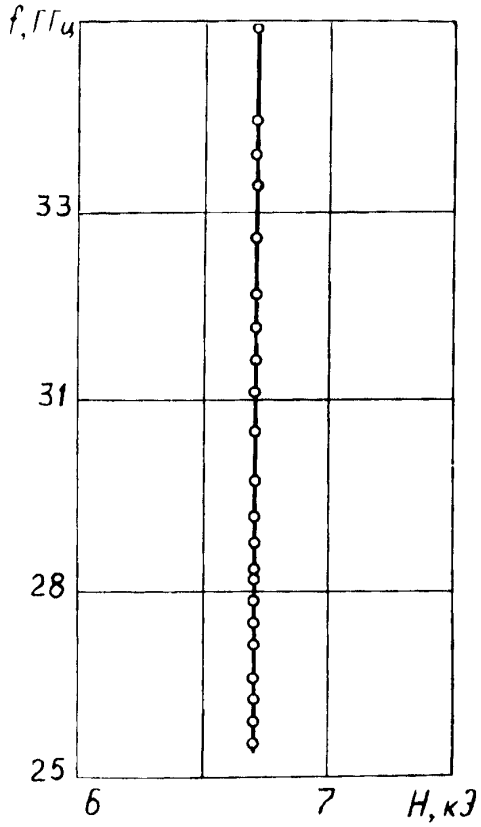

Figure 4.5. Magnetic field dependences of resonance frequencies with H aligned with a-axis in $CuCl_2 \cdot 2H_2O$ at T=1.65 K [96].

orientation of the external field along both with easy and hard planes. For $CuCl_2 \cdot 2H_2O$ in the metal phase, the resonance absorption in the region of modes corresponding to high magnetic fields results from the influence of magnetoelastic factor on the electronic system at resonance conditions.

4.2. Peculiarities of resonance absorption in the region of structural phase transition in inclined magnetic fields

A detailed investigation of the resonance in $CuCl_2 \cdot 2H_2O$ exposed a new additional absorption of high-frequency power at frequencies of 9.0, 4.2 GHz [93] and 3 GHz [84, 100] in the region of small angles of magnetic-field deviation from a-axis. This phenomenon has the form of abroad non-resonant absorption of upper resonance field satellite dependent on the angle. The line of additional absorption was detected in a small interval of angles and fields [93]. With the external field deviation from the easy a-axis, the position of the additional absorption is displaced upward with respect to the field and its width is growing.

The mechanism of such absorption is possible in the process of transition to a new phase state characterized by electronic properties responding to high-

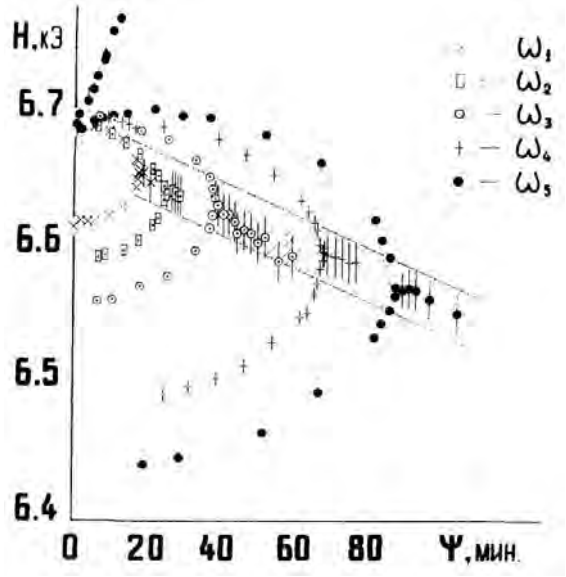

Figure 4.6. Angular dependences of the resonance fields of varied frequencies in $CuCl_2 \cdot 2H_2O$ [101]:
ω_1=1.8 GHz, T=1.64 K; ω_2=2.02 GHz, T=1.65 K; ω_3=2.42 GHz, T=1.66 K; ω_4=2.98 GHz, T=1.66 K; ω_5=3.34 GHz, T=1.66 K.

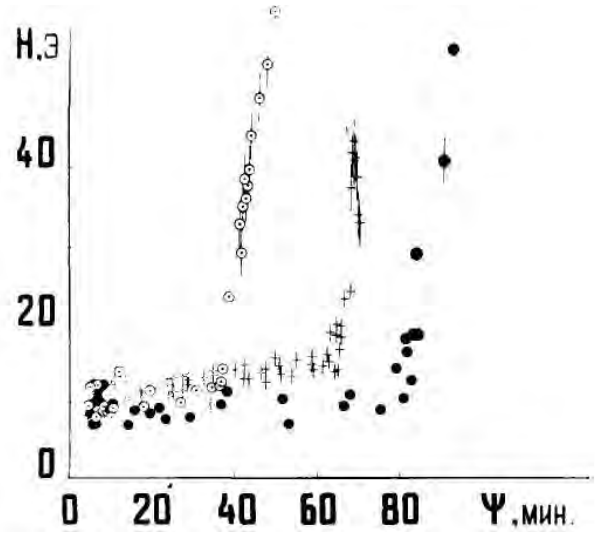

Figure 4.7. The width of the line of the resonance field [101].

frequency environment of the resonator. The process is accompanied by a newly formed resonance absorption observed near a-axis. Similar results were observed at the frequency of 3 GHz for T=1.57 K [84, 100] with the lines of additional absorption fixed at small angles of magnetic field deviation. For small angles of 0.2^o, the resonance field value was found to be relative and permanently corresponding to the field of the structural phase transition, whereas the field of additional absorption is growing with the gradual decrease of the intensity and with the temperature rise up to 2 K in this interval of angles.

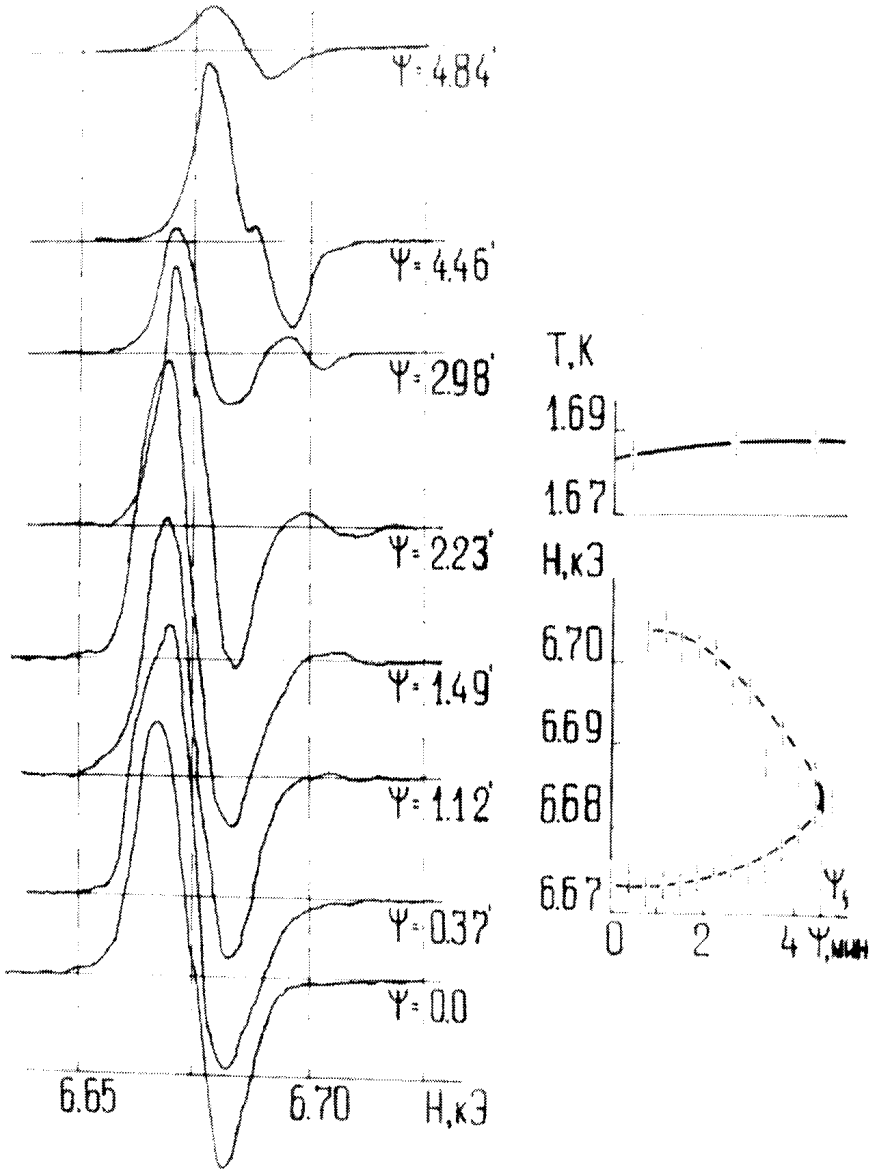

Figure 4.8. The dependence of the lines of resonance absorption on the angle of deviation of the magnetic field H from a-axis at the frequency of 1.085 GHz [104].

One of the mechanisms of non-resonant absorption can be related to the character of HF-field polarization and to electronic mobility of the phase relating to the region of the phase state.

The resonance investigations have one more interesting peculiarity developing in ab-plane of the easy plane in a wide interval of angles [84, 90, 102]. In this interval, the highest and the lowest resonance fields superpose. There was broad resonance absorption of low intensity (Fig. 4.6, 4.7). It should be noted that the auxiliary non-resonant absorptions on the background of the basic resonance effect have not been studied beforehand. To elucidate the mechanisms forming the structural phase transitions and separate phases, the nature of the whole of resonance peculiarities should be known.

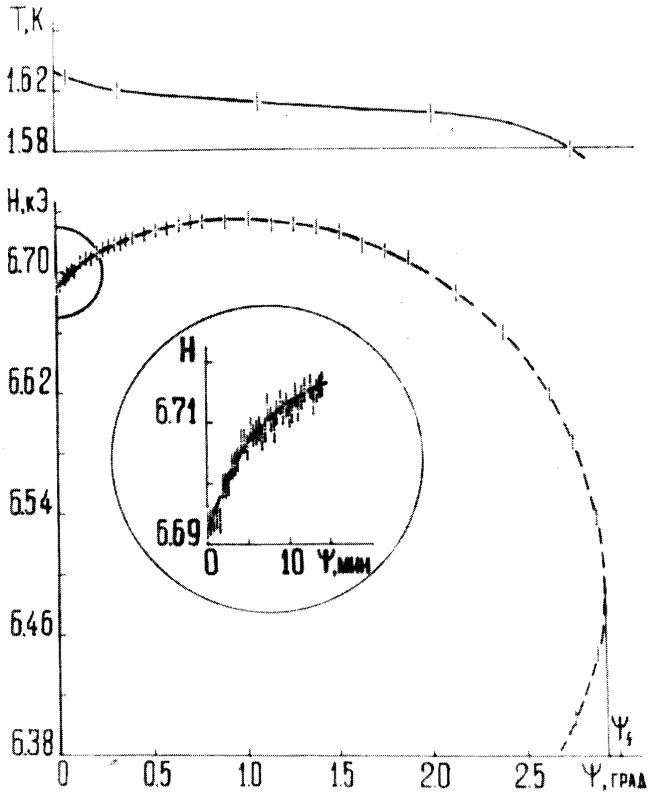

Figure 4.9. The dependence of the field of resonance on the angle of deviation of the magnetic field H near a-axis at the frequency of 4.55 GHz, T=1.6 K [104].

For a systematic presentation of resonance peculiarities in a two-axial magnetodielectric, the authors of [101] studied samples of different shape in a wide frequency range. The absorption was studied in the low-frequency range $\nu = 0.39 - 4.55\,GHz$ in a spiral-type resonator where frequencies can be changed without sample removal. It is the range that represents the region of superconducting phase state and the phase transition [6]. Detailed information is illustrated on Figures 4.8-4.10. The recorded is the derivative of the circuit of resonance absorption band for the frequency of 1.085 GHz and T1.68K. In the vicinity of easy axis, the system is not sufficiently sensitive to discriminate the absorption. With the magnetic field deviation of 0.3, there is an absorption line with the well-resolved maximum (10 Oe wide). The absorption lines approach (Fig. 4.8) and merge to the form of a single line as a result of angle increase. The regularity of alignment of lines depends on the frequency (Fig. 4.11). The descriptive picture of the results of resonance - frequency experiments in inclined magnetic field (Fig. 4.6, 4.7) is given for 5 frequencies. It is also typical of another frequencies observed earlier. At these frequencies, there is a wide absorption line at the side of higher resonance field if the region of PT (Fig. 4.6). It fixes the strong dependence on the angle between easy axis and the field of the easy axis H. It is also symmetrical with

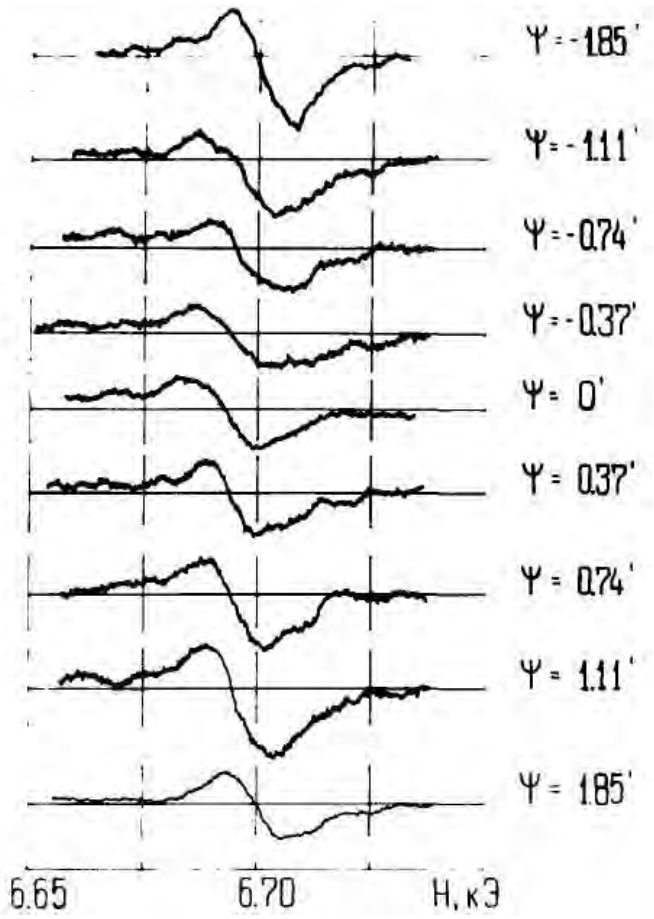

Figure 4.10. The dependence of the line of absorption of the higher resonance field at small deviations of the magnetic field from a-axis at ω=4.55 GHz, T=1.63 K [104].

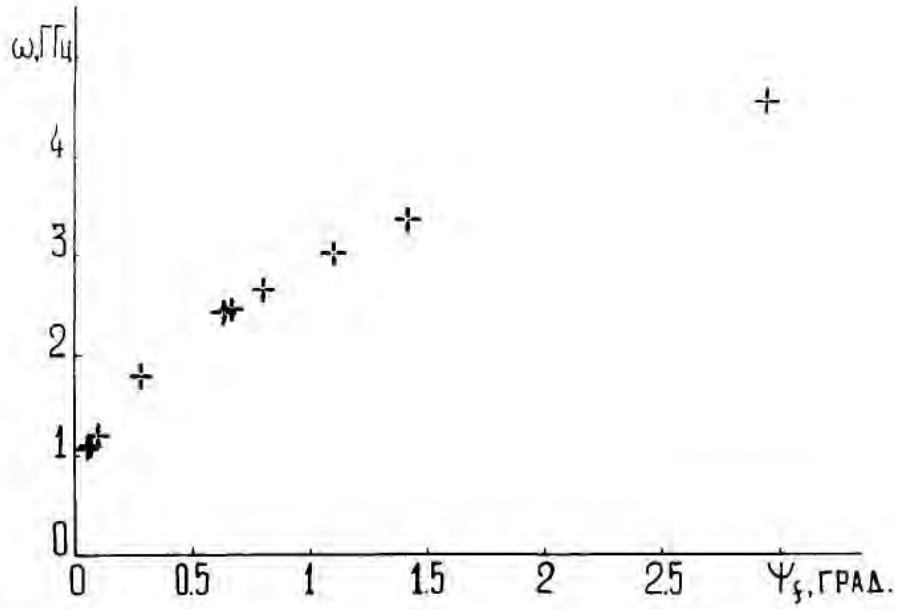

Figure. 4.11. The resonance frequency dependence of the angles of shedding at T=1.58 K [104].

respect to the symmetry plane (ac-plane of the crystal). The magnitude is wide under exact orientation of the magnetic field. This effect enables fixing of the field direction to within 20-30`. We can suppose that the resonance absorption related to the established features is of relaxation origin. The most important fact is that variable results for resonance absorption observed in a wide temperature range are consequences of changes of the structural phase transition at 0^o K followed by distinguished phase states under magnetic field. The next important fact is the resonance absorption related to both the phase state properties and the region of the phase transition. The mentioned non-resonant absorption in the vicinity of the external field orientation with respect to the easy axis can result from peculiarities of high-frequency field polarization.

4.3. Effect of sample shape on resonance high-frequency properties

Experimental investigation of the effect of sample shape for $CuCl_2 \cdot 2H_2O$ is of interest because of the typical change of the low-frequency resonance with selective absorption of HF-electromagnetic field in the region of phase state and phase transition. While studying the resonance absorption for the samples of different shapes and phase states in the external magnetic field, we can generalize and unite the conditions of the resonance mode development in the region of the structural phase transition as well as the methods of observation. The purposeful application of this method is of high value for the study of PT and phase states.

The standard was a $CuCl_2 \cdot 2H_2O$ single crystal, 4x4x4 mm in size. The structure inhomogenities were detached during the observation in a polarizing microscope. By means of X-ray diffractometer, the samples were disoriented and a-, b- and c-axes were grinded to the dish form.

The investigations of the region of structural phase transition with the observed jump of the properties were the most interesting. This region is characterized by the behavior of the upper resonance absorption line (Fig.4.12). The experiment shows that as the angle between the easy axis and the field H decreases, the resonance absorption intensity decreases and becomes low at $\psi=0$. The intensity was enhanced by an insignificant increase of the amplitude of the modulating field. As a result, the absorption line was somewhat distorted but the position remained practically unchanged. The deviation of the position of the maximum with respect to the field was registered by NMR transducer.

Considering the results of the phase transition state in magnetic field H || easy axis, we should mention the presence of the temperature. The combined influence of H and T on the structural changes in the region of PT, the same as the anisotropy of elasticity, magnetoelasticity, responds to any changes of the shape of the sample. The magnetoelasticity anisotropy is the most evident on both angular diagrams and additional absorption lines at the fixed temperature below 2 K.

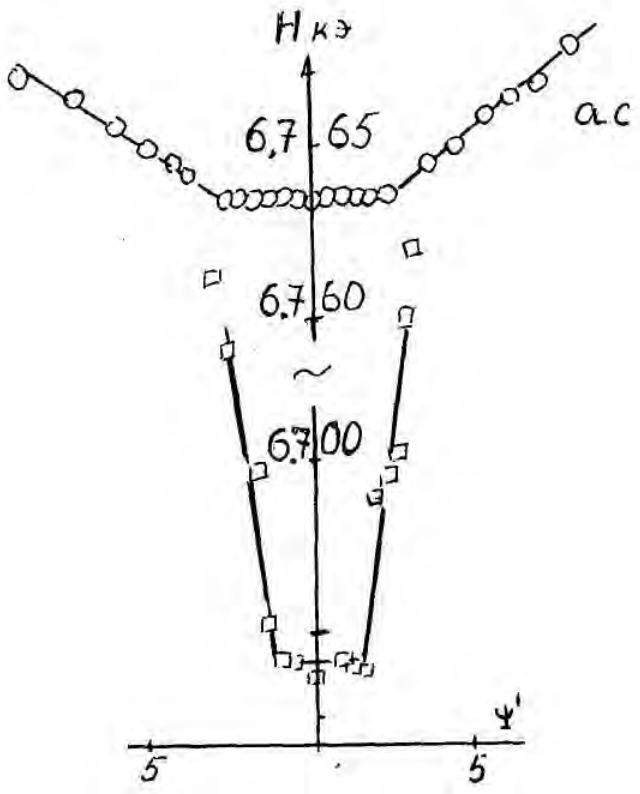

Figure 4.12. The higher resonance field near a-axis for a cubic sample at T=1.68 K and for a plate at T=1.98 K at ω=5 GHz.

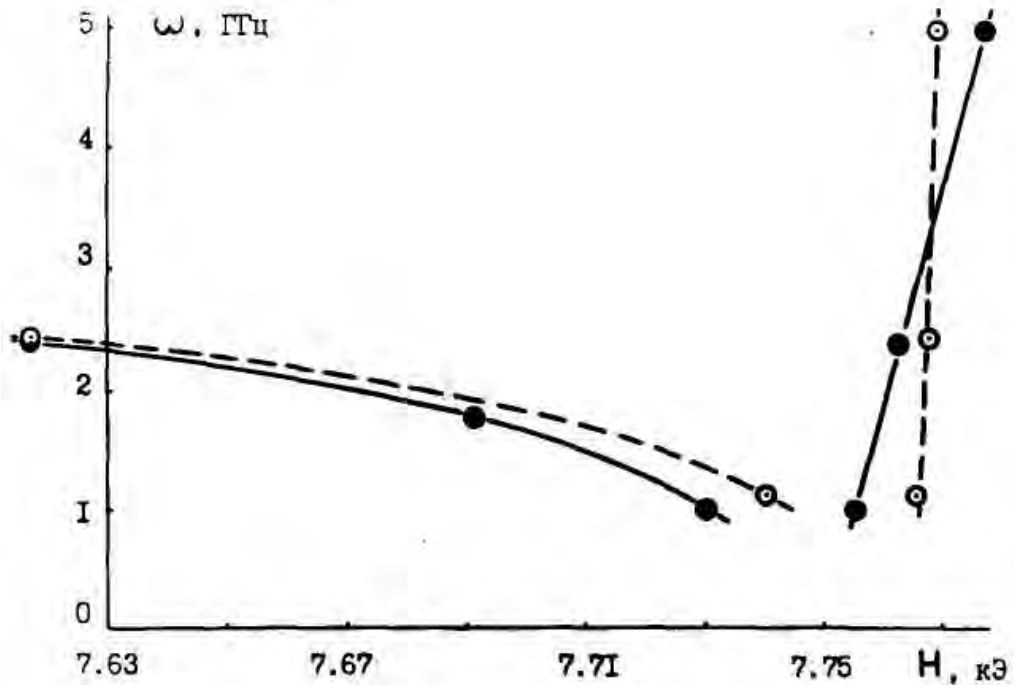

Figure 4.13. Frequency-field dependence of the field of resonance absorption in $CuCl_2 \cdot 2H_2O$ at T=1.94 K ((•) denotes a disk normal to a-axis and (o) means a disk normal to b-axis).

On the illustrated dependences (Fig. 4.13) of the resonance absorption frequencies for bc- and ac-plates, we note the vertical region with a weak field dependence of the frequency for the upper resonance line. At the same time, the dependence is essential for bc-plate. Here the slope has changed very much. But in the both cases, the resonance absorption responds to the first-order phase transition.

The first resonance line is related to the high-frequency field absorption in the superconducting phase state during H effect on the electron density change through mechanisms of magnetoelastic stresses at the fixed temperature. The position of the line slightly changes depending on the shape of the sample. In the region of formation of the structural phase transition, the resonance occurs in the form of the upper resonance field. It covers a narrow range of magnetic-field values with a thermodynamically stable PT and shows qualitatively the difference between resonance absorption in ac- and c-plates.

The discussion of the experimental results relates to the analysis of the nature of the upper resonance absorption field at frequencies of 2-5 GHz. The process of the structural phase transition is connected with the rupture and the change of bonds in the mechanisms of structure rearrangement and with the jump of properties including the high frequency ones. The nature of the resonance absorption is interpreted in view of the electron density in the region of PT and the relaxation and polarization peculiarities.

The changes of the upper resonance field with the magnetic field orientation along easy axis (Fig. 4.13) can be interpreted as those resulting from structure changes and elasticity properties. We see on the field-temperature dependences that the resonance fields are of the same value for ac-plate and three frequencies of about 20 Oe. They form the vertical part of the dependence. This part is 15 Oe for bc-plates. The elastic stresses and the anisotropy of elasticity are involved to the mechanisms of the influence of magnetic field and temperature. These quantities are tensor-like. The redistribution and changes of both the elastic stresses and anisotropy of elasticity are initiated by changes of the shape of a sample. Is it not the fact that defines the processes of the evolution of the shape of a sample?

4.4. Regularities of PT and resonance absorption in the vicinity of the hard plane

In $CuCl_2 \cdot 2H_2O$, the resonance absorption was studied in the easy plane and assigned easy axis for the magnetic field oriented along ab-plane of the crystal. The behavior of this magnetodielectric has not practically been investigated in magnetic fields oriented along ac-plane called the difficult one. In [92], the resonance method was used and the resulting were dependences of changes of resonance absorption in ac-plane in the form of a hyperbola (Fig 4.14). The studies of PT peculiarities and the low-frequency branch of resonance

absorption in the hard plane [101, 103, 104] may help in throwing light on wide domain of phenomena and effects by using the fine resonance procedures and give an answer to important problems of formation of the structural phase transition in the hard plane. These researches of the character and peculiarities of PT in magnetic field lying in the hard plane of $CuCl_2 \cdot 2H_2O$ helping revealing

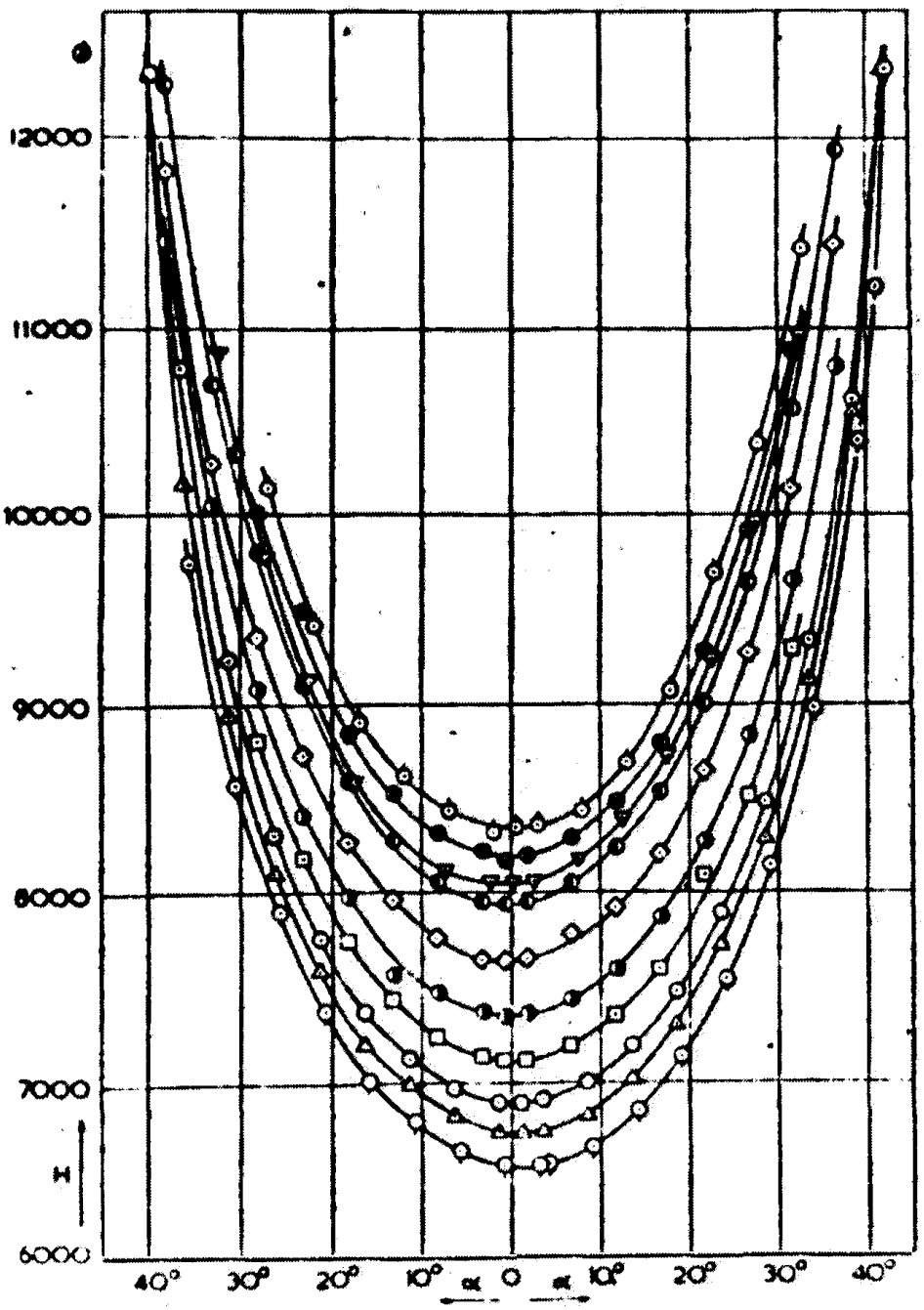

Figure 4.14. The dependence of the higher resonance field at the 3 deviation of H magnetic field from a-axis on $\overline{ac}$ hard plane in $CuCl_2 \cdot 2H_2O$ at T_1= 1.22 K, T_2= 1.939 K, T_3= 2.275 K, T_4= 2.672 K, T_5= 3.018 K, T_6= 3.411 K, T_7= 3.783 K, T_8= 4.067 K, T_9= 4.206 K, T_{10}= 4.235 K [92].

of regularities for relationship between elastic properties and magnetism in the region of low temperatures.

Single-crystalline samples of 1x1x1 mm in size were pre-oriented by X-ray diffractometer DRON-1.5 along a, b, c axes. Then, the sample was fixed with ac-plane of the substrate base. So, the sample could be mounted in resonator with b-axis movable in horizontal plane. The accuracy of orientation makes 25. In the course of the measurements, the sample was oriented completely by signal intensity and the position of the resonance fields. The frequencies of the lower branch had two resonance lines each. The signal level was fixed at any magnetic field deviation. Fig.4.15 illustrates experimental results for dependences of resonance fields of both the fixed angle in the hard plane and varying magnetic field in the soft plane. Angular diagrams show that when the magnetic field in ac-plane is changed, the intensity of higher resonance field decreases and vanishes near ac-plane, i.e. the region of PT realization.

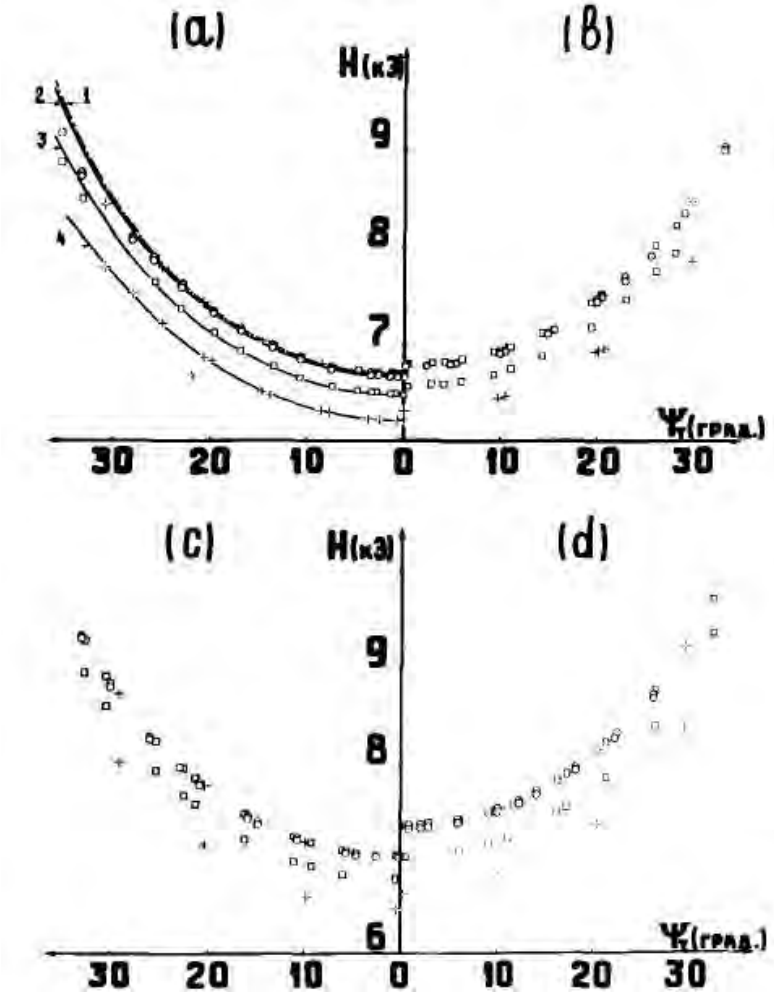

Figure 4.15. The dependence of resonance fields at the deviation of the magnetic field H on the hard plane [103] at T_1= 1.63 K (a), T_1= 2 K (b), T_3= 2.5 K (c), T_4= 3.01 K (d) at the frequencies ω_1=1.1 GHz, ω_2=3.01 GHz, ω_3=4.5 GHz.

The dependences of fig. 4.15 illustrate the systematic displacement to the region of high fields with both the temperature increase and the rise of the angle of deviation from the axis of easy magnetization toward the hard axis. Here, the attention is paid to the correspondence of results of [81, 103] to analogous data represented on fig. 4.16 in a more explicit form. The resonance absorption lines are in planes parallel to *ab*-plane in the magnetic field with the varying fixed angle directed to the hard axis and H varying its direction in the easy plane. The type of the dependence is found to be recurrent. But at low temperatures of 2 K, the valley near the axis of hard magnetization becomes increasing much (Fig. 4.17). The application of orientation methods near the axes under consideration helps in finding identity for the low-frequency absorption line in the both planes (Fig. 4.18).

The analysis of results of the observed resonance absorption in magnetic fields lying in the hard plane demonstrates that the higher resonance field does not depend on the frequency within the experimental accuracy. This behavior of frequencies was analyzed in [6, 81, 104] and related to the absorption in the region of structural phase transition. The resonance absorption pattern lasts under H change near the easy axis followed by the orientation thereof near the

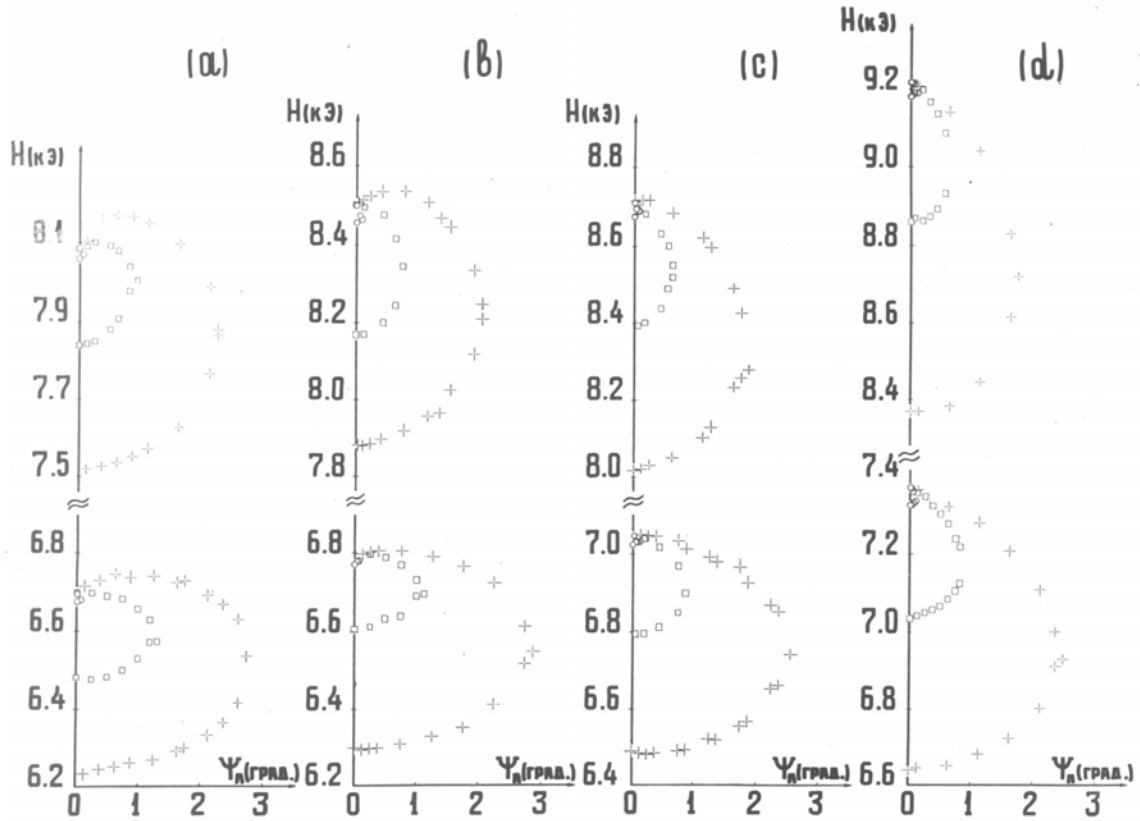

Figure 4.16. The dependence of the resonance fields at the deviation of the magnetic field on the easy plane at the fixed angles of deviation on the hard plane: a) $\psi_1=0^o$, $\psi_2=28^o$; b) $\psi_1=0^o$, $\psi_2=30^o$; c) $\psi_1=0^o$, $\psi_2=29^o$; d) $\psi_1=0.3^o$, $\psi_2=29.5^o$.

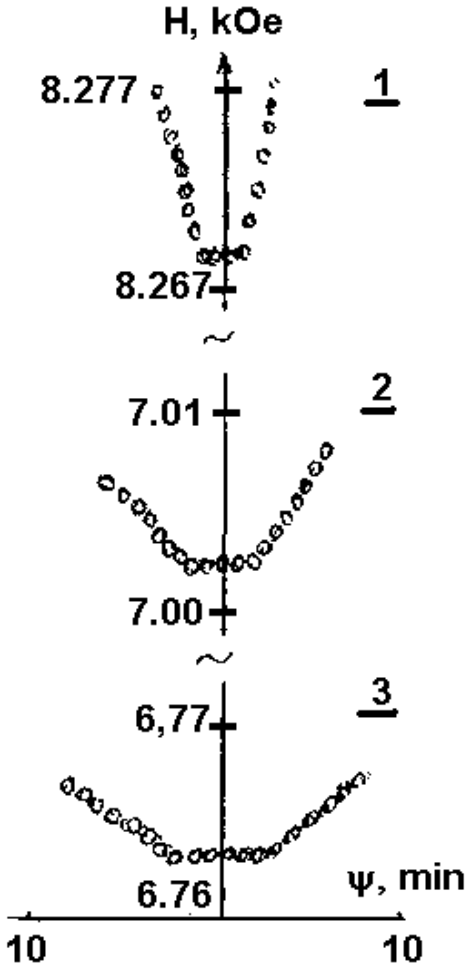

Figure 4.17. The dependence of the higher resonance field near the hard plane [103] for $\overline{ac}$ plate at T=1.98 K. 1: $\psi_T=29.7^o$, $\psi_T=14.7^o$, $\psi_T=0^o$.

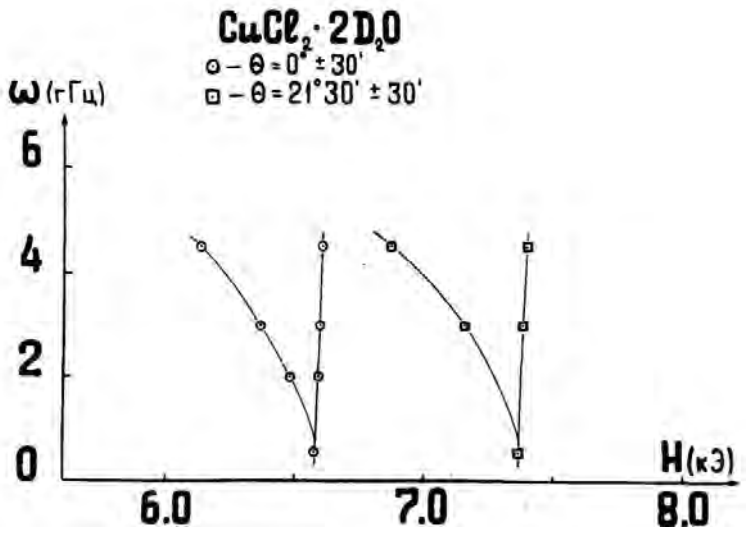

Figure 4.18. Frequency-field dependence of the resonance absorption in $CuCl_2 \cdot 2D_2O$ at $\psi_T=0^o$ and $\psi_T=21^o30'$ (T=1.68 K)[104].

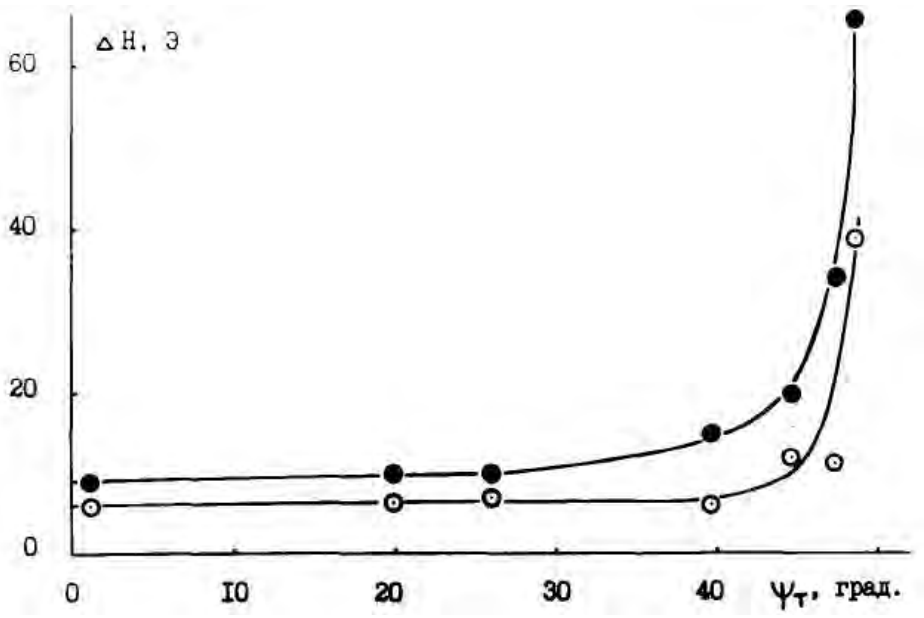

Figure 4.19. The width of lines of resonance fields for ω=2.4 GHz, T=1.94 K ((•) denotes ΔH_1 and (o) means ΔH_2).

hard plane [6]. The absorption remains near the hard plane even at very low angles. It does not practically depend on the frequency up to 30° deviation of the magnetic field in the hard plane, i.e. the PT character remains unchanged though the symmetry of phase states changes very much.

Analogous results of the resonance absorption in $CuCl_2 \cdot 2D_2O$ single crystals in the magnetic field lying near the hard axis are represented in [107]. The difference was in the position of resonance fields at all angles, it was 130 Oe lower. The same behavior was observed in ab-plane [105].

By extending the limits of magnetic field to16 kOe, it becomes possible to treat angles of 48° in the hard planes and to observe changes of the dependences of resonance absorption fields. For every investigated frequency, there are two lines of the resonance absorption for the high-frequency field and the behavior of the lines is similar till the angles of deviation in the hard plane of 40°. With the angle increase, noticeable changes of the resonance fields took place. A growth of the resonance field results in the resonance absorption line broadening and the lines become 5-fold broadened for angles of 48° (Fig. 4.19). The distance between absorption fields becomes much longer, the intensity reduces and the lines are not visible for angles of 43°. The behavior of resonance absorption lines is limited under magnetic field orientation change in the hard plane for 40° deviation. The above results give us grounds to state that the recorded resonance fields of the low-frequency branch of the field-frequency dependence determine the position of phase state and of the region of the first-order structural phase transition for the all angles of magnetic field deviation in the hard plane with the typical change of PT region where

magnetoelastic properties and the anisotropy of magnetoelasticity are specific and typical of two-axis magnetodielectrics. The role of magnetoelastic anisotropy for PT state is also noted. Being in correspondence with the position in the easy plane, it has the dependence for the critical line in exponent form showing the position of the first-order structural phase transition if the hard plane.

4.5. Conclusions

The investigation of the resonance peculiarities in the inclined magnetic field, the revealed changes of the resonance spectra in magnetic fields directed along the assigned directions helped in identification of both the character of the first-order phase transition and the phase states.

The observations demonstrate that the frequency independent part of the upper resonance field belongs to the region of the structural phase transition while the frequency-dependent part of the lower resonance field is of a phase state. The available experimental data make it possible to analyze the resonance spectrum in the easy plane for varying T and H in the selected directions and in samples of different shape in detail.

The resonance absorption in the vicinity of the easy axis is of low intensity. Strict requirements to the magnetic field orientation allow us to confirm the existence of the first-order structural phase transition from estimates of the critical angles as well as a sample shape and temperature effects. It means that the chosen region of resonance absorption studies is a community of several factors that is the role of thermo- and magneto-elasticity anisotropy, the state of the electronic system at varied parameters T and H. The mentioned results point to high importance of high-accurate external field orientation to the symmetry plane of the single crystal. Using these results, it was possible to select and to evaluate the region of the structural phase transition in order to offer mechanisms of the resonance absorption [6] and to show the first-order phase transition boundaries.

With a single crystal in the resonator, it is possible to vary the properties of the structural and magnetic symmetry with respect to the magnetic field orientation in the vicinity of so-called hard axis, i.e. going through the easy axis normal to the easy plane, where the critical region with the first-order phase transition is present. At the hard plane, there are numerous phenomena and effects among PT peculiarities. Thus, when H is directed from the easy axis toward the hard plane, the resonance absorption character is preserved to within 40^{o} and the resonance field is shifted towards increase in this case.

Comparative investigations of $CuCl_2 \cdot 2H_2O$ and $CuCl_2 \cdot 2D_2O$ show the coincidence in the character of the field-temperature dependences. With the varying sample shape and a constancy of the upper resonance field (after the structural PT) for different angles of the hard plane, the resonance fields

demonstrate that the absorption is independent of the angle of deviation, i.e. that the region of PT formation is uniform. The represented results make us to conclude that the component appearing in the hard plane is a consequence of the displacement of properties in the processes of elastic deformation. Resonance absorption of the low-frequency branch satisfies the condition of the formation of critical points and aids in restoration of the picture of structural phase transitions induced by T and H due to the mechanisms of thermoelastic and magnetoelastic stresses in the region with structure peculiarities (in the hard plane). In this case, PT character is not changed.

It follows that the observed low-frequency resonance-absorption fields occur in the region of the phase state and structural phase transition for all the investigated angles of deviation (in both the easy and hard plane) with the typical features of magneto- and thermoelastic anisotropy that is typical of the two-axis low-temperature magnetodielectrics.

Chapter 5

Resonance properties of low-temperature magneto-dielectrics under hydrostatic pressure

The radio-frequency and microwave microscopy methods make it possible to obtain information on interrelation between electronic states and positions of atoms and ions in the structure of a solid. Being sensitive to any changes of the structure, the resonance methods combined with hydrostatic pressure evoking changes of the structure parameters are effective ways of investigations of complex processes in the vicinity of structural phase transitions [106-109].

The design and creation of high-pressure and resonance techniques relates largely to the parameters of loading, resonance conditions and the degree of compressibility of a sample.

Rich bibliography on the high-pressure technology and resonance and magnetic investigations can be found in [110-112] showing the level of achievements in this field. The analysis of the results of the studies of phase transitions by resonance methods under pressure has shown that they contribute a lot to changes of the properties of ferroelectrics and ferromagnets [113]. The relationship between the magnetic properties and changes of the lattice parameters shown by the example of compressibility for MnF_2 and Cr_2O_3 as well as the numerical value of $dT/dP = 1.6\ cal/kbar$ tell about the second-order PT indicated by negative changes of the critical temperature under pressure [114-116].

The shift of the resonance frequency modes F_0^{2x} MnO, MNF_2 under hydrostatic pressure makes it possible to specify features of the structural phase transition [117]. The pressure realizes transformations of the structure, the dynamics of the phase states that is accounted for, in model representations through the renormalization of the constants [118]. The authors of [119] have theoretically shown the dynamics of changes of the resonance properties during the formation of the structural phase transition. The analysis of the data on $CuCl_2 \cdot 2H_2O$ NMR studies under pressure was the basis for the high-frequency branch calculation with the pressure parameter taken into consideration [120]. For the low-frequency spectrum [6], the region of the field-temperature dependence was shown in the form of resonance absorption both in the phase state and in the region of the first-order structural phase transition in the easy and hard planes.

By determining the thermodynamic state of a solid through relationship of the temperature and the volume, we can place the dependence of the temperature change in correspondence with the structural changes of the volume and the

properties, consequently. There occurs a transformation process: first we deal with one type of the energy which is the heat transformed into the energy of elastic stresses deforming the structure and changing the properties. A similar process of elastic changes of the structure results from the hydrostatic pressure effect.

The studies of regularities and phenomena in the physical process of structure changes in the low-temperature range and under the influence of magnetic field and high hydrostatic pressure together with the resonance registration procedure for objects of good compressibility enable us to determine the interactions under the formation of phase transitions and to compare the effects of pressure, temperature and magnetic field. The hydrostatic pressure effect conforms to the effect of thermoelastic and magnetoelastic compression. In the physics of magnetic phenomena, there are not so many papers dealing with the investigation of high-density samples at variable temperature and magnetic field and under pressure effect. In this case, the efficiency of high hydrostatic pressure action on the structure parameters and as a consequence on the magnetic properties on magnet-containing media is obvious but insignificant. For such investigations, the most promising are model single crystals of good compressibility. These are magnetodielectrics $CuCl_2 \cdot 2H_2O$ and its isotopic analogue $CuCl_2 \cdot 2D_2O$.

5.1. Resonance properties and pressures in inclined magnetic fields

The sensitivity of the resonance properties to the hydrostatic pressure observed during complex investigations of the low-frequency branch has shown dynamic changes of the phase state prior to PT as well as the dependence of the region of first-order structural phase transition realization on the mechanisms of elastic stresses. The investigations were done at frequencies of the decimeter range in a broad pressure range to 10kbar. The preliminary result [18, 102] has shown that for 3.7 GHz and 0.9 GHz, the resonance absorption lines for a higher H, pressure increase and a fixed temperature, coincide in the whole pressure range (Fig. 5.1). The changes of the form of a dip observed at small angles and low temperatures disappear with the pressure and the temperature increase.

More detailed investigations were done for a minimal temperature of 1.68 K at frequencies of 2.85-3.15 GHz, 4.5-4.8 GHz and 0.75-0.63 GHz under the fixed pressures of 5.2, 9.2, 11.2 kbar (Fig. 5.2, 5.3).

The external magnetic field H was oriented in the ab-plane and varied to within 6.2 kOe (Fig. 5.3). In this case, the resonance absorption lines belonged tone and the same field for all the frequencies and fixed pressures. There were no changes of the character of the low-frequency branch. For H to a-axis, the resonance fields were displaced thus pointing to the first-order structural phase transition.

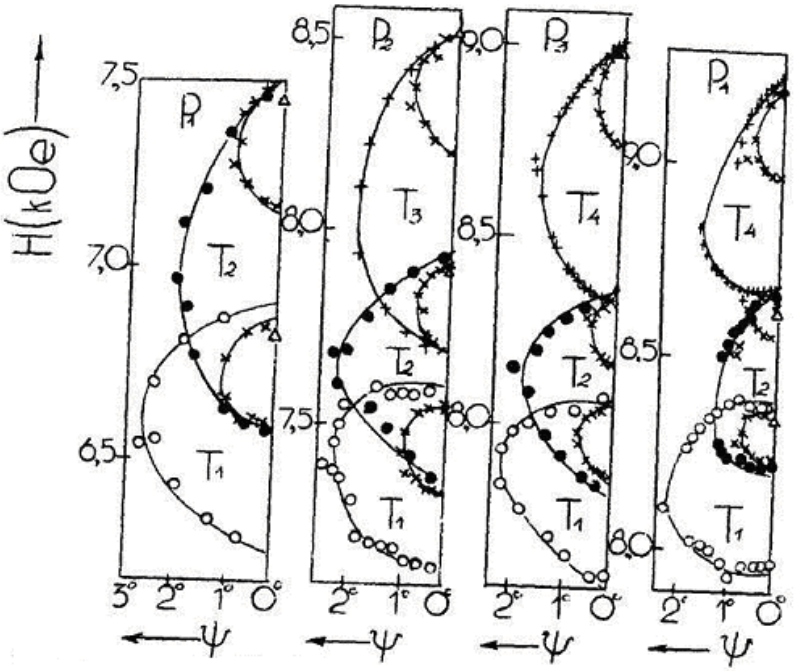

Figure 5.1. The dependence of the fields of resonance absorption on the deviation of the magnetic field at easy plane and fixed temperatures and pressures in $CuCl_2 \cdot 2H_2O$: T_1=2 K, T_2=3 K, T_3=4 K, T_4=4.2 K; P_1=0, P_2=5.2 kbar, P_3=9.2 kbar, P_4=11.2 kbar; $\omega_1(\Delta)$=0.76 GHz, $\omega_2(\times)$=3.14 GHz, $\omega_3(\circ)$=4.88 GHz [18].

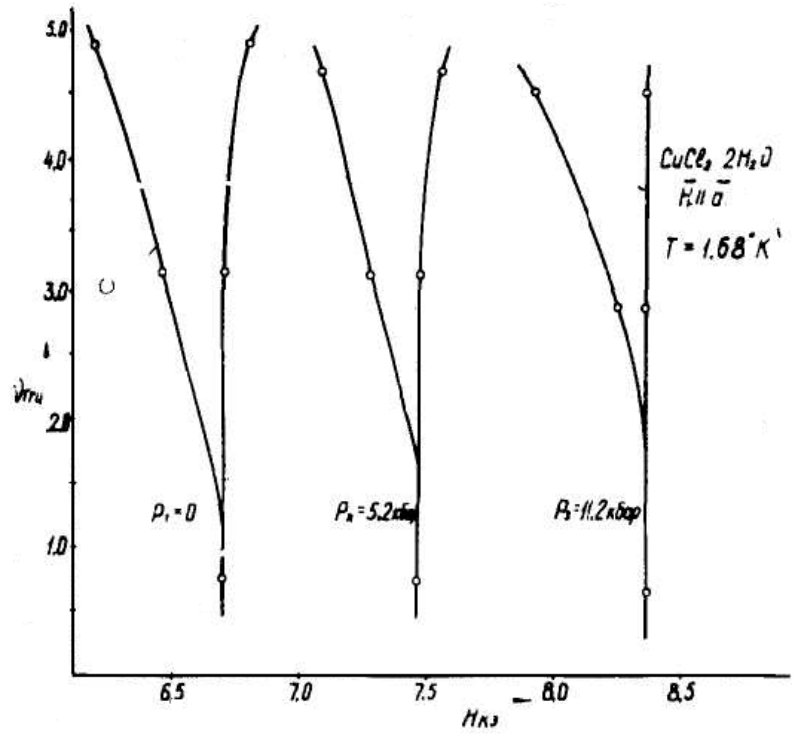

Figure 5.2. Frequency-field dependence of the fields at fixed pressures P_1=0, P_2=5.2 kbar, P_3=11.2 kbar and T=1.68 K.

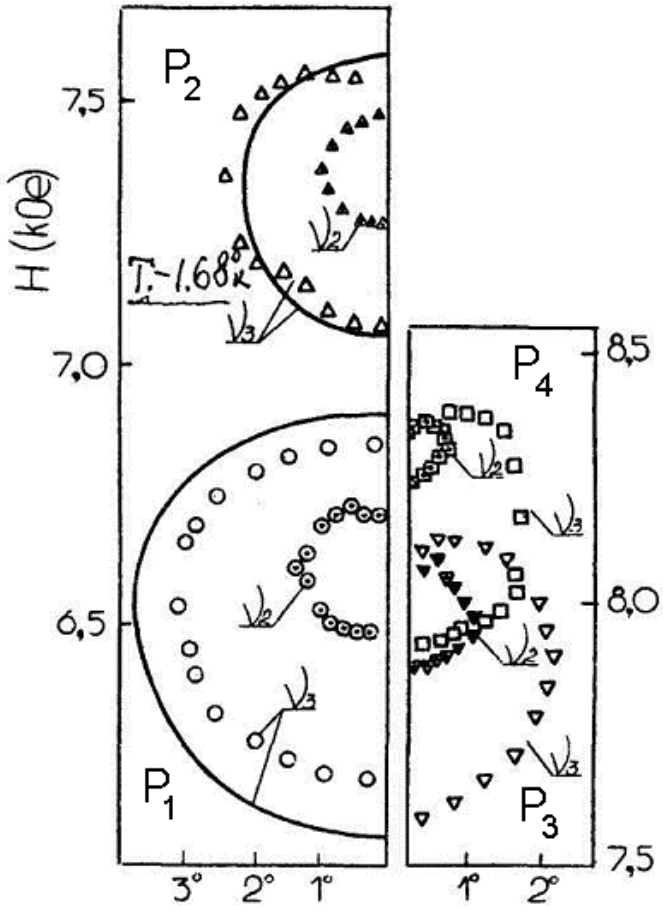

Figure 5.3. The fields of the resonance at H deviation on the easy plane at P_1=0, P_2=5.2 kbar, P_3=9.2 kbar, P_4=11.2 kbar and ω_1=2.85 GHz, ω_2=4.88 GHz at T=1.68 K [18].

From the analysis of the experimental data on the position of H field, the resonance in the PT region for different pressures and temperatures, it follows that with hydrostatic pressure increase, the conditions for structural phase transition realization are equivalent to the temperature decrease by their effect.

Another case relates to studying the conditions of resonance absorption with the fixed temperature growing from 1.68 up to 4.2 K. The magnetic field was oriented in ab-plane. For T≠0, the region of stable resonance observation propagated to the maximum of 3K. And the position of low-frequency section of the field-temperature dependence was unchanged. With the pressure increase, the boundaries of stable resonance observation reached 4.2 K. The broadened temperature range is shown on the field-temperature dependences which are shifted to higher fields with angular diagram change. Characterizing the nature of the observed phenomena in all the investigations, we note changes in H-resonance in the region of the structural phase transition while the dynamics of the changes corresponds to the first-order phase transition. A lower resonance field belongs to the phase state discussed in [6]. In view of the results of [64], it is concluded that the resonance absorption branch covers the

region of PT formation on the whole of the low-frequency branch (up to the frequency of 4.62 GHz). With the pressure increase, the region changes very much, making it possible to relate the uniform compression to the energy of structural interactions that provide perfect information on the dynamics of the first-order structural phase transition in a magnet-containing media. So, the constants $\lambda = 44\,kbar^{-1}$, $\lambda = 2\,kbar^{-1}$, $\lambda = 0.14\,kbar^{-1}$ have been evaluated enabling the binding of energies to restore the curves of the phase states.

5.2. Resonance and pressure in magnetodielectric $CuCl_2 \cdot 2D_2O$

The investigations of single crystals distinguishable by minor structure changes and prepared by X-ray methods and H_2O substantiation for D_2O resulting in changes of the distance between the lattice sites. This substantiation results in negligible stretching of the lattice along b- and c-axes. The low-frequency branch of the resonance absorption was studied in $CuCl_2 \cdot 2D_2O$ at the frequencies $\nu_1 = 0.832\,GHz$, $\nu_2 = 2.206\,GHz$ and $\nu_3 = 4.531\,GHz$ in 1.74-4.2 K temperature range and under pressures between 0-7 kbar. In H field of the easy magnetization of a-axis and at T=1.74 K (Fig. 5.4), the field-temperature dependence resembles the dependence for $CuCl_2 \cdot 2H_2O$ [65]. The curves for $CuCl_2 \cdot 2D_2O$ are 80-100 Oe displaced to lower fields. The type of the dependences

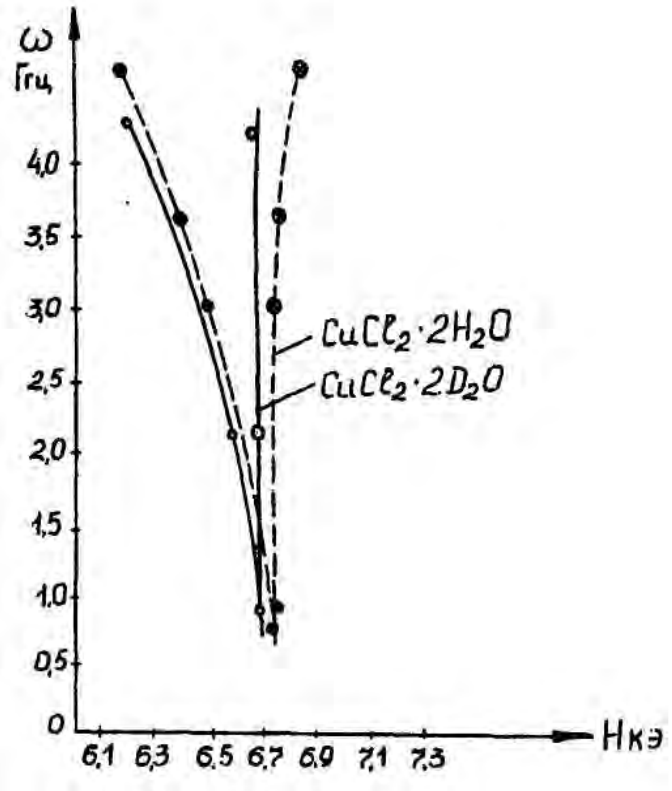

Figure 5.4. Frequency-field dependence for $CuCl_2 \cdot 2H_2O$ and $CuCl_2 \cdot 2D_2O$ at T=1.74 K [122].

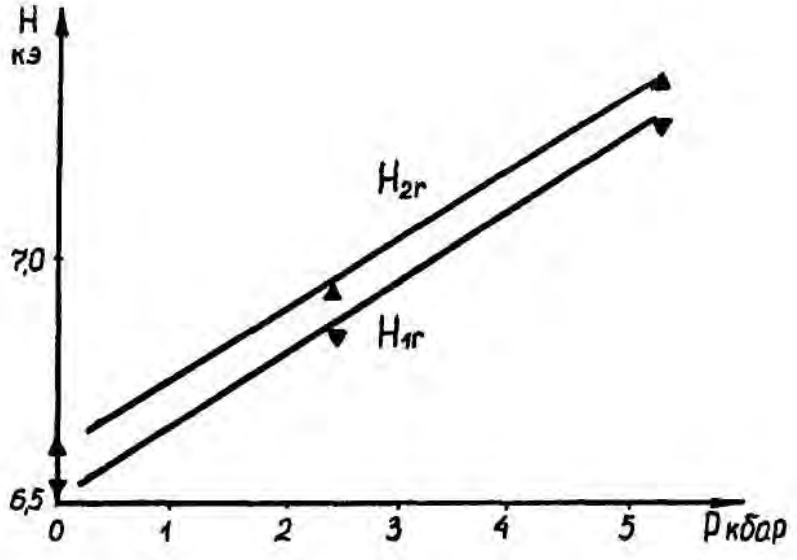

Figure 5.5. The pressure dependence of the resonance fields in $CuCl_2 \cdot 2D_2O$.

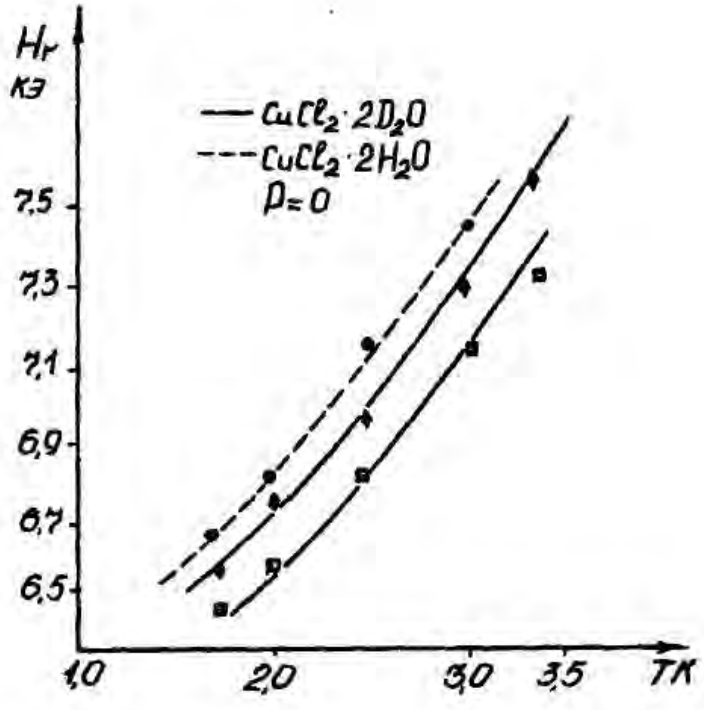

Figure 5.6. The resonance fields of PT in $CuCl_2 \cdot 2H_2O$ and $CuCl_2 \cdot 2D_2O$.

remains unchanged pointing to the invariant character of the first-order structural phase transition and the resonance absorption in both the phase state and the region of the phase transition [121]. The phase transition character retains with the introduction of the hydrostatic pressure parameter [122]. The dependence of Fig. 5.5 shows a linear growth of the resonance absorption fields in the area of PT with the derivatives with respect to the pressure $\lambda = 0.143 kOe \cdot kbar^{-1}$

and $\lambda = 0.14\,kOe \cdot kbar^{-1}$, respectively. The discrepancy of the parameters is a consequence of the changes of the parameters and the decrease of binding energies and stresses.

The temperature dependences of the resonance absorption fields are lower than those for $CuCl_2 \cdot 2H_2O$ for all the pressures and repeat the regularities of the changes in PT region. There are also differences in the values of the resonance fields of 100-200 Oe (Fig.5.6 of the preprint) [65, 122].
The temperature dependence of the field of the structural phase transition can be written as [120, 123]:

$$H(T) = H_0 + xm^2 \text{ , where } H_0 = 65\,kOe \text{ and } L = 0.07\,kOek^{-2}$$

This expression describes the character of temperature changes in the field of the first-order structure phase transition in a qualitatively correct way. For $CuCl_2 \cdot 2D_2O$, L parameter is equal to 0.0803 kOe·cal^{-2} and it is somewhat different from the analogue. For T=0 K, H_0=6.38 kOe. The investigation of the temperature dependence of resonance fields for different pressures [122] changes similarly for $CuCl_2 \cdot 2D_2O$ and its analogue, i.e. there is a decrease in dH/dP gradient value.

Dependence of resonance fields upon the displacement of the external magnetic field. The regularities are repeated in the whole the temperature range (1.74-4.2 K) and for the pressures to 5.3 kbar as well as in the dynamics of stall-angle behavior. The angles are decreasing with pressure.

5.3. Dynamics of width and intensities of resonance absorption lines under pressure and temperature

For a more complete study of the changes of the character of phase states we consider the dependencies of intensities and width of resonance absorption lines in the low-frequency region.

With the magnetic field H oriented strictly along the easy magnetization axis a, the line corresponding to the absorption in the phase state is an order of magnitude intensive with respect to the line that fixes the region of the phase transition. Under magnetic field deviation by the angle of 0.3^o, the intensities relate as 2 to1, respectively, they coincide in the region of stall angles (Fig. 5.7). This behavior was regular for all the studied frequencies.

The resonance fields were studied simultaneously with the half-width of resonance absorption lines [122]. With H || to the easy magnetization axis a, for T=1.74-3, the half-width did not exceed 20 Oe (Fig. 5.8). For the pressure of 0,53 GPa, the temperature range increases to 4.2 K and till 2.5 K the widths decrease to10 Oe and are increasing to 50 Oe at 4.2 K (Fig. 5.9).

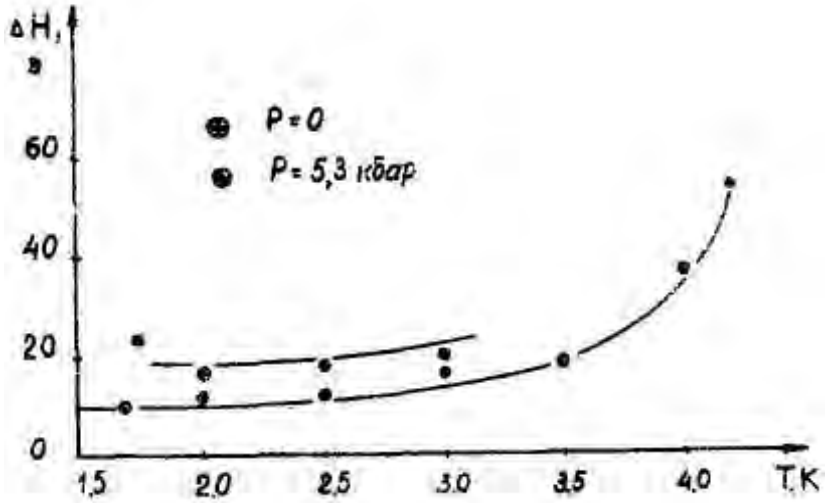

Figure 5.7. Temperature-field dependence of the width of the resonance fields in $CuCl_2 \cdot 2D_2O$ at the fixed pressures P_1=0 and P_2=5.3 kbar; ω=0.806 GHz [122].

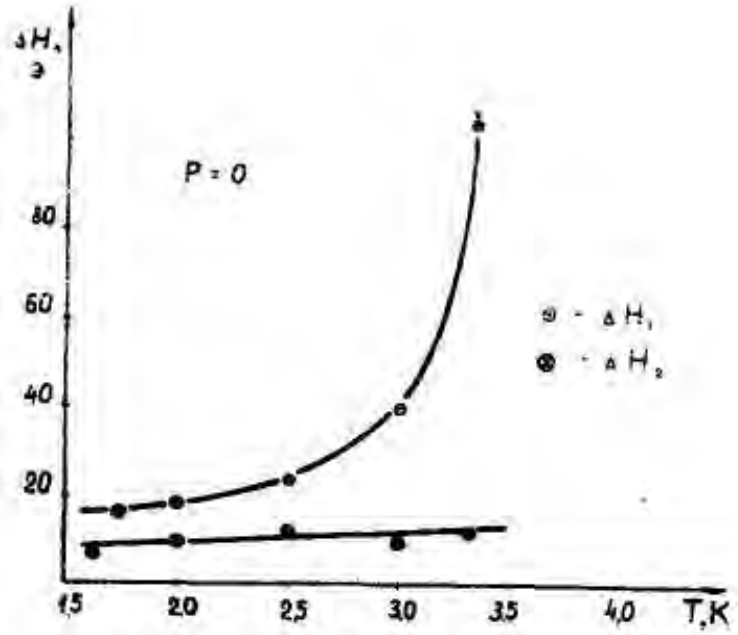

Figure 5.8. The temperature dependence of the resonance width at P=0; ω=2.206 GHz [122].

It follows that there is the essential difference in the dynamics of the behavior of the resonance absorption like half-width in the phase state and in the area of the phase transition. The half-width of the resonance absorption corresponding to the phase state field does not practically depend on the temperature and is insignificantly influenced by the frequency and the pressure. In the area of the structural phase transition, the resonance absorption half-width considerably varies with the temperature and toa less degree with the pressure increase.

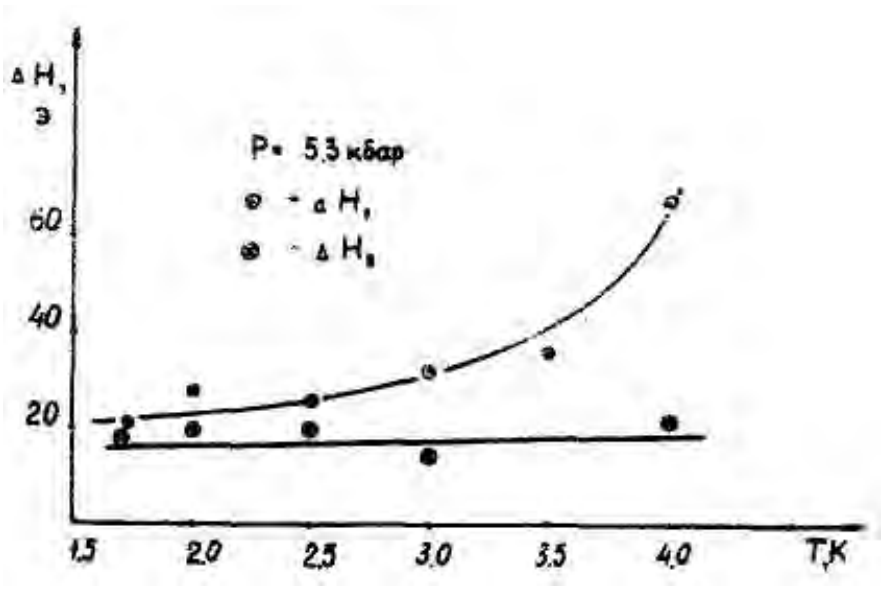

Figure 5.9. The temperature dependence of the resonance width at P=5.3 kbar; ω=2.206 GHz.

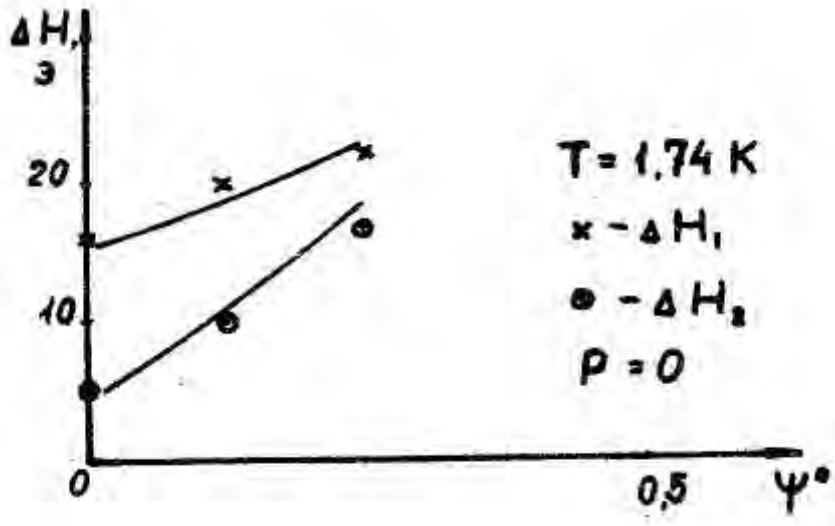

Figure 5.10. The dependence of the width of resonance absorption at the deviation of the magnetic field on the easy plane at T=1.74 K; ω=2.206 GHz.

It should be noted that the growth of the hydrostatic pressure changes parameters of the structure at the expense of compression, redistributes the relationship between the binding energies and elastic stresses and influences the electron mobility. For a more detailed analysis, an additional set of the experimental results is required. However, even this result differs very much from analogous investigations done at other frequencies [124] where the width of ~5Oe and lower were obtained due to a special processing of the samples. It is difficult to compare the results of [125] because there are practically no

calculations done for low-temperature magnetodielectrics studied, as a rule, for T lower than the critical one.

The measurements made on the studied dielectrics show that there exist regularities in the changes of the half-width of the resonance absorption lines when the magnetic field H deviates from the easy magnetization axis a. The results demonstrate that at low temperature, minor changes in the area of the phase transition correspond to 20 Oe and the same is observed with the temperature increase (Fig. 5.10). The region of the phase state fixed by H varies within 90-120 Oe with the temperature growth and under a 0.5^{o} deviation of the field from a-axis (Fig. 5.11). In this case and in the mentioned conditions, the resonance line widths are little influenced by the pressure (Fig. 5.12).

By comparing the results of $CuCl_2 \cdot 2H_2O$ and its isotopic analogue investigations, we can note the identical dynamics of changes of the properties in the area of the first-order structural phase transition as well as some difference in lattice parameters along b and c-axes. As a result, there is a difference in phase diagrams and a 100-120 Oe difference in the fields. The character of the first-order phase transition was unchanged for all ranges of frequency, temperature and pressure.

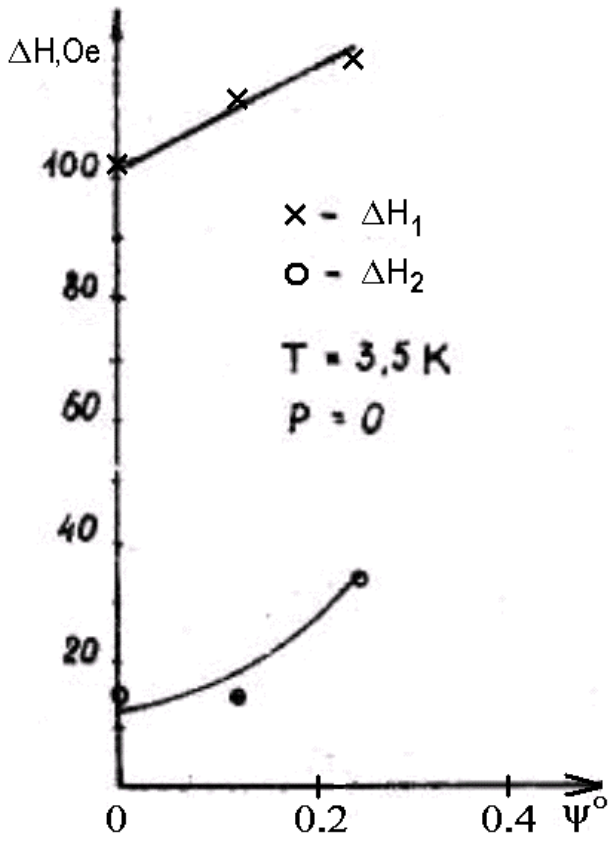

Figure 5.11. The dependence of the width of the resonance absorption at the deviation of the magnetic field on the easy plane at T=3.5 K; ω=2.206 GHz.

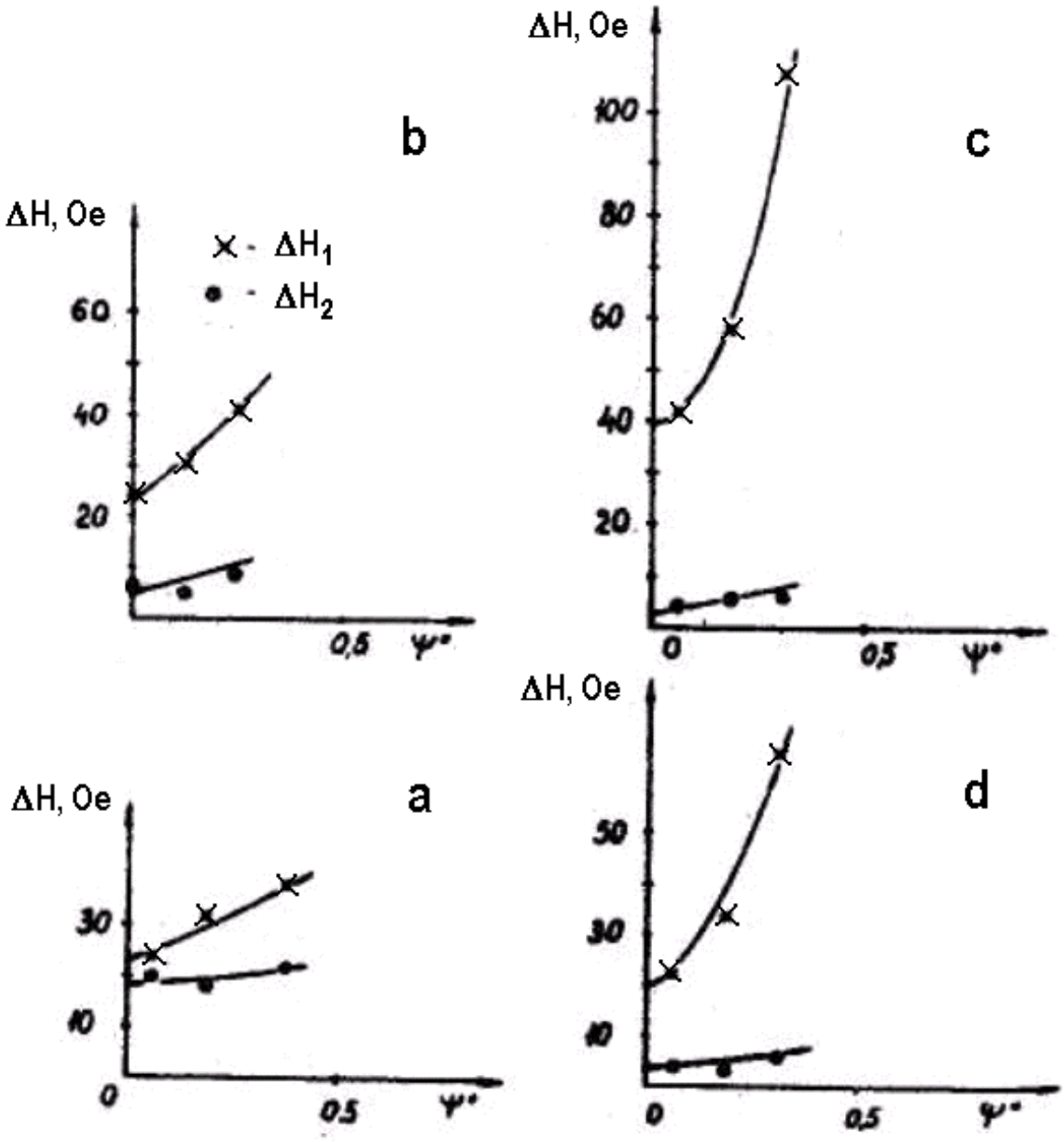

Figure 5.12. The dependence of the width of the resonance absorption at the deviation of the magnetic field on the easy plane at the fixed pressure P=5.3 kbar and the temperatures: a) T_1=2.5 K, b) T_2=3 K, c) T_3=3.5 K, d) T_4=4 K.

5.4. Conclusions

The resonance methods are sensitive to any changes of the crystal structure influenced by elastic stresses. Thus, it is possible to investigate complex processes developing in the neighborhood of structural phase transitions and phase states under T-H effect and uniform compression by hydrostatic pressure P. The meaningful dependence of the parameters of hydrogenated single crystal and good compressibility make it possible to distinguish experimentally the parameters of bonds and interactions that correlate with interatomic

distances. The results of investigations explaining how the pressure affects the resonance properties in the region of the phase states and structural phase transition establish the regularities for the critical points and the lines separating the phase states as well as for the resonance spectrum.

The represented dependences give us regularities of the resonance absorption showing that the increase of the pressure broadens the temperature range of resonance observation that is shifted to higher fields. On the dependence of the resonance fields, the depth of the dip increases near the distinguished easy axis. In the considered phases, the difference between the fields becomes smaller, the temperature range with stable resonance field fixation becomes broader and the PT critical line is shifted to higher fields.

It follows that the hydrostatic pressure increases the resonance fields and demonstrates the role of elastic stresses in the considerable change of interatomic distances with fixed T and H. As far as the nature of the upper resonance field correlates with the region of the first-order structural phase transition and the pressure from the uniform compression influences the anisotropy of interatomic and structural interactions, the dynamics of their changes gives us the information on PT state in magnet-containing medium within the low-temperature region. As a result, it has become possible to estimate the magnetoelastic constants.

Chapter 6

Relationship between magnetoelastic and elastic properties of orthorhombic magnetodielectrics

Multiple experimental results obtained by resonance methods possess rich information on the properties of $CuCl_2 \cdot 2H_2O$ and the values of typical parameters of this magnetodielectric [49, 53, 63, 68, 71] listed in Table 1. The peculiarities of the resonance studies in the region of the structural phase transition [6] are the fact, which has been proved experimentally. In the external field parallel to a-axis, in the region of the low-frequency branch, the resonance absorption is of a specific type. There are two resonance absorption lines, one of which corresponds to the value of the resonance field equal to the resonance magnetic field at low frequencies. It is the value corresponding in the magnitude to the filed of the first-order PT. The authors of related the lines of the high-frequency field energy absorption to two phase states.

Among important generalizing characteristics of magnet-containing media, there are magnetostriction parameters and dependencies of the structural changes of properties on the hydrostatic pressure. So, the role of elastic stresses in compressible structures can de determined and shown. The influence of the pressure on the high-frequency properties, fields of the phase states, critical temperatures of the structural phase transitions and the linear dependence of the mentioned parameters on the pressure make us to conclude that both dP/dH and dTp/dP , the same as changes of the critical line of the first-order phase transition Tp(H) are of positive sign.

Table 6.1.

M_0 ед CGS	$\delta \cdot 10^3$	ρ	ρ'	β	β'	$10^4 \chi_{\perp 0} = \delta^{-1}$
42	1,87	-22,4	-28,8	-102	- 122	5,36
$H\alpha_1$	$(\rho-\rho')\cdot M_0$	$2\delta M_0$	$10^4 \chi_{\perp 0}^{(a)}$	$10^4 \chi_{\perp 0}^{(b)}$	$10^4 \chi_{\perp 0}^{(c)}$	$\frac{\beta-\beta'}{\rho-\rho'} = \gamma$
кЭ			5,35	5,44	5,68	3,00
6,28	0,27	1,57				
$H\delta_{x_1}$	$H\delta_{x_2}$	$H\delta_{y_1}$	$H\delta_{y_2}$	$H\delta_{z_1}$	$H\delta_{z_2}$	-
кЭ						
148	148	155	154	156	157	-

Pressure effect on the magnetic properties is conditioned by magnetostriction. That is why the total parameters describing the influence can be useful for studying the magnetoelastic properties of $CuCl_2 \cdot 2H_2O$. The theoretical analysis of magnetoelastic properties of orthorhombic magnetodielectrics gives us a possibility to derive expressions for finding the magnetostriction constants [64].

The density of the free energy of magnetically ordered crystal can be represented as

$$\omega = \omega_m + \omega_{me} + \omega_e \tag{1}$$

where ω_m, ω_{me}, ω_e are the densities of magnetic, magnetoelastic, elastic energy, respectively.

The density of the elastic energy of D_{2h}^7 symmetry group crystals in the double sublattice model is [126]:

$$\omega_m = \frac{1}{2}A_0 M^2 + \frac{1}{2}B_0 L^2 + \frac{1}{2}\left(a_{10}M_x^2 + a_{20}M_y^2 + b_{10}L_y^2\right) - \vec{M}\vec{H} - k_B T\left[S\left(M_1\right) + S\left(M_2\right)\right] + \omega_m^{(ex)} \tag{2}$$

Here $\vec{M} = \vec{M}_1 + \vec{M}_2$ is the vector of weak thermomagnetic moment, $L = \vec{M}_1 - \vec{M}_2$ is the vector of ferromagnetism, M_1, M_2 are the magnetizations of sublattices, A_0, B_0 are dimensionless constants of the uniform exchange interaction, a_{10}, a_{20}, b_{10}, b_{20} are dimensionless constants of anisotropy, $\vec{H}$ is the external constant magnetic field, $S(M)$ is the entropy correspondingto the magnetic moment $\vec{M}$:

$$S(M) = v_0^{-1} \int_{M/M_0}^{1} B^{-1}\left(x\right)dx \tag{3}$$

where v_0 is the volume of crystal unit cell, M_0 is sublattice magnetization at the absolute zero, $B^{-1}\left(x\right)$ is the inverse Brillouin function and k_B is Boltzmann's constant.

The term $\omega_m^{(ex)}$ describes the non-uniform exchange energy and it has a standard form [126]. The constants A_0, B_0, a_{10}, a_{20}, b_{10}, b_{20} are related to the exchange and anisotropy constants by which the energy of two-axis magnetodielectrics [127] is written as

$$A_0 = \frac{1}{2}\delta; \quad a_{10} = \frac{1}{2}(\beta + \beta'); \quad b_{10} = \frac{1}{2}(\beta - \beta');$$
$$B_0 = \frac{1}{2}\delta; \quad a_{20} = \frac{1}{2}(\rho + \rho'); \quad b_{20} = \frac{1}{2}(\rho - \rho'); \tag{4}$$

The density of the magnetoelastic energy can be written down in the form

$$\omega_{me} = \frac{1}{2}\Lambda_{\alpha\beta\rho\mu}u_{\alpha\beta}L_\rho L_\mu + \frac{1}{2}\tilde{\Lambda}_{\alpha\beta\rho\mu}u_{\alpha\beta}M_\rho M_\mu + \frac{1}{2}\Lambda^{(e)}_{\alpha\beta}u_{\alpha\beta}L^2 + \frac{1}{2}\tilde{\Lambda}^{(e)}_{\alpha\beta}u_{\alpha\beta}M^2 \tag{5}$$

The tensors $\Lambda_{\alpha\beta\rho\mu}$ and $\tilde{\Lambda}_{\alpha\beta\rho\mu}$ describe the relativistic magnetoelastic interactions, the tensors $\Lambda^{(e)}_{\alpha\beta}$ and $\tilde{\Lambda}^{(e)}_{\alpha\beta}$ describe the exchange magnetoelastic interactions. The doubly repeated indices imply summation. There are no terms like $\Lambda_{\alpha\beta\rho\mu}$, $u_{\alpha\beta}L_\rho M_\beta$ since in $CuCl_2{\cdot}2H_2O$ and $CuCl_2{\cdot}2D_2O$, the unit cell is doubled as compared to the chemical one moreover such combinations are impossible because the sublattice atoms change places with each other during the translation and $\vec{L}$ changes its sign. The structure of tensors Λ and $\tilde{\Lambda}$ is totally determined by the symmetry of the crystal that is non-zero elements Λ and $\tilde{\Lambda}$ are those with which there are combinations of strain tensor components and components of vectors of antiferromagnetism, all being invariant with respect to all the transformations of D_{2h}^7 symmetry group. Here and below, the indices written in Greek are for writing down the components of vectors and tensors in Cartesian coordinate system, so they take values from 1 to 3. The indices written in Latin are for tensors in Feught designations, they take the values from 1 to6. The Cartesian indices relate to Feught indices as follows:

Cartesian indices	xx	yy	zz	yz	xz	xy
Feught indices	1	2	3	4	5	6

If we rewrite (5) in Feught designations, we get

$$\omega_{me} = \frac{1}{2}\Lambda_{ik}u_i L_k^2 + \frac{1}{2}\tilde{\Lambda}_{ik}u_i M_k^2 + \frac{1}{2}\Lambda^{(e)}_{\alpha}u_\alpha L^2 + \frac{1}{2}\tilde{\Lambda}^{(e)}_{\alpha}u_\alpha M^2 \tag{6}$$

Here we took the following designations: $L_1^2 = L_x^2$, $L_2^2 = L_y^2$, $L_3^2 = L_z^2$, $L_4^2 = L_y L_z$, $L_5^2 = L_x L_z$, $L_6^2 = L_x L_y$, the designations for M_k^2.

For (6), the tensors of exchange striction have only three components other than zero. The tensor of relativistic striction satisfying the properties of D_{2h}^7

symmetry group is defined by nine independent magnetoelastic constants and is of the form

$$\lambda_{ik} = \begin{pmatrix} \lambda_1 & \lambda_3 & \lambda_5 & 0 & 0 & 0 \\ \lambda_2 & \lambda_4 & \lambda_6 & 0 & 0 & 0 \\ -(\lambda_1+\lambda_2) & -(\lambda_3+\lambda_4) & -(\lambda_5+\lambda_6) & 0 & 0 & 0 \\ 0 & 0 & 0 & 4\lambda_9 & 0 & 0 \\ 0 & 0 & 0 & 0 & 4\lambda_8 & 0 \\ 0 & 0 & 0 & 0 & 0 & 4\lambda_7 \end{pmatrix} \tag{7}$$

The structure of $\tilde{\Lambda}_{ik}$ tensor is analogous to (7).

Next, for the study of magnetoelastic properties under external pressure, we write down the density of magnetoelastic energy in terms of stress tensor $\sigma_{\alpha\beta}$ using [128]:

$$\omega_e = \frac{1}{2} c_{ik} u_i u_k = \frac{1}{2} \tilde{K}_{ik} \sigma_i \sigma_k \tag{8}$$

where c_{ik} is the tensor of elastic moduli, $\tilde{K}_{ik}$ id the tensor of moduli of elastic compliance. As known, $\tilde{K}_{ik}$ is reverse to c_{ik} tensor. The structure of c_{ik} tensor for rhombic crystal is given in [128].

The tensor of moduli of elastic compliance can be written in the form

$$\tilde{K}_{ik} = \begin{pmatrix} K_{11} & K_{12} & K_{13} & 0 & 0 & 0 \\ K_{12} & K_{22} & K_{23} & 0 & 0 & 0 \\ K_{13} & K_{23} & K_{33} & 0 & 0 & 0 \\ 0 & 0 & 0 & 4K_{44} & 0 & 0 \\ 0 & 0 & 0 & 0 & 4K_{55} & 0 \\ 0 & 0 & 0 & 0 & 0 & 4K_{66} \end{pmatrix} \tag{9}$$

Using the relationship

$$u_i = \tilde{K}_{ik} \sigma_k \tag{10}$$

and substituting (10) into(5), we have

$$\omega_{me} = \frac{1}{2} Z_{ik} L_k^2 \sigma_i + \frac{1}{2} \tilde{Z}_{ik} M_k^2 \sigma_i + \frac{1}{2} Z_\alpha^{(e)} \sigma_\alpha L^2 + \frac{1}{2} \tilde{Z}_\alpha^{(e)} \sigma_\alpha M^2 \tag{11}$$

In this expression, we have already the stress tensors, and new tensors of magnetoelastic constants Z_{ik}, $\tilde{Z}_{ik}$, $Z_{ik}^{(e)}$, $\tilde{Z}_{ik}^{(e)}$ are related to those in (6) through the following relationships:

$$\begin{aligned} Z_{ik} &= \Lambda_{mi} \tilde{K}_{mk}; \qquad \tilde{Z}_{ik} = \tilde{\Lambda}_{ji} K_{jk}; \\ Z_\alpha^{(e)} &= \Lambda_\beta^{(e)} \tilde{K}_{\beta\alpha}; \qquad \tilde{Z}_\alpha^{(e)} = \tilde{\Lambda}_\beta^{(e)} K_{\beta\alpha} \end{aligned} \tag{12}$$

Thus, the total density of the free energy of orthorhombic AFM is of the form

$$\begin{aligned} \omega = \frac{1}{2} A_0 M^2 + \frac{1}{2} B_0 L^2 + \frac{1}{2}\left(a_{10} M_x^2 + a_{20} M_y^2 + b_{10} L_x^2 + b_{20} L_y^2 \right) - k_B T \left[S(M_1) + S(M_2) \right] - \\ - \vec{M}\vec{H} + \frac{1}{2}\left[Z_{0ik} L_k^2 + \tilde{Z}_{0ik} M_k^2 \right] \sigma_i + \left[Z_{0\alpha}^{(e)} L^2 + Z_{0\alpha}^{(e)} M^2 \right] \sigma_\alpha + \frac{1}{2} \tilde{K}_{ik} \sigma_i \sigma_k - k_B T S(\sigma) \end{aligned} \tag{13}$$

The last term of (13) describes the entropy of the lattice including the stresses σ. Going over from magnetization M and the vector of antiferronmagnetism $\vec{L}$ of the unit volume to the magnetization $\vec{\mu} = \vec{\mu}_1 + \vec{\mu}_2$ and the vector of antiferromagnetism of the unit cell $\vec{l} = \vec{\mu}_1 - \vec{\mu}_2$ for the free energy of orthorhombic AFM per one gram/mole we obtain

$$\begin{aligned} \frac{F}{N_0} = \frac{1}{2} A\mu^2 + \frac{1}{2} B l^2 + \frac{1}{2}\left(a_1 \mu_x^2 + a_2 \mu_y^2 + b_1 l_x^2 + b_2 l_y^2 \right) - \vec{\mu}\vec{H} - \\ - k_B T \left[\mathbb{S}(\mu_1) + \mathbb{S}(\mu_2) \right] + \frac{1}{2}\left[Z_{ik} l_k^2 + \tilde{Z}_{ik} \mu_k^2 \right] \sigma_i + \frac{1}{2} v_0 \tilde{K}_{ik} \sigma_i \sigma_k - \\ - k_B T \mathbb{S}(\sigma) + \frac{1}{2}\left[Z_\alpha^{(e)} l^2 + Z_\alpha^{(e)} \mu^2 \right] \sigma_\alpha \end{aligned} \tag{14}$$

Here $A = \frac{A_0}{v_0}$, $B = B_0 v^{-1}$ etc., $Z_{ik} = Z_{0ik} v_0^{-1}$, $\mathbb{S}(\mu_1) = v_0 S(M_1)$, N_0 is Avogadro number. The values of unit cell magnetization are related to spins of ions as follows

$$\vec{\mu} = g\mu_B \left(\vec{S}_1 + \vec{S}_2 \right), \quad \vec{l} = g\mu_B \left(\vec{S}_1 - \vec{S}_2 \right) \tag{15}$$

where g is Lande splitting factor and μ_B is Bohr magneton.

The equilibrium values of strain, magnetization and the vector of ferromagnetism are found from the system of equations

$$u_i = \frac{\partial F}{\partial \sigma_i}; \quad \frac{\partial F}{\partial \mu_\alpha} = 0; \quad \frac{\partial F}{\partial l_\alpha} = 0 \tag{16}$$

Using the expression for the free energy of a magnetodielectric (14), we have the first equation of the system (16) in the form

$$u_i = v_0 \tilde{K}_{ik}\sigma_k - k_B T \frac{\partial \mathbb{S}(\sigma)}{\partial \sigma_i} + \frac{1}{2}\left[Z_{ik} l_k^2 + \tilde{Z}_{ik}\mu_k^2 \right] + \left[Z_\alpha^{(e)} l^2 + \tilde{Z}_\alpha^{(e)} \mu^2 \right]\delta_{i\alpha} \tag{17}$$

The second and the third equations in (16) define both the vectors of magnetization and ferromagnetism and their dependence on the stresses:

$$A\vec{\mu} + a_1\mu_x\vec{I}_x + a_2\mu_y\vec{I}_y - H + k_B T\left\{ B^{-1}\left(\frac{\mu_1}{\mu_0}\right)\frac{\vec{\mu}+\vec{l}}{2\mu_1\mu_0} + B^{-1}\left(\frac{\mu_2}{\mu_1}\right)\frac{\vec{\mu}-\vec{l}}{2\mu_2\mu_0}\right\} + \frac{1}{2}\tilde{Z}_{ik}\sigma_i\frac{\partial\mu_k^2}{\partial\vec{\mu}} + Z_\alpha^{(e)}\sigma_\alpha\vec{\mu} = 0; \tag{18}$$

$$B\vec{l} + b_1 l_x\vec{I}_x + b_2 l_y\vec{I}_y + k_B T\left\{ B^{-1}\left(\frac{\mu_1}{\mu_0}\right)\frac{\vec{\mu}+\vec{l}}{2\mu_1\mu_0} - B^{-1}\left(\frac{\mu_2}{\mu_1}\right)\frac{\vec{\mu}-\vec{l}}{2\mu_2\mu_0}\right\} + \frac{1}{2}Z_{ik}\sigma_i\frac{\partial l_k^2}{\partial l} + Z_\alpha^{(e)}\sigma_\alpha\vec{l} = 0 \tag{19}$$

Here $\vec{I}_x$, $\vec{I}_y$ are the unit vectors aligned with x,y-axis. The derivatives $\partial l_k^2 / \partial l_0$ are determined by the expressions

$$\begin{aligned} &\frac{\partial l_1^2}{\partial \vec{l}} = 2l_x\vec{I}_x; \quad \frac{\partial l_2^2}{\partial \vec{l}} = 2l_y\vec{I}_y; \quad \frac{\partial l_3^2}{\partial \vec{l}} = 2l_z\vec{I}_z; \quad \frac{\partial l_4^2}{\partial \vec{l}} = l_z\vec{I}_y + l_y\vec{I}_y; \\ &\frac{\partial l_5^2}{\partial \vec{l}} = l_z\vec{I}_z + l_z\vec{I}_z; \quad \frac{\partial l_6^2}{\partial \vec{l}} = l_y\vec{I}_x + l_x\vec{I}_y; \end{aligned} \tag{20}$$

The derivatives $\partial\mu_i / \partial\mu$ are found in the analogous way.

By the known tensor of the crystal strain, the magnetostriction value is easily found as a function of any direction in the crystal.

$$\frac{\delta a}{a} = \frac{|\vec{a}| - |\vec{a}_0|}{|\vec{a}|} = u_{\alpha\beta}\left(\vec{l},\vec{m}\right)n_\alpha n_\beta \tag{21}$$

where $\vec{a}_0$, $\vec{a}$ is a vector in the crystal prior to and after the magnetic ordering, respectively; $\vec{n} = \vec{a}_0 a_0^{-1}$ is the unit vector in $\vec{a}_0$ direction.

The most important and interesting case relates to magnetostriction in the absence of the external stresses $(\sigma_i = 0)$. For this case, expression (21) takes the form

$$\frac{\delta a}{a} = \frac{1}{2}\left\{ Z_{\alpha\beta\gamma\delta} l_\gamma l_\delta + \tilde{Z}_{\alpha\beta\gamma\delta} \mu_\gamma \mu_\delta + \left(Z_\alpha^{(e)} l^2 + \tilde{Z}_\alpha^{(e)} \mu^2 \right) \delta_{\alpha\beta} \right\} n_\alpha n_\beta \tag{22}$$

For instance, this formula describes the relative changes of the lattice parameters due to the magnetostriction. To determine the magnetostriction constants Z, $\tilde{Z}$, $Z^{(e)}$, $\tilde{Z}^{(e)}$, the magnetostriction along the ribs and diagonals of the parallelepiped should be known. The formulas are collected in Table 2.

The relative bulk magnetostriction is

$$\frac{\delta a}{a} = \left(\frac{\delta a}{a}\right)_{100} + \left(\frac{\delta a}{a}\right)_{010} + \left(\frac{\delta a}{a}\right)_{001} \tag{23}$$

Table 2.

n_α	$\delta a/a$
100	$\frac{1}{2}\left\{ Z_{xx\gamma\delta} l_\gamma l_\delta + Z_x^{(e)} l^2 + \tilde{Z}_{xx\gamma\delta} \mu_\gamma \mu_\delta + \tilde{Z}_x^{(e)} \mu^2 \right\}$
010	$\frac{1}{2}\left\{ Z_{yy\gamma\delta} l_\gamma l_\delta + Z_y^{(e)} l^2 + \tilde{Z}_{yy\gamma\delta} \mu_\gamma \mu_\delta + \tilde{Z}_y^{(e)} \mu^2 \right\}$
001	$\frac{1}{2}\left\{ Z_{zz\gamma\delta} l_\gamma l_\delta + Z_z^{(e)} l^2 + \tilde{Z}_{zz\gamma\delta} \mu_\gamma \mu_\delta + \tilde{Z}_z^{(e)} \mu^2 \right\}$
$\frac{1}{\sqrt{2}}$ $\frac{1}{\sqrt{2}}$ 0	$\frac{1}{2}\left\{ \left(\frac{\delta a}{a}\right)_{100} + \left(\frac{\delta a}{a}\right)_{010} \right\} + \frac{1}{2}\left\{ Z_{xy\gamma\delta} l_\gamma l_\delta + \tilde{Z}_{xy\gamma\delta} \mu_\gamma \mu_\delta \right\}$
$\frac{1}{\sqrt{2}}$ 0 $\frac{1}{\sqrt{2}}$	$\frac{1}{2}\left\{ \left(\frac{\delta a}{a}\right)_{100} + \left(\frac{\delta a}{a}\right)_{001} \right\} + \frac{1}{2}\left\{ Z_{xz\gamma\delta} l_\gamma l_\delta + \tilde{Z}_{xz\gamma\delta} \mu_\gamma \mu_\delta \right\}$
0 $\frac{1}{\sqrt{2}}$ $\frac{1}{\sqrt{2}}$	$\frac{1}{2}\left\{ \left(\frac{\delta a}{a}\right)_{010} + \left(\frac{\delta a}{a}\right)_{001} \right\} + \frac{1}{2}\left\{ Z_{yz\gamma\delta} l_\gamma l_\delta + \tilde{Z}_{yz\gamma\delta} \mu_\gamma \mu_\delta \right\}$
$\frac{1}{\sqrt{3}}$ $\frac{1}{\sqrt{3}}$ $\frac{1}{\sqrt{3}}$	$\frac{1}{3}\left\{ \left(\frac{\delta a}{a}\right)_{100} + \left(\frac{\delta a}{a}\right)_{010} + \left(\frac{\delta a}{a}\right)_{001} \right\} + \frac{1}{3}\left\{ \left(Z_{xy\gamma\delta} + Z_{yz\gamma\delta} + Z_{xz\gamma\delta} \right) l_\gamma l_\delta + \left(\tilde{Z}_{xy\gamma\delta} + \tilde{Z}_{yz\gamma\delta} + \tilde{Z}_{xz\gamma\delta} \right) \mu_\gamma \mu_\delta \right\}$

If an external stress σ is applied now to the sample, then, in linear approximation, the strains due to the external stresses and magnetostriction effect are added together.

The expression for the free energy (14) consists of many phenomenological constants characterizing the magnetic, magnetoelastic and elastic energies. However, these can be found only experimentally with arbitrary components of stress tensors, variations of the direction and the value of the external magnetic field and by the measurement of the strains of any directions and the components of $\vec{l}$, $\vec{\mu}$ vectors. In such experiments, the set of data will be much larger than the set of unknown parameters in (14). It will become possible to have experimental results andtocontrolthe validity ofthre experimental data and the theoretical statements.

$CuCl_2 \cdot 2H_2O$ and $CuCl_2 \cdot 2D_2O$ crystals are very brittle, so it is very difficult to study them experimentally. A question arises of finding another way to determine the parameters, which describe the free energy of the crystal. Thus, in [50], the components of the tensors of elastic-compliance moduli for the orthorhombic $CuCl_2 \cdot 2H_2O$ have been found by measuring the sound velocity in the crystal.

Another convenient external parameter that influences AFM properties,is hydrostatic pressure. It has been shown that the magnetic properties of $CuCl_2 \cdot 2H_2O$, i.e. Neel temperature, the field of sublattice magnetic moment flip-flop, frequencies depend on the pressure very strongly. The pressure dependences of the basic magnetic characteristics of the crystal, i.e. $T_N = T_N(P)$, $H_n = H_n(P)$, $\omega_r = \omega_r(P)$ and so on can be used to determine some combinations of magnetoelasticconstants for this dependence is conditioned by magnetoelastic interactions present in the crystal.

This effect can be traced better in the case of the hydrostatic pressure that is when the stress tensor can be represented as $\sigma_k = \left\{\frac{1}{3}P, \frac{1}{3}P, \frac{1}{3}P, 0, 0, 0\right\}$. At the given σ_k, the magnetostriction energy takes the form analogous to the expression for the magnetic energy (see (14)). Therefore, it is possible to describe the influence of the external pressure by a simple renormalization of the constants of the energy magnetic part

$$\frac{F_m}{N_0} = \frac{1}{2}\tilde{A}\mu^2 + \frac{1}{2}\tilde{B}l^2 + \frac{1}{2}\left(\tilde{a}_1\mu_x^2 + \tilde{a}_2\mu_y^2 + \tilde{b}_1 l_x^2 + \tilde{b}_2 l_y^2\right) - \vec{\mu}\vec{H} + k_B T\left[\mathbb{S}(\mu_1) + \mathbb{S}(\mu_2)\right] \quad (24)$$

Here

$$\begin{aligned}
\tilde{A} &= A+\frac{1}{3}P\sum_{\alpha=1}^{3}\left(\tilde{Z}_{\alpha}^{(e)}+\tilde{Z}_{\alpha 3}\right)\equiv A+\frac{1}{3}P\tilde{L}^{(e)}\\
\tilde{B} &= B+\frac{1}{3}P\sum_{\alpha=1}^{3}\left(\tilde{Z}_{\alpha}^{(e)}+\tilde{Z}_{\alpha 3}\right)\equiv B+\frac{1}{3}P\tilde{L}^{(e)}\\
\tilde{a}_1 &= a_1+\frac{1}{3}P\sum_{\alpha=1}^{3}\left(\tilde{Z}_{\alpha 1}-\tilde{Z}_{\alpha 3}\right)\equiv a_1+\frac{1}{3}P\tilde{L}_1\\
\tilde{a}_2 &= a_2+\frac{1}{3}P\sum_{\alpha=1}^{3}\left(\tilde{Z}_{\alpha 2}-\tilde{Z}_{\alpha 3}\right)\equiv a_2+\frac{1}{3}P\tilde{L}_2\\
\tilde{b}_1 &= b_1+\frac{1}{3}P\sum_{\alpha=1}^{3}\left(\tilde{Z}_{\alpha 1}-\tilde{Z}_{\alpha 3}\right)\equiv b_1+\frac{1}{3}P\tilde{L}_1\\
\tilde{b}_2 &= b_2+\frac{1}{3}P\sum_{\alpha=1}^{3}\left(\tilde{Z}_{\alpha 2}-\tilde{Z}_{\alpha 3}\right)\equiv b_2+\frac{1}{3}P\tilde{L}_2
\end{aligned} \tag{25}$$

In such a way, the external hydrostatic pressure results in the renormalization of exchange and anisotropy constant, the combination of which affects such parameters as Neel temperature, the field of the sublattice magnetic moment flip-flop, the resonance frequency? The temperature of the triple point of the phase (H-T) diagram, etc. The above-mentioned parameters are pressure-dependent and the combinations of magnetostriction constants can be determined from the experimental pressure dependences. The expressions relating the parameters with the anisotropy and the exchange constants are of the form [129]:

$$T_N=\frac{2\mu_B^2}{k_B}\left|\tilde{B}\right| \tag{26}$$

$$T_3=T_N-\frac{3\mu_B^2}{k_B}\tilde{b}_2 \tag{27}$$

$$H_n^2=\mu_B^2\tilde{b}_2\left(\tilde{A}-\tilde{B}-b_2\right)\left(\frac{\mu(T)}{\mu_B}\right)^2 \tag{28}$$

Here the fact that for $CuCl_2{\cdot}2H_2O$ and $CuCl_2{\cdot}2D_2O$ the copper ion spin $s=1/2$ has been taken into account and g-factor can be considered to be equal to 2. $\mu(T)$ is the magnetization of the sublattice at the temperature T. The

field corresponding to the triple point is found from the relation $H_3 = H_n(T_3)$. The calculations of the resonance fields and angles of the resonance field separation as the functions of the frequency gave the following expressions:

$$H_r^2(\nu) = H_n^2 - \left(\frac{h\nu}{2\mu_B}\right)^2 \left(\frac{r+3}{r-1}\right) \tag{29}$$

$$\sin\psi_f(\nu) = \frac{(h\nu)^2}{(2\mu_B H_n)^2} A(r) \tag{30}$$

where $r = \tilde{b}_1\tilde{b}_2^{-1}$ and *v* is the frequency. The value $A(r)$ has the form

$$A(r) = \frac{1}{2}\left[(r+1)\left(1+b^2\right)^{1/2} + 2b\right](r-1)^{-1}\left(1+b^2\right)^{-1} \tag{31}$$

and the parameter b from this expression is equal to

$$b = (2q)^{-1}\left\{\sqrt{(q+3)^2 + 4q} - (q+3)\right\}, \qquad q = \left(\frac{r+1}{2}\right)^2 - 1.$$

By differentiating formulas (26)-(28), we have

$$L^{(e)} = \frac{3k_B}{2\mu_B{}^2}\frac{dT}{dP} \tag{32}$$

$$2L^{(e)} - 3L_2 = \frac{3k_B}{\mu_B^2}\frac{dT_3}{dP} \tag{33}$$

$$\frac{\tilde{L}^{(e)} - L^{(e)}}{A-B} + L_2\left(\frac{1}{b_2} - \frac{1}{A-B}\right) = \frac{6}{H_n}\frac{dH_n}{dP} \tag{34}$$

With formulas (32)-(34) and the known experimental dT_N/dP, dT_3/dP dH_n/dP values, we find the combinations of magnetoelastic constants denoted by $\tilde{L}^{(e)}$, $L^{(e)}$, L_2. Formulas (29), (31) are used for writing down an expression for insufficient combination of magnetoelastic constants

$$L_1 - r_0 L_2 = 3b_2 \frac{(r_0 - 1)^2}{2}\left(\frac{\gamma}{\nu}\right)^2 \left[H_r' H_r - H_n' H_n\right] = \\ = \frac{3b_2}{A'(r_0)}\left\{\left(\frac{rH_n}{\nu}\right)^2 \psi_f' \cos\psi_f + \frac{2H_n'}{H_n} A(r_0)\right\} \tag{35}$$

Here $r_0 = b_1 b_2^{-1},\ H_r' = dH_r/dP,\ H_n' = dH_n/dP,\ \gamma = 2\mu_B/h,\ \psi_f' = d\psi_f/dP,\ A(r_0) = \left(dA(r)/dr\right)_{r=r_0}$

It should be noted hat the account of the quadratic terms with respect to pressure would have been an excessive accuracy. This is because we do not take into account the quadratic terms with respect to the stress tensor into account in the expression for the magnetoelastic energy and in (25), consequently.

Experimental investigations of $CuCl_2 \cdot 2H_2O$ and $CuCl_2 \cdot 2D_2O$ properties done under pressure have made it possible to determine typical parameters and to calculate combinations of magnetoelastic constants by (32)-(35).

The pressure dependences of Neel temperature, field of the spin-flop transition were studied by NMR[7], EPR and resonance absorption methods [64, 65, 84]. Now, we calculate magentostriction constants for two data sets. Such values as dT/dP, H_r, dH_r/dp have been determined by only one method: the former parameter was treated by NMR and the latter ones used the resonance method, respectively.

First we give the results of calculation of magnetoelastic constants by resonance absorption method. Table 3 lists the basic parameters to be used in calculations.

For $CuCl_2 \cdot 2H_2O$, the values of resonance and transition fields were taken for the temperature of 1.68 K and the frequency $\nu = 3GHz$. For the deuterated crystal, H_r and H_t have been determined for T=1.74K and $\nu = 2.206\ GHz$. The values of the derivative with respect to pressure of the triple point were taken from [71, 130].

Using (32), (33) for the aqueous crystal, we have $L^{(e)} = 4.45 \cdot 10^{23}\ Oe^2/erg\ .kbar$, $L_2 = 0.51 \cdot 10^{23}\ Oe^2/erg\ .kbar$ For $CuCl_2 \cdot 2D_2O$, these parameters are $L^{(e)} = 4.33 \cdot 10^{23}\ Oe^2/erg\ .kbar$, $L_2 = 0.42 \cdot 10^{23}\ Oe^2/erg\ .kbar$. The decrease of the

Table 3.

AFM	$\frac{dT_N}{dP}, \frac{K}{kbar}$	$H_n,\ kOe$	$\frac{dH_n}{dP}, \frac{kOe}{kbar}$	H_r, kOe	$\frac{dH_r}{dP}, \frac{kOe}{kbar}$	$\frac{dT_3}{dP}, \frac{K}{kbar}$
$CuCl_2 \cdot 2H_2O$	0.185	6.7	0.147	6.48	0.152	0.153
$CuCl_2 \cdot 2D_2O$	0.18	6.62	0.14	6.52	0.143	0.154

value of $L^{(e)}$ for the deuterated crystal is because its dT_N/dP value is lower than that for $CuCl_2 \cdot 2H_2O$. The increase of L_2 in $CuCl_2 \cdot 2D_2O$ is because dT_3/dP is higher than in the aqueous crystal.

For getting the totality of the magnetoelastic constants, the values of AFM constants (A,B) and b_2 should be known. They are found from (4) and the parameters of the uniform part of AFM Hamiltonian. From (34), it follows for $CuCl_2 \cdot 2H_2O$ $\tilde{L}^{(e)} = -2.8 \cdot 10^{25}\ Oe^2/erg \cdot kbar$, and for $CuCl_2 \cdot 2D_2O$ $\tilde{L}^{(e)} = -2.3 \cdot 10^{25}\ Oe^2/erg \cdot kbar$. The decrease of the amount of the magnetoelastic constants for the deuterated sample is due to the lower (A-B) and b_2 (because of the unit cell tension under deuteration) and lower H_r and H_t and their derivatives with respect to pressure, as compared to those for the aqueous crystal.

When calculating the latter set of magnetostriction constants L_1, we considered that r_0=3 to be the same for the both samples. For $CuCl_2 \cdot 2H_2O$, we find by (35) $L_1 = 1.53 \cdot 10^{23}\ Oe^2/erg \cdot kbar$ and for $CuCl_2 \cdot 2D_2O$ $L_1 = 1.27 \cdot 10^{23}\ Oe^2/erg \cdot kbar$.

Now let us to calculate the same values using the data of Table 4 based on NMR [71].

The values of all the fields are for T=2 K, the value of the resonance field and dH_r/dP are taken for $CuCl_2 \cdot 2H_2O$ at 3 GHz frequency [121], those for $CuCl_2 \cdot 2D_2O$ [65] for $\nu = 2.206\ GHz$. As a result, we have the following values for the amount of magnetostriction constants (Table 5).

While comparing the values of magnetically ordered constants calculated with two data sets, it can be concluded that in the both cases, the magnetoelastic constants for the deuterated crystal are lower than those for the aqueous one.

Table 4.

AFM	$\frac{dT_N}{dP}, \frac{K}{kbar}$	$H_n,\ kOe$	$\frac{dH_n}{dP}, \frac{kOe}{kbar}$	H_r, kOe	$\frac{dH_r}{dP}, \frac{kOe}{kbar}$	$\frac{dT_3}{dP}, \frac{K}{kbar}$
$CuCl_2 \cdot 2H_2O$	0.18	6.78	0.142	6.64	0.143	0.153
$CuCl_2 \cdot 2D_2O$	0.172	6.67	0.138	6.53	0.14	0.154

Table 5.

AFM	$L^{(e)}$	$\tilde{L}^{(e)}$	L_1	L_2
	$Oe^2 \cdot erg^{-1} \cdot kbar^{-1}$			
$CuCl_2 \cdot 2H_2O$	$4.34 \cdot 10^{23}$	$-2.36 \cdot 10^{25}$	$1.28 \cdot 10^{23}$	$0.43 \cdot 10^{23}$
$CuCl_2 \cdot 2D_2O$	$4.15 \cdot 10^{23}$	$-1.54 \cdot 10^{25}$	$0.86 \cdot 10^{23}$	$0.29 \cdot 10^{23}$

Conclusions

The magnetostriction constants are rather important characteristics of magnet-containing systems. The results of investigations of hydrostatic pressure effect on high-frequency magnetic properties, PT parameters enable us to show their correlation with the magnetic field effect through magnetic elasticity.

With the correlation between strain and stress parameters under the loading with hydrostatic pressure taken into account, the theory embraces the whole of interactions in magnet-containing structures. The expression for the density of magnetic energy per gram/mole includes all types of the interactions, e.g. binding energy present in the single crystal.

In the expression for the free energy, there is a large number of phenomenological constants that characterize magnetic, magnetoelastic and elastic energies. Hydrostatic pressure is the most successful parameter that influences the energies through elastic stresses. Our investigations have shown the role of uniform compression effect in the regularity of structural phase transition critical line and its influence on the high-frequency properties. As a result, we have combinations and estimates of magnetoelastic constants that define the influence of interactions of the magnetoelastic stresses.

The analysis of magnetoelastic properties is supplemented by investigations of elastic properties of hydrated crystals. The estimation of compressibility factors aids if establishing the relationship between elastic stresses and deformation of the structure to be used in the expression for the interaction energies. Complex investigations reveal the nature of elasticity mechanisms participating in formation of the first-order phase transitions in magnet-containing structures studied.

Chapter 7

Lows of bulk elasticity in the formation of PT and properties in magnetic semiconductors and dielectrics

7.1. Linear regularities of elasticity in resistivity properties in the processes of P-H-T effect in $La_{0.7}Mn_{1.3}O_3$

Rare-earth manganites are attracting a heightened interest because of the colossal magnetoresistive (CMR) effect [131-133] observed in these perovskite like metal oxides when doped with divalent ions: $R_{1-x}Me_x^{2+}Mn_{1-x}^{3+}Mn_x^{4+}O_3^{2-}$ (R is La^{3+}, Pr^{3+}, Nd^{3+}, or Sm^{3+}; Me^{2+} is Ca^{2+}, Sr^{2+}, Ba^{2+}, or Pb^{2+}). In spite of a large number of papers, including review articles [134, 135], the nature of the unusual coupling of the electric and magnetic properties in these materials remains in dispute.

Elucidation of the nature of the CMR effect and the development of new magnetoresistive materials based on rare-earth manganites are topical problems in science and technology. To help solve them it is useful to investigate the influence of temperature, magnetic field, and especially high hydrostatic pressures, about which little information is available [136].

The present study is devoted to a comprehensive investigation of the influence of temperature, magnetic field, and high hydrostatic pressure over wide ranges on the resistivity and magnetoresistive effect (MRE) for a ceramic sample and a single-crystal laser film of the same cationic compound $La_{0.7}Mn_{0.3}O_{3\pm\delta}$.

The ceramic samples of manganite-lanthanum oxides of the series $La_{1-x}Mn_{1+x}O_{3\pm\delta}$ [136a] with x = 0.3 were obtained by a synthesizing anneal of a mixture of ChDA-grade powders of La_2O_3 *(Ia3, a* = 11.498 Å) and Mn_3O_4 *(I*4_1*/amd, a* = 5.77 Å, c = 9.38 Å) at 900 °C (20 h) and sintering the pressings at 1150 °C for 24 h, followed by a slow cooling.

The single-crystal films were deposited by laser sputtering at 800 °C on a $LaSrGaO_4$ single-crystal substrate. For saturation of the film with oxygen it was subjected to additional annealing at 780 °C.

The phase composition and crystal lattice parameters were determined by x-ray diffraction in Cu radiation on a DRON-2 diffractometer.

The resistance *R* and the value of the magnetoresistive effect $\Delta R/R_0 = (R_0 - R_H)/R_0$ were determined by a four-probe method over a wide range of temperatures 77-350 K at several different values of the magnetic field (*H* = 0, 2, 4, 6, and 8 kOe). High hydrostatic pressures *P* were obtained in a special two-layer chamber[20] made of nonmagnetic 40Kh-NYu refined steel, with a channel diameter of 6.5 mm and an outer diameter of 31 mm. The pressure was

determined from the load on the press and was monitored by measuring the resistance of a manganese pressure sensor. The errors of measurement of the quantities mentioned were within the following limits: phase composition — 3%, lattice parameters — 1%; resistivity — 0.7%, temperature — 0.1%, magnetic field – 1.5%, hydrostatic pressure – 3%.

According to the x-ray data, the ceramic targets had a rhombically distorted *(Pnma)* lanthanum manganite perovskite structure with the parameters a = 5.464 Å, b = *5.515* Å, c = 7.728 Å. The Curie temperature of the sample was T_c = 255 K.

The temperature dependence of the resistivity of the ceramics and laser-deposited film is shown in Fig. 7.1 for H =0 and 8 kOe and P = 0 and 1.8 GPa. One notices substantial differences not only in the value of pressure but also in the character of its temperature dependence for the ceramics and film. The higher values of the resistivity of the ceramic samples arc possibly due to their porosity and the different degree of nonstoichiometry.

For the ceramic sample, but not for the film, there is an additional smaller, smeared peak (T'_{ms} =210 K) at temperatures below the main resistivity peak (T_{ms} = 250 K), which, like the main peak, decreases markedly with increasing pressure, i.e., the used ceramics have two metal-semiconductor transitions. The main transition, depending on the magnetic field and pressure, lies in the interval from T_{ms} = 235 K *(H = 0, P = 0)* to T_{ms} = *215* K (H=8 kOe, P = 1.8 GPa). The second transition lies between T'_{ms} = *200* K *(H = 0,* P = 0)

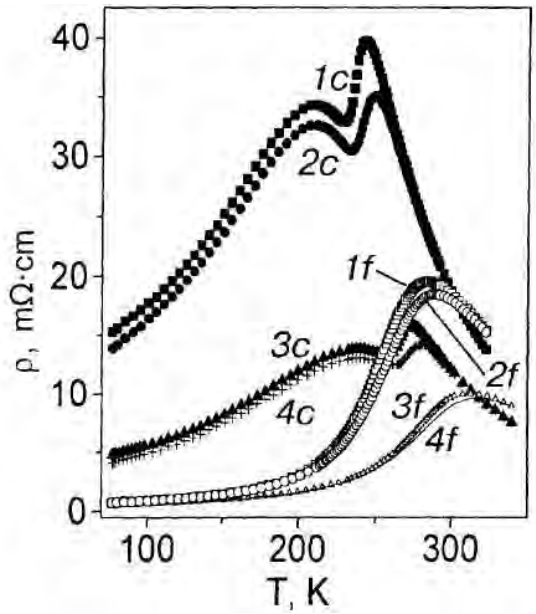

Figure 7.1. Temperature dependence of the resistivity of a ceramic sample (*c*) and a single-crystal film (*f*) of $La_{0.7}Mn_{0.3}O_{3\pm\delta}$ for various pressures and magnetic fields: *1c, 1f — P = 0, H = 0; 2c, 2f — P = 0, H= 8* kOe*; 3c; 3f — P = 1.8* GPa, *H = 0; 4c, 4f — P = 1.8* GPa, *H = 8* kOe.

and T'_{ms} = 235 K (H = 8 kOe, P= 1.8 GPa). The two resistive transitions in the ceramic samle are apparently due to the intercrystallite zones, to the mesoscopic structural and magnetic [137] inhomogeneities, the nature of which is in dispute and is now being clarified. One notices that the temperature of the main resistivity peak for the ceramics (T_{ms} = 235-275 K) is substantially lower than for the film (T_{ms} = 275-300 K). This may be due to the different oxygen content and nonstoichiometry of the ceramic and film samples, or to the difference in the characteristic dimensions of the crystallites of the ceramic ($D \approx 10$ μm) and the thickness of the single-crystal film (d ≈ 1 μm) and also to the influence of the substrate. These factors may be the cause of the different influence of high hydrostatic pressures (P = 1.8 GPa) on the resistivity and value of the MRE in the ceramics and film.

The temperature dependence of the magnetoresistive effect $\Delta R/R_0$ at P = 0 and various values of the magnetic field (H = 2, 4, 6, and 8 kOe) for the ceramic and film samples is shown in Fig. 7.2. One notices first the large values of the MRE in the ceramics and the less smeared $\Delta R/R_0$ peak in comparison with the film. Here the temperature of the peak of the MRE is

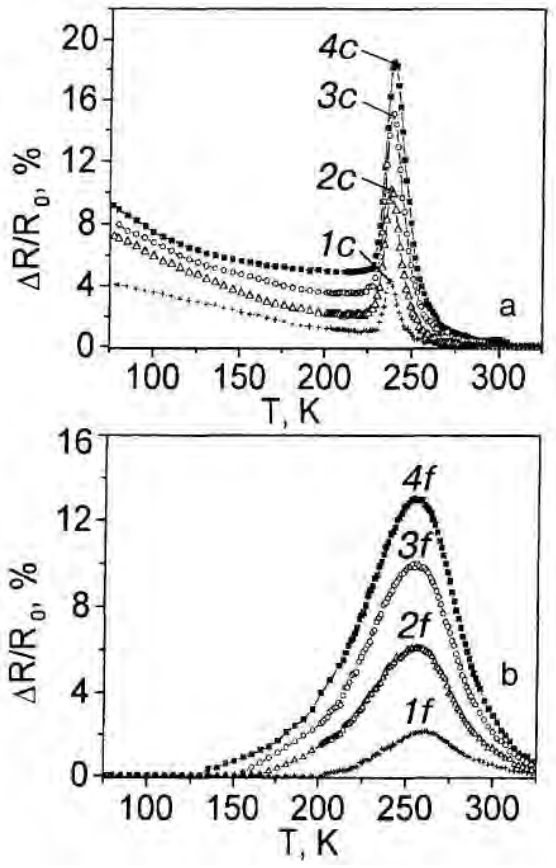

Figure 7.2. Temperature dependence of the magnetoresistive effect at P = 0 and various magnetic fields for the ceramics (a) and film (b): *1c, 1f*— H = 2 kOe; *2c, 2f*— H = 4 kOe; *3c, 3f*— H = 6 kOe; *4c, 4f*— H = 8 kOe.

lower in the ceramics (T_p = 237 K) than for the film (T_p = 257 K). As the magnetic field is increased from 2 to 8 kOe for the ceramic target, the MRE increases from 4 to 18.5%, i.e., by a factor of 4.6, while for the single-crystal film it increases from 2 to 13%, i.e., by a factor of 6.5.

The influence of the magnetic field strength on the MRE at P= 1.8 GPa for the ceramics and film is shown in Fig. 7.3. At high hydrostatic pressures the value of the MRE decreases and the temperature of its peak increases. $\Delta R/R_0$ increases with increasing H from 2 to 8 kOe: for the ceramics from 3.8 to 16%, i.e., a factor of 4.2, and for the film from 1.8 to 9.8%, i.e., a factor of 5.4. In spite of the lower MRE in the film, it is influenced by the magnetic field to a greater degree.

Fig. 7.4 shows the effect of high hydrostatic pressures on the resistivity of the ceramics and film at *H=0.* As the pressure is increased to 2.2 GPa the resistivity decreases: by a factor of 1.75 for the ceramics and 2.5 for the film. It appears as if the resistivities of the ceramics and film should converge somewhere in the region of negative hydrostatic pressures.

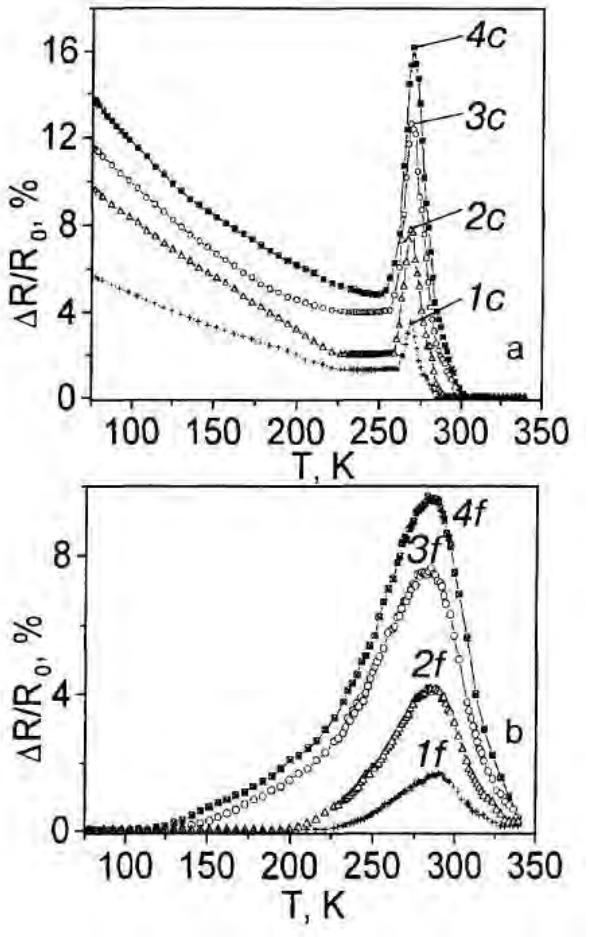

Figure 7.3. Temperature dependence of the magnetoresistive effect at P = 1.8 GPa and various magnetic fields for the ceramics (a) and film (b): *1c, 1f*— H = 2 kOe; *2c, 2f*— H = 4 kOe; *3c,3f*— H = 6 kOe; *4c,4f*— H = 8 kOe.

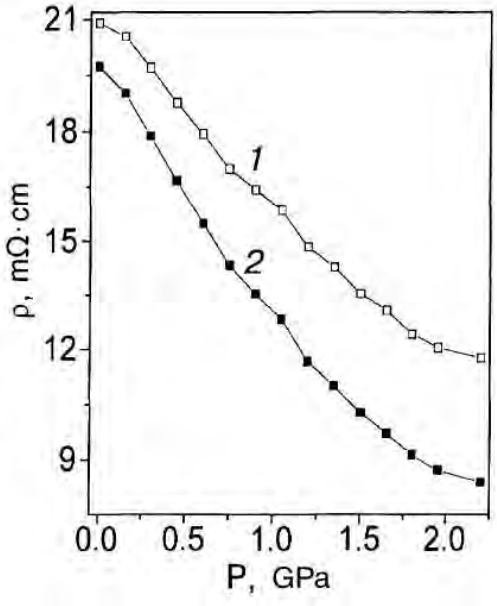

Figure 7.4. Effect of high hydrostatic pressures on the resistivity of the ceramic (1) and film (2) at $H = 0$.

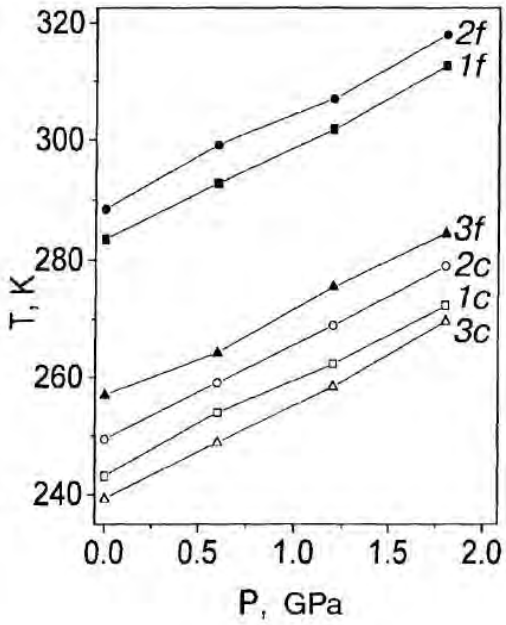

Figure 7.5. Effect of high hydrostatic pressures on the metal-semiconductor phase transition temperature T_{ms} at $H = 0$ and 8 kOe and the peak temperature T_p of the MRE for the ceramics (c) and film (*f*): *1c,lf* — T_{ms}, $H = 0$; *2c,2f*— T_{ms}, H=8 kOe; *3c,3f*— T_p, H=8 kOe.

The effect of high hydrostatic pressures on the metal-semiconductor transition temperature T_{ms} at $H=0$ and 8 kOe and the temperature of the magnetoresistance peak T_p for the ceramic target (the unfilled symbols) and the single-crystal film (filled symbols) is illustrated in Fig. 7.5. With increasing *P*

the temperatures T_{ms} and T_p increases practically linearly in the entire pressure interval investigated, and their temperature coefficients are close in value. The reason is apparently the decrease in the inter-ion distances and the change in the exchange interaction, which shifts the region of the “metallic” state to higher temperatures.

Comprehensive studies of the influence of temperature, magnetic field, and high hydrostatic pressures on the resistivity and magnetoresistive effect of ceramic and film samples of the lanthanum manganite perovskites $La_{0.7}Mn_{0.3}O_{3\pm\delta}$ have established the following:

1) the resistivity of the ceramic target is higher than that of the laser film;
2) the temperature of the metal-semiconductor transition is substantially higher for the film;
3) for the ceramic samples two temperature peaks of the resistivity are observed, which are explained by a cluster type of mesoscopic inhomogeneity;
4) for the ceramics the MRE is larger and its peak temperature is lower than for the film, on account of the different nonstoichiometry;
5) with increasing magnetic field the MRE increases in both the ceramics and film, the effect being stronger in the film;
6) high hydrostatic pressures decrease the resistivity and increases the temperatures of the metal-semi conductor transition and of the peak of the MRE.

7.2. Baro- and magnetoresistive effects in properties of $La_{0.9}Mn_{1.1}O_3$ and $La_{0.56}Ca_{0.24}Mn_{1.2}O_3$

In spite of a large number of publications, the nature of a unique interrelation between magnetic and electric properties in manganites remains debatable [135, 138]. Recently, the works with an unconventional approach to rare-earth materials investigations, in which changes of conductivity as a result of changes in temperature, magnetic field and hydrostatic pressure were observed, have increased in number [139-141]. A variety of investigations in the resistive properties under influence of temperature, pressure and magnetic field [30-32, 142] reveals some new effects.

The main goal of the present work is to establish the correlation between elastic, resistive and magnetoelastic properties and explanation of effects in magnetic semiconductors influenced by temperature, magnetic field and pressure.

$La_{0.9}Mn_{1.1}O_3$ and $La_{0.56}Ca_{0.24}Mn_{1.2}O_3$ bulk and film samples were obtained by standard methods [143]. Pressure was generated by a technique described in Ref. [19].

Investigations of the resistivity of the materials influenced by temperature, magnetic field and pressure are illustrated in Fig. 7.6a and 7.6b(l —6),

Fig. 7.8(1-6), where the temperature dependence of resistivity (thermoresistivity)—curve (1); is shown under different magnetic field intensities (thermo-magnetoresistivity) (2) and hydrostatic pressures (thermobaroresistivity) (3-5). Resistivity behavior in magnetic field at fixed pressures (thermo-baromagnetoresistivity) in the whole of the temperature range is demonstrated in Fig. 7.6a and 7.6b(6), Fig. 7.8(6). In all the dependences, the “metal-semiconductor” transition temperature shifts, as a result of the application of pressure and magnetic field.

Temperature dependences of the magnetoresis-tive effect $(\rho_0 - \rho_H)/\rho_0$, (H = 8 kOe) are presented in Fig. 7.7a and 7.7b(6), Fig. 7.9(6); baroresistive effect $(\rho_0 - \rho_P)/\rho_0$ under different hydrostatic pressures in Fig. 2a and b(2,3,5),

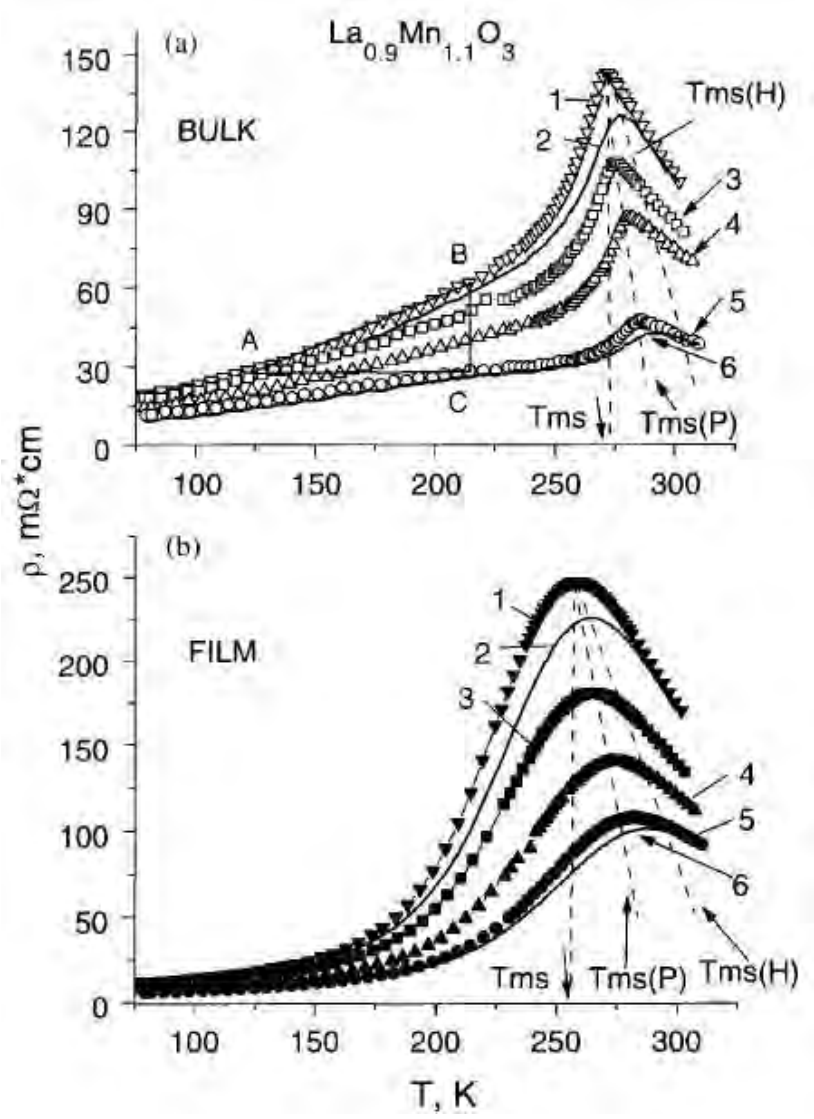

Figure 7.6. Temperature dependences of $La_{0.9}Mn_{1.1}O_3$ bulk (a) and film (b) samples resistivity: 1—P = 0 kbar; 2—P = 0, H = 8kOe; 3—P = 6 kbar; 4—P= 12 kbar; 5—P= 18 kbar; 6—P = 18 kbar, H = 8 kOe.

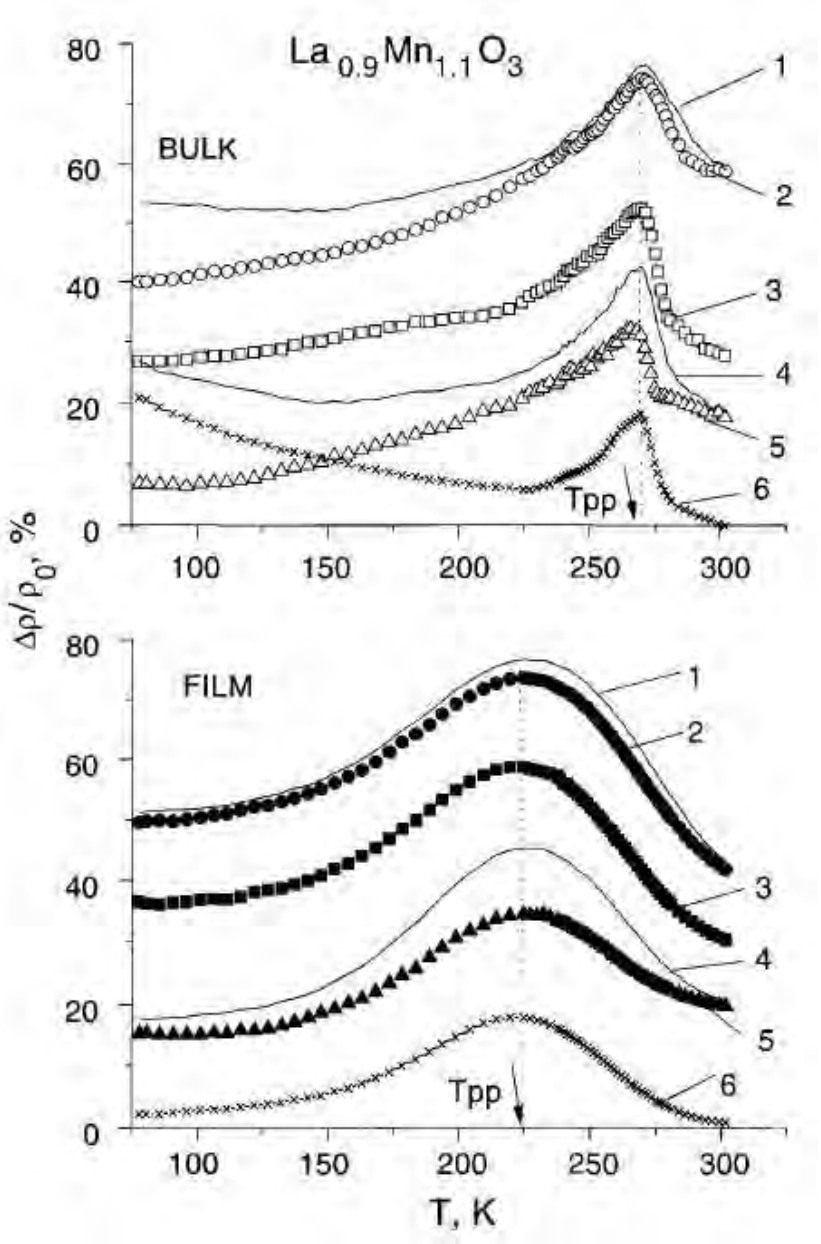

Figure 7.7. Temperature dependences of $La_{0.9}Mn_{1.1}O_3$ bulk (a) and film (b) samples baroresistive effect: 2 - P = 18 kbar; 3 - P= 12 kbar; 5 - P = 6 kbar; Baromagnetoresistive effect: 1 - P = 18 kbar, H = 8 kOe; 4 - P = 6 kbar, H = 8 kOe; Magnetoresistive effect: 6 - P = 0, H = 8 kOe.

Fig. 4(2,3,5); baromagnetoresistive effect $(\rho_0 - \rho_{PH})/\rho_0$ at different magnetic field intensities and hydrostatic pressures - in Fig. 7.7a and 7.7b(l,4), Fig. 7.9(1,4).

Here ρ_0 is the resistivity of the sample;
ρ_H is the resistivity in magnetic field;
ρ_P is the resistivity at hydrostatic pressure;
ρ_{PH} is the resistivity in magnetic field at a fixed applied pressure.

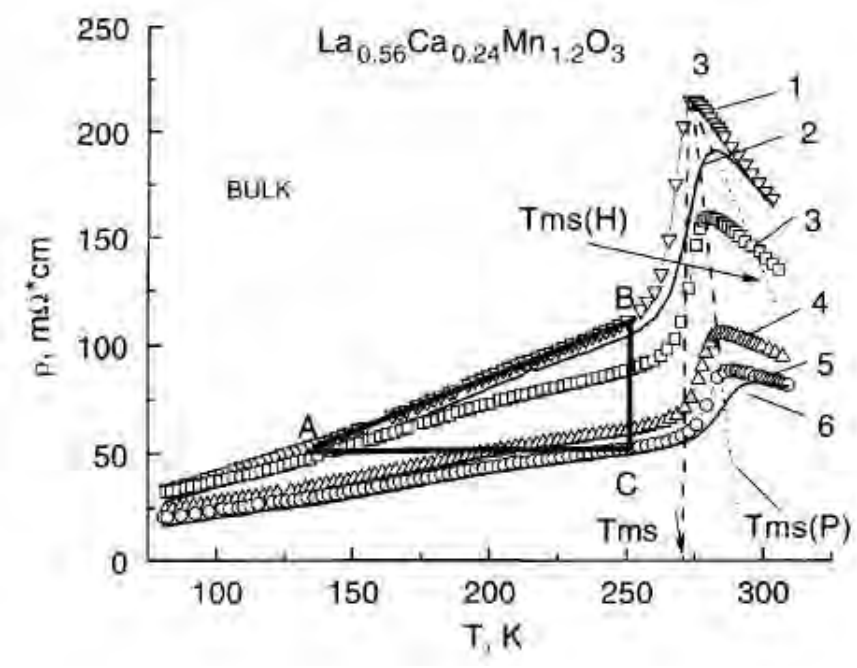

Figure 7.8. Temperature dependences of $La_{0.56}Ca_{0.24}Mn_{1.2}O_3$ bulk sample resistivity: 1—*P* = 0 kbar; 2—*P* = 0, *H* = 8 kOe; 3— *P* = 6 kbar; *4*—*P*= 12 kbar; *5*—*P* = 18 kbar; 6—*P* = 18kbar, *H* = 8 kOe.

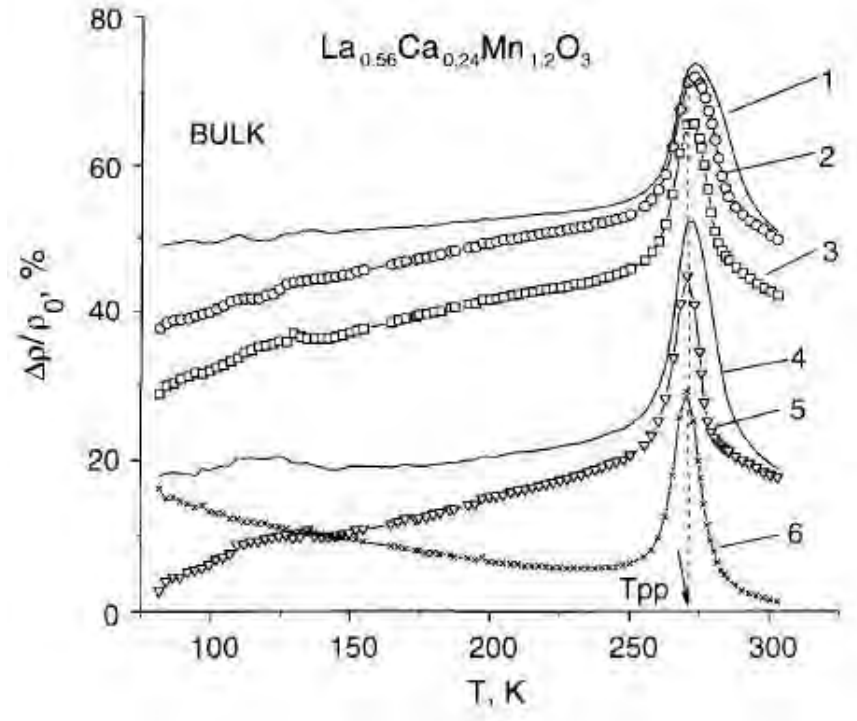

Figure 7.9. Temperature dependences of $La_{0.56}Ca_{0.24}Mn_{1.2}O_3$ bulk samples resistivity: 2—*P*=18 kbar; 3—*P*= 12 kbar; 5— *P* = 6 kbar. Baromagnetoresistive effect: 1—*P* = 18kbar, *H* = 8 kOe; 4—*P* = 6 kbar, *H* = 8 kOe. Magnetoresistive effect: 6—*P* = 0, *H* = *8* kOe.

Investigation of electronic properties of bulk and film samples $La_{0.9}Mn_{1.1}O_3$, $La_{0.56}Ca_{0.24}Mn_{1.2}O_3$ as a result of magnetic field H — 0-8 kOe and hydrostatic pressure P = 0-18 kbar are presented in this paper. These results were partly published previously [142]. It is necessary to mark that the resistive properties are the most sensitive to any structure changes.

1. Special attention is paid to studying the resistivity properties of the samples under magnetic field and pressure influences. The illustrated data shown in Fig. 7.6a and 7.6b, Fig. 7.8 thermoresistive (1), thermomagnetoresistive (2,6), thermobaroresistive (3,4) and thermobaromagnetoresistive (5) behaviours are identical in the whole temperature range. In all dependences resistivity peak temperature (T_{ms}) monotonously shifts as a function of pressure and magnetic field, at the same time peak intensity is reducing. Thus, the identity of magnetic field and pressure effect on resistivity is traced. Note that in Fig. 7.6a and 7.6b(2), Fig. 7.8(2) resistivity behaviors at H = 0; 8 kOe are illustrated, but in H = 2, 4, 6 kOe the regularity is preserved [142]. Connected resistivity peaks in Fig. 7.6a and 7.6b(l,2), Fig. 7.8(1,2) illustrated a regularity of magnetic field effect on $T_{ms}(H)$ shifting. This regularity is linear. The same features were noted in works [30, 142]. Analogously, the $T_{ms}(P)$ dependence will be plotted with shifting the resistivity peak temperature under hydrostatic pressure; the regularity is linear (Fig. 7.6a and 7.6b(l,3-5) and Fig. 7.8(1,3-5)). These experimental data are presented in Refs. [30, 142, 144].
2. The magnetoresistive effect is well studied in a large variety of magnetic semiconductor samples. An interesting regularity of magnetoresistive peak temperature (T_P) constancy under different magnetic field intensities, Fig. 7.7a and 7.7b(6), Fig. 7.9(6), was observed. It is noted that peak temperatures (T_{PP}) of baroresistive, Fig. 7.7a and 7.7b(l,3,4), Fig. 7.9(1,3,4), and baromagnetoresistive Fig. 7.7a and 7.7b(2,5), Fig. 7.9(2,5) effects are the same and coincide with magnetoresistive peak temperature, Fig. 7.7a and 77.7b(6), Fig. 7.9(6). In bulk samples $La_{0.9}Mn_{1.1}O_3$and $La_{0.56}Ca_{0.24}Mn_{1.2}O_3$ temperature, T_{PP} coincides with the “metal-semiconductor” transition temperature T_{ms} without any influences of magnetic field and pressure. Taking the above results into account, these regularities allow us to conclude that mechanism of hydrostatic pressure and magnetic field effect on resistive properties and phase states of magnetic semiconductors is identical. Realization of these mechanisms is conditioned by elastic, thermoelastic and magnetoelastic properties of the material.
3. On thermoresistive, thermomagnetoresistive and thermobaroresistive dependences one observes a linear area of resisitivity close to 225 K, Fig. 7.6a(l-5), Fig. 7.8(1-5), and a reduction of slope angle with increasing pressure and magnetic field.

This observation makes it possible to carry out some estimations. Resistivity increment $\Delta\rho$ per 1K amounts to $\Delta\rho/\Delta T = 0.37\Omega$/deg, Fig. 7.6a (l). Resistivity change vs. pressure increase at fixed temperature, T≈225K, amounts to $\Delta\rho/\Delta P \approx 2.29$ Ω/kbar. It may be seen from triangle ABC Fig. 7.6a (l,5). These estimations show that in the linear resistivity area temperature changes by δT = 6.2 K at the expense of thermoelastic expansion changes the resistivity in the same way as the elastic deforming compression by hydrostatic pressure of 1 kbar. The same correspondence underlines the role of elastic properties in formation of resistivity behavior.

4. The character of the observed thermoresistive, thermomagnetoresistive and thermobaroresistive dependences Fig. 7.6a and 7.6b (l-5), Fig. 7.8 (1-5) is analogous. It allows one to estimate action of pressure and magnetic field in the linear resistivity area and in the area of resistivity peaks. From curves of Fig. 7.6a (l,2) it is seen that magnetic field intensity (H = 1 kOe) action corresponds to resistivity change $\Delta\rho/\Delta H$ = 2.2Ω/kOe. Resistivity change under pressure, in this temperature range, amounts to $\Delta\rho/\Delta P$ = 6 Ω/kbar. It shows that the magnetic field intensity increase by δH = 2.7 kOe brings the same resistivity change as in the case of hydrostatic pressure increase by 1 kbar. The compressive mechanism of magnetic field action is also evidenced by phase transition temperature shifting, which is commensurate with hydrostatic pressure effect.

   From this point of view, a giant magnetoresistive effect is a result of the sudden change in resistivity due to magnetoelastic compression mechanism caused by magnetic field effect.

   To confirm a role of elastic properties, we may consider dependencies of the resistivity peak temperature $T_{ms}(H)$, $T_{ms}(P)$ and also a linear dependence of resistivity vs. pressure at T = 300 K Fig. 7.6a(l-6). They are linear in all the investigated magnetic field and pressure range. The same features are pointed in Refs. [30, 142, 144]. We pay attention to the fact that the curves $T_{ms}(PH)$, at simultaneous action of magnetic field and hydrostatic pressure, are placed between T_{mi},(H) and $T_{ms}(P)$. Linear behavior and difference in temperature dependencies $T_{ms}(H)$ and $T_{ms}(P)$ are explained by the anisotropy in elastic and magnetoelastic properties.

5. Thermoresistive, thermomagnetoresistive and thermobaroresistive dependences Fig. 7.6a(l-6) demonstrate that pressure and magnetic field effect on resistivity realises the “cooling” effect—elastic and magnetoelastic compression reduces resistivity in proportion to temperature decreasing. The estimations show the magnitude of these strains: magnetic field intensity increasing by 2.7 kOe or pressure increase by 1 kbar correspond to sample cooling by 6.2 K and vice versa. Decreasing the hydrostatic pressure or magnetic field intensity has the same influence on resistivity as the increase in temperature.

The given conformities in the resistive properties under *T—P—H* influence reveal one more feature of the system. The influence of pressure and magnetic field implements the “cooling” effect. The magnetic field growth or pressure increase through elastic mechanisms change resistivity equivalently to temperature decreasing. Moreover, the reverse, “heating” effect takes place. A reduction of pressure and magnetic field intensity changes the sample resistivity equivalently to a relevant temperature rise.

What do the “cooling” and “heating” effects in magnetic semiconductors explain? First of all, it explains linear dependence of temperature T_{ms} under pressure and magnetic field, and the basic role of elastic properties in this process. The “metal-semiconductor” phase transition is a property of the thermoelastic expansion of sample structure and is fixed by the resistivity peak temperature T_{ms} Fig. 7.6(1). The application of hydrostatic pressure and magnetic field lead to the "cooling" effect. When reducing, the resistivity magnitude becomes equal to initial one taken at a lower temperature. In this case, for the phase transition, it is necessary to increase the temperature. It is an additional thermoelastic expansion compensating the structure compression by both pressure and magnetic field, accompanied by rising $T_{ms}(H)$ and $T_{ms}(P)$. Thus, the magnetoresistive, baroresistive and baromagnetoresistive peak temperature T_{PP} remains constant at different pressures and magnetic fields. It means that the phase transition takes place at some condition, which is constant for the given sample.

If the process occurs in reverse order, as the initial dependence we will take $\rho(T)$ under magnetic field and pressure influence. Then, at lowering these actions, the rising resistivity magnitude will correspond to initial dependence taken at a higher temperature. Thereby, the “heating” effect of pressure and magnetic field is determined. For the phase transition realization, by analogy, in this case, it is necessary to decrease the temperature—an additional thermoelastic compression compensates the structure expansion by decreasing both pressure and magnetic field. It means, that the removal of an external influence demands a lesser overheat of the system for reaching the conditions of the phase transition realisation. $T_{ms}(H)$ and $T_{ms}(P)$ are decreasing.

The revealed “cooling” and “heating” effects, and linear dependence of $T_{ms}(H)$ and $T_{ms}(P)$ testify to a compensative interaction of elastic and magnetoelastic expansion, on the one hand, and thermoelastic expansion on the other hand. However, in this case the conditions of the phase transition realisation remain constant irrespective of pressure and magnetic field magnitude. The confirmation of this fact is one and the same temperature T_{PP} of baroresistive, magnetoresistive and baromagnetoresistive peaks and linearity of $T_{ms}(H)$ in magnetic properties. And, as a consequence, the equality of the both: phase transition temperature T_{ms} (without pressure and magnetic field influence) and T_{PP}, confirms a similar nature of elastic-deforming mechanisms

of temperature, magnetic field and pressure action, and also testifies to an invariable condition of “metal-semiconductor” phase transition.

The carried out consideration of resistivity behaviour allows one to reveal and to prove that temperature, magnetic field and pressure have the same mechanism of the influence on the magnetic semiconductors.

1. The baroresistive effect has been discovered—a result of elastic compression and thermoelastic expansion, which becomes apparent on relative resistivity change.
2. The baromagnetoresistive effect has been observed—a result of elastic, magnetoelastic compression and thermoelastic expansion, which becomes apparent on relative resistivity change.
3. It is established that peaks of magnetoresistive, baroresistive and baromagnetoresistive effects have the same temperature T_{PP}. It evidences that the mechanisms of temperature, magnetic field and pressure effect are identical.
4. The “cooling” and “heating” effects have been found. They explain the mechanism of elastic deforming corresponding with the change of resistivity, $T_{ms}(P)$ and $T_{ms}(H)$ linearity, and also T_{PP} constant at *T—H—P* influence.
5. All the demonstrated conformity regularities in the elastic deforming mechanism of the change of resistive properties and phase states under *T—P—H* influence, establish the correlation between elastic, resistive and structural properties in magnetic semiconductors.

7.3. “Cooling-heating” effects in properties of $La_{0.9}Mn_{1.1}O_3$ and $La_{0.56}Ca_{0.24}Mn_{1.2}O_3$ under the influence of P and H

The influence of hydrostatic pressure on resistance magnitude in films is shown in fig. 7.10. Curves behavior indicates monotonous resistance decreasing in the whole of pressure range. The same dependence of standard manganin gauge is shown for comparison (inset). Experimental data of film samples are summarized in Table 7.1.

The dependence of ceramic samples' resistance on applied hydrostatic pressure (fig. 7.11) shows the same behavior as in films but coefficient *K* is smaller Experimental data of ceramic samples are summarized in Table 7.2.

The resistance reduction in these structures with applied hydrostatic pressure is caused by reduction of bond length and increasing of the covering factor between Mn *d*-orbital and O *p*-orbital that leads to rise in the Mn-O-Mn exchange interaction. It should be noted that all resistive changes of all samples are reversible.

Fixed linear resistance behavior of ceramics and, especially, of film allows to propose the using of film samples of the same compositions as pressure gauges.

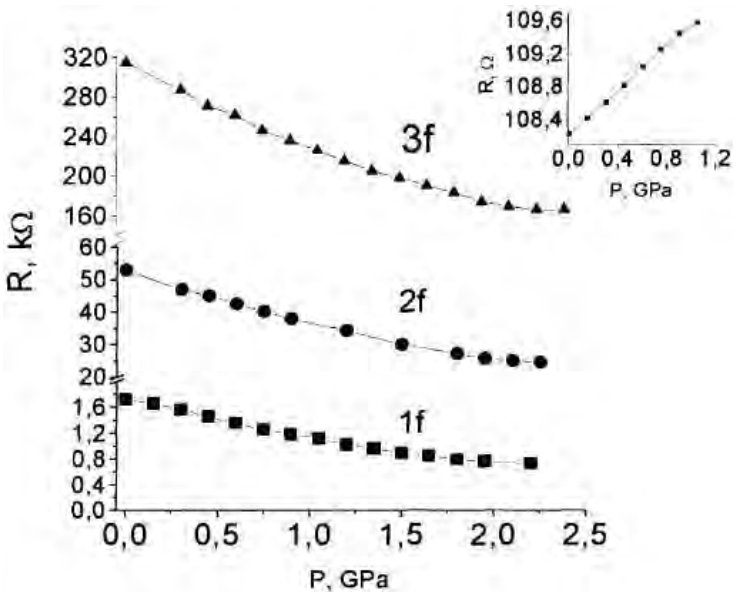

Figure 7.10. Influence of hydrostatic pressure on the resistance of standard manganin gauge (inset) and films: *1f*- $La_{0.7}Mn_{1.3}O_{3-\delta}$; *2f*- $La_{0.9}Mn_{1.1}O_{3-\delta}$; *3f*- $La_{0.56}Ca_{0.24}Mn_{1.2}O_{3-\delta}$.

Table 7.1.

Material	R, [kΩ]	P, [GPa]	*K*, [ΔΩ/ΔGPa]
$La_{0.7}Mn_{1.3}O_{3-\delta}$	1.8-0.8	0-2.2	454
$La_{0.9}Mn_{1.1}O_{3-\delta}$	53-25	0-2.2	12720
$La_{0.56}Ca_{0.24}Mn_{1.2}O_{3-\delta}$	320-165	0-2.45	63265
Manganin	0.108-0.1095	0-1	1.5

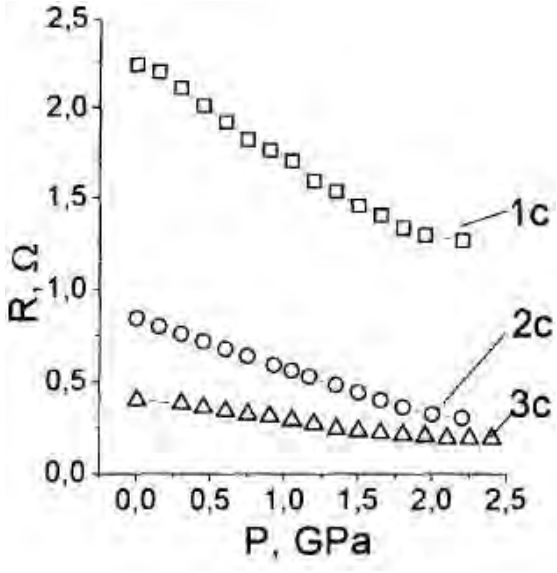

Figure 7.11. Influence of hydrostatic pressures on the resistance of ceramics: *1c*- $La_{0.7}Mn_{1.3}O_{3-\delta}$; *2c*- $La_{0.9}Mn_{1.1}O_{3-\delta}$; *3c*- $La_{0.56}Ca_{0.24}Mn_{1.2}O_{3-\delta}$.

Table 7.2.

Material	R, [Ω]	P, [GPa]	*K*, [ΔΩ/ΔGPa]
$La_{0.7}Mn_{1.3}O_{3-\delta}$	2.25-1.25	0-2.2	0.454
$La_{0.9}Mn_{1.1}O_{3-\delta}$	0.81-0.30	0-2.2	0.232
$La_{0.56}Ca_{0.24}Mn_{1.2}O_{3-\delta}$	0.42-0.20	0-2.45	0.090

The sensitivity as pressure gauges of the investigated film samples of following compositions $La_{0.7}Mn_{1.3}O_{3-\delta}$, $La_{0.9}Mn_{1.1}O_{3-\delta}$ and $La_{0.56}Ca_{0.24}Mn_{1.2}O_{3-\delta}$ is about 10^3-10^5 times as high as that of standard manganin gauge. They may be used in investigations with hydrostatic pressures up to 2.5 GPa.

Non-trivial effects in solid-state physics have been revealed practically at one and the same time: in experimental works [145, 146] during the investigation of properties of the dielectric manganese perovskites a sudden correlation was found between electric conduction and ferromagnetism.

A number of papers have been recently devoted to investigations of properties and PT influenced by temperatures (T), magnetic field (H), and high hydrostatic and quasi-hydrostatic pressures (P). Significant results have been obtained, new effects and regularities have been revealed. We pay attention to a consecutive and generalizing analysis of studies of phase transition and properties change for magnetic semiconductors influenced by T-H-P [148-151]. There, the role of thermodynamic mechanisms of the elastic anisotropically deforming stresses in the changes of PT and properties of manganites has been determined, and the notions of sign alternation for T-H-P effect have been first introduced. That was a prerequisite for finding identical mechanisms of elastic stresses in changes of PT and properties of the magnet-containing materials of another class.

First, we mark that the results of papers [148-151], where polycrystalline samples of magnetic semiconductors were studied, are consecutive. Thus, in paper [149], the baroresistive and baromagnetoresistive effects were first described, a correspondence of T-H-P effect on resistivity in polycrystalline samples was estimated and the role of thermodynamic mechanisms of elastic stresses was determined. In paper [147], the “cooling”, “heating” effects from the influence of pressure and magnetic field were substantiated, their regularity in changes of critical lines $T_{ms}(P)$, $T_{ms}(H)$ has been determined. It was also noted that the misfit of $T_{ms}(P)$, $T_{ms}(H)$ dependences is due to a difference in the elastic and magnetoelastic anisotropies in those samples. An important feature consisting in constancy of T_{PP}, the temperature of magneto-, baro-, baromagnetoresistive effects peaking, which coincides with the temperature of structural phase transition T_{ms}, has been revealed. By the analysis of changes in PT, resistive and magnetostrictive properties under the influence of T-H [150],

the correlation through the elastic properties is grounded, the notion of sign alternation in properties and effects is introduced. $H_g(T)$ and $T_{ms}(H)$ correspondence with respect to magnetostriction properties has been determined, critical points P_X and T_X have been revealed. In paper [151], an improved experimental procedure is described for the case of high hydrostatic pressures; the characteristics are given for 0 to 25 kbar pressure transducers based on film samples of magnetic semiconductors.

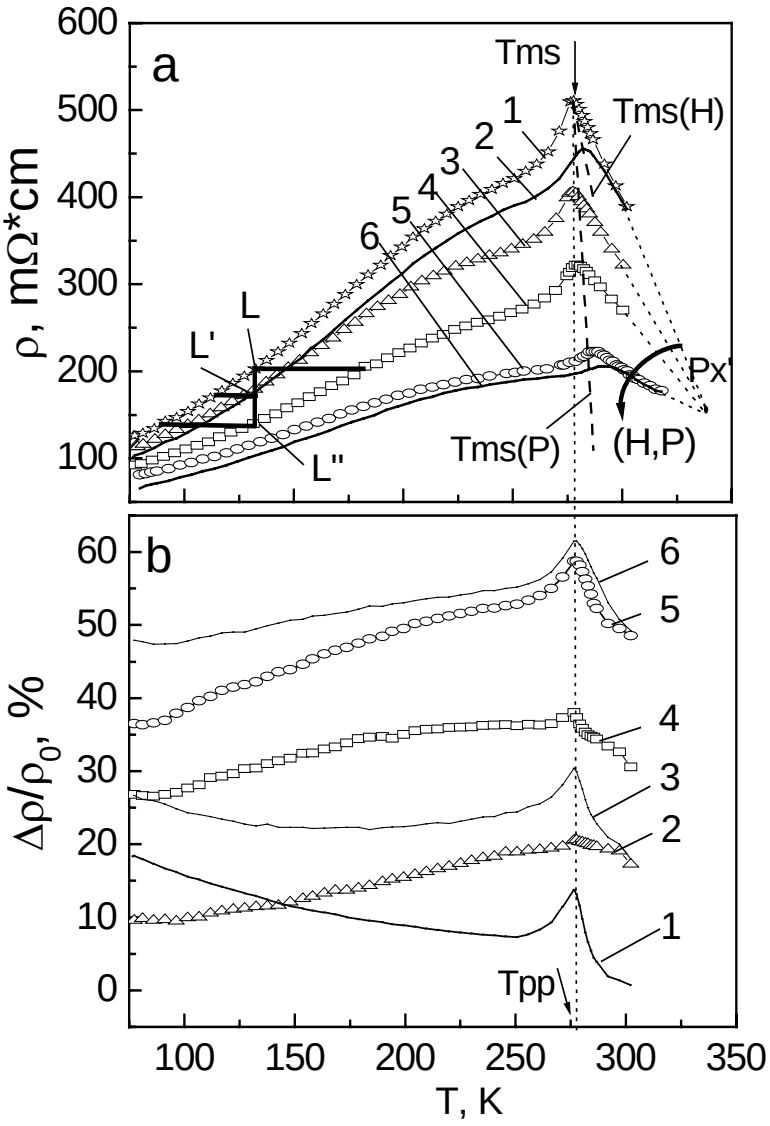

Figure 7.12. Temperature dependence of resistivity (a) and magneto-, baro-, baromagnetoresistive effects (b) of $La_{0.7}Ca_{0.3}MnO_3$ polycrystalline sample under influence of magnetic field and hydrostatic pressure: (a) 1 – P=0, H=0; 2 – P=0, H=8 kOe; 3 – P=6 kbar, H=0; 4 – P=12 kbar, H=0; 5 – P=17 kbar, H=0; 6 – P=17 kbar, H=8 kOe; (b) *1* – P=0, H=8 kOe; *2* – P=6 kbar, H=0; *3* – P=6 kbar, H=8 kOe; *4* – P=12 kbar, H=0; *5* – P=17 kbar, H=0; *6* – P=17 kbar, H=8 kOe.

We pay attention to the given estimations of T-H-P influence on resistivity of polycrystalline $La_{0.7}Ca_{0.3}MnO_3$ (5.1 K~2.42 kOe~1 kbar) (fig. 7.12a), which insignificantly differ in value from those for such compositions as $La_{0.56}Ca_{0.24}Mn_{1.2}O_3$ (6.2 K~2.37 kOe~1 kbar); $La_{0.9}Mn_{1.1}O_3$ (6.2 K~2.7 kOe~1 kbar) [147, 150, 151] and to their relative equality in the case of bulk polycrystalline samples. Noting the role of thermoelastic expansion on the dependences of magneto-, baro- and baromagnetoresistive effects in the wide temperature range (fig. 7.12ab), one can state that in their names there is prefix thermo. Since in magnetic semiconductors the shift in $T_{ms}(H)$ and $T_{ms}(P)$ under the influence of H and P is a regularity of elastic properties and of a difference in anisotropies of elasticity and magnetic elasticity, the estimate of their correspondence in PT parameters change in the sample of $La_{0.7}Ca_{0.3}MnO_3$ shows (fig. 7.12a) is that the magnetic field of 2.12 kOe shifts T_{ms} by the same value as the hydrostatic field of 1 kbar does.

The most important result noted in papers [147, 150] demonstrates that the peaks of baro-, magneto- and baromagnetoresistive effects (see fig. 7.12b) have one and the same temperature T_{PP} coinciding with that of the metal-semiconductor PT T_{ms}. It follows that thermo-elastic stresses are the basic factor in realization of structural phase transitions and, as a consequence, of the jump in properties, whereas the magneto- and baro-elastic stresses realize the “cooling”, “heating” effects. On the dependences of fig. 7.12a we see that changes in properties from L to L’ and L” are connected with the influence of H and P, a direct “cooling” effect in properties, subsequent increase in T-heats the properties to L. The estimates of conformable influence of temperature and pressure (5.1 K~1 kbar) determine quantitatively and rather truly the changes in PT and the differences in the dynamics of resistivity, and stress the role of the mechanism of elastic stresses to be the main reason for the formation and changes in resistivity as a function of temperature at different fields and pressures. It should be added that by a simple construction of approximate dependences of resistivity on temperature with P and H varied (fig. 7.12a), one can single out the point of their intersection, P_X, which is a consequence of changes in properties under the influence of elastic stresses. Such a construction could be shown in some other papers investigating the properties under pressure [150].

7.4. The role of bulk elasticity in formation of second-order structural PT and in magnetic properties of critical lines, points in $LaMnO_3$

To continue the analysis, and having shown the regularities of elastic stresses in resistive properties, it is very important to estimate the significance of the above mechanisms for magnetic properties that was in part done in

paper [150]. There, the correspondence of H and T effect on properties of $LaMnO_3$ single crystal magnetostriction has been estimated, the relationship between T_{ms} and $H_g(T)$ has been determined (fig. 7.13), the $H_g(T)$ dependence and positions of points P_X and T_X with the parameter $H_X(T=0)$ have been found.

We pay attention to regularities of the "cooling", "heating" effect from H influence in the properties of magnetostriction. On the represented dependences we take point L corresponding to T and H (fig. 7.13). Decreasing T with H unchanged, we have changes in properties corresponding to L'. Decreasing H with relief in backpressure magnetostriction, we see how the "heating" effect restores the properties corresponding to L.

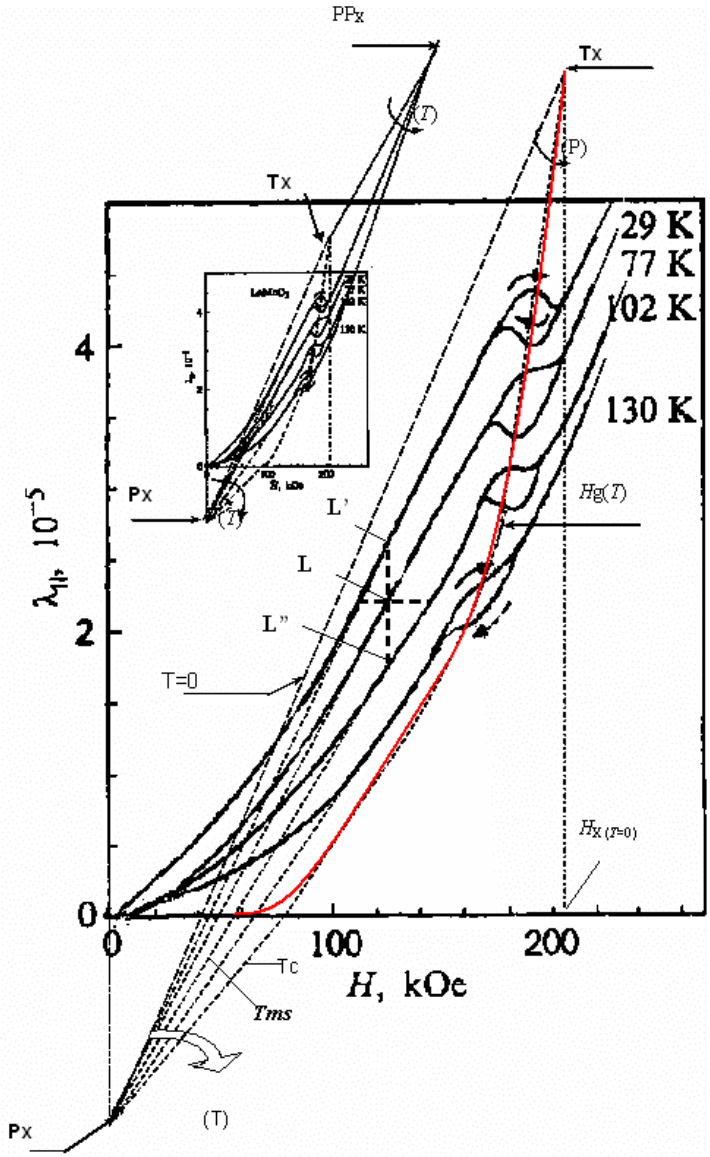

Figure 7.13. Field dependence of the longitudinal magnetostriction of $LaMnO_3$ single crystal.

And the reverse “cooling” effect. When T is increased with H unchanged, the change of properties corresponds to L”. By increasing H and, thus, the magnetostriction pressure, we restore the properties corresponding to L.

Due to the given results it becomes possible to carry out a generalizing analysis of a variety of magnetic semiconductors. The role of elastic stresses is most obviously displayed in regularities of linearity and nonlinearity in the field dependences of magnetostriction, in the case of $LaMnO_3$ single crystal (fig. 7.13). The features observed in nonlinearity of properties are a consequence of the competing influence of T and H through the mechanisms of elastic stresses, they can be explained by the introduction of a more detailed explanation of sign alternation:

a) at fixed low temperatures, in the initial region of the field, the dependence of magnetostriction prior to the PT, is nonlinear (fig. 7.13). This is a consequence of the competing influence of the fixed thermoelastic expansion and magnetoelastic compression, thus, we have the linear dependence under a fixed thermoelastic expansion;
b) at temperatures higher than that of phase transition, the thermoelastic expansion is prevails over the magnetoelastic compression. A sudden growth of magnetostriction is observed, the magnetic hysteresis is formed and the sign alternation range of magnetic properties arises;
c) the effect of sign alternation also develops under a conformable influence of T and H through the competing mechanisms of elastic stresses on $H_g(T)$ dependence, with anisotropies of elasticity and magnetoelasticity equal to T_C, the Curie temperature (fig. 7.13);
d) this is more obvious with changes in the priorities of thermomagnetic EAD stresses, under a simultaneous action of T and H, in the form of a non-linear $H_g(T)$ dependence. Temperature T_{PP} remains constant.

As a whole, the study of thermo- and magnetoelastic effect reveals strong interrelations between the magnetic and lattice-symmetry features of the structure, as well as the causal role of the mechanism of EAD stresses. A particular significance of regularities of thermo- and magnetoelastic anisotropies is a consequence explaining a large quantity of anomalies observed in magnetic poly- and single-crystalline samples.

Let us note the following regularities relating to the critical points. Thus, the point of intersection for the extrapolated linear dependence $H_g(T)$ and the approximated dependence $\lambda_{||}(H)$, for T=0, (fig. 7.13) is denoted by T_X. This parameter is responsible for the state of structural PT in the sample of $LaMnO_3$, when T=0. The position of point PP_X is found as the intersection of the approximated dependences of magnetostriction properties at different

temperatures past the phase transition. Critical points T_X and PP_X emerge from participation of the priority mechanisms of magneto-elastic stresses.

It is noteworthy that such an approach determines the role and the basic importance of magneto-elastic stresses and magnetoelastic anisotropy in the mechanisms of structural PT realization in fields $H_X(T=0)$ with T=0 K. This fact is very important for the understanding of regularities, since the opposite effect of thermoelastic anisotropy is defined by the metal-semiconductor phase transition temperature T_{ms}. It corresponds to T_{ms}=275 K ~ P≈50 kbar for $La_{0.7}Ca_{0.3}MnO_3$, but for H=0 (see fig. 7.12a). The anisotropy of thermo- and magnetoelasticity is the most evident under these extreme conditions of T and H effect on changes in namely structural PT, it also demonstrates the role of elastic properties and sign-alternating priorities of their influence. It should be noted that these statements are valid for a variety of magnet-containing samples, where the influence of T and H through the mechanisms of elastic stresses affects the structural PT and properties and values of anisotropies of thermo- and magnetoelasticity are the basic ones. Such methodological approach makes it possible to consider changes in resistive, magnetic properties and of PT in unified context of both temperature and magnetic field effect through the mechanisms of elasric stresses.

It follows that the position of critical points T_X, $H_X(T=0)$, P_X, PP_X and P_X'is a regularity defined by the chemico-technological and lattice-symmetry features of a sample, while the T-H-P effect is a regularity of the influence of mechanisms of thermo-, baro- and magneto- elastic stresses observed in properties, phase transitions, conformities, sign alternation and effects.

7.5. Relation of bulk elasticity to changes in parameters of properties and in PT

The generally accepted basis kinetics microprocess in lanthanum manganites demands the analysis of complex investigations results.

The one point of view are described in work [1]. The phenomenological approach of influence parameters (T-P-H) has a clear physical sense.

The influence of detailed thermodynamic parameters through mechanisms of volume elasticity to structural changes is leaded to following structural phase transitions and result in properties.

Take into account the high-temperature fact formation structures possibly to give basis of basic peculiarity of temperature dependences, one from which attend forever.

The physical process of temperature-elastic compresses is necessary factor of influence temperature on the whole range.

The results of work [6] are shown the process is related with influence of P-baro-elastic, H-magneto-elastic changes of parameter due to volume elasticity.

Therefore linear change of temperature dependence parameter structure is more significantly.

As fluent from the X-ray structure date the investigated samples $LaMnO_3$ and $La_{0,7}Sr_{0,3}MnO_3$ are homogeneous with rhombohedric distortion lattice and have parameters at room temperature $a=5,531A$; $c=13,360A$ and $a=5,486A$; $c=13,352A$ consequently [169].

High-temperature investigations are carried out at X-ray difractometer in Cu-radiation in standard goniometer attachment GPVT-1500.

The measuring precision of temperature was controlled by platinum-rhodium thermocouple with precision ±3 degree.

The scanning of sample surface was carried out with pitch $0,02^0$. The results of measurement are exhibited at Fig. 7.14.

Monotonous linear increase of crystal lattice parameter of investigated samples is observed with increase temperature.

The change of structure type from rhombohedric to cubic are observed at temperature range 660^0C (for $LaMnO_3$) and 150^0C (for $La_{0,7}Sr_{0,3}MnO_3$).

The X-ray investigations of parameters along of detailed directions in $La_{0,875}Sv_{0,125}MnO_3$ [170] are leaded to the same result.

The stability of linear changes (Fig. 7.15) in whole temperature range 1500 – 350^0K with take into account of experimental errors are exhibited important factor of elasticity strain, which are inalienable reason of volume elasticity behavior.

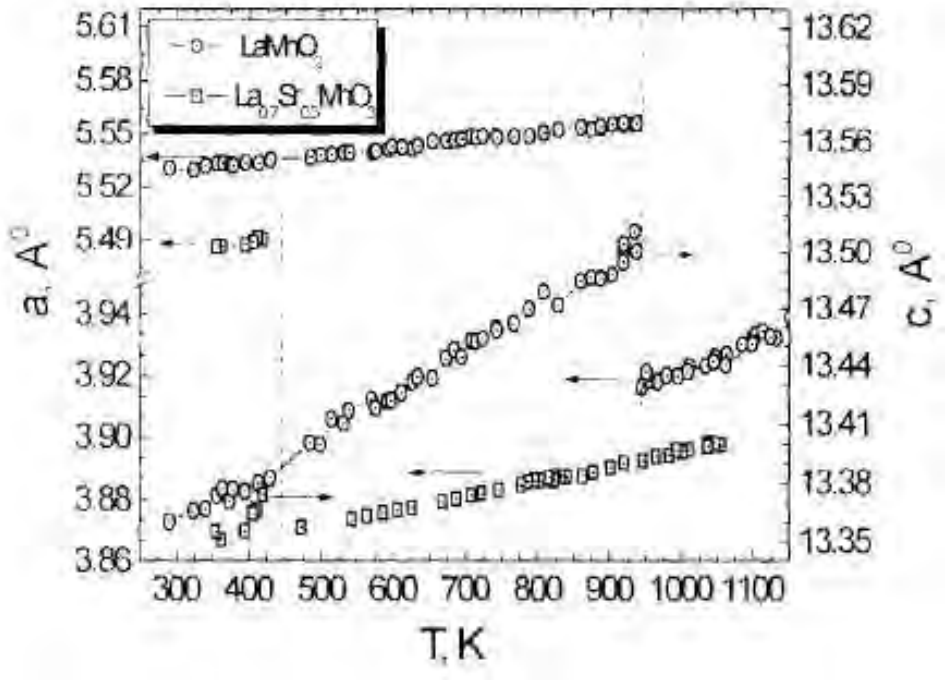

Figure 7.14. Monotonous linear increase of crystal lattice parameter of $LaMnO_3$ and $La_{0.7}Sr_{0.3}MnO_3$ polycrystalline samples [169].

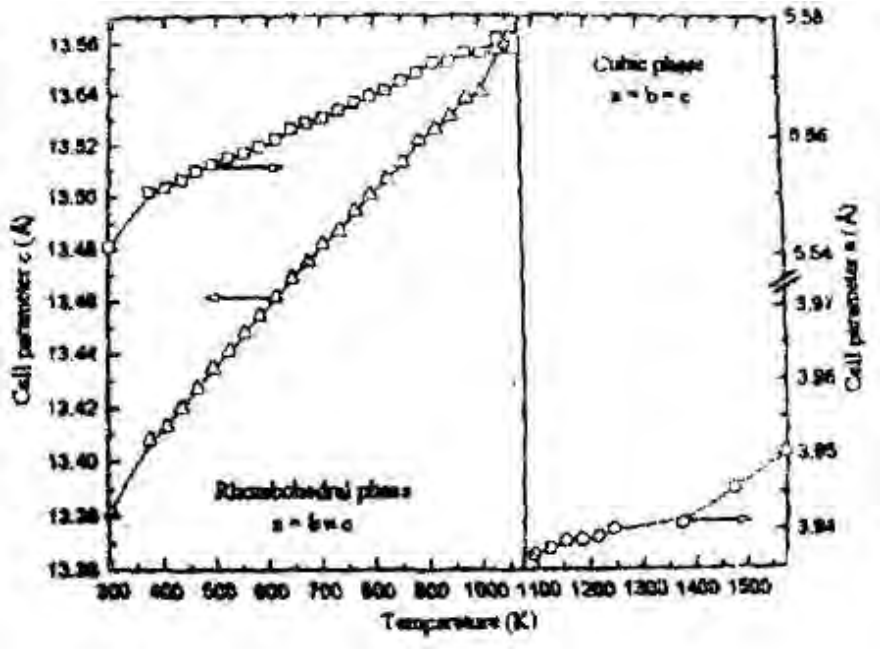

Figure 7.15. The stability of linear changes in $La_{0.7}Sr_{0.3}MnO_3$ in whole temperature range 350 - 1500°K [170].

The fixed jumps at temperature dependencies of parameter are characterized availability of obligatory structural changes – phase transitions.

7.6. Linear regularities in magnetization properties and in structural PT in low-temperature magnetodielectric $CuCl_2 \cdot 2H_2O$

Also in the earlier works of Holland investigators [7, 152, 153], unusual changes of magnetic, magnetothermal and resonance properties of the low-temperature magnetic dielectric $CuCl_2 \cdot 2H_2O$ have been revealed. The noted features and the related physical properties were being studied in detail during the last decade. The results have contributed much to the fundamental physics of phase transitions. However, the discovery of the so-called "supereffect" – a colossal influence of the external magnetic field H on the resistive properties of manganites in the vicinity of Curie point and the discovery of conductivity in HTSC put a question to investigators [135]. The understanding of the mechanisms of effects and processes under investigation, the penetration into casual bases of PT and properties would favour the application of such effects and could be the achievement for the physical science as a whole.

By using the procedures to analyze the experiments on magnetic semiconductors [147-151], we consider the studies of AFM resonance in copper chloride dehydrate under T-H-P effect [102, 165, 166].

The resonance was observed at frequencies ν_1=0.7 GHz, ν_2=2.85-3.15 GHz, ν_3=4.5-4.88 GHz in the temperature range $1.68 \leq T \leq 4.2$ K, under hydrostatic

pressure P of 0; 5.2; 9.2; 11.2 kbar by a specially developed method [166]. The experimental results have been obtained on single crystals and, what is important, under the accurate optical and x-ray orientation. In this respect, the demonstrative is the study by direct x-ray method of the features of structure lattice and anisotropy of the elastic properties of the critical directions under hydrostatic pressure effect in $CuCl_2 \cdot 2H_2O$ [64].

We pay attention to experimental procedure. The external magnetic field of 0 to 12 kOe is oriented in plane ab of the crystal structure of the sample. The resonance was observed for all the selected frequencies (apart from ν_1=0.7 GHz), in the pressure range 0 to 11.2 kbar for two values of the magnetic field, if angle ψ between field H and easy magnetization axis a was not in excess of the angle of AFMR failure ψ_f. With ν_1=0.7 GHz, the resonance was only observed in magnetic field H_{2P} pertaining to the field of phase transition. The resonance disappeared at slight deviations of field H from axis a in the ab-plane.

In the whole of the temperature range, on the isochronous diagrams, the resonance absorption was truly observed only for T≤3.5 K and P=0. With pressure increase (P>9 kbar), there was an increase in the resonance absorption temperature range to 4.2 K.

On the field-temperature dependences [165, 166] we take the field-temperature changes (fig. 7.16a) of the phase transition and denote it $H_{ST}(T)=H_P(T)$, influenced by T-H-P. It is noteworthy that $H_P(T)$ with H||a, in the temperature range to 3.5 K, and P=0 (fig. 7.16a, curve 1) has a linearity of peculiar character, that was also observed in a wider temperature range [92, 96]. Some discrepancy in numerical values is explained by high response of the resonance fields to orientation of the sample with respect to the magnetic field. However, on the dependences, the regularities of linearity are maintained.

It is this result that enables us to study and analyse the linear regions on the field-temperature dependences of fig. 7.16a, to estimate the conformity parameters of T-H-P effect on phase transition shifting using the estimate of the linear changes in PT as a function of T and H, observed on the dependencies (fig. 7.16a) under fixed pressures P_1=0 kbar (curve 1), P_2=5.2 kbar (curve 2), P_3=9.2 kbar (3), P_4=11.2 kbar (4). It follows that $\Delta P/\Delta T$=3 kbar/K and $\Delta H/\Delta P$=1.3 kOe/kbar. These results show that temperature variation by ΔT=1 K and magnetic intensity change by ΔH=4 kOe result in shifting the PT field on the $H_P(T)$ dependencies by the same quantity as the pressure of 3 kbar does. This means that the numerical estimations of T-H-P effect (1 K~4 kOe~3 kbar), for the represented dependencies confirm the important role of the mechanism of elastic stresses, but already in the low-temperature region.

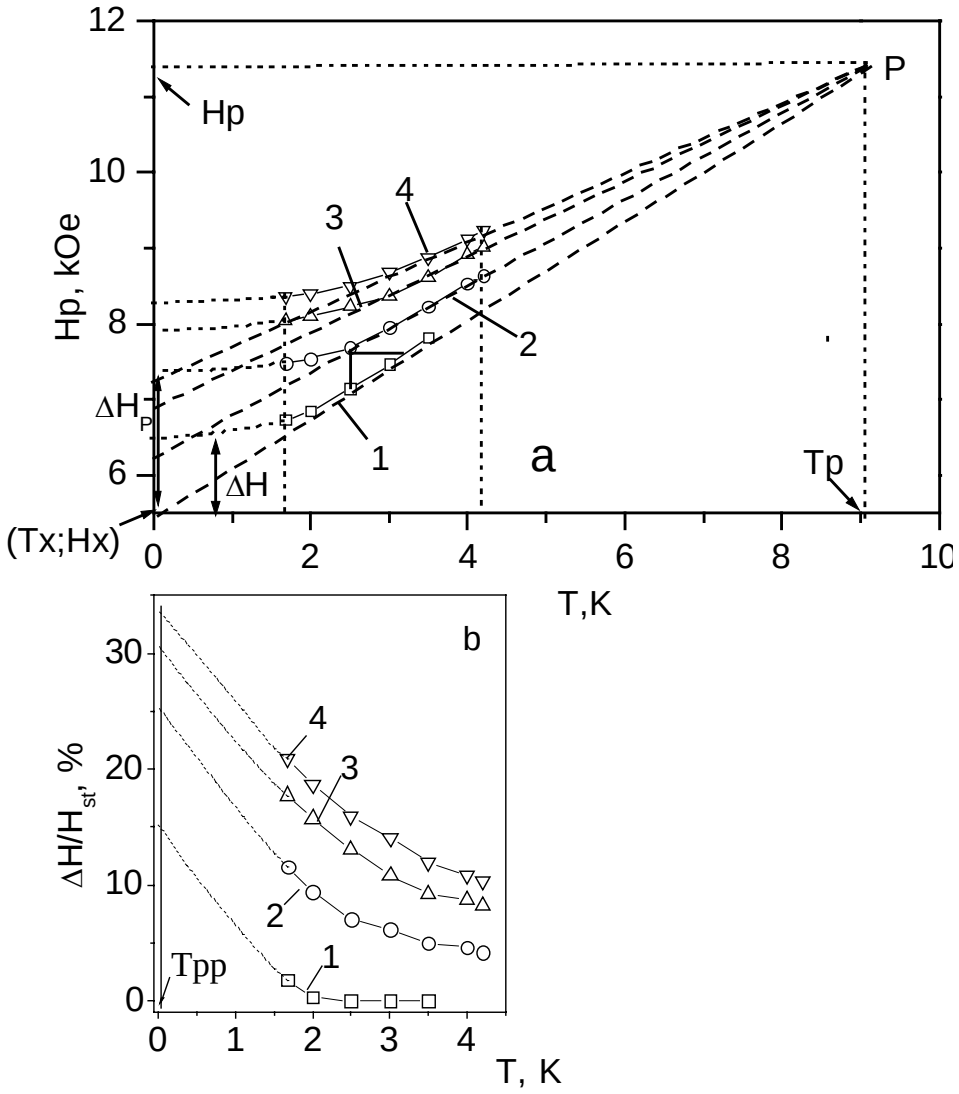

Figure 7.16. (a) Temperature-field dependence of the field of the phase transition at different presures on a frequency ν=0.73 GHz: 1 – P=0; 2 – P=5.25 kbar; 3 – P=9.25 kbar; 4 – P=11.2 kbar. (b) Temperature dependence of thermomagnetic effect 1 – P=0 and thermobaromagnetic effect: 2 – P=5.25 kbar; 3 – P=9.25 kbar; 4 – P=11.2 kbar.

Drawing the analogies and making comparisons with the results for magnetic semiconductors, we pay attention to the revealed effects and the determined temperature of maxima T_{PP} there, which corresponds to T_{ms}, the temperature of metal-semiconductor phase transition. This appears as a regularity of a jump in properties in the structural PT. By the same methods we consider and ascertain the analogies in magnetodielectric. To this end we analyze the field-temperature dependencies of fig. 7.16a and make our complements. We introduce a concept of thermomagnetic $\{H_{st0}(T)- H_{stH}(T)\}/H_{st0}(T)$, % and thermobaromagnetic effects $\{H_{st0}(T)- H_{stHP}(T)\}/H_{st0}(T)$, % (fig. 7.16b), where $H_{st0}(T)$ is the approximated linear dependence with the initial parameter

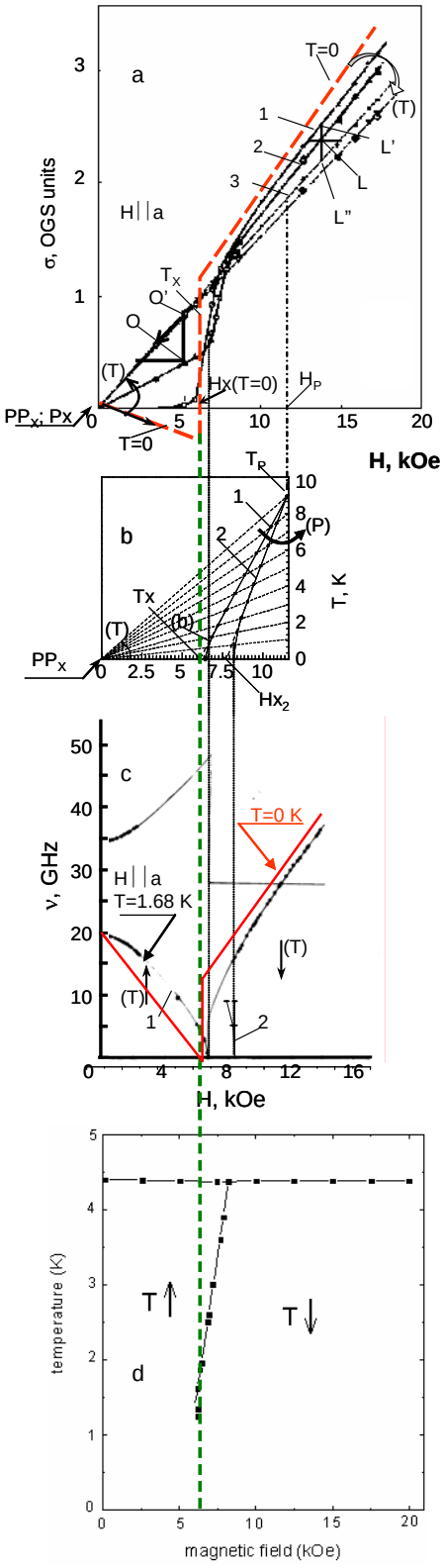

Figure 7.17. (a) Behavior of magnetization of $CuCl_2 \cdot 2H_2O$ monocrystal at external magnetic field directed along the easy axis: 1 – 1.59 K; 2 – 3.02 K; 3 – 4.1 K. (b) temperature-field dependence of the field of the phase transition at pressures: 1 – P=0; 2 – P=11.2 kbar. (c) Frequency-field dependence of AFMR in $CuCl_2 \cdot 2H_2O$ at H$\|$a and T=1.65 K: 1 – P=0; 2 – P=11.2 kbar. (d) magnetic phase diagram of $CuCl_2 \cdot 2H_2O$ monocrystal.

H_X=5.5 kOe. H_{stH}(T) is the regularity of PT shifting under the influence of H; H_{stHP}(T) is the dependence of PT temperature change under the influence of magnetic field and pressure. Such operations substantiating the final result do not contradict the physical sense and show the potentialities of a consequent analysis, which is somewhat different from the conventional one.

Thus, from the results of fig. 7.16b it follows that the maxima of the revealed effects correspond to one and the same temperature T_{PP}=0 K. By analogy with the similar result (fig. 7.12b) but for the magnetic semiconductor, where the temperature T_{PP} of the maxima of magneto-, baro- and baromagnetoresistive effects coincided with T_{ms}, we can state that in magnetic dielectric, T_{PP}=0 K also corresponds to the temperature T_{ST} of the structural phase transition. Proceeding from the obtained result shown for the first time in paper [167], and to continue the analysis the following can be found. Upon approximating the dependence shown in fig. 7.16a, curve 1, we can single out point T_X with magnetic-field parameter H_X≈5.5 kOe. The same regularities of magneto-EAD stresses and of magnetoelastic anisotropy, but in a higher fields, are denoted by the critical point T_X with parameter H_X(T=0) on the dependencies of magnetostriction, (fig. 7.13) for single-crystalline $LaMnO_3$. In the above results, the found regularities show that in the both cases the mechanisms of EAD stresses and of anisotropy are identical.

Next, we pay attention to the estimates of conformity in the influence of T, P and H (1 K~3 kbar~4 kOe) and explain the importance of the mechanisms of EAD stresses and regularities of the “cooling”-“heating” effects from the influence of P and H, which were first shown in papers [147, 150], but already from the point of view of dynamics of T_P(H), T_P(H,P) change. The substitution of indices H_{ST}(T) on the field-temperature dependence by T_P(H) does not contradict the physical sense (fig. 7.16a, fig. 7.17b).

First, with H increase from H_X=5.5 kOe with P=0, the mechanism of magnetoelastic striction on the T_P(H) dependence leads to the “cooling” effect, while the conditions for PT realization acquire an additional thermoelastic expansion and, thus, the temperature increase. T_{PP} remains constant. And the reverse, “heating” effect is as follows: with diminution of magnetic intensity, the magnetostriction effect weakens, and temperature decrease is necessary for conditions of PT realization be satisfied. In this case, T_{PP} is constant once again.

Second, regularities of the effect of simultaneous influence of hydrostatic pressure and magnetic field are of the most interest. The sign alternation of the effects is a very important result. “Supercooling” at the expense of pressure increase to 11.2 kbar is overcome by an additional change in magnetic field to H_{X2} at the expense of magneto-elastic stresses, i.e. the “heating” effect near the same critical point T_{ST}=0 K, where the magnetoelastic anisotropy realizes the PT. Further growth of magnetic intensity results in regularities of “cooling”

effect. It follows that changes in P and H are shifting the PT by the mechanisms of sign alternation in the effects. Conditions for PT realization remain the same, T_{PP} – constant. The like "heating" effect of the magnetic field is realized in $LaMnO_3$ at temperatures below the structural phase transition, this is illustrated on the $H_g(T)$ dependence of fig. 7.13.

This means that the "cooling", "heating" effects create a competition between baro- and magnetoelastic compression, on the one hand, and thermoelastic expansion, on the other hand, under elastic stresses influence. The role of these mechanisms is in the form of sign alternation for properties and PT from T, H effect [150]. With the allowance for the estimates of the parameters (T-H-P) influencing the PT shifting, we can explain the linear and non-linear regions of the field-temperature dependencies (fig. 7.16a), where the thermoelastic expansion prevails over the magnetoelastic compression, in the whole range of H change upon the increase of temperature. Such an explanation of $T_P(H)$, $T_P(H,P)$ dependencies and of the role of "heating" and "cooling" effects from the influence of field H and pressure P confirms the regularities of EAD stresses being pointed to by sign alternation.

Now, we pay attention to further analysis of the investigation results, which pointed to sign alternation, and show that at different pressures the field-temperature dependencies of fig. 7.16a tend to approach each other. By simple operation we take and denote the more important regularity – at points T_X and P.

T_X is the initial point of the approximated field-temperature dependence (fig. 7.16a, curve 1) having the coordinates H_X=5.5 kOe and T_X=0 K. This result has already been used in the analysis, it shows that at T=0 K and H_X=5.5 kOe the PT is realized at the expense of magnetoelastic anisotropy.

Critical point P results naturally from the mechanisms of EAD stresses. It is at the intersection of the field-temperature dependencies, at fixed pressures, at the point having coordinates T_P=9.2 K and H_P=11.5 kOe (fig. 7.16a).

It is noteworthy that the temperature parameter of the critical point T_P=9.2 K more than twice exceeds the critical temperature T_N=4.33 K known from papers [152, 153, 168]. Such unordinary has result stimulated an additional research of true thermodynamic mechanisms in the chosen magnetic dielectric.

7.7. Secondary signs of the first-order structural PT and the role of elastic properties in the distinguishing of critical lines and points, resonance properties and phase states

To elucidate the role of the found regularities in the properties of magnetization, let us consider and analyze the results of experimental investigations of the megnetic properties in single crystal of $CuCl_2 \cdot 2H_2O$

(fig. 7.17a) obtained in paper [7]. These results were among the important arguments for the formation of basic concepts of antiferromagnetism. Here we pay attention to a study of magnetization in single-crystalline sample in the form of round disks (2.5 mm×5 mm) aligned manually with no optical or X-ray control that gave error in measurements and affected the interpretation of results.

Now we interpret the dependence of fig. 7.17a illustrating the dynamics of magnetization with H directed along the "easy" axis and T_1=1.59 K, T_2=3.02 K, T_3=4.1 K. Here we note some interesting features:

a) for $H<H_0$ ($H_0=H_{ST}$) and at T_1, T_2, T_3 the author [7] observed slight changes in magnetization vs field rise dependence, while the temperature variation (thermoelastic expansion) essentially influences the slope of magnetization in each the dependencies, which have a single point of convergence PP_X. With temperature increase the above dependencies tend to deviate counter-clockwise, i.e. the growth in T and H affects the increase in magnetization. Consequently, in the same figure it is possible to construct an approximation of the dependency (fig. 7.17a, the dashed line) for T=0 K, that does not contradict the logic of the experiment.
b) For $H>H_0$ (fig. 7.17a) the magnetization increases with H and decreases with changes in T_1, T_2, T_3, i.e. changes in T and H affect the magnetic properties in antiphase. The growth in T is shown by the arrow. It is noteworthy that the approximation of all the dependencies has a single point of convergence P_X near the origin of coordinates. Logically follows the behavior of properties at T=0 shown by the dashed line. Here we also point to the regularity due to changes in T and H. By the position of critical points L, L', L'' one can follow the "heating"-"cooling" effects of the magnetic field. With T decrease, the properties are transferred from L to L'. By H decrease, the returning of properties to L results in the "heating" effect. On the contrary, the properties are returned to L and we have the "cooling" effect. In this case, both the magnetization and magnetostriction in $LaMnO_3$ (fig. 7.13 and fig. 7.17a) are of similar tendency.

For a better understanding of the jump in properties (fig. 7.17a) we superimpose the behaviour of magnetization on the field-temperature dependencies $T_P(H)$, $T_P(H, P)$ of fig. 7.17b by the method of common coordinates of both the magnetic field and the temperature. In fig.7.17b the changes in temperatures are shown in the angle coordinates. Such coordinates are more evident for the explanation of the dynamics of properties and PT under the influence of thermo-, magneto- and baro- elastic stresses. However, during this procedure it is very difficult to make allowance for the main

mistake originating from the orientation of a single crystal with respect to the magnetic field, however, the main tendencies are maintained.

What does the jump at point with coordinates T_X=0 K, H_X(T=0)=5.5 kOe mean? In fig. 7.17a it is marked by the dashed line. It defines, through the properties, the position of structural phase transition for T=0 K. Such a methodology of the analysis is justified and there is an agreement with the analogous result for $LaMnO_3$ (fig. 7.13). In the figure, there is the analogous point T_X with parameters T=0; H_X(T=0). The mentioned methodology of analysis and construction helps in the revealing and explaining the role of elastic stresses from the influence of T-H-P on the structural phase transition, properties and in determining the significance of structural peculiarities. Such peculiarities are due to chemical-and-technological as well as the symmetry-lattice characteristics of the magnet-containing samples. In this respect, the matched critical point P_X (PP_X) in the origin of coordinates is a regularity of changes in properties under the influence of magnetic field and temperature namely for magnetodielectric (fig. 7.17a). At the same time, it is noted [150] that on the dependence of magnetostriction in $LaMnO_3$, the critical points P_X, PP_X, resulting from a similar extrapolation (fig. 7.13) are spread on different sides of the phase transition. This is a regularity of the chemical-and-technological as well as structural features of magnetic semiconductors.

The described results and their substantiation are important for the interpretation of regularities in changes and formation of properties and phase transitions in the physics of low-temperature magnetic dielectrics and of another materials. The following generalization can be done:

First, from the above construction and estimation of the found conformities (fig. 7.17a and fig. 7.17b) we reveal the regularities in PT changes and in dynamics of magnetization under the influence of temperature and “cooling”, “heating” effects from H and P through the mechanisms of elastic stresses;

Second, on the example of “cooling” effect, as a result of magnetic field influence on T_P(H) shifting and properties, a regularity of the opposite effect of thermoelastic stresses on magnetization properties before and after the phase transition has been shown. In fig. 7.17a and fig. 7.17b this is shown by the dashed line for T=0 and it is seen from changes in properties under T effect with respect to overlapping points PP_X, P_X, meaning that the effect of temperature change for the properties develops in counterphase . This fact shows that there is a mechanism of thermoelastic deforming striction (compression), which fixes the structural phase transition as a jump during the increase of temperature. Such a redistribution of stresses induced by the temperature (fig. 7.17a) can be termed as the effect of TSS.

What does the TSS effect mean? It means changes in the structural PT under the influence of temperature through the mechanism of thermo elastic

stresses. In the investigated sample, under the structural PT temperature of 0 K, the properties are changing in a jump-like manner (the dashed-dotted line in fig. 7.17a). This means that with temperature rise, in the region of PT, there occurs a sudden change in properties at the expense of thermoelastic compression mechanism. On magnetization curve there is a jump, or as we think, a jump in conductivity, but already under the superconductive effect.

We pay attention to the found regularity in magnetization properties, which is realized by TSS effect. On the dependencies we observe changes in properties prior to magnetization jump (PT) in low field H (fig. 7.17a). T and H affect the properties unambiguously. This means that the magnetization increases with T and H, while there is a monotonous lowering of the properties with T and H decrease. The resulting is an unusual sign alternation in the influence of T and H.

This is proved by the analysis of changes in magnetization under the influence of T and H. To this end, we take point O on the dependencies of fig. 7.17a. With T increase, there is a shift of properties from O to O'. Next, by decreasing H and removing the magnetostriction backpressure, we return the properties typical of point O. By decreasing H we realize the effect corresponding to a decrease in T. This is a consequence of the effect of TSS.

Such representation and the found regularities relating to the role of elastic stresses enable us to substantiate their causal value in some more properties and effects. This will be done later on.

The carried out analysis, the shown results, the grounding of the effect of TSS give us a possibility to state that the like regularities in changes of PT and properties are the case with samples of some other compositions and classes.

It was already mentioned that the understanding of regularities in structural PT in the low-temperature magnetic dielectric $CuCl_2 \cdot 2H_2O$ is a key to the comprehension of the superconducting effect and as we believe, of the properties of conductivity in HTSC. And the magnetic field effect realizes, at the expense of causal role of magneto-EAD stresses, conditions for a colossal magnetoresistance in magnetic semiconductors.

The obtained results and further studies of the role of the mechanisms of elastic stresses in regularities of changes in PT and properties have made it interesting to find out the nature of the high-frequency properties in $CuCl_2 \cdot 2H_2O$ influenced by H and T.

A great number of papers [76, 77, 86, 154-157] deal with the investigation of the resonance properties in a model sample of copper chloride dehydrate in a wide range of frequencies, magnetic fields and temperatures. A more complete explanation of the models and theory by using the molecular field approximation is represented in papers [76, 77]. Changes in the resonance properties in the rotating magnetic field were theoretically explained in papers [86, 96, 101, 102, 159, 165, 166]. However, the proposed models can't find the

mechanisms, determine the constants, nor show the whole spectrum of the field-frequency dependencies at the fixed temperature T=0 K. An extensive data on experimental investigations of properties in the low-temperature region, in a whole range of the magnetic fields have defined the purpose of our analysis.

We pay attention to a low-frequency branch of the field-frequency dependence, (fig. 7.17c), [96], which is a generalized result of the experiments. It shows that there is a conformity in magnetic field changes to the described above results (fig. 7.17a,b,c).

The low-frequency branch is expressed by a dependence showing how the properties are changed for T=1.68 K in field H directed along the a-axis.

Let us look at the position of critical point b (fig. 7.17b). It is a matched point, its position is shown on the $T_P(H)$ curve of fig. 7.17c. All the regularities in changes are considered with the allowance for the estimates of conformity in T-P-H effect (1 K~4 kOe~3 kbar).

a) point b with the coordinate H_{ST}=6.8 kOe, which corresponds to P≈4.8 kbar, and T=1.68 K (P≈5 kbar). The position of point b is a consequence of the “cooling” effect from the magnetic field influence on changes in PT (fig. 7.17c).
b) in the initial segment of frequency behavior in fields from 0 to 6.8 kOe, that corresponds to P change from 0 to 4.8 kbar, under a fixed thermoelastic expansion (T=1.68 K), the non-linear dependence is explained by the alternating-sign priorities in the competing mechanisms of thermoelastic expansion and magnetostrictive compression;
c) on the field-frequency dependence (fig. 7.17a,c) the changes in temperature affect the dynamics of properties in counterphase, this is explained by sign alternating influence of T and H. Thus, the priority of thermoelastic expansion fixed at T=1.68 K (corresponding to P≈5 kbar) is changed, the magnitude of field H=6.8 kOe corresponding to P~4.8 kbar. On the dependence of fig.4c we observe a change in slope.

As a result, the low-frequency branch of the field-frequency dependence is nothing but resonance in properties prior and past the structural PT, with regularities in changes being a consequence of the mechanisms of EAD stresses from T, H effects.

Such an explanation of the noted low-frequency dependencies enables us to treat the conditions for the resonance absorption in a new way. Since in the structure the changes in conduction electron coupling are determined by the mechanisms of EAD stresses, in the electromagnetic field of the resonator tuned to resonance, the high-frequency current is realized, which is an active component of the absorption. This is registered by the equipment.

The given results and the revealed regularities prove that the mechanisms of EAD stresses from T-H-P effects are identical in both the low- and high-temperature range. Consequently, we can consider the phase diagram for $CuCl_2 \cdot 2H_2O$ illustrated in fig. 7.17d and discussed in papers [81, 86, 153] somewhat differently.

What is it the dependence for properties, when the role of competing influence of T and H through the EAD stresses and the effect of TSS are taken into account? At the initial segment of the dependence, T and H unambiguously are forming the magnetic properties with the account for the TSS effect. Next, the changes in PT obey the regularities of the "cooling" effect from the magnetic field at T=4.3 K. The following segment is a consequence of regularities of monotonic change in the properties under the influence of competing mechanisms of thermo- and magnetic EAD stresses. Here the change of priorities from T to H can be estimated from T-H-P (1 K~4 kOe~3 kbar) conformities. We note that the dynamics of changes in PT propagates to the critical point P_C having the coordinates H_P, T_P, where $T_P \approx 9.2$ K is much different from T_N of 4.3 K.

Such interpretation of the role of EAD stresses is preferable for the explanation of regularities in phase diagrams for the given class of samples. The carried out analysis and the obtained results have proven this interpretation to be correct.

7.8. Linear lows of elasticity during the selection of critical lines and points

The studies have shown that the experimental results for changes in PT and properties point to the existence of critical points and lines participating in the construction of typical singes. They also help in judging the mechanisms of changes in magnetization, magnetic susceptibility, heat capacity, resonance properties not only in phenomenological models and theory, but can be a subject of independent investigations.

At present, there is no a consecutive analysis of the critical phenomena realized in critical lines and points. The analytical methods to study them in a variety of compositions and properties in both physically accessible and inaccessible regions have not been developed. This is a missing link in the chain of researches. This deficiency can be made up by finding and analyzing the true peculiarities of the revealed thermodynamic mechanisms of elastic stresses. The understanding of physical regularities taken directly from the experimental results and appearing as a variety of critical lines and points makes it possible to relate the chemico-technologycal and lattice-symmetry features of the structure in the changes of PT and properties, as well as to show the causal role of elastic stresses.

On the example of changes in resistivity of polycrystalline $La_{0.7}Ca_{0.3}MnO_3$ we derive the following critical lines and points (fig. 7.12a):

$T_{ms}(H)$, $T_{ms}(P)$ are the temperatures of the metal-semiconductor phase transitions under H, P effect. The regularities of their changes become formed by the difference in magnetoelastic and elastic anisotropies;

P_X' is the critical point resulting from the intersection of approximated dependencies of resistivity on temperature under the influence of variable parameters P and H;

T_{PP} is the temperature corresponding to the maxima on the dependencies of baro-, magneto-, baromagnetoresistive effects (fig. 7.12a,b), which coincides with T_{ms}.

It is noteworthy that all the critical lines and points are a regularity of the chemical composition, the technology of treatment, symmetry-lattice features of structure and T-H-P effect through the mechanisms of elastic stresses.

The next result, which applies to magnets as well, are the critical lines and points concerning the changes in magnetostriction in $LaMnO_3$ under the influence of magnetic field and temperature, fig. 7.13 where:

$H_g(T)$ is the critical line of changes in PT hysteresis field parameters versus the temperature. Differences in thermo- and magnetoelastic anisotropies define the parameters of hysteresis under the PT;

P_X, PP_X are spaced apart points resulting from the intersection of the approximated linear segments of the field dependencies of magnetostriction prior and past the PT; they are a regularity of changes in properties under the influence of T and H through the elastic stresses. The magneto-elastic stresses are of priority, when PP_X is found;

T_X is the critical point of intersection of $H_g(T)$ approximation with the dependence of magnetostriction (T=0 K) $H_X(T=0)$, fig. 7.13. In this case, of priority are magneto-elastic stresses;

T_C is the Curie temperature corresponding to the point of intersection of the critical line $H_g(T)$ with axis H on the magnetostriction dependence. It is a consequence of the competing conformities of thermo- and magneto-elastic stresses. It also holds the structural PT fixed with thermo- and magnetoelastic anisotropies being equal.

This variety of critical lines and points makes it possible to relate them to each other and to determine the role of elastic stresses. Now, we carry out a comparative analysis of the mentioned results for magnetic semiconductors.

a) We pay attention to resistivity change, fig. 7.12a (curve 1), where the temperature realizes, through thermo-elastic stresses and regularities, a resistivity jump in the region of the structural metal-semiconductor PT, with T_{ms}=275 K corresponding to pressure P~45 kbar and H=0, in compliance with our estimates. A subsequent influence of the magnetic

field affects the properties and $T_{ms}(H)$ dependence through the "cooling" effect. In $LaMnO_3$ $T_{ST}\approx300$ K [5];

b) Proceeding from the revealed relative equality of the estimates of a correlative influence of T and H in a variety of polycrystalline and single-crystalline samples, it can be assumed that changes in magnetostriction under the influence of the "heating" effect of the magnetic field (fig. 7.13) show that the magneto-elastic stresses realize the properties of magnetoelastic anisotropy in the form of the structural PT, with $H_X(T=0)\approx210$ kOe, at the critical point T_X for T=0. Such coordinates correspond to pressure of approximately 75 kbar. Subsequently, the mechanism of thermo-elastic stresses results in the changes of the hysteresis field on $H_g(T)$ curve. This is a regularity of differences in thermo- and magnetoelastic anisotropies;

c) Now we analyse the result of a combined influence of H and T (fig. 7.12a, fig. 7.13). Here we observe the linear and non-linear critical lines $T_{ms}(H)$, $H_g(T)$. With the role of elastic stresses and the estimates of a correlative influence of T-H-P taken into account one can see that changes in critical lines is a regularity of changes of H and T prevailing influence on PT and properties. In this case, the influence of the elastic stresses is of alternating sign character, and the location of T_C is a consequence of such alternation. Thus, the mechanisms are correlative and there is equality of elastic and magnetoelastic anisotropies. The analysis and the results show that there are the laws for elastic stresses, sign alternation, T_{PP} constancy, correspondence of elastic and magnetoelastic anisotropies (the Curie temperature). It is also shown that the magneto-EAD stresses play the basic role in a giant magnetoresistance.

As a consequence, the position of critical points $T_{ms}=T_{PP}$, T_X, $H_X(T=0)$, P_X, PP_X and P_X' and lines $H_g(T)$, $T_{ms}(H)$, $T_{ms}(P)$ is a regularity determining the relation between chemical-and-technological, symmetry-lattice features of the structure and the regularities of T-H-P effects through the mechanisms of thermo-, baro-, magnetoEAD stresses in properties, phase transitions, correlations, sign alternation and effects.

The analysis of the experimental results reveals the casual role of thermo-elastic stresses in changes of the structural phase transition taking place prior and past the PT, whereas the influence of H through magneto-elastic stresses is a consequence of "cooling", "heating" effects. The regularities are also valid for the magnets.

Now we define more exactly the regularities in the construction of critical lines and points for the magnetic dielectric $CuCl_2\cdot2H_2O$ by the results of PT magnetization and high-frequency properties change (fig.7.16a, fig. 7.17abc):

$T_P(H)$, $T_P(H, P)$ are field-temperature dependencies of changes in phase transition under the influence of H and P;

P_X, PP_X are superposed points of intersection of extrapolated linear dependencies of magnetization showing the regularities of T and H effect through the mechanisms of elastic stresses prior and past the PT (fig. 7.17a);

T_X is the point of intersection of the approximated field-temperature dependence $T_P(H)$ with the axis of temperatures, it shows the location of PT with T=0 K, $H_X(T=0)$=5.5 kOe (fig. 7.16a, fig. 7.17ab);

$T_{PP}=T_X=0$ K is the temperature of the thermomagnetic and thermo-baromagnetic effect maxima, it corresponds to the temperature of structural PT (fig. 7.16b);

P is the critical point with the coordinates T_P=9.2 K, H_P=11.5 kOe. It is a point of regular intersection of the approximated field-temperature dependencies $T_P(H)$, $T_P(H,P)$ corresponding to changes in PT for different fixed pressures (fig. 7.16a and fig. 7.17b). At this point, thermoelastic and magnetoelastic anisotropies are conformable;

T_P=9.2 K is the temperature parameter of the critical point P.

Such arrangement of the critical lines and points and their conformity help in finding regularities in correlation between the structural features and the mechanisms of thermo- baro-, magneto-elastic stresses, which result in changes of the structural PT and properties of the given sample.

By using the methodology of the analysis of magnetic semiconductors, we now analyse critical lines $T_P(H)$, $T_P(H,P)$ and points T_X, $H_X(T=0$ K), $T_{PP}=T_{ST}=0$ K, P_X, PP_X for the investigated magnetodielectric.

a) By comparing the properties of magnetization (fig. 7.17a), field-temperature (fig. 7.17b) and field-frequency (fig. 7.17c) dependencies, we pay attention to their location for T=0 K and note that any changes in T are connected with the mechanism of thermo-EAD stresses, when the anisotropy of thermoelasticity realizes the structural PT at point T_X, and the effect of TSS is developing with temperature increase for H=0. Moreover, it has been revealed that $T_X=T_{PP}=T_{ST}=0$ K is a regularity of the structural PT.
b) On the dependencies of magnetization (fig. 7.17a) we observe the regularities of magneto-EAD stresses: by analogy with the magnetic semiconductors (fig. 7.13), we pay attention to the fact that the influence of the magnetic-field “heating” effect through the magneto-EAD stresses and the magnetoelastic anisotropy realize the structural PT (T=0 K) in the form of magnetization jump in field $H_X(T=0)$=5.5 kOe, which, according to the estimates, is equivalent to the influence of P≈4.2 kbar and correspond to the critical point T_X. A subsequent increase of the magnetic intensity gives the “cooling” effect in the behavior of $T_P(H)$;
c) Finally, we consider the combined effect of H and T through the mechanisms of EAD stresses, (fig. 7.17abc). Their role in the properties of

magnetization (fig. 7.17a) is seen by regularities of equivalent T, H effect prior to PT and by the sign-alternating influence past it. It is also seen by the changes in field-temperature dependencies $T_P(H)$, $T_P(H,P)$ (fig. 7.17a,b) and by the TSS influence of T, the “cooling”, “heating” effects of H, and by the determined regular location of critical point P; linear and non-linear changes in PT, field-temperature dependencies (fig. 7.17bc) and phase diagrams (fig. 7.17d). This determines the causal role of T, H, P effects through the mechanisms of EAD stresses in the represented results of the analysis of investigation of changes in PT and properties in $CuCl_2 \cdot 2H_2O$.

A detailed consideration of the obtained results allows us to characterise one more important regularity, which determines the correspondence and differences in structural PT and properties of magnetic semiconductors and magnetic dielectrics. Primarily, it is a consequence of the chemical composition, technical processes of sample preparation and, as a result, of lattice-symmetry peculiarities of the structure. The properties and the structural PT are realized under the influence of thermodynamic parameters T-H-P through the revealed mechanisms of elastic stresses, the anisotropy of elasticity and magnetoelasticity manifesting itself in high and low H and T, respectively. These regularities were revealed when the notion of sign alternation in the position of critical lines and points was introduced.

Now, we consider the variety of critical lines and points in the two systems. We pay attention to changes of resistivity in polycrystalline samples (fig. 7.12a) and to the revealed adequacy of T-H-P effects, as well as note the dependencies of magnetostrictive properties and correspondences (T-H) in single-crystalline $LaMnO_3$ on the critical lines $T_{ms}(H)$, $T_{ms}(P)$, $H_g(T)$ and of points $T_{PP}=T_{ms}$, T_C, P_X, PP_X and T_X for $H_X(T=0)$ (fig. 7.13), which relate the structural, electronic, magnetic, elastic properties and the mechanisms of elastic stresses in magnetic semiconductors.

For the low-temperature magnetic dielectric, the critical lines $T_P(H)$, $T_P(H,P)$ (fig. 7.16) and points $T_{PP}=T_{ST}=0$ K, P_X, PP_X, T_X with the coordinates T=0; $H_X(T=0)$, and critical point P for $T_P=9.2$ K as well as the effect of thermoelastic deforming striction (compression), fig. 7.17abc, relate the peculiarities of structural, magnetic, elastic, high-frequency properties to the mechanisms of elasticstresses.

As a result, by specifying the location of critical points T_X and P_X, PP_X of fig. 7.13, fig. 7.17ab, we see that their location is different, but the role in the investigated systems is unambiguous. From the analysis and comparison of the mentioned critical lines in the form of the $H_g(T)$ dependence and its relation to $T_{ms}(H)$ and T_C, in one case, and to the $T_P(H)$, $T_P(H,P)$ dependencies and critical points $T_X=T_{ST}=0$ K and P, in the other case, as well as their relation to the effect

of TSS it can be stated that their significance is, by definition, unambiguous, and characterising the regularities of changes in structural PT, but the position of the lines and points is of sign-alternating character. This is the proof of regularities in the conformities and differences of the investigated samples.

The investigation results make it possible to conclude that in the chemical compositions of multicomponent magnet-containing systems subjected to a specific treatment, the symmetry-lattice peculiarities of the structure are formed, when the structural PT are formed and changed with the variety of properties, effects and anomalies. This happens under the influence of T-H-P by the laws of elastic stresses.

The grounded analysis of the results of experimental investigations, where the significance of elastic stresses has been revealed, is very helpful. It differentiates between real and unreal models and their theoretical substantiation. The understanding of such regularities in thermodynamic influence of T-H-P helps in the improvement of potentialities of thermodynamic and phenomenological methods for the sake of elaboration of new models and theories.

7.9. Conclusions

The carried out analysis of the experimental results for $La_{0.7}Ca_{0.3}MnO_3$ and their analogies, such as $LaMnO_3$, $CuCl_2 \cdot 2H_2O$, makes it possible to tie together the chemical-and-technological as well as the symmetry-lattices peculiarities of the samples, the electrical, magnetic and other properties through the elastic properties. The revealed role of T-H-P effect in their conformities for the properties and PT through the mechanisms of elastic stresses in both a relatively high-temperature and a low-temperature regions for substances of different classes makes the generalization of the obtained results possible.

By the investigation results on the behaviour of resistivity in $La_{0.7}Ca_{0.3}MnO_3$ and of magnetostriction in $LaMnO_3$, it has been noted:

1. a relative adequacy and conformity of T-H-P influence of the resistive properties of $La_{0.7}Ca_{0.3}MnO_3$ samples (5.1 K~2.42 kOe~1 kbar), as well as $La_{0.9}Mn_{1.1}O_3$ samples (6.2 K~2.7 kOe~1 kbar), and $La_{0.56}Ca_{0.24}Mn_{1.2}O_3$ samples (6.2 K~2.37 kOe~1 kbar) [147, 150, 151];
2. regularities of “cooling”, “heating” effects, constancy of T_{PP}, the temperature of maxima on the dependencies of baro-, magneto-, baromagnetoresistive effects, its equality to T_{ms} – the temperature of the metal-semiconductor phase transition, the differences being related to those in anisotropies of elasticity and magnetoelasticity;
3. regularities for EAD stresses and differences in anisotropies of elasticity and magnetoelasticity for changes in $T_{ms}(H)$ and $T_{ms}(P)$;

4. an adequate influence of H and T (2.5 kOe~5.2 K) on the magnetostrictive properties in $LaMnO_3$ single crystal;
5. a regularity in changes of hysteresis parameters $H_g(T)$ as a function of T and H in the region of PT, the role of equality and inequality of elastic and magnetoelastic anisotropies in T_C – to the Curie temperature;
6. a correspondence between $H_g(T)$ and T_{ms}, substantiation of "heating", "cooling" effects in magnetic properties prior and past the PT, as a result of the influence of magnetic field;
7. a sign-alternating competing influence of thermo- and magneto- elastic stresses on changes in properties and structural PT at T_C.

The results of the analysis of the experimental investigations of magnetization and high-frequency properties under the influence of hydrostatic pressure, magnetic field and temperature in single-crystalline $CuCl_2 \cdot 2H_2O$ have revealed:

- the linear regularity for changes in PT on $T_P(H)$, $T_P(H,P)$ dependencies, the estimates of conformities in T-H-P (1 K~4 kOe~3 kbar) effects;
- significance of thermomagnetic and thermobaromagnetic effects with the maxima at point T_{PP} that corresponds to the temperature of structural phase transition T_{ST}=0 K;
- the role of "cooling", "heating" effects in the properties of magnetization and of sign alternation for changes in PT under the influence of H and P on $T_P(H)$, $T_P(H,P)$ dependencies;
- critical point P as a result of regularity in correspondence for the elastic and magnetoelastic anisotropies with temperature parameter T_P=9.2 K.
- a regularity in changes of magnetization determining the effect of thermo-elastically strain striction (compression) (TSS)– is a result of relationship between chemical-and-technological and symmetry-lattice peculiarities, as well as of T and H effect on changes in structural PT;
- the basic role of elastic stresses in a single-valued and sign-alternating influence of T and H on changes in magnetization prior and past the PT, as a consequence of TSS effect;
- the role of regularity in T and H effect through the mechanisms of elastic stresses on high-frequency properties explaining the existence of two resonances on the properties prior and past the PT;
- regularity of the competing mechanisms of thermo- and magneto-elastic stresses and TSS effect during the construction of phase diagrams.

The reasoning from the analogies between various critical lines and points for the investigated samples has revealed:

- the roles of critical lines and points in a general problem of studying the physical processes and regularities;
- a variety of critical points T_X, P_X, PP_X, T_C, $H_X(T=0)$ and lines $T_{ms}(H)$, $T_{ms}(P)$, $H_g(T)$ and their relation to peculiarities of composition and structure to resistive, magnetic properties and PT through the mechanisms of elastic stresses;
- conformity and sign alternation in changes of properties and PT represented on critical lines $T_{ms}(H)$, $T_{ms}(P)$, $H_g(T)$ and at points T_X, P_X, PP_X, $T_{ms}=T_{PP}$, T_C and the role of the mechanisms of elastic stresses from T, H, P effect in magnetic semiconductors;
- a variety of critical lines $T_p(H)$, $T_P(H,P)$ and points T_X, P_X, PP_X, $H_X(T=0)$ and P;
- conformity and sign alternation of a competing influence of T and H observed in changes of properties and PT on critical lines $T_p(H)$, $T_P(H,P)$ and at points P_X, PP_X, $T_{PP}=T_{ST}=0$, critical point P (with $T_P=9.2$ K) showing the role of the mechanisms of elastic stresses from T, H, P effects in magnetodielectric;
- conformity and sign alternation in the location of critical points T_X, P_X, PP_X, $H_X(T=0)$, T_C, P and lines $H_g(T)=T_{ms}(H)$ and $T_P(H)$ in the investigated samples show the identity of T-H-P effect through the elastic stresses and the regularities in position of structural phase transitions with the TSS effect taken into account.

The described results enable us to make a generalizing conclusion.

The found regularities in properties, PT, effects, anomalies are a consequence determined by the chemical composition, manufacturing technology, symmetry-lattice peculiarities, presence of magnet in multicomponent systems. In these objects and not only there, the influence of T-H-P through values of thermo-, magneto-, baro- elastic stresses results in regular structure changes directly connected with anisotropy of elasticity and magnetoelasticity. This is a causal basis for all the regularities that should be taken into account during the analysis of investigation results within various thermodynamic and phenomenological models and theories, what is very important for the kinetics of microprocesses.

It can be stated without exaggeration that such interpretation of the experimental results shows that it is necessary and very important to take the revealed regularities of thermo-, magneto-elastic stresses into account, as they are forming and changing the properties and phase states. The understanding of these regularities allows us to predict the participation of the same mechanisms in realization of long-studied effects of a colossal magnetoresistance (CMR) and of conductivity in HTSC structures.

By drawing analogies for the influence of the mechanisms of elastic stresses, in manganites and copper chloride dihydrate, on the dynamics of changes in structural phase transition, properties, effects, with the revealed critical lines and points taken into account, it can be stated that there exist the laws of bulk elasticity. Here we agree with the authors of paper [135] that the understanding of the obtained results would favour a quicker and a forecasted application of the results to elaborate new models and theories, to substantiate various interesting phenomena and effects in solid-state physics.

This conclusion means that the revealed regularities can be used for studying a wide class of substances. Their application would promote the revealing and understanding of physical processes in solid-state physics and would interpret the law of correlated states as that of the elastically deforming conformities, and the revealed regularities in the influence of temperature, magnetic field, pressure as the laws of elastic anisotropically deforming stresses and of sign alternation. And, finally, the constancy of T_{PP} – as the law of elastic and magnetoelastic anisotropy conformities.

Chapter 8

The role of bulk elasticity in the mechanisms of the realization of the structural PT

Introduction

At present, the number of papers dealing with the study of magnet-containing multi-component manganite systems increases due to high experimental potentialities. Some uncertainty presents in the form of anomalies, peculiarities, numerous effects with contradictory interpretation of mechanisms of the colossal magnetoresistance (CMR) realization. While studying magnetic–phase states, an attempt was made to relate the formation of the CMR state to the changes of the bulk magnetostriction in single crystals of different manganites, as noted in reviews [171, 172] and papers [173-175]. But it is not clear what phases and mechanisms are responsible for the changes. A number of anomalies, effects, features have been revealed for manganites modified by different chemical additives of varied percentage, e.g. giant negative magnetostriction, identity of modification of electronic properties influenced by both the temperature and the magnetic field H. Unfortunately, the role of phase transition (PT) has not been understood and grounded completely in the course of analysis and substantiation of the majority of anomalies and effects in properties where the main attention was paid to the determination of strong bonds between unfilled electron shells and to their reaction to the influence of thermodynamic parameters with magnetic properties taken into account. Moreover, an interpretation of the Curie temperature was indistinct to some extent. The interest to the correspondence between hydrates and manganates with respect to similarities and divergences of lattice and magnetic effects was shown in review [172]. The conception of two co-existing phases was used as the approach to the analysis of colossal magnetostriction phenomenon. The elastic energy was separated from the Hamiltonian and omitted, being replaced by the term of phonon degrees of freedom.

The results of investigations of peculiarities are demonstrative for magnetic and electric properties [175]. Here the colossal magnetoresistance in $Sm_{1-x}Sr_xMnO_3$ (x=0.45) was explained by high negative bulk magnetostriction, and changes in parameter (x) are considered as a correlation of magnetoresistance, magnetostriction, magnetization resulting in anomalies and singularities. Paper [176] is of a special interest, where peculiarities of semiconducting regions with varying conduction current in $Eu_{0.7}Sr_{0.3}MnO_3$ were analyzed and an original explanation of a giant maximum on the

isotherms within the low-temperature range was suggested. Besides, the differences were shown between magnetization at varied temperature of the sample with the field and without it, which are typical for the studied system from the viewpoint of the authors.

The role of the oxygen-isotopic substitution in the $Sm_{1-x}Sr_xMnO_3$ system was studied in [177], where peculiarities of the metal – dielectric transition and regularities of changes of the low-temperature phase of a unclear nature were substantiated.

In [9, 6, 181, 182], new approaches and explanation have been used to study T-P-H influence on properties and PT in single–crystal samples of low-temperature magnetodielectric $CuCl_2 \cdot 2H_2O$, magnetic semiconductor $LaMnO_3$ and its analogues.

An impact of bulk elasticity mechanisms on the structure has been shown to be identical. In the mentioned papers, the specified variety of critical lines and points underlined the causal basis of the mechanisms of elastic stresses and their role in processes of a sign inversion, change of parameter priorities, and a sign inversion of thermodynamic parameter effect on the properties in different phase states. The direct correlation was supposed to exist between changes of the structure, magnetic and electronic properties; the dominating role of mechanisms of bulk elastic stresses was grounded. Numerical values of P-T-H impact were suggested, a correspondence was established between the linear change of properties and critical lines for $La_{0.56}Ca_{0.24}Mn_{12}O_3$ (1kbar- 6.1 K – 2.3 kOe), $CuCl_2 \cdot 2H_2O$(3 kbar – 1 K – 4kOe), $LaMnO_3$ (5.2 K – 2.5 kOe). The role of thermoelasticity, magnetoelasticity, baroelasticity was shown separately.

It should be noted that just results [6] generated new approaches to the grounding of the specified critical points. In [181], it was shown that the binding energies of electrons located from the center to a periphery of an atom or a molecule differed by two and more orders of magnitude as followed from the analysis of P-T-H impact and general conclusions. This tendency of the binding energy was less noticeable for peripheral electrons participating in the formation of a lattice structure of a multi-component system. It relatively agreed the energy of elastic stresses, a decisive factor of any thermodynamic influence. The results allowed us to conclude that any construction of model theoretical presentations remained incomplete without an account of the causal role of volume changes of the structure forming the PT and properties under the T-P-H influence.

In order to emphasize the role of bulk elasticity laws of for properties and PT, we should draw attention first to the following example given as early as 1931. P.A. Kapitsa [178] and noted a high interest in the results of studies of resistance changes in different metals under high magnetic fields. In some cases, the resistance value was shifted by 20-30%. In the field, the resistance changed linearly. It was found in another study of magnetostriction in high

fields for bismuth that the parameter (tension) changed along a trigonal axis while the compression was normal to it.

Unfortunately, methods of investigations under the hydrostatic pressure were far from being perfect at that time. Our result shows only a combined T-P-H effect through mechanisms of ED stresses. It provides an objective consideration of physical processes; otherwise, new approaches cannot be elaborated. Far in the past, the lack of experiment could not give an impulse to the development of model-theoretical representations to substantiate real physical processes.

The object of the present paper is an analysis, drawing analogies and generalization of regularities of an evolution of structural phase transitions and properties in multi-component structures of magnet-containing systems of $CuCl_2 \cdot 2H_2O$, $Eu_{0.55}Sr_{0.45}MnO_3$, $Sm_{1-x}Sr_xMnO_3$. It is also aimed at the presentation of unambiguous T-P-H impact through mechanisms of EAD stresses and settling the question of the presence of anomalies and regularities in view of the laws of the bulk elasticity. We will also specify the peculiarity of a structural phase transition at T=0 K and an opportunity to treat this critical point as a triple one.

As the considered problem is ambiguous, I should like to cite academician P.L. Kapitsa: ”Science develops as follows - the ascertained facts remain unshakable, while theory is constantly changing, developing and is under revision. The most powerful spur to the development of a theory is from a new experimental fact which contradicts a settled view…”. So, the main motive power in the development of physics is the search for and the revealing of contradictions.

8.1. The regularities of the elastic properties in the processes of formation of direct and inverse hysteresis effects

Numerous studies of copper chloride dehydrate $CuCl_2 \cdot 2H_2O$ [6, 64, 181] were taken as a basis for drawing analogies and correspondences in mechanisms and regularities of changes of structural phase transitions and properties of the mentioned multi-component magnet-containing systems. The interrelation of elastic mechanisms was established for the joint thermodynamic influence of P-T-H on multi-component magnet-containing structures.

Let us pay attention to [64, 65] where X-ray diffraction studies were done under hydrostatic pressure. Basing on experimental results, the authors have directly evaluated numerical parameters of bulk elasticity and estimated both the changes of elastic properties along the considered directions and the anisotropy of compressibility in $CuCl_2 \cdot 2H_2O$ orthorhombic single crystal at room temperature. Considerable changes in position of the resonance

absorption lines were revealed by resonance methods due to an important factor of the shape and relationship of parameters in the sample [187]. The role of elasticity anisotropies in the bulk was stated to be the decisive one for the formation of the position of PT and for changes of magnetic and electronic properties, as believed. This was the reason of considerable differences in the results for bulk samples as compared to films of the same composition.

In [6], the method of analogies and comparison was used to set up a correspondence between changes in magnetostrictive properties in $LaMnO_3$ and magnetization in $CuCl_2 \cdot 2H_2O$. The causal role of thermoelasticity and magnetoelasticity in mechanisms of the effect on regular linear changes of properties has been specified (Fig. 8.1a, 8.2a). Note that there was a very important regularity of the identical effect of T and H on both the magnetostriction dependence (Fig. 8.1a) prior to phase transition and on magnetization properties (Fig. 8.2a) after the phase transition. It can be assumed that the considered areas have identical mechanisms of the effect and belong to the conducting (metallic) phase in the region where changes of the properties under H and T impact are antipodal. One more very important result has been established for magnetization properties at the initial part of the dependence (Fig. 8.2a). The stable tendency of evolution of the properties under unambiguous T and H influence was separated and the sign reversion of the position of the critical line of the field – temperature dependence with critical point $P(T_P, H_P)$ was found. An essential jump of the properties was observed at this line, and the position of the structural phase transition area was determined by T_{st} equal to 0 K, according to the approximation method. These regularities were believed illustrating that changes revealed in this region affiliated it to the superconducting phase. Such statement implies new approaches to the substantiation of regularities for phase diagrams [6, 181], low-frequency properties at 0^oK and at specified temperatures in $CuCl_2 \cdot 2H_2O$. These important results emerged from new methods of an analysis where elastic linearity appeared to be defining for changes of properties. The corresponding plots do not contradict the logics of reversible physical processes under study in principle, making it possible to distinguish the structural phase transition in $LaMnO_3$ T_x (H_x, T=0 K) and in $CuCl_2 \cdot 2H_2O$ T_x (H_x=5.5 kOe, T=0 K).

Since it is a problem to obtain experimental results just at 0 K, it is very important to find general signs of evolution of properties accompanying PT that are formed under T-P-H impact (so-called secondary indications). The presence of these signs in another systems and samples will help in defining the generalizing role of the mechanisms of EAD stresses in structural transformations. So we could distinguish these regularities with full confidence in a large number of papers where the authors considered them as effects, anomalies and peculiarities.

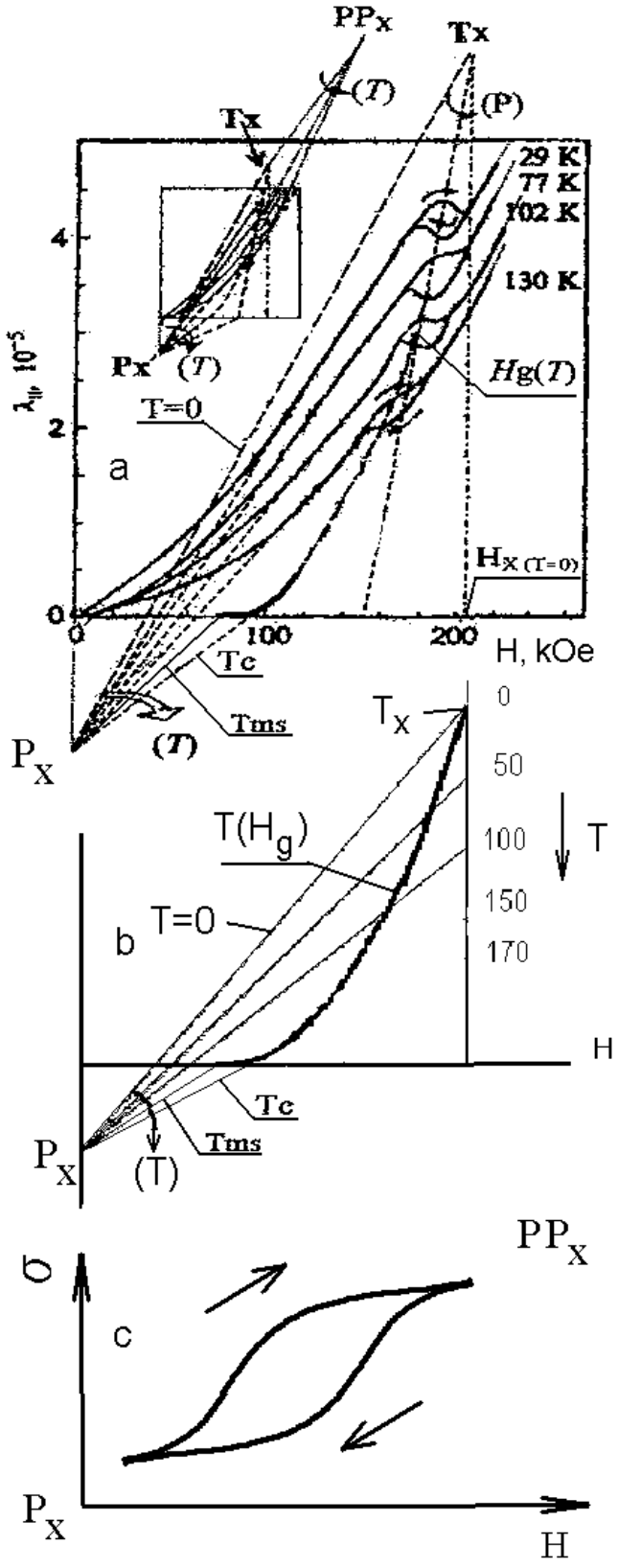

Figure 8.l. a) Field dependences of the longitudinal magnetostriction for $LaMnO_3$; b) Field-temperature dependence $T_p(H_g)$ of PT. c) Dependence of magnetization change in hysteresis effect.

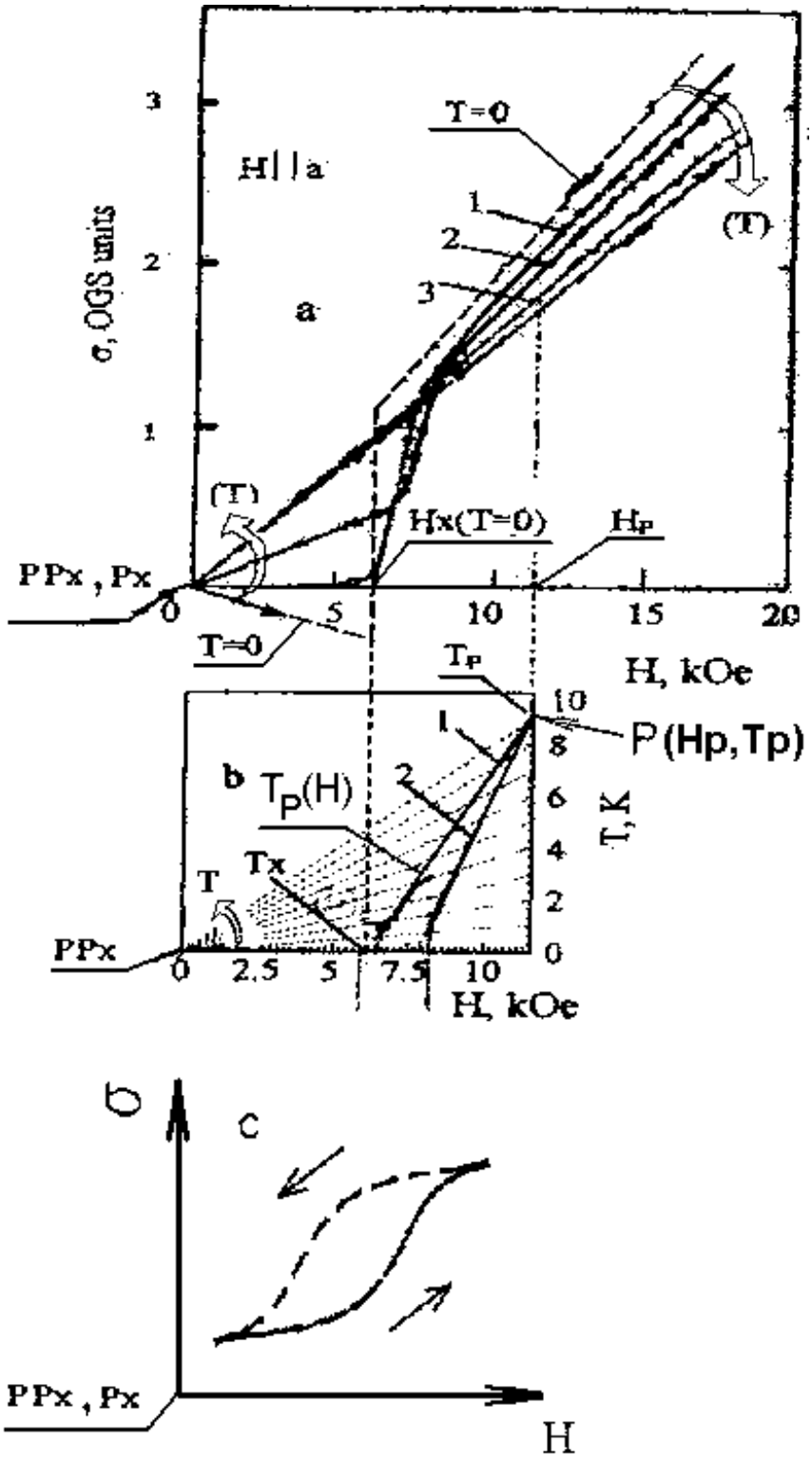

Figure 8.2. a) Field dependences of longitudinal magnetostriction for $CuCl_2*2H_2O$; b) Field-temperature dependence of changes in the phase transition $T_P(H)$, T_P (H, P) for P = 11,2 kbar in $CuCl_2*2H_2O$; c) Dependence of magnetization change in the effect of inverse hysteresis in $CuCl_2*2H_2O$.

It should be added that the analysis of the mentioned dependences illustrates the relation between the features of magnet-containing structure and the positions of critical points P_x, PP_x on Fig. 8.1a, 8.2a. Both the content of magnetic material and structural changes connected with the composition and technology of sample preparation displace the position of critical points P_x, PP_x and T_x (Fig.1a,b) and metal – semiconductor interfaces, as a consequence of critical lines in the form of PT field-temperature dependences $T(H_g)$. That is why the point of PP_x and P_x coincidence (Fig. 8.2a,c) as well as the sign reversal of position of the critical line of PT field – temperature dependence $T_P(H)$ shows that the critical line separates both the conducting (metallic) phase and, I suppose, the superconducting phase in this case. The result qualifies the effect of thermo-elastically deforming compression as regularity of antiphase temperature impact and points to a peculiarity of the structure and the anisotropy of EAD stresses. It also emphasizes their causal role in formation of essential changes such as a jump in the region of PT at 0^oK. With regularities revealed for a model structure, new multicomponent systems are to be found where similar mechanisms of the effects repeat conditions for the formation of structural PT and changes of properties.

One of the examples of considering the revealed regularities of T and H impact through mechanisms of EAD stresses and the definition of the role of specified critical lines $T_P(H)$ and points P_x, PP_x is the analysis of various experimental results relating immediately to the modification of properties of direct and inverse hysteresis effect.

Prior to the consideration of the effect of the conventional hysteresis (Fig. 8.1a, c) on magnetostriction dependences in the area of the phase transition in $LaMnO_3$, we pay attention to the significance of the role of thermo-magnetically EAD stresses in mechanisms of the impact of thermodynamic parameters (T,H) determined and grounded in [6]. It was shown that P and H influence through “cooling – heating” effects and sign inversion, i.e. changes of priority of thermo – and magnetically EAD stresses in structural phase transitions, magnetic and resistive properties. A conformity of regular changes in magnetization has been determined in phase states (diagrams) of low- temperature magneto-dielectric $CuCl_2 \cdot 2H_2O$ [181].

These results and regularities as well as position of critical lines and points relating to $LaMnO_3$ properties rise a question of their role in hysteretic evolution near the structural phase transition.

Thus for $LaMnO_3$ magnetostriction behavior, the role of “cooling” effect from the magnetic field is related to regularities of P_x critical point at the initial section. It should be noted that the temperature change is in antiphase with the dynamics of evolution of magnetization properties influenced by H. The next regularity is the behavior of the dependence after PT in a new phase state

where the properties are changed in compliance with regularities of changes with respect to PP_x critical point (Fig. 8.1c).

At this section of the dependence, the properties are influenced by "heating" effect under the reverse run, i.e. upon magnetic field (H) release. In this case, the jump of properties follows directly from changes in the sample, but already with respect to the position of PP_x critical point where the properties return to the initial phase with the temperature rise (Fig. 8.1a, c).

This physical process is a conventional hysteresis in the region of structural phase transition. It is formed by regularities of mechanisms of elastic stresses and obeys the primary role of the critical points and lines.

The next example of the change of $CuCl_2 \cdot 2H_2O$ magnetization properties allows to find a regularity (Fig. 8.2a, c) corresponding to the effect of reverse hysteresis and to explain it from viewpoint of PP_x and P_x critical points and changes in $T_P(H)$ field-temperature dependence of the structural phase transition taken into account. The result shows that in our case, the dependence of the form of critical line separating $T_P(H)$ phases is controlled by the position of PP_x critical point (Fig. 8.2b); the changes of magnetization at the initial section belonging to the superconducting phase are regularities of magnetic field "cooling" effect, they are fixed in antiphase to T change with respect to the position of PP_x critical point (Fig. 8.2c).

There is one more phase change on the dependence of Fig. 8.2a, b with H increases: a jump in magnetization, but already in the metallic phase and with respect to a P_x critical point (Fig. 8.2c). As a consequence, there follows magnetic field H release at the expense of the elastic expansion. And the "heating" effect develops on magnetization dependence with respect to P_x accompanied with a phase change, but now in view of PP_x critical point. That is why the properties are unambiguously influenced by both T and H. This is a wide-spread result supported by the revealed regularities.

Such a conclusion is an example of a new definition of the effect of direct and inverse hysteresis studied for a long time. It detects the principle sources of changes of properties in the region of a structural phase transition, which are related to the position of PP_x and P_x critical points. The analysis gives a convincing proof of the role of mechanisms with investigated differences, it can be also a demonstrating example of the presence of secondary signs that confirm the causal role of EAD stresses in regularities of direct and inverse hysteresis.

8.2. The structural first-order phase transition in $Sm_{1-x}Sr_xMnO_3$ and $Eu_{0.55}Sr_{0.45}MnO_3$ systems

The analysis of magnetization dependences and critical PP_x and P_x points (Fig. 8.2a) before and after structural phase transitions shows that the influence of temperature change on properties prior to and after the PT is of a sign-

alternating character. It means that the magnetization increases with T and H increase first (any changes are to be considered with respect to a PP_x critical point). The temperature affects the magnetization value as well. As noted, these changes of properties are associated with the superconducting phase. The dynamics of T and H influence after the phase transition is in antiphase at the next section of the dependences where changes of properties are examined starting from P_x critical point. The magnetization increases with the field and decreases with the temperature rise. It follows that the changes of properties belong to superconducting (metallic) phase for both $LaMnO_3$ magnetostriction properties and $CuCl_2 \cdot 2H_2O$ magnetization on the mentioned sections. As a consequence, the critical line of $T_P(H)$ (Fig. 8.2b) was the interface between phase states with sign-alternating influence of the temperature. This result can also be considered as a secondary factor.

By drawing analogies in regular changes of magnetization properties for $CuCl_2 \cdot 2H_2O$ (Fig. 8.2a) and magnetization for $LaMnO_3$ (Fig. 8.1a) and marking the alternation of sign in position of $T(H_g)$ (Fig. 8.1c) and $T_P(H)$ (Fig. 8.2b) critical lines, we can conclude that:

a) in the first case, the field – temperature dependence $T(H_g)$ separates metallic and semiconducting phases;
b) in the second case, the structural phase transition realized at T_{st}=0 K and the field-temperature dependence $T_P(H)$ is none other than the interface (and what is important) between superconducting phase and conducting (metallic) one;
c) the critical line of $T_P(H)$ (Fig. 8.2b) which generalizes structural phase transition changes after the jump of properties and after the effect of thermoelastic – deforming compression (Fig. 8.2a,b) under the magnetic-field cooling effect, terminates at the fixed temperature T_P=9.2 K. The location of $P(T_P, H_P)$ critical point fixing the boundary position of a structural phase transition may be specified as the point of the intersection of approximated $T_P(H)$ and $T_P(H, P)$ critical lines.

The estimated role of secondary indications observed in changes of properties in the course of reversible physical processes in varied magnetic fields and temperatures as well as the determined position of critical points and their sequence PP_x and P_x in property change enables one to state convincingly that the primary influence of thermodynamic parameters T,H,P is a regularity of the mechanisms of EAD stresses.

Analyzing the regularities and determining secondary indications, we can treat the results of a number of papers [5, 175-177, 180] in order to trace anomalies and peculiarities. It should be noted that the experimental results refer to investigation of multi-component magnet-containing mono – and polycrystalline samples for the taken manganite compositions.

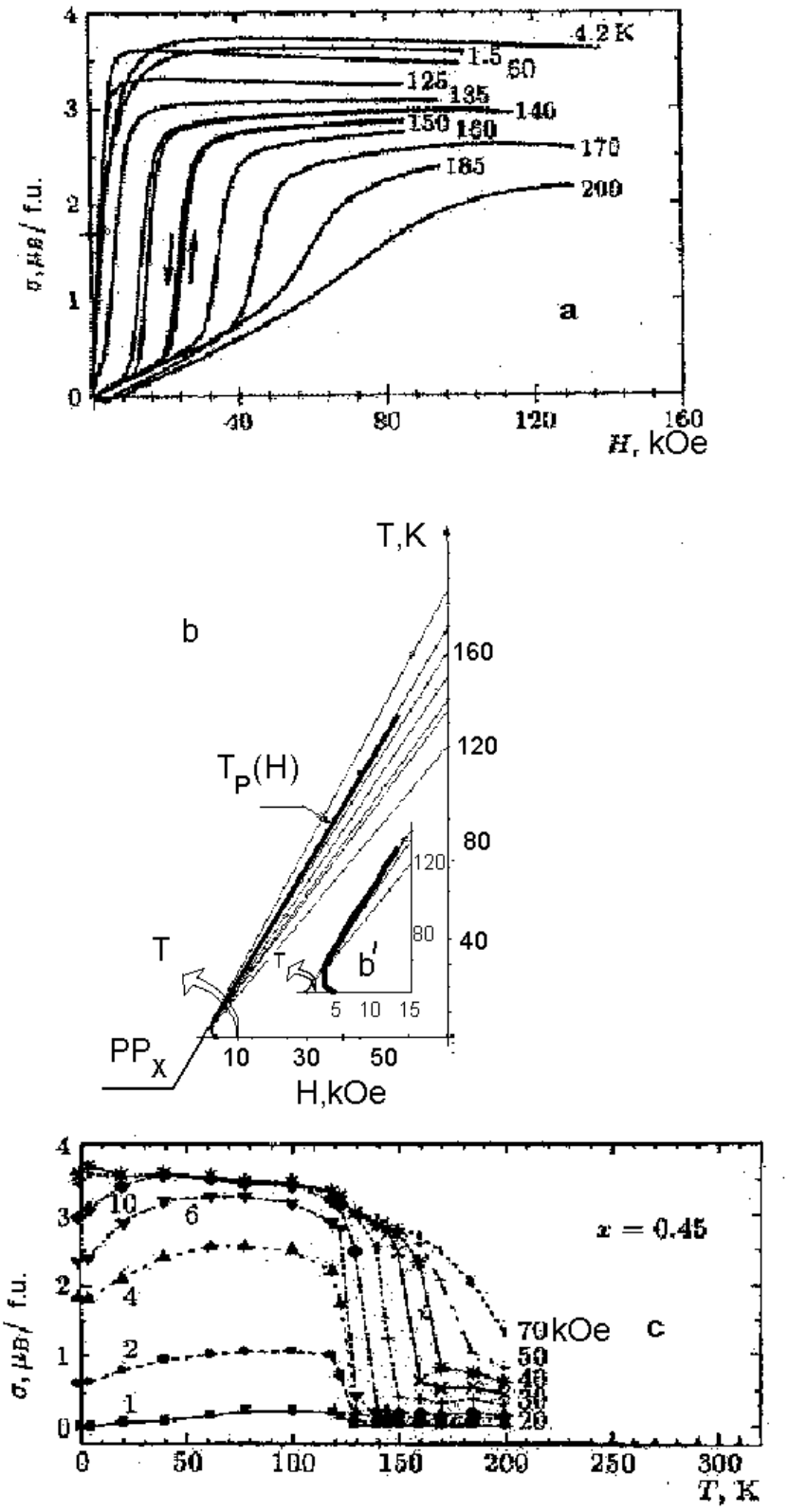

Figure 8.3. a) Magnetization isotherms for different temperatures in $Sm_{1-x}Sr_xMnO_3$ compounds for x = 0.45; b) Field-temperature dependence of changes in $T_P(H)$ - the phase transition in $Sm_{1-x}Sr_xMnO_3$; c) Temperature dependence of magnetization in variable magnetic fields.

For the analysis, the most demonstrative are experimental results for manganites of combined $Sm_{1-x}Sr_xMnO_3$ composition [175] with their peculiar magnetic, elastic and magnetoelastic properties. The authors consider dependences of changes of properties for samples with x=0.45. Magnetization isotherms (Fig. 8.3a) have a singularity in the form of a jump of properties at the initial section of the dependence for fixed temperatures. With H increase, a relative linearity at the region of saturation tends to maintain the magnetization, while the process of temperature growth changes the properties towards decreasing. The authors state that the maxima of conductivity on ρ(T) dependences change by several orders of magnitude at low temperatures for all the investigated compositions, and magnetoresistance of samarium manganites of the taken composition (as stressed by the authors) reaches colossal values in relatively low magnetic fields. For instance, the magnetoresistance makes 44% for composition with x=0.45 and H=0.84 kOe. The attention is attracted to a stable regularity of changes at isotherms (Fig. 8.3c) with a jump of properties at the initial section of the dependence for all H fixed. The conformities retain in the whole temperature range up to 125^oK. With changing T, the magnetization decreases in the region of the jump, i.e. with T increase in high magnetic fields, the magnetization diminishes linearly.

This result has made it possible to characterize and to substantiate the presence of general secondary indications in changes of properties of that structure:

a) the inverse hysteresis observed in the region of phase transition allows us to treat the changes as a structural phase transition with the typical field – temperature dependence $T_P(H)$ with changes occurring at PP_x critical point (Fig. 8.3b);
b) stable changes of magnetization isotherms after the jump of properties corresponding to PT, where the magnetic field enhances the properties whereas the temperature growth results in a significant decrease of the properties. It should be noted that this region of the phase state corresponds to the metallic conductivity;
c) regularities of the magnetization increase under T,H influence observed on Fig. 8.3c show that at the initial section prior to the structural phase transition, the changes of properties under T and H effect occur in one phase (in view of position of PP_x critical point). After the PT, the magnetization changes in antiphase to relative changes of T and H (Fig. 8.3b,c). This result repeats changes in the magnetization for $CuCl_2 \cdot 2H_2O$ (Fig. 8.2a,b).

Such regularities broaden the region of applicability of the specified critical lines and points and confirm the presence of mechanisms of EAD stresses in the formation and changes of first-order structural phase transition and properties, as a consequence.

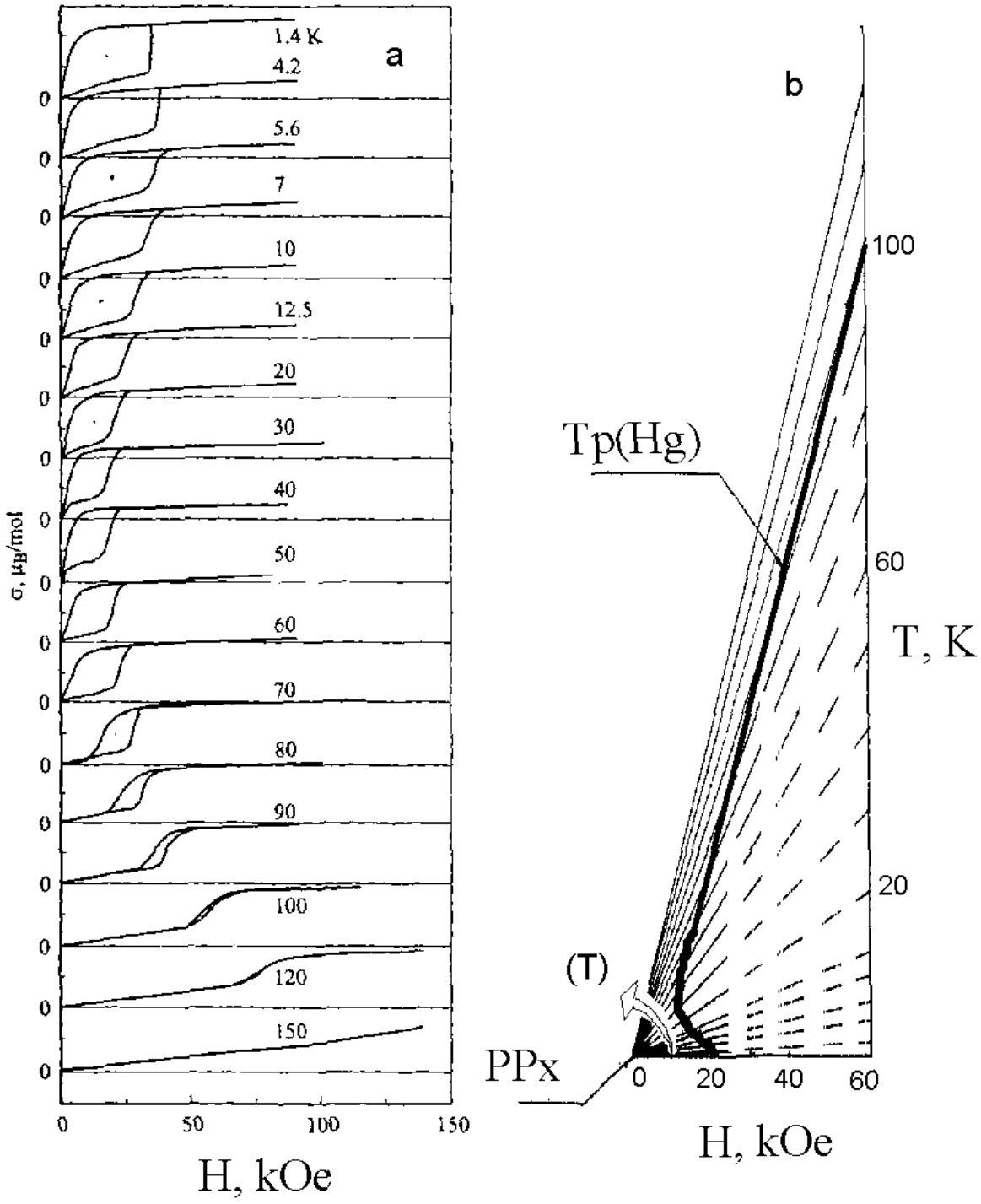

Figure 8.4. a) Magnetization isotherm for different temperatures in $Eu_{0.55}Sr_{0.45}Mn0_3$; b) Field-temperature dependence of changes in phase transition $T_P(H_g)$ in $Eu_{0.55}Sr_{0.45}Mn0_3$.

For further substantiation of regularities of elastic stresses in the formation and changes of structural phase transition and properties, we analyze magnetic, elastic, magnetoelastic, resistive and magnetoresistive properties of polycrystalline $Eu_{0.55}Sr_{0.45}MnO_3$ [176]. The paper presents a large bulk of experimental results. The authors show that the studied ceramics is a

polycrystalline single-phase perovskite of orthorhombic structure and, what is very important, they pay attention to the identity of the results to the properties of ceramic samples of other compositions: $Sm_{1-x}Sr_xMnO_3$ (x=0.4, 0.45), $EuMnO_3$. Let us examine the changes of magnetization (Fig. 8.4a) where hysteresis changes in magnetization jump within the temperature range of 1.4^oK-150^oK are explicitly seen on isotherms. Here we note the run of inverse (anomalous) hysteresis (Fig. 8.5b) analogous to the behavior of magnetization for $CuCl_2 \cdot 2H_2O$ (Fig. 8.2c). The authors suppose that the structure remains dielectric in a wide range of low temperatures according to the resistivity properties (Fig. 8.5a). This important notice enables us to assume that the structural phase transition at 0^oK can be triple-point regularity and magnetic field H displays a jump in magnetoresistivity through mechanisms of magneto-EAD stresses due to superconducting phase realization.

It should be noted that the resistivity should be much beyond the limits of changes in resistance with T decreasing, as follows from the logics of the experiment (Fig. 8.5a). Most probably, the sensitivity of measurements was not high enough to register the peak of ρ change at a level of 10^{10}-10^{12} at temperatures tending to 0^oK. And it is shown in fact that the temperature dependence of thermoelastic expansion is practically linear with the low-temperature measurement errors being taken into account (Fig. 8.5a).

The above result makes it possible to note one more regularity shown on T and H dependences of magnetization (Fig. 8.5d). Here we see a jump-like increase of the magnetization at the initial section of isotherms with H fixed as well as magnetization decrease with T rising at the final part of the dependence. These changes are similar to those on the isotherms of Fig. 8.2a. They are the regularities of unambiguous change of the magnetization as a function of T and H at the initial section of the corresponding superconducting phase with $T_P(H)$ critical line separating phase states and corresponding to PP_x critical point (Fig. 8.2b). The subsequent evolution results from the antiphase impacts of T and H in the conducting (metallic) phase, i.e. there is a sign-alternating temperature effect after the phase transition. In $CuCl_2 \cdot 2H_2O$, the behavior of properties is similar (Fig. 8.2a). The changes observed on magnetization isotherms (Fig. 8.5c) make it possible to consider this result as a secondary indication for this composition.

The analytical results emphasize peculiarities of formation of structural phase transition and make it possible to construct and to single out $T_P(H_g)$ field – temperature dependence basing on changes of parameters of inverse hysteresis, Fig. 8.4b. It is a regularity attached to the position of PP_x critical point. The critical line of $T_P(H_g)$ separates two phase states (superconducting and conducting (metallic) phases). It also displays the regularities of structural phase transition at $T_{st}=0^oK$ and it is a dependence of the dynamics of changes influenced by the position of the averaged magnetic field H_g determined in this paper.

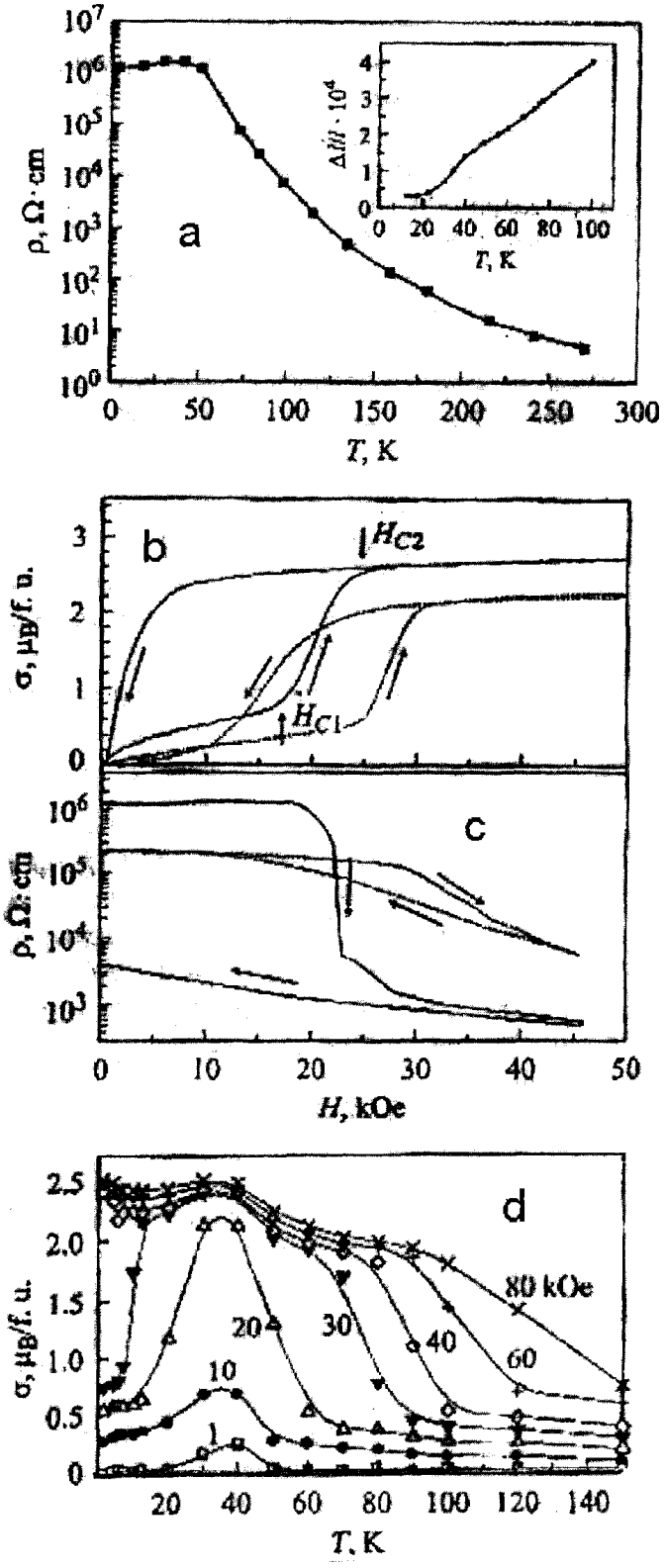

Figure 8.5. a) Temperature dependence of resistivity. Temperature dependence of thermal expansion in $Eu_{0.55}Sr_{0.45}MnO_3$. b) Magnetization isotherm p(H) in changes of inverse hysteresis for T = 20 K, 60 K; c) Isotherms of changes in electrical resistance (H) for T = 20 K, 60 K; d) Temperature dependence of magnetization p(T) in different magnetic fields.

It follows that the role of field and temperature influence through mechanisms of EAD stresses is a causal basis of volume change and the formation of structural phase transition and properties, as a consequence. Moreover, the position and sign alternation of critical lines and points determine the regularities of the impact in the form of changes of properties in both phases separated by the structural phase transition. Such an explanation implies that the role of elastically deforming stresses is the basic one as the binding energy directly corresponds to and interacts with elastically and anisotropically deforming mechanisms of volume change in this case. They are also the primary cause of PT changes and properties at the expense of mechanisms of thermoelastic and magnetoelastic effects of T and H.

An extensive experimental result [175] of studies of phase states and peculiarities of electrical properties in manganites of $Sm_{1-x}Sr_xMnO_3$ system was also treated in [177] in the course of investigations of a similar sample. The authors believe that the peculiar isotopic oxygen substitution helps in the identification of the metal - dielectric phase states. They pay attention to a composition with x between 0.4 and 0.5 where a jump of electrical resistance and sudden changes of the coefficient of volumetric expansion and magnetostriction were found out. High sensitivity of all physical characteristics to negligible composition changes, the lack of information for the explanation of properties of the above manganates have made us to propose the analysis of our own in view of the role of T-H-P influence through EAD-stress mechanisms. We take the data for $Sm_{1-x}Sr_xMnO_3$, x=0.500. For the sample with x=0.500 and isotropic substitution, there is a phase transition separating metallic and dielectric phases within the low-temperature range. And a relatively weak influence of external magnetic field on magnetostrictive dependence (Fig. 8.6a) via mechanisms of magnetoelastic compression brings the system to a new phase state and, what is important, the corresponding maxima of the electrical resistance have much decreased and shifted to the region of higher temperatures under the influence of H. The temperature hysteresis decreases as well. As the result of resistivity change is incomplete, we show changes of ρ for $T=0^oK$ (the dot-and-dash line) to be of the order of 10^{11}-10^{12} by approximation (Fig. 8.6a). This behavior of the dependence makes us to ascertain a regularity, that changes in thermoresistivity under magnetic-field effect (H=1T, 2T, 4T) fix the position of temperature maximum at T_{PP} point. The specified effect corresponds to T_{PP}=0 K on the dependences (Fig. 8.6a). So, we can state that the structural first-order phase transition is realized at 0 K in this sample.

It is also noted that the maximum MR is shifted in magnitude attaining colossal values for the mentioned samples. So, we can construct the field – temperature dependence of changes in PT showing the behavior of $T_P(H)$, Fig. 8.6c. It is the critical line separating superconducting and conducting phases

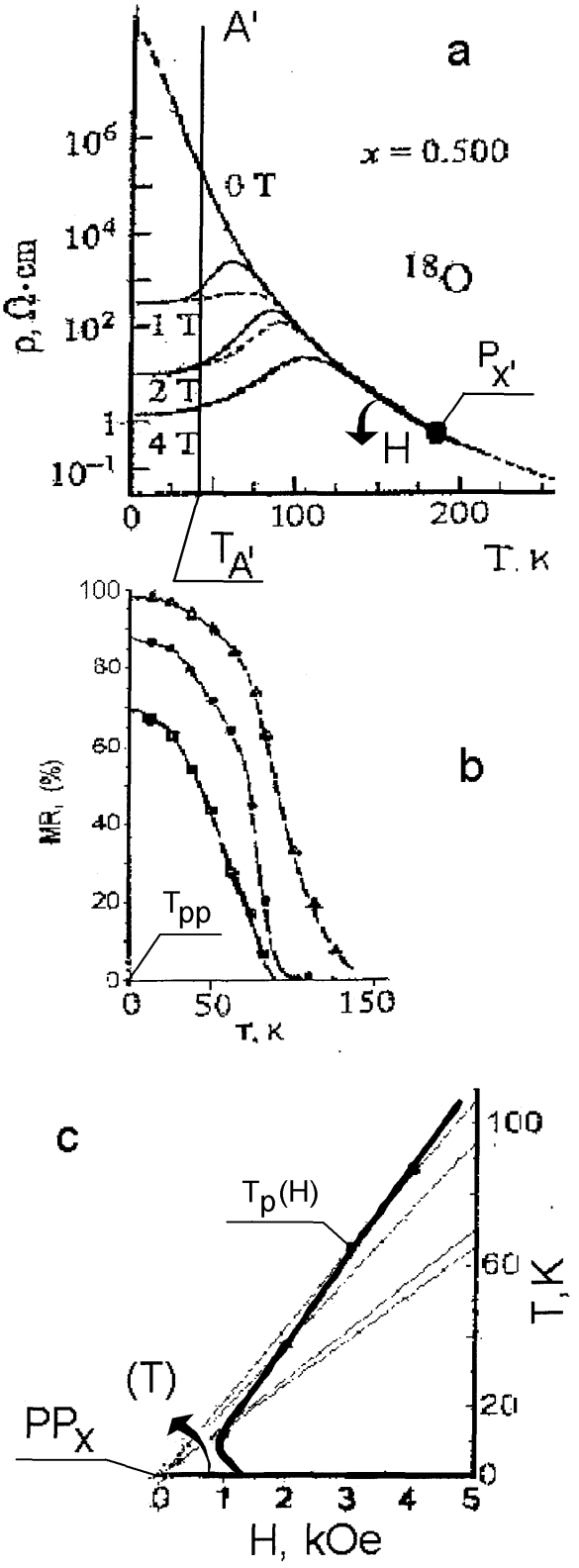

Figure 8.6. a) Temperature dependence of electrical resistance for $Sm_{1-x}Sr_xMn0_3$ samples (x = 0.500) with ^{18}O and magnetic field of 1 T, 2 T, 4 T; b) Dependence of magnetoresistive effects MR (%); c) Field-temperature dependence of changes in phase transition $T_p(H_g)$.

with the position directly related to PP_x critical point responding to a real physical process. The authors stress that both the peculiarities of crystalline structure and the obtained results are similar to properties of single-crystalline samples of $Sm_{0.55}Sr_{0.45}MnO_3$ composition [179] having the rhombic space symmetry as well. The authors note that there are no structural phase transitions in the temperature range of 1.4-300^oK but this statement is not entirely correct. It follows from our conceptions and secondary indications of T_{PP}-const=0^oK rule that the pointed critical temperature fixes the structural phase transition and $T=0^oK=T_{PP}$ responds to the position and properties of a triple point. The real character of the structural phase transition is $T_P(H)$ field-temperature dependence and changes of magnetic and electronic properties are consequences of peculiarities in different phase states revealed by the analysis.

With important factors of secondary indication taken into account, the given results make it possible, first, to show the role of T-H impact through mechanisms of EAD stresses and, second, to confirm convincingly the importance of the discussed critical lines and points and the role of bulk elasticity.

8.3. The causal role of regularities of the elasticity in the formation of the colossal magneto-resistivity

The consecqutive analysis of the effect of elastic stresses on the formation of structural phase transition and magnetic properties of the mentioned magnet-containing media raised a question, how the properties of conductivity behave at any changes of structure influenced by elastic stresses.

The demonstrative are results of [181] considering mechanisms involved in formation of the dynamics of resistive properties in magnetic semiconductors. The authors studied the behavior of resistivity in a bulk ceramic sample $La_{0.56}Ca_{0.24}Mn_{1.2}O_3$ as a function of three thermodynamic parameters T-P-H (Fig. 8.7a). The revealed regularities, with respect to the linearity in a wide T-P-H range, show the role of mechanisms of elastically deforming stresses in the region of metallic phase and, what is very important, make it possible to ascertain the correlations (6.3^oK-1 kbar-2.3 kOe). It follows that the hydrostatic pressure of ~18 kbar creates conditions at the expense of volume decrease, through mechanisms of backpressure, thus resulting in changes of conductivity properties, which are in turn analogous to the temperature decrease by ~120 K. Similar effect is observed in the case of magnetoelastic compression of 8 kOe corresponding to changes in resistivity analogous to temperature decrease by ~21^oK. As formulated, there is an important regularity in such processes, i.e. conductivity redistribution because of the relaxation of inner stresses during volume reduction. As the thermoelastic expansion is associated with considerable inner stresses, the

influence of elastic and magnetoelastic compression induced by the backpressure diminishes the inner stress. The process clarifies that any volume change due to thermoelastic, baroelastic, magnetoelastic compression relates directly to the inner-stress reduction in the system, while a volume decrease is directly related to the enhancement of the energy of atom-electron coupling, by definition.

On the dependence (Fig. 8.7a) the denoted important factor of a nearly double jump in the region of PT where the phase states are separated implies that changes have occured already in the semiconducting phase. Such changes of properties are based on the presence of structural phase transition in a reversible physical process. In this case, the regularity is the equality of temperature maxima of thermobaroresistive, thermomagnetoresistive and thermobaromagnetoresistive effects $T_{PP}=T_{mc}$ that corresponds to the temperature of the structural phase transition. It can be consequently stated that the regularity T_{PP}-const is the law of conformity conservation for elasticity and magnetoelasticity anisotropies, which was first proved in [6] (Fig. 8.7b).

Next, the shown critical lines of $T_{ms}(P)$ and $T_{ms}(H)$ are regularities of phase state separation and dynamics of their changes under the influence of hydrostatic pressure and magnetoelastic compression (Fig. 8.7a). It is obvious that the field-temperature and thermobaric dependences reflect mechanisms of elastic stresses and the important role of thermo- and magnetoelasticity anisotropy participating in the processes. It is stressed that the dynamics of both the jump and resistivity reduces in two coexisting phases under P and H effect.

Now we consider typical changes of properties of semiconducting phase. Here we single out P_x point of intersection of the dependences by means of approximation. The critical state defines the relation between T-P-H induced change of properties and the real physical process of elastic-compression mechanisms. It means that any changes in volume towards reduction, e.g. a decrease of temperature parameter, affect the regularities of changes of properties in a way similar to hydrostatic pressure P effect and magnetic field H effect through magnetoelastic compression. These mechanisms directly relate to changes in volume and correspond one to another. As a consequence, it can be stated that position of P_x' critical point functions as a relatively conforming equality of interacting binding energy and energy of elastic stresses in the system.

It follows that a decrease in volume at the expense of the revealed mechanisms of T-P-H influence modifies the binding energy of the atomic-electron system, and the structural phase transition separates a large symmetry volume in one phase from a smaller symmetry volume in another new phase. The extent of changes depends on values of thermo-elastic stresses.

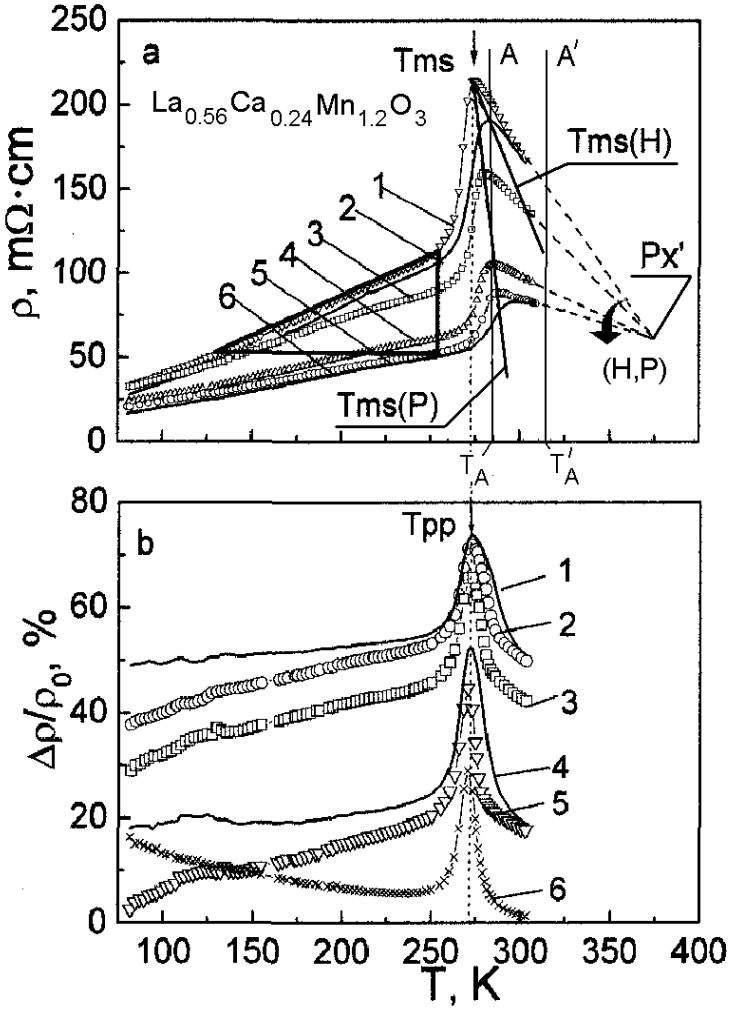

Figure 8.7. a) Temperature dependence of resistivity of $La_{0.56}Ca_{0.24}Mn_{1.2}O_3$ ceramic sample: 1 - P = 0 kbar; 2 - P = 0, H = 8 kOe; 3 - P = 6 kbar; 4 - P = 12 kbar; 5 - P = 18 kbar; 6 - P = 18 kbar, H = 8 kOe; b) Temperature dependence of baroresistive, baromagnetoresisitive, magnetoresistive effects: 1 - H = 8 kOe, P - 18 kbar; 2-P-O, H = 8 kOe; 3 - P = 12 kbar; 4 - P = 6 kbar; 5 - P = 6 kbar H = 8 kOe; 6 - H = 8 kOe.

Methods applied for revealing regularities in the formation and changes of structural phase transitions, for determining the metal-semiconductor, dielectric-superconductor-conductor phase states, as well as triple point positions enable us to show the role of magnetoelastic mechanisms in the colossal magnetoresistance effect by means of the results of changes of resistivity:

a) to begin with, we pay attention to the behavior of dynamics of dependences of resistivity change under T-P-H effect (Fig. 8.7a). With changing T and P, we have a region on $T_{mc}(P)$ dependence marked by T_A temperature. Following the change of pressure with respect to P_x' critical point, it is stated that with P increase, including the “cooling” effect, we

observe resistivity change for fixed T_A and this corresponds to the semiconductor-metal phase transition. The process is fixed by a sudden (not so high jump) change of properties n $T_{ms}(P)$ critical line. Similar regularity of changes in resistivity properties is found at T_A and in the "cooling" effect of magnetoelastic compression by magnetic field H. A sudden (jump-like) resistivity change will be observed during semiconductor-metal transition through the critical line of $T_{mc}(H)$, Fig. 8.7;

b) following result is the most demonstrative and the analogy can be drawn by regularities of changes of properties according to investigations of electrical resistance for $Sm_{1-x}Sr_xMnO_3$ (Fig. 8.6a). With T_A' fixed, the "cooling" effect results first in dielectric-superconducting transition and there occur more essential changes in this range with further H increasing, i.e. resistivity reduction under the influence of mechanisms of magnetoelastic stresses. The process of the change of properties becomes apparent by a noticeable resistivity jump in the region of phase separation where $T_P(H)$ critical line has an intersection.

That are these regularities that explain the behavior of resistivity isotherms P(H) in a wide range of magnetic fields. This is illustrated on Fig. 8.5a by dependences for fixed $T_1=20^oK$, $T_2=60^oK$ in $Eu_{0.55}Sr_{0.45}MnO_3$. At the initial section for $T_1=20^oK$, the change of properties with H increase corresponds to regularity of the "cooling" effect, when it is obvious that resistivity ρ is invariably high, so it is the dielectric phase. We note that there is a jump of resistivity in the field of 20 kOe (Fig. 8.5c) that conforms the field-temperature dependence of the structural phase transition toward the superconducting phase with a considerable reduction of resistivity at the field raising. During the inverse process of H decrease (Fig. 8.5c), the "heating" effect presents in resistivity properties as a transition from superconducting to conducting (metallic) phase followed by changes in the region of dielectric phase with $H\rightarrow 0$. Thus, it can be noted that the mechanisms of magneto-elastic stresses relate directly to conductance and they are the primary cause of the colossal magnetoresistivity effect currently studied.

An analysis of changes of properties represented on Figs. 8.7a and 8.6a attracts out attention to dynamics of resistivity change in semiconducting phase and to the position of critical point P_x' (Fig. 8.7a) and dielectric phase on isotherms of electrical resistance (Fig. 8.6a). This result clearly shows the scheme of changes of properties in the course of volume reduction as a result of T decrease and P increase. Similar result is observed in the case of H effect. In other words, the influence of these parameters on structural changes occurs involving the elasticity. This influence is unambiguous and conformal. The correspondence allows us to take P_x' critical point into consideration and to represent P and H effects by mechanisms of baroelastic and magnetoelastic

compression backpressure. It should be noted that anisotropy of thermo- and magnetoelasticity plays the principal role in the formation of structural phase transition, and the anisotropy of elastic stresses creates conditions for volume decrease in a reversible physical process. It is also an important factor for concentration of stresses preventing the mobility of conduction electrons in both semiconducting and dielectric phase till the boundaries where the structural phase transition develops accompanied by jumps of heat capacity and properties.

A consecutive determination of the role of elastic stresses (compression) reveals regularities for the discontinuity of structure in the range of PT in a reversible physical process [182 – 184]. There is also a jump of properties (heat capacity) and temperature increase giving negligible changes of properties due to high stresses developed in the system, as shown by our analysis. This is also indicated by the observed accordance of temperature-to-pressure correlations and by a comparatively low binding energy. At low temperatures, such changes occur in the form of a large jump of properties due to low energies of elastic stresses but with enhanced binding energy.

8.4. Secondary signs of the structural phase transitions and their role in the establishing of the regularities of ED stresses

The performed analysis makes it possible to generalize and systematize the results of ascertaining of secondary indications in regularities of magnetic, elastic and magnetoelastic properties in $Sm_{1-x}Sr_xMnO_3$ compounds [175], they are:

a) inverse hysteresis is fixed, the jump in properties and the tendency of magnetization decrease with temperature growth are observed (Fig. 8.3a);
b) unambiguous growth of magnetization properties under T and H effect (the initial section of the dependence) is present as well as sign-alternating change of properties under the influence of H and T after the jump in properties. Temperature parameter affects the properties of different phase states in antiphase (Fig. 8.3c);
c) the regularity of changes in the field-temperature dependence $T_P(H)$ is revealed by averaging the position of jump of properties with the typical role of the initial point relating to PP_x under the temperature change in angular coordinates (Fig. 8.3b,c);

Similar results with the revealed regularities corresponding to secondary indications have been observed in studies of peculiarities of magnetic, elastic, magnetoelastic properties in $Eu_{0.55}Sr_{0.45}MnO_3$ compounds [176]. Here we note dependences obtained at $T=1.4^oK$, that are close to those for $T=0^oK$:

a) the parameter was changing linearly within the whole interval of measurements because of thermoelastic compression (Fig. 8.5a). The method of approximations makes us to show the maximum of resistivity at the level of 10^{11}-10^{12} in dielectric phase (Fig. 8.5a);
b) considerable and obvious changes of the inverse hysteresis were present on the magnetization isotherms including T=1.4^{o}K, as well as the typical reduction of properties with T increasing (Fig. 8.5c);
c) unambiguous growth of magnetization with T and H increase was observed at the initial section of the dependence followed by the antiphase effect of T and H at the final stage (Fig. 8.5d);
d) the analysis of the dynamics of changes on magnetization isotherms (Fig. 8.4a) makes it possible to mark and represent the regularity of the field-temperature dependence as $T_P(H_g)$, i.e. as the critical line of the structural phase transition with T_{st}=0^{o}K, separating superconducting and conducting (metallic) phases with the typical position of PP_x critical point and respective change of the temperature.

It should be added that the observed character of evolution of properties and the determined critical temperature T_{st}=0 K meets the requirements set forth for the formation of superconducting and conducting phase. It is also a regularity satisfying the conditions of the triple point.

Hence, it can be concluded that one more critical point P with H_P and T_P coordinates can be taken into account for the samples under investigation. This point was shown first in [6] and determined by approximation and intersection of changes in the field-temperature $T_P(H)$ and field-baro-temperature dependences $T_P(H,P)$ presented on Fig. 8.2b. To determine such a point in studied structures, a cycle of investigations of properties and PT influenced by thermodynamic parameters T-H and by one important parameter (the hydrostatic pressure P) should be performed.

By extending potentialities of the analysis on revealing secondary indications, the same regularities can be found in so-called anomalies of magnetic and magnetoelastic properties in $Nd_{1-x}Ca_xMnO_3$ single crystals in strong magnetic fields [180]. The represented dependences of magnetization for composition with x=0.45 demonstrate inverse hysteresis of change of properties and make it possible to show definitely that changes of the field-temperature dependence of PT are in correspondence with respect to PP_x critical point. It should be noted that magnetization decreases with temperature rise, and $T_P(H_g)$ field-temperature dependence is a consequence of temperature of the structural PT detected at 0^{o}K. The results to be analyzed might be more reliable provided investigations accounting for selected directions. The same conclusion follows from the analysis of properties and anomalies of changes of phase transitions in $La_{1-x}Sr_xMnO_3$ single crystals [6].

While analyzing the technology of structure formation, we should note that this process is followed by weakening of energies of atom-electron bonds at high energies of thermo-elastic stresses when a combination of chemical elements is exposed to high temperature. The further volume change at the rate of T-P-H influence is connected with the redistribution of these energies.

Therewith, physical influence of parameters (e.g. T decrease, P raise, H increase by the mechanisms of elastic stress (compression)) is the basis of formation of structural phase transitions and the realization of a jump of properties at the boundary of phase states. Hence we can state that the role of energies of elastic stresses prevails at high temperatures. The analysis carried out shows that the reduction of the temperature in the course of volume compression redistributes the energy of elastic stresses toward reduction.

Special attention should be paid to the extreme variant determining the energy state of the system at the temperature varied with taking into account the minimal volume at 0^oK. The volume is minimal, the binding energy is maximal due to electrostatic Coulomb interactions at comparatively small elastic stresses which are neglected in used theoretical models of quantum mechanics. That was the fact created the necessary prerequisites for introduction of conception of an equilibrium state in Bohr-Levin postulate as well as magnon definition in the theory of spin magnetism [11, 183].

Taking into account the proven mechanisms of realization of physical processes using real experimental results (significant hysteresis of magnetization at $T=1.53^oK$ in $CuCl_2 \cdot 2H_2O$ (Fig. 8.2a) and at $T=1.4^oK$ in $Eu_{0.55}Sm_{0.45}MnO_3$ (Fig. 8.4a)), we can doubt theoretical models based on ideal postulates and containing significant restrictions [183]. The existence of considerable binding energies verified by quantum-mechanical definitions side-by-side with elastic stresses forming a structural phase transition (a triple point) exactly at 0^oK is the driving force of a real physical process. The evidence of the existence of a structural phase transition at 0^oK is the availability of a number of secondary indications enlisted in a number of papers in the form of jumps of heat capacity, magnetization, HF-properties, striction etc. that emphasizes the real importance of the mechanisms of elastic stresses.

As a consequence, the formulated regularities contradict to the statement about the absence or insignificant value of elastic stresses. They are hardly small enough, to deny or neglect the elastic energy forming the phase transition exactly at 0^oK.

While generalizing and emphasizing the role of elastic stresses, we should suppose their importance in both dielectric and semiconducting phases. The reduction of the volume down to the boundary of the phase transition forms a phase state as a concentrator of elastic stresses preventing electron motion.

Here the superconducting and conducting phases are manifestations of PT at 0^oK with the reversible jump in properties (a rupture) of the structure.

The revealed regularities of elastic stresses treated as the main cause of volume change under T-P-H effect through mechanisms of bulk elasticity as well as the relation of these mechanisms to changes in electric conduction let us to assume that not all the electrons participate in conduction. Some of them are located at the filled shells that are most bound to nodal points (ions) and at the same time least relate to the processes of electric conduction. The mobility originates from the fact that the binding energy of electrons located from atom or molecular center to periphery is two and more orders of magnitude lower in the case of multi-component systems. Since the binding energy of peripheral electrons participating in the formation of lattice structure can be in a relative correspondence with the energy of elastic stresses, and then namely the electrons can play a principal role in structure changes and be a defining factor of T-P-H thermodynamic influence.

As known, every single-crystalline or polycrystalline structure is formed by repetition of groups of ions, molecule, atoms in the bonds, thus forming sites, and the experiment shows that in lattice sites the atomic and molecular magnetism develops as magnetic non-compensation. Such non-compensation is the maximum at $T=0^oK$ (Fig. 8.1a- magnetostriction dependence; Fig. 8.2a – magnetization dependence) and it goes to zero at high temperatures directly connected with processes of volume change. Showing the role of the laws of cubic elasticity we stress that if changes in volume are not accounted for completely, any methods of theoretical modelling remain an approximate solution with the empirical selection of coefficients to define changes in the exchange. The approximations taking these volume changes into account need much correlation.

The presented methods of analysis, the established regularities of elastic stresses in physical processes of formation of phase transitions and properties in multi-component magnet-containing structures are separated among fair quantity of results and facts. The main goal of the present paper is the demonstration of universality of the chosen methods of analysis. This aim demanded the intuitive formulation of principles of correct account for macro- and mezoscopic properties.

The establishment of causing role of elastic stress energies and natural fact of their separation at formation of critical lines and points [6] attracted our attention to [171, 177, 180, 185]. There a wide spectrum of studies of multi-component magnet-containing structures is presented in the form of varied parameter dependences of phase diagrams of $Re_{1/12}Al_{1/2}MnO_3$ [171, 185] compounds, $Pr_{1-x}Ca_xMnO_3$ monocrystals and $Pr_{1-x}Sr_{1/2}MnO_3$ [177] and $Nd_{1-x}Ca_xMnO_3$ [180], too. Presented in [6] for $LaMnO_3$ and $CuCl_2$ $2H_2O$ properties, the selected methods of analysis allow us to establish analogous

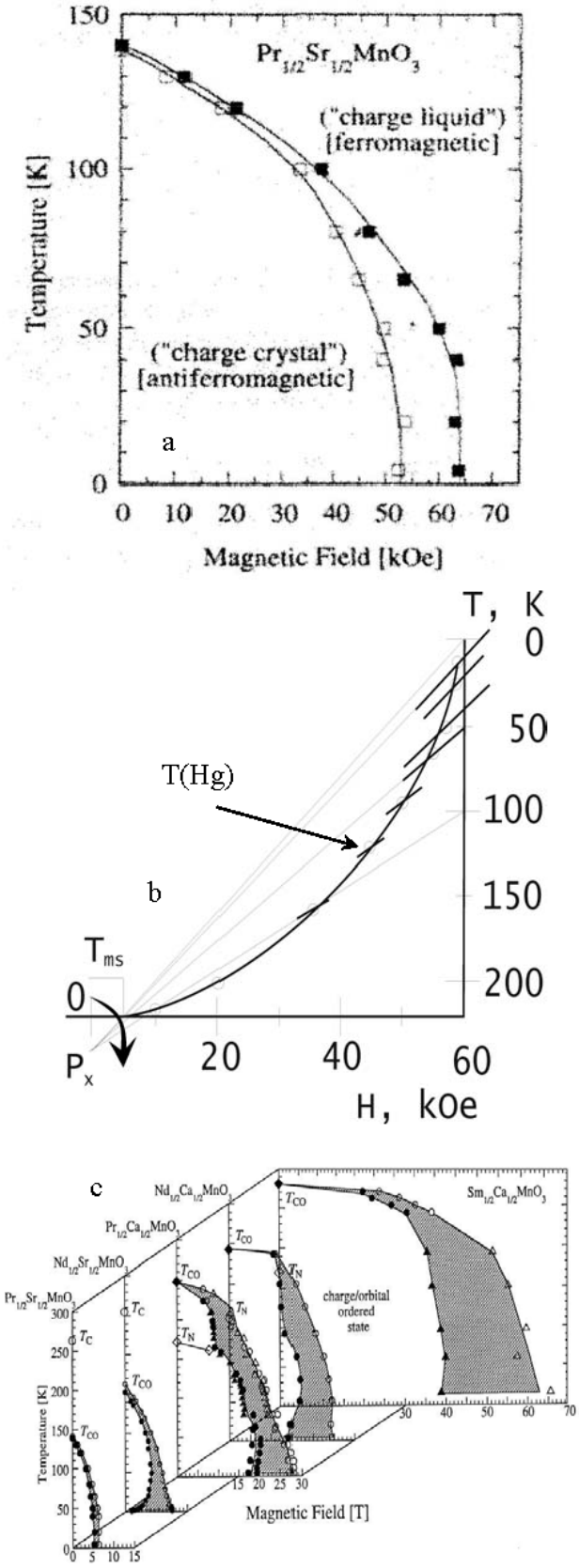

Figure 8.8. a) phase diagram [177] of $Pr_{1/2}Sr_{1/2}MnO_3$; b) Temperature-field dependence of phase transition with critical point Px; c) The charge-ordered phase of various compounds $Re_{1/2}Ae_{1/2}MnO_3$ plotted on the magnetic field-temperature plane.

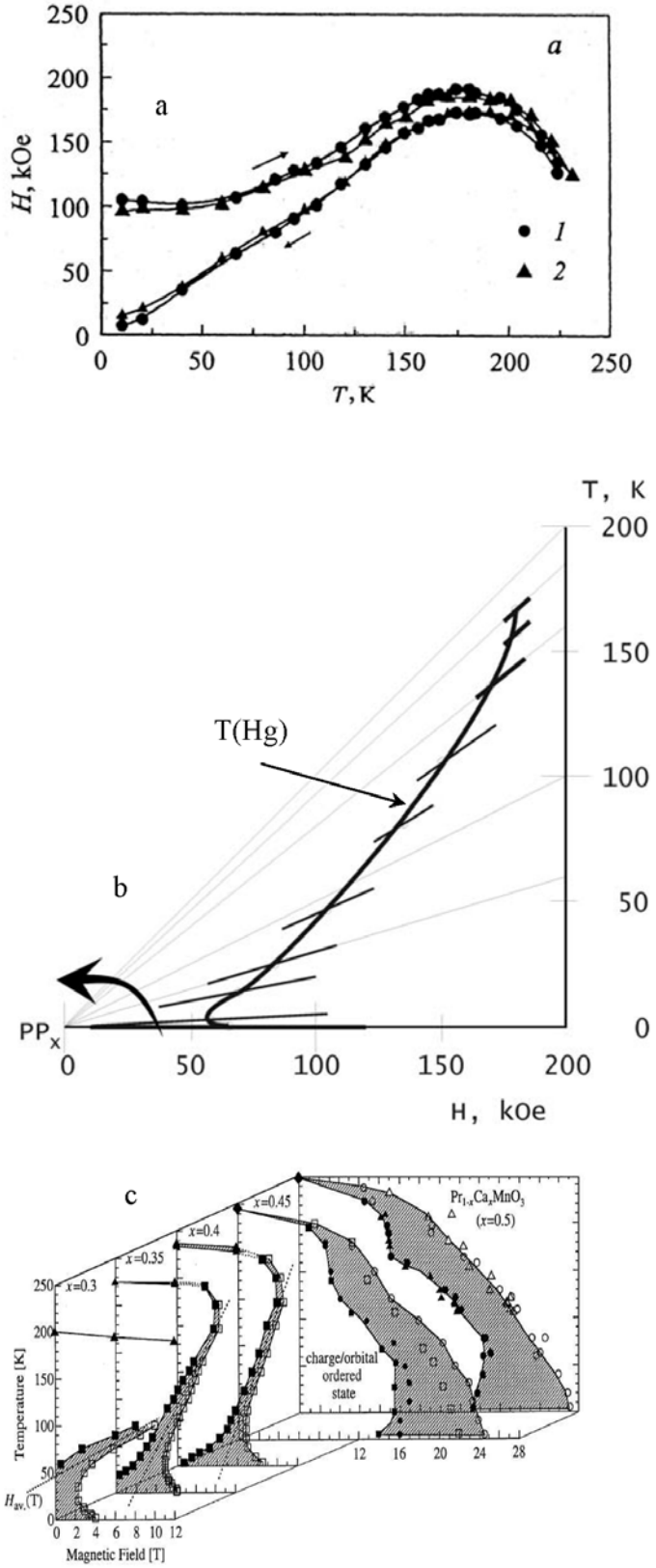

Figure 8.9. a) phase diagram [180] of $Nd_{1-X}Ca_xMnO_3$ (x=0.45); b) Temperature-field dependence of phase transition with critical point PPx; c) The charge-ordered state of $Pr_{1-X}Ca_xMnO_3$ at several hole concentration plotted on the magnetic field-temperature plane.

regularities also in these papers. We should note that the singled-out T(Hg) dependence (figs. 8.8b, 8.9b) is the average result of the handling of changes of magnetization and magnetostriction. The identity of these properties shows their complete dependence on the mechanisms of magnetoelasticity.

The exhibition of $Pv_{1/2}Sv_{1/2}MnO_3$ phase diagram [177] (fig. 8.8a) as T(Hg) dependence with separated Px critical point and Tx(Hx T=0) shows common regularities with $LaMnO_3$ (fig. 8.1a,b). Only the positions of the singled-out critical points are changed. Similar dependences can be established for the whole manifold of phase diagrams of the varied compositions of $Re_{1/2}Al_{1/2}MnO_3$ (fig. 8.8c). The character of the singled-out dependences is analogous (fig. 8.8b), except the position of the critical lines and points.

The succeeding result is presented in the form of a phase diagram of magnetization and magnetostriction of $Nd_{1-x}Ca_xMnO_3$ monocrystal [180], fig. 8.9a. The cited results have the form of temperature-field dependence $T(H_9)$ (fig. 8.9b) separating superconducting phase and metal analogous to phase transition in $CuCl_2$ $2H_2O$, fig. 8.2b.

The established position of the critical points PPx allowed us to separate the same regularities in phase diagrams of monocrystal $Pr_{1-x}Ca_xMnO_3$ too, where small concentrations of the composition x=0.3; 0.35; 0.4 can be treated as a phase transition (fig. 8.9c) analogous to the corresponding structural phase transition in $CuCl_2$ $2H_2O$. The succeeding changes of the composition x=0.45; 0.5 result in sign alteration of the position of the critical line (fig. 8.8b) [6] corresponding to the phase transition analogous to monocrystal $LaMnO_3$ behavior (fig. 8.1b, 8.8b) with the singled critical point Px.

We should note that the magnetization of the superconducting phase changes under the influence of T and H in single-phase state.

The derived regularities are justified by the methods of the carried analysis where the causing role belongs to the energy of elastic stresses. If the volume elasticity is not taken into account in model presentations, it means the abandonment of the analysis of the role of elastic energy in formation and evolution of structural phase transitions and properties.

8.5. Conclusions

Contemporary problems related to conducting magnet-containing media entail study of numerous experimental results obtained for systems of various compositions. Being based on the laws of bulk elasticity, new methods are to be used to analyze reversible physical processes induced by thermodynamic parameters.

The investigated objects are finite-size samples prepared by the conventional technology. By the method of high-temperature annealing, the chemical compounds are formed with repeated sites and bonds in the structure. The atomic-electronic binding energy is optimally minimal in that process of

high-temperature heat removal, while stresses are maximal. These are the structure-forming principles of energy distribution. Subsequent cooling directly relates to heat removal and the mechanisms of thermo-elastic compression involved. An obvious evidence is the linearity of the lattice parameter within the temperature range of 300-1000^{o} K [170] in $La_{0.875}Sr_{0.125}MnO_3$ and down to 0^{o}K as shown by our analysis. This is a clear acknowledgement of the role of bulk elasticity in physical processes under the temperature, magnetic field or hydrostatic pressure influence. Such a consideration shows that any heat transfer is also a causal basis of the involvement of mechanisms which modify (expansion-compression) internal elastic stresses. As a consequence, there follows the sign-alternating influence on structure change, i.e. heat application (heating) means the increase of elastic stresses, heat removal (cooling) results in the decrease of elastic stresses. Form this standpoint, similar processes are observed when baroelasticity and magnetoelasticity mechanisms are involved as shown by the results of our analysis [185].

The relation between thermodynamic effect through heat-transfer processes and mechanisms of elastically deforming stresses in structure changes has not been exposed finally, that is why their causal role in the formation of properties and PT has not been studied completely by model theoretical representations. This is because there in no complete understanding of relations between heat capacity (heat transfer) and elastic stresses and because of uncertainty in substantiation of the role of these mechanisms and significance of the estimating values of energies in a variety of physical processes studied.

Being a complex inhomogeneous process with peculiar linear regularities, elastic-anisotropic deforming stress can be taken into account with respect to power distribution by means of coefficients, but not always grounded. Moreover, the heat transfer, the heat conduction and elastic stresses are bound in the structure of energies of mobile electrons, and linear changes observed in properties and PT determine the causal role of elasticity, more exactly of bulk elasticity in the processes of T-P-H effect.

When treating the heat transfer as a factor forming elastically deforming stresses in the structure and also redistributing the energy of interactions, we can conclude that in the laws of interactions and conformities one should take into account:

a) the energy of quantum-mechanical forces determined by the short-range atomic-electronic bonds;
b) the energy of heat transfer and the related mechanisms of elastically deforming stresses (partially accounted for in molecular-field models) resulting in structure changes.

The T-P-H effect through the properties of elasticity varies the volume, redistributes the energies, thus forming the structural phase transition and properties in each phase state.

The analyzed processes of a fast (linear) increase of magnetization or magnetostriction in the magnetic field show that particles (sites and bonds in the structure) are a great vector (magnetic moment) of magnetic non-compensation. This phenomenon results from the participation in structure formation of numerous individual non-compensated spins, bound electrons in intermolecular (modal) space. It was not possible completely to explain the interactions or the role of elastically deforming stresses in non-compensative processes in theoretical molecular-field models.

Consequently, the model-theoretical representations of the quantum-mechanical statistics are more preferable for the magnetic non-compensation in structure at $T=0^oK$ and with the maximal energy of the atomic-electronic bond and the minimal energy of elastic stresses. Next, the volume increase with thermo-elastic stresses influences the state of structure sites and bonds due to the expansion, and then the long-range forces start operating and magnetic non-compensation goes to zero.

The analysis of the role of magnetic properties and relation thereof to elastic regularities of T and H effect on structure changes rises a question about the formation of conditions for origination of T_c critical point. As the internal energy is a factor of conformities and interactions between binding energies and internal stresses, then T_c is the temperature of conformity for thermoelastic expansion and magnetoelastic compression.

Numerous results obtained for $LaMnO_3$, $CuCl_2 \cdot 2H_2O$, $Eu_{0.55}Sr_{0.45}MnO_3$, $La_{0.56}Ca_{0.24}Mn_{1.2}O_3$ are based on new representations, which assume that there exists the direct correlation between structure changes and regularities of elastically deforming stresses. Let us state that there is the redistribution between interactions and conformities of the atomic-electronic binding energy and the energy of elastic stresses in physical processes. In other words, this correlation of structure changes can be treated as the law determining the degree of conformity and correlation between heat flow (heat capacity) and the energy of elastic stresses. As noted, this correlation is always present.

Accounting for direct relationship between structure, regularities of elasticity, electronic and magnetic properties, PT, new approaches make it possible to explain the anomalies, peculiarities, effects through described regularities. The applied analytical methods allowed to determine the role of stresses in the formation of structural phase transitions with the unusual location of critical points and phase states at 0^oK. This fact was a reason for finding generalizing principles named secondary indications that determine and fix the position of PT at 0^oK. These indications are:

a) unambiguous location of maxima of thermo-baro-resistive, thermo-baro-magneto-resistive effects at $T_{PP}=0^oK$ corresponding to the structural phase transition, Fig. 8.6d;
b) single-phase influence of T and H on changes of magnetization properties at the initial section of the dependence and the antiphase influence on the same properties after the phase transition, Figs. 8.2a, 8.3c, 8.5c;
c) the revealed regularity of magnetization properties in the region of structural phase transition into inverse (anomalous) hysteresis effect, Figs. 8.2a, 8.3a, 8.4a, 8.5d;
d) a sign-alternating effect of temperature on magnetization properties in different phases, Figs. 8.2a, 8.3a, 8.4a, 8.5d;
e) succession in positions of mentioned points PP_x and P_x and their direct relation to the field-temperature dependence $T_P(H)$, the boundary separating the superconducting and conducting phase states, Figs, 8.6c, 8.4, 8.3b, 8.2b.

The given results (Figs. 8.5a, 8.6a) show that the phase with dielectric properties becomes apparent in physical processes of volume change at the expense of mechanisms of the decrease of stresses down to the temperature of the structural phase transition at 0^oK. That is the process that determines the mechanisms of stress concentration preventing the mobility of conduction electrons. The stress concentration is also present in the region of semiconducting phase (Fig. 8.7a) where the parameter changes from the critical point P_x' and the volume starts decreasing. This is observed for the dependence of resistivity with T decrease and P, H increase and change of structure symmetry from a high value down to lower one (Fig. 8.6a). These facts enable us to conclude that the critical point of the structural phase transition at $T=0^oK$ meets the requirements of a triple point, i.e. the point of dielectric, superconducting and conducting (metallic) phase convergence.

For a more complete understanding of the laws of bulk elasticity in physical processes it is very important to analyze the significance of the mentioned critical lines and points for the formation of structural phase transitions and properties.

The demonstrative is the result of intersection of approximated dependences at the critical point P_x' (Fig. 8.7a). The presence of three parameters (T-P-H) and the revealed regularities of their influence on the resistance has specified the approaches to substantiate the role of mechanisms of elastically deforming compression in the formation of structural phase transitions and the region of stress concentrators in semiconducting phase. The position of P_x' critical point (Figs. 8.7a, 8.6a) shows the sequence of the physical process forming the region of PT in the form of a jump of resistivity followed by the transition to conducting (metallic) phase where the changes

obey the law of linear elasticity. This result has made it possible to establish a very important factor of conformities in T-P-H ratio (6.3^{o}K-1 kbar-2.3 kOe) and to assume that the backpressure and H decrease the level of elastic stresses in the structure. This is confirmed by changes (decrease) of resistivity properties by analogy with the thermoelastic compression.

Being the most prominent in regularities of hysteresis, differences of anisotropy, magnetoelasticity and thermoelasticity are shown by linear changes of $T_{ms}(H)$ and $T_{ms}(P)$, Fig. 8.7a.

Here we add the result of distinction of the temperature maxima of magneto-, baro-, magneto-baro-resistive effects $T_{PP}=T_{mc}$ (Fig. 8.7b). This is a straight confirmation of the formed structural phase transition. For this result the physical processes are located in the region of thermoelasticity priorities. This follows from the revealed correspondences between T, H and P.

One more important result adds to the role of bulk elasticity in magnetostriction dependences (Fig. 8.1a), which are linear by definition due to priorities of magnetoelasticity. It became possible to specify P_x, PP_x critical points and the regular changes of the field-temperature dependence $T(H_g)$ (Fig. 8.1b). Those are the regularities of the dependence of complex processes of elastically deforming stresses in the structure that point to the separation of phase states limited by P_x and PP_x. Here we also pay attention to the antiphase effect of temperature and to the formation of structural phase transition in the region where magnetoelastic stresses are of priority for H increasing; the mechanisms of thermoelasticity are involved with T decrease, and this is demonstrated by the revealed regularities. It becomes possible to approximate the magnetostriction properties on the dependences for T=0^{o}K and to show the role of mechanisms of magnetoelastic stresses under the maximal magnetic non-compensation resulting from the minimal volume for T=0^{o}K. As a result, the position of PT has been determined and the role of magnetoelastic anisotropy has been shown to be defining T_x (H_x – 205 kOe, T=0), Fig. 8.1a,b. It follows that position of T_c is, by definition, a fact of averaged conformity of elastic stresses with the change of priorities, under the realization of structural phase transition between $T_{mc}(H=0, T_{PP})$ and $T_x(H_x, T=0)$.

Positions of critical points are connected with changes in volume; it is also a consequence of chemical composition, technology of preparation and the intrinsic magnetic non-compensation as well as the reaction of volume on T-P-H effect through the mechanisms of elastic stresses. It is worth to note the regularities in the hydrostatic pressure (P) effect (Fig. 8.1a), all the critical points are invariable for the composition under consideration, while the properties and position of PT dependence vary anti-clockwise with respect to $T_x(H_x, T=0)$.

The most demonstrative is the result where regularities in changes of properties and PT allow to register superposition of critical points PP_x and P_x

(Figs. 8.2a, 8.3b, 8.4b, 8.6c). The elastic regularities of T-P-H effect have been revealed. They corresponded to 1^oK-4kOe –3kbar by the linear change of magnetization properties.

The analysis of relationship between structure peculiarities and bulk elasticity in a real physical process has shown that the structural phase transition may exist at $T=0^oK$. Moreover, the experiment gave the result close to that parameter. This effect is accompanied by a high jump of the properties, including heat capacity and susceptibility. Its parameters are $T_x(H_x=6.5$ for $T=0^oK)$, Fig. 8.2a,b. This means that the magnetoelastic ($H_x=6.5$ kOe) stresses correct the position of the structural phase transition for $T=0^oK$. Next, the field-temperature dependence differentiates the phase states of superconducting and conducting phases. Here we note that $T_P(H)$ dependence(Fig. 8.2a,b) much differs from $T(H_g)$ (Fig. 8.1a,b) first of all by critical line position of different sign [6] and by existence of critical point $P(H_P, T_P)$. This regularity of changes in phase transition is connected with position of point PP_x, in the results under consideration, and this is the defining factor for the formation of superconducting phase. It also shows the role of stresses in the effect of anomalous hysteresis within the region of structural phase transition. These results demonstrate the antiphase effect of the temperature on properties for separate phases.

The critical point of the phase transition at T=0 K functions as a triple point. In this region under thermo-elastic compression, the mechanisms concentrating the stresses start operating to realize a jump of properties when the region of phase transition is formed and this hinders the dynamics of the conduction-electron mobility. Subsequently, structural phase transition results in considerable changes of heat capacity, resistivity, magnetization, thus characterizing the superconducting and conducting phases as they are.

Our attention is paid next to numerical parameters of conformal influence of T-P-H. They are equal to 1^oK-3 kbar- 4 kOe. We also note the position of the parameter where the region of field-temperature dependences $T_P(H)$ and $T_P(H,P)$ (Fig. 8.2a) is limited by $P(H_P, T_P)$ point. This critical point limits the region of existence of phase states, it can be determined for any structures by investigating properties and PT under the influence of high hydrostatic pressures.

The analysis of the role of P_x' point where resistive dependences intersect each other (Fig. 8.6a, 8.7a) in the physical process of volume change under T-P-H influence through mechanisms of elastic compression is worth mentioning too. These results confirm regular participation of the mechanisms in the effect of colossal magnetoresistance being under study for many years.

By using new approaches to analyze the results of investigations, when the defining role of the effect of thermodynamic parameters T-P-H is considered in view of the mechanisms of elastic stresses, it is possible to explain

numerous anomalies, peculiarities and effects by relationships between structure and elasticity.

The presented generalizing analysis shows the correspondence and interaction of binding energy and elastic energy. The neglecting of this energy [172] in the course of model theoretical analysis results in practical refusal of an important part of the energy that forms and changes the phase transition and properties.

Chapter 9

The relation of bulk elasticity with the parameters of the influence in magnet –containing metals, dielectrics and ferroelectrics

9.1. Regularities of the first-order structural phase transition in MnF_2

The magnetic and magnetoelastic properties of magnetodielectrics are vast ranges of investigations in the solid-state physics. While analyzing results of experimental investigations near the region of phase transition, we pay attention to the common nature of the magnetic states in the vicinity of the structural phase transitions. The influence of magnetic field H on the properties of magnetostriction has been analyzed for the simplest two-component representatives of magnetodielectrics that are MnF_2 single crystals being uniaxial, low-compressible and prepared by high-temperature annealing and based on transition metals with the declared first-order phase transition at 0^oK [188].

The magnetic properties of the substances with the jump of the magnetization observed at the magnetic field other than zero have been widely investigated. It should be added that for this system, the first-order structural phase transition develops with the positive dynamics of dT_p/dH and dT_p/dP changes. For the distinguished phases, the magnetization is different in the absolute value and direction.

The first-order phase transitions in the external magnetic field are discussed in [1] with mentioning the jump of the properties where the values of the field H are critical and the specific magnetization on the phase states is of different value and of different dynamics of the changes of each phase.

MnF_2 is a popular magnetodielectric for the experimentalists. It has a rutile-type crystal structure (the space group D_{4h}^{14}). The tetragonal unit cell with the parameters a=4.87 A and c=3.30 A [189] contains two Mn^{2+} ions. The manganese ion has the half-filled d-shells, five uncompensated electrons, i.e. the total spin of the ion is 5/2. The decompensation magnetic moment is of purely spin origin. For T-67 K [190], the phase transition and the jump of the magnetic susceptibility are noted [191].

The elastic constants of the crystal have been estimated [192], the thermal properties are investigated in [193], the magnetic ordering on the temperature dependence of the heat capacity have been stated [194], the coefficient of the

thermal expansion is determined as $\frac{1}{T_N}\frac{dT_N}{dP} = 4.5 \cdot 10^{-2}\ cm^2/erg$ [195], as well as the state of the additional compression (the volume change) of the crystal along the axis of the symmetry has been revealed. The magnetoelastic properties and their regular change during the PT under pressure have been distinguished [196].

In [197], the temperature dependence of the magnetic susceptibility in low fields is studied. At temperatures higher than the critical one associated with PT, the magnetic susceptibility is isotopic and obeying the Curie-Weiss law. At low temperatures, $X=10^{-3}$ units CL-SM is normal to the axis of symmetry and does not depend on the temperature. In the field aligned with the axis of symmetry, the susceptibility drops to zero with T decrease [198].

The demonstrative are studies of magnetic properties at low temperatures and high magnetic fields [199]. On the dependence of the magnetization, there is a jump of the properties typical of the first-order phase transition (Fig. 9.1b). The properties are shown at the distinguished point for T=4.2 K and for varied magnetic field orientation. Thus, in the field parallel to the axis of symmetry, there is a magnetization jump for H of 10^5Oe. The investigations show that $H_e \sim 1.1 \cdot 10^6\ Oe$, $H_a \sim 8.6 \cdot 10^3\ Oe$, i.e. there is a correspondence between exchange and anisotropic fields [200]. The rare results do not enable us to judge the first-order phase transition by the character of the magnetization curves.

Let us now to consider the experiments with ultrasound adsorption in the region of PT [201] and to analyze the magnetic properties by using the phase diagram of MnF_2 (Fig. 9.1a). On Fig. 9.1b, the considered $T_p(H)$ dependence is a field-temperature curve with the critical points PP_x and the temperature parameter evolution corresponding to the regularity of the first-order phase transition for T_{cm}(T_x=0 K, H_x~90 kOe) and of the phase transition changes with the plus sign. The anomalies of the ultrasound absorption observed near this dependence of PT can be related to the critical region separating phase states.

It has been detected that for H=93 kOe directed along the axis of the symmetry, the magnetostriction has demonstrated a jump of the crystal size [190], a change of the length in high H that is also typical of the first-order structural phase transition. These studies help in the estimation of the magnetoelastic constants for MnF_2: $A_0=8.6 \cdot 10^{-13}$cm^2/erg, $A_1=2.1 \cdot 10^{-13}$cm^2/erg, $A_2=1.07 \cdot 10^{-13}$cm^2/erg.

Investigations of the region where the structural phase transition is formed impose demands upon experimental methods. Broad temperature range is implied starting from 4.2 K and lower. For MnF_2, the magnetic fields are of 10^5-10^6 Oe with high homogeneity of the fields, high accuracy of the

orientation of the external field with respect to crystallographic axes as well as the detailed study of the field-temperature dependence of the resonance absorption in the vicinity of PT.

The explicit jumps of the magnetization properties (Fig. 9.1c) let us to assume that in MnF_2, the first-order structural phase transition restricts the phase states, changes the volume and the symmetry of each phase. This results in differences in the magnetization as well as in changes of the direction of magnetic non-compensation along crystallographic axes (different specific magnetizations) of neighbor phases relatively to changes of the crystal symmetry.

The magnetization jumps are natural factors of the formation of the structural phase transition.

The considered investigations make us to conclude that the phenomenon of jump-like magnetization change is a typical sign of physical processes of T, H effect under which the PT is formed through the mechanisms of elasticity, magnetic elasticity and important elastic and magnetoelastic anisotropy. The jump-like magnetization change is a sudden change of the properties in a narrow range of fields H~670 Oe. On the background of repeated jumps, there is a region of angles of the field deviation with respect to crystal symmetry, to within $\psi \sim 30'$. This is shown by magnetization properties on the oscillogramm of Fig. 9.1b'.

The studied phase states differ by the degree of magnetization, first of all. The experimentally observed changes are characterized by different intensity of magnetic non-compensation and magnetization jump in MnF_2 for H_c=92 kOe makes 100 units of CG-SM. The inhomogeneity of the phases in the course of PT realization is revealed by the critical range of fields and angles. While considering and drawing analogies with formation of the first-order structural phase transition in $CuCl_2 \cdot 2H_2O$ and MnF_2, let us now to analyze the field-frequency resonance absorption branch [202]. For MnF_2, the field-frequency dependence was realized in the temperature range of 4.2 K with high-accurate magnetic field orientation along the tetragonal crystal axis for frequencies of 3.5-16.5 cm^{-1}. For two single crystals of highly accurate orientation, the resonance absorption decreases the intensity of the second absorption line to the level of resolution near the PT. At low angles of deviation, the absorption was restored. For MnF_2, the fields of Pt region correspond to H~0.1+0.005T. The investigated samples were in the form of plates, L=3.5 mm and h=0.07-1.5 mm [188].

Form the above results, it can be concluded, that the regularity of the formation of the jump of the properties under the first-order structural phase transition is common of magnetodielectrics having different composition and compressibility factors. The results obtained for MnF_2 are observed for another systems of different compositions still their properties are varied in a similar

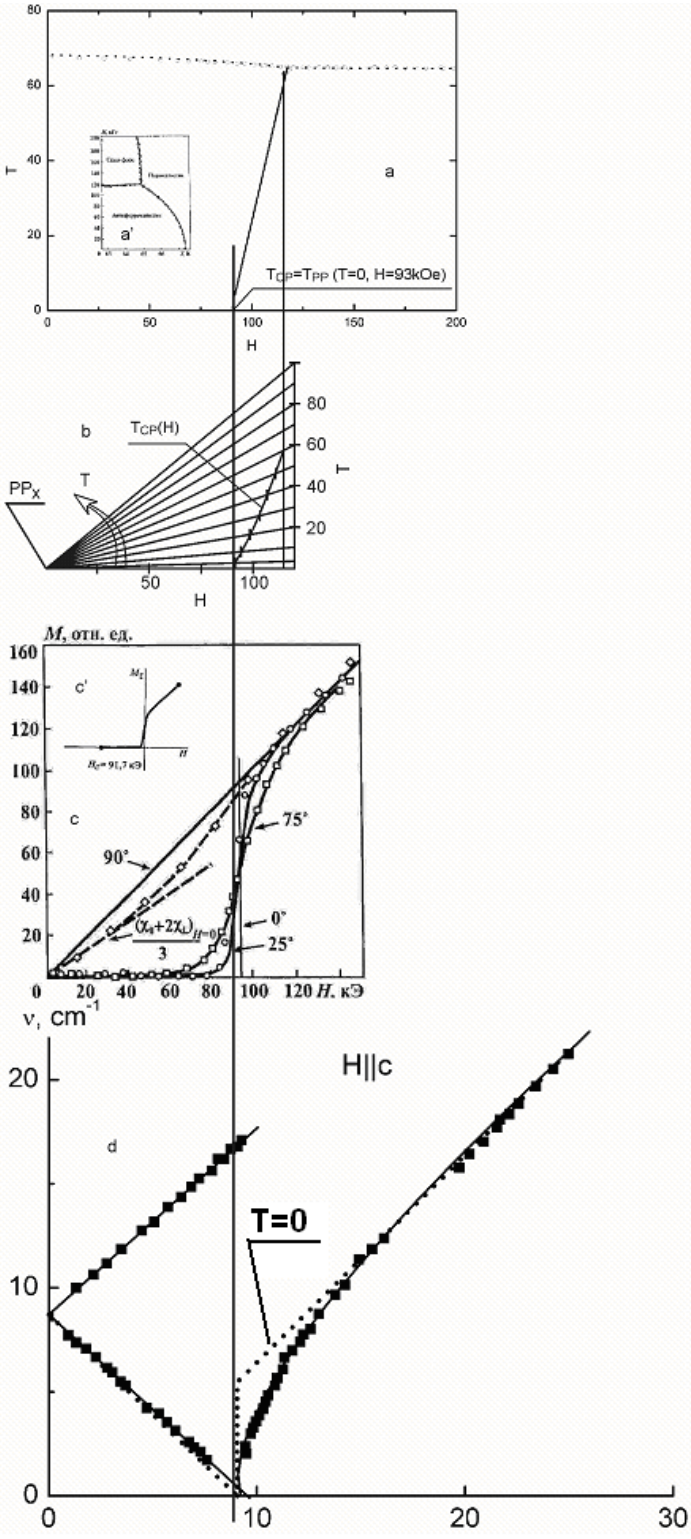

Figure 9.1. (a, a') Magnetic phase diagram MnF_2 in the field parallel to (001) axis. (b) Temperature and field dependence of a structural phase transition of the first order with separated critical point PP_x and T_{pp} (T_x=0, H_x~93 kOe). (c, c') The jump of magnetization of MnF_2 at varied orientation of magnetic field with respect to (001) axis at T=4.2 K. (d) Frequency and field dependence of resonance absorption of MnF_2 in the field parallel to (001) axis at T=4.2 K [202].

way [188]. The magnetic non-compensation is maximal along the principal crystallographic axis c, which is relatively small and for the transition to be realized at the point of 0 k, high magnetic field H=90 kOe is necessary (see the dotted line on Fig. 9.1d).

The crystal and magnetic structure of MnF_2 as well as the elastic deformation of the crystal lattice in high magnetic fields are related to the magnetostriction through the mechanisms of magnetoelastic influences under magnetization of the crystal and this is the causal basis for the changes of the properties, which are generalized by regularity of the bulk elasticity effect.

Another confirmation of the results on determination of the region of the structural phase transition in MnF_2 is work [199] where the magnetic susceptibility was studied using the samples of different shape. The specific run of the magnetization curves in the region of the jump of the properties for H~92 kOe and T=4.2 K is noted in the initial section. In low fields, the magnetization is low. Then, there follows a jump and a considerable change of the properties (Fig. 9.1c). Here we remark the analogies of the results. A correspondence to the magnetization jump in $CuCl_2 \cdot 2H_2O$ is present in lower fields and another temperatures (see [7]).

It follows that as dT/dH, $T_p(H)$ regularity is of positive sign and in the both cases we have the first-order phase transition. Thus, we get $T_p(T_x=0, H_x=90$ kOe) for MnF_2 and $T_k(T=0, H_x=5.5$ kOe) for $CuCl_2 \cdot 2H_2O$. It is also seen that for those single crystals the compared coefficients of compressibility differ by an order of magnitude, but there are regularities of H change in higher fields and PT dynamics corresponds to the “cooling-heating” effect that is an increase of H resulting in T increase at $T_p(H)$, and on the contrary, the reduction of H decreases T. Note that single crystal orientation and the sample shape are in direct correlation with the physical process of the structure change at the expense of elasticity anisotropy restricting the region of PT formation to 0.4kOe for a cylinder and 0.9 kOe for a disc.

Form the analysis of the field-temperature dependences for MnF_2 (Fig. 9.1c) and approximation thereof to 0 k we can distinguish the frequency – independent region which has not been determined in the low-temperature range for 4.2 K. With the highly accurate orientation of the magnetic field, the same was observed and characterized by the position of the structural phase transition in $CuCl_2 \cdot 2H_2O$ single crystal (Fig. 7.8). Thus, it can be concluded that from the results obtained for alloys based on 3d and 4d tetragonal structure elements, the role of mechanisms of elastically deforming stresses and the anisotropy of elasticity is the determining one with respect to the physical properties of the volume change. The result confirming the analogies with the regular change of the properties on Fig. 9.1a,b,c,d for MnF_2 and Fig. 7.8a,b,c for $CuCl_2 \cdot 2H_2O$ is the identity of the field-temperature dependences for the first-order PT, T_p with the distinguished critical point PP_x and of the field –

frequency dependence with the change at 0 K shown by the dotted line as well as with the region that fixes the positions of PT and phase states.

While separating the changes of the magnetic properties under magnetoelastic effect in the superconducting phase state and drawing analogies with the alternating mechanism of hydrostatic pressure effect on the structure inhomogeneity and PT character, it is possible to relate the regions of the superconducting phase state and magnetism with the processes of the changes of the volume and the symmetry.

The analysis of the results of the changes of the field dependences is concentrated on magnetoelastic, magnetic, electronic, structural interactions connected with the structure rearrangement at the expense of the stresses created by the magnetic field through the mechanisms of magnetic elasticity, which affect both the structural changes and the processes of formation of the region of the first- and second-order structural PT that are recorded by the resonance methods in high magnetic fields and under the hydrostatic pressure. Showing the experimental results for real physical processes, we try to attract the attention of researchers stating that theoretical models are needed taking into account the energies of elastically deforming stresses and applied to a practical case. The analysis and the methods used to ground the analogies in the study of magnetodielectrics and superconductors enable us to generalize and to connect the regularities of magnetostriction and structural changes occurring during the formation of the first-order structural phase transition. As a consequence, the changes of magnetization and magnetostriction are in accordance with the general regularities of magnetoelasticity that is a part of the total bulk elasticity.

9.2. The laws of elasticity in the mechanisms of T-H-P effect on the formation of the structural phase transitions and properties of metals

As far back as the 20-30ies of the last century, the origination and the development of the methods employing high magnetic fields and low temperatures stimulated the investigation of the electronic properties of metals. The changes of the electrical resistance in magnetic fields were studied first in bismuth. Later, this phenomenon was found in all the metals and explained by the electron conduction theory by J. Thomson [204]. The theory showed that the change of the resistance was proportional to the square law. However, in fields of about 300 kOe [205], the regularity was found violated and substituted for stable linear changes. More than 30 metals of high purity were investigated and the low-field conductance followed the square law of the changes in every metal. In high magnetic fields, the changes were linear (Fig. 9.2). For all the investigated metals, there was one more interesting

phenomenon: a chemical additive changed the position of the square dependence without changes of the linear behavior. This meant that whereas the crystallographic lattice of the metal was distorted by a physical or chemical factor, the linear law of the changes was connected immediately with the high magnetic field effect on the elastic stresses thorough magnetic elasticity resulting also in deformation of the structure. This pointed to a close relation between the state of the metal crystal lattice and the magnetic field effect.

The results of experimental investigations of physical and chemical imperfections of crystals show the phenomena due to resistance growth to be similar. The introduction of such parameter as the temperature revealed the similar changes as well [206], but with some exceptions. On Fig. 9.3, there are typical curves of the resistivity changes for copper studied at 86 K liquid hydrogen temperature as well as 63 K and 20 K of liquid hydrogen. They consist of square sections in low fields and linear ones in high fields.

With this result, some more regularity can be distinguished. In view of the influence of two thermodynamic parameters, it can be concluded that the above dependence is a consequence of two mechanisms resulting in crystallographic changes. At the beginning, the thermoelastic expansion and themagnetoelastic compression form the square dependence of the changes.

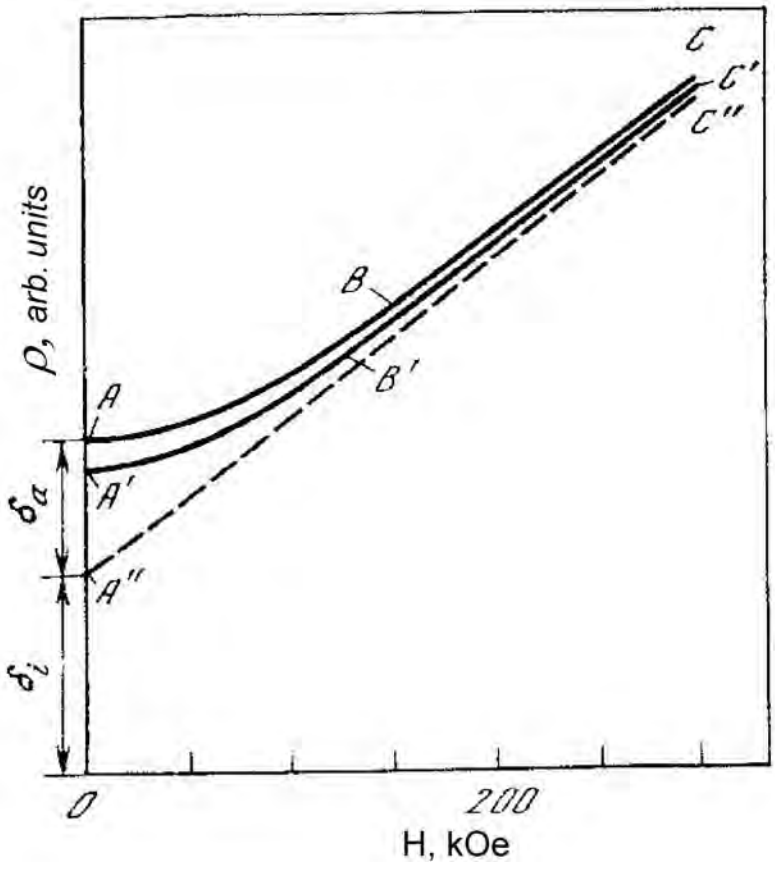

Figure 9.2. The magnetoresistivity in pure metals [205].

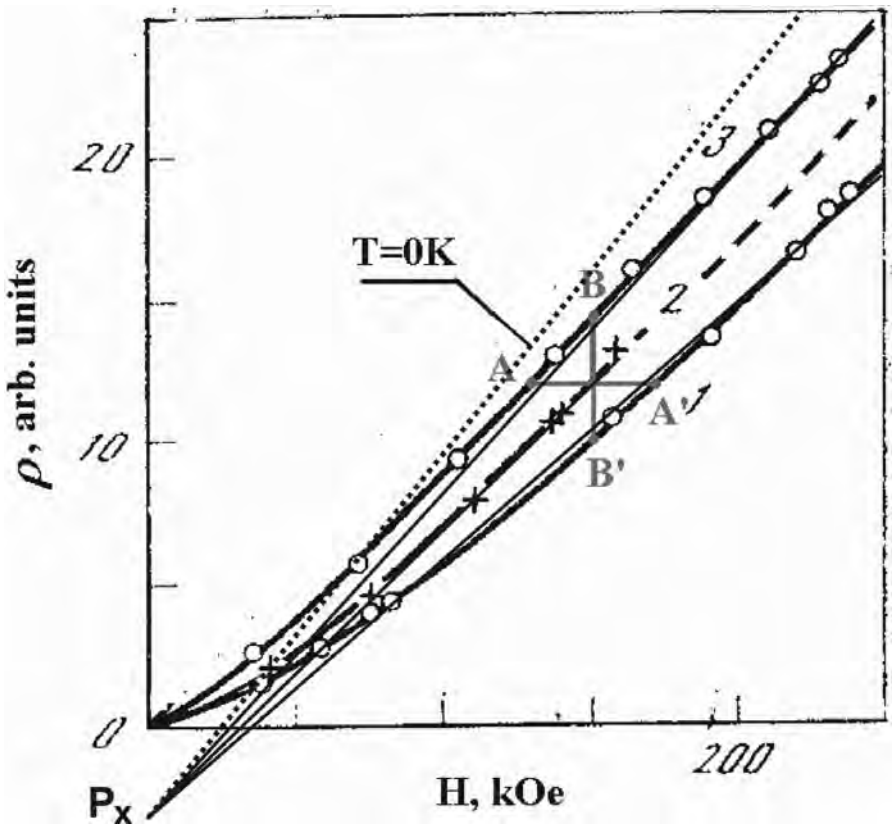

Figure 9.3. The magnetoresistivity in copper at fixed temperatures: T_1=86 K, T_2=63 K, T_3=20 K [206].

Then, a sign change follows with the preference given to the magnetoelastic effect resulting in the linear dependence due to crystallographic changes through the mechanisms of elastic stresses. The next fact of T and H effect on the physical process allows us to show the regularities of the changes (dotted line, by approximation) of the resistivity at 0K and those of cooling-heating effect from magnetic field H. The triangles ABC show how the temperature reduction increases the parameter of resistivity of fixed H (Fig. 9.3). The consequent decrease of H brings the system to the “heating” effect that is to the initial resistivity value. There is an opposite “cooling” effect which is compensated by the properties and the temperature effect with H rising. This means that the thermoelastic expansion effect brings the structure back to the initial state due to the counteraction to the magnetic compression.

Such presentation differs from the proofs suggested by Sommerfeld [206] and other theoreticians being sure that the magnetic field influences the trajectory of conduction electrons thus resulting in the changes of the properties.

Here, it is worth to mention the definitions by P.L.Kapitsa [207]. He stated that the resemblance between the resistivity growth due to crystal lattice imperfections and due to the changes of the magnetic field means that

theoretical presentations should be based on direct disturbance of the lattice structure by magnetic field. This opinion is also supported by the fact that in a number of diamagnetic substances, the magnetic field effect at low temperatures becomes apparent in magnetostriction properties. There, it was also assumed that the magnetostriction effect is a direct factor determining the relationship and the interaction of atoms in the lattice.

The lattice distortions by the deformation can be distinguished experimentally by X-ray diffraction method. However, X-rays show change of the relative intensity of the reflections of different order. The observation of the changes is difficult under short-term strong magnetic fields. Such results could not be convincingly explained from the position of the structural changes and T-H effect for about 30 years. From the position of the classical theory of the electronic properties of metals, the energy spectrum of conduction electrons does not practically differ from that of free electrons. According to this model, the energy of charge carrier is a square function of the pulse, the same as with free electrons, however their masses differ very much.

The action of crystal-lattice periodic potential on the conduction electrons is accounted for by the effective mass thereof that differs much from the mass of the electron. As a consequence, it should be taken into account that the atoms of magnet-containing sites (molecules) form the crystal lattice while the electron orbits of neighbor (valence or free) electrons intersect each other. This means that the electrons of onsite make bonds (intersect) with another site and vice versa. This implies that the energy of electrostatic interactions of the electrons will correspond to and form magnetic non-compensation or compensation with respect to the spin orientation.

While analyzing the resistivity change under H influence, the author of [207] assumed that the strong magnetic field induced changes of the crystal structure similar to the influence of impurities and defects. This means that H did not influence the electron motion but disturbed the structure of the lattice-site bonds through magnetoelastic stresses, thus modifying the conduction electron energy state. The methods for application of model presentation based on the quantum mechanics were discussed in parallel. The notions relating to classical mechanics (elasticity, magnetoelasticity) that explained real physical processes in the kinetics of microprocesses had not been developed properly. This also concerned the investigations under hydrostatic pressures. The use of quantum mechanics causal basis has resulted in generalizing theories with numerous parameters.

The followed the investigation of galvanomagnetic phenomena using the methods of hydrostatic pressure generation [208, 209]. The pressure varied the structure parameters and resulted in phenomena related to the electron density change as well as to typical anomalies in thermodynamic and kinetic

processes. The mechanisms of continuous lattice deformation stimulated the deforming stresses similar to T and H effect.

The complexity of the procedure depends on the object of the investigation. For a metal, the elastic compression modulus equals to 10^{-6}, this is identical to P~100 kbar and the pressure of 1-2 kbar is commensurate, the effect is low and as a consequence, the pressures about 30 kbar should be generated to determine the regularities.

In [210, 211], a series of materials such as Sn, Zn, Pb, Hg, Al, Cd, Nb has been investigated. They are typical of the regular change of the crystal temperature T_c with phase transition and dT_c/dP with the minus sign is considered to be the second-order phase transition. For La, Ti, Zr, V, dT_c/dP varies with plus sign that is the first-order phase transition.

While analyzing the properties of tin, indium, lead and tantalum with identical tendencies of the pressure effect corresponding to the second-order phase transition [212], we paid attention to an unusual change of the phase transition in Thallium (Fig. 9.4a). At the initial stage of the temperature shift to 0.02^o, for P to 7 kbar, T(P) varies non-monotonously in view of the measurement error for a shelf-like dependence. Subsequent dT/dP changes with the minus sign are typical of the second-order phase transition. Using the results of [6], we defined the critical point P_x indicating the position of the structural second-order phase transition and place $T_p(P)$ in correspondence with the position of P_x with respect to the temperature change (Fig. 9.4b) clockwise. For P under 30 kbar, the non-linear component shows the sign change region for the priorities of thermoelastic effect of baroresistivity as well as the role of properties in the formation of elastic anisotropy of the electron density. The influence of impurities results in structure changes and the evolution of the state of electron density. This can be followed by barotemperature dependence of the second-order phase transition [213, 214]. For the structural phase transition, this regularity of $LaMnO_3$ magnetostriction properties is unambiguous (Fig. 7.2 of [6]).

For this metal, the mentioned pressures realize the mechanisms of elastic stresses corresponding to the values of the compressibility factor of 10^4 (10^{-6}-10^{-7}) which is insignificant for this method of investigations. But the observed tendency reflects the state of the second-order phase transition and the dependence of Fig. 9.4a is due to both the deforming influence of the stresses on the structure affecting PT formed to 0 K and to the consequence of the conduction-electron density change in the metallic phase.

Under 30 kbar, the non-linear component reflects the conformity of the pressure effect on the structure changes similar to the effect of impurities of the dynamics of the changes and PT formation and, as a consequence, the formation of the properties and the phase states.

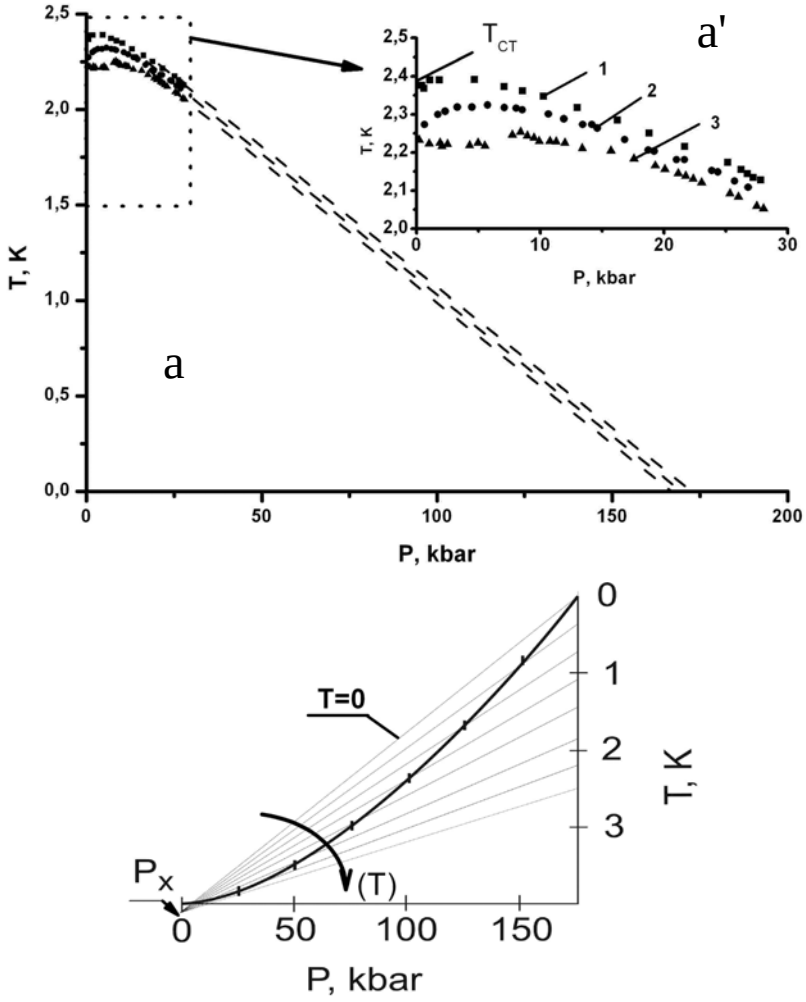

Figure 9.4. (a) Temperature and pressure dependence of the phase transition in Tl (1) doped by Hg (0.45%) (2) and Hg (0.9%) (3). (b) Temperature and pressure dependence of the phase transition in Tl with the separated critical point P_x: $T_{pp}=T_{mc}$~2.4 K, $T_x=T=0$, P_x~160 kbar.

The application of pressures has determined the relationship and analogy between the structure changes and the topology of the spectrum of phase-state electron density and the impurity concentrations. The distinguished crystallographic anisotropy apparent in the mechanisms of elastic stresses is a phenomenon of the shape.

While considering the superconducting phase state through the dependence dT_p/dP with the positive sign, we see that the pressure influencing the structure changes and varying the parameters is a factor bringing the system and the magnetoelasticity to the metallic phase state.

The pressure and the magetnostriction are factors changing the shape and the volume at the expense of baro- and magnetoelasticity exactly due to bulk elastic stresses. The factor of elasticity anisotropy is the defining one in the changes of the topology of the phase state electron density on the background

of the structural phase transition. It is the dependence of the magnetic field effect on the structure, that develops the changes of the magnetic susceptibility in cadmium, beryllium, magnesium, tin, indium single crystals through the magnetoelastic mechanisms.

The analysis of the results and the fact of distinguishing the linear law of the resistance change (Kapitsa) make us to state that the electron mobility induced by the magnetic field is connected with the crystal structure disturbances which affect the conductivity in a way similar to impurities or defects. In the low-temperature range, the magnetic field affects the structure of atomic bonds or the whole lattice that is the primary reason of the influence on the electron mobility. The changes of the field direction are related to the fact of distinguished directions of magnetic non-compensation in the structure. As a consequence, the direction of the disturbance is changed due to the anisotropy of magnetic properties and magnetic elasticity.

9.3. Structural phase transition in ferroelectrics in varied T and P parameters

The studies of the critical phenomena in the processes of structure rearrangements under T and P effects are not simple because researches are scare and the results are doubtful. The correlation between the parameters of the changes conforms the temperature and pressure dependences. Thus, for a ferroelectric $BaTiO_3$ [215], dT/dP equals 8.4 K/kbar, and dT/dP makes 5.1 K/kbar in manganates $La_{0.7}Ca_{0.3}MnO_3$ [6], the compressibility is good. At the same time, dT/dP equals 0.37 K/kbar for EuO during the ferromagnetic transition [216], i.e. the structure changes under the influence of dT/dP with the positive sign are a first-order structural phase transition with a high enough hysteresis. The regularity is also typical of $CaCl_2 \cdot 2H_2O$ [6] with 0.33 K/kbar and dH/dP of 1.34 kOe/kbar.

A non-trivial grounding of the investigations of the critical phenomena in systems of the perovskite family differs much from ferroelectric phase transitions with the compressibility of ~ 10^{-3}-10^{-4} found experimentally because of multi-component system and coefficient of Om compressibility of 10^{-6}as well as because of the instability at the boundaries of the phase states. The most reliable results give methods of the elastic neutron scattering and resonance methods.

The structural phase transition is considered to be a reversible physical process where non-uniformities and the strong bond between the structure parameters and elastic stresses are reflected in the smearing of the phase transition and in the shift of phase transition temperature T, consequently.

It is the difficulty of interpretation of the experimental results that does not permit us to distinguish and to predict the state of structural changes in

processes of stress strain under the PT and to provide an adequate model theoretical grounds that take the real physical process into account. In this process, changes of the volume and the energy of bulk elasticity are not completely considered by classical theories which treat the phase states.

Analyzing the position of the critical states for perovskite family where the parameters at the phase transition boundary are unstable $T_{mc}=T_{pp}$ [6] and correspond to the second-order phase transition with the critical points P_x and PP_x, it is noted that these critical points distinguished from regular changes of magnetostriction properties determine the phase state under P and H effect through baroelasticity and magnetoelasticity mechanisms. The mentioned regularities propagate to the physical properties of PT realization to temperatures T=0 K [217, 218]. Analogous results of Figs. 9.5ab for a mixed $Kta_{1-y}Nb_yO_3$ system [219] help in application of the results of [6] qualitatively to study the second-order PT and properties of ferroelectrics.

In the crystal, the presence of imperfections is the most obvious in the dynamics near critical points. To classify the processes, we need differentiate between the principal and the minor things. The main item is the determination of the causal basis for the elasticity mechanisms realized during the development of the structural phase transitions as well as the analogies for the defining role of parameters T-H-P through thermo-, magneto- and baroelasticity that result in PT and structure changes. It is also important to consider the same mechanisms under the formation of discontinuous structural phase transitions giving bulk and symmetry changes, anomalous hysteresis, i.e. resulting in the first-order structural phase transitions at 0 K where quantum-mechanical grounds are not important for the critical region [200].

In thee presence of defects, the nature of the critical phenomena is followed in the dynamics of property changes in the vicinity of the critical points due to the mechanisms that form the phenomena. A physical process could hardly be modeled without the critical phenomena.

The process of experimental analysis has not been finished yet. The nature of the mechanisms forming the critical phenomena in ferroelectrics still remains not properly understood. It sees highly interesting to make an experiment to study samples under high hydrostatic pressure with varying T and H and to analyze the results basing on the existing preconditions for relationship between the bulk elasticity, structure and properties.

The regularity of quasi-elastic phenomena such as the elastic stresses and the elasticity anisotropy is the basis of current understanding of the dynamics of the critical phenomena in the vicinity of the structural shift-type phase transitions. No matter how paradoxical it is, the developed theoretical representations are not considered from such a viewpoint, and now it is even hard to conceive how these mechanisms can characterize changes in perfect crystals.

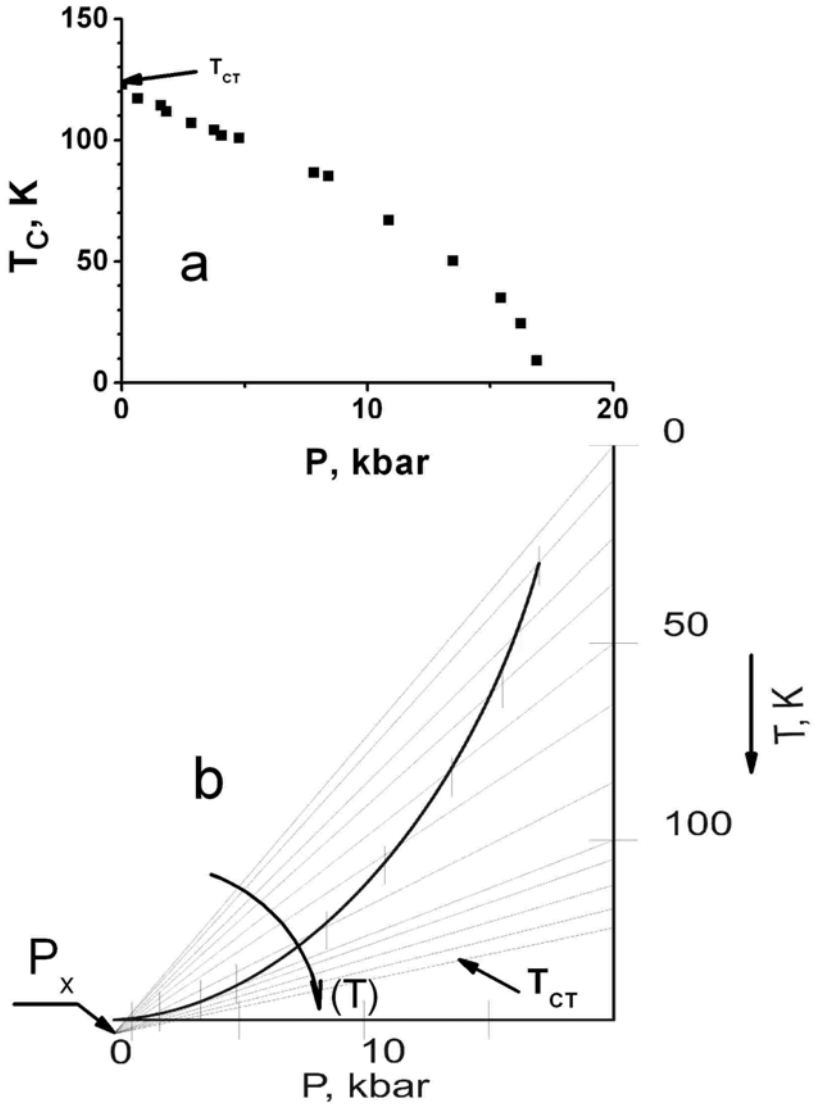

Figure 9.5. (a,a') Temperature and pressure dependence of the phase transition in a ferroelectric in KDP [219]. (b) Temperature and pressure dependence of the structural phase transition of the second order with the separated critical point P_x and $T_{pp}=T_{mc}$~122 K, $T_x(T=0)$, P_x~17 kbar.

9.4. Conclusions

While studying a complex state of material, a researcher faces a great amount of information without proper treatment of the results. The empirical principles are not formulated correctly that does not contribute to the understanding of reality. A very complex task of a researcher is the control of intuition that allows one to distinguish sign of objective universality. Otherwise, it is impossible to suggest a real model of the studied physical process where any quantitative changes do not influence the basic physical principles forming the structure of a solid and cover a wide variety of macro- and microscopic properties of the studied system.

Now we shall evaluate the levels of energy contribution in the course of consideration of critical phenomena and properties. This matter touches upon principal questions of the direct relation between thermodynamic parameters and structure evolution through the mechanisms of elastic stresses affecting the volume and other parameters controlling the structural phase transitions and the properties of phase states.

We shall estimate the energy of Coulomb interactions as 1÷10 eV, the influence of the crystal field as 0.1÷1 eV, spin-orbit relationship as 10^{-2}÷10^{-1} eV, spin-spin (magnetic) bond as 10^{-4} eV, electron-nuclear bond as 10^{-4}÷10^{-5} eV. According to our estimations, the energy of elastic stresses with taking into account the coefficient of compressibility is 1÷10 eV.

The magnetism of magnet-containing structures can get the most effective consideration from the viewpoint of the experiment. There the real physical process is registered if the form of the evolution of the properties of a solid that testifies the regular bond of the changes of the crystal structure and the electronic and magnetic properties.

Model representations treat the energy to a first approximation without sensibility to phase transitions. Directly calculating the energy, the models do not pay proper attention to magnetoelastic interactions and magnetization.

We should keep in mind that magnetoleastic interactions are nothing but bulk striction based of the elastic bond between neighbor non-compensated spins. Thus, all changes of interatomic distances result in both the changes of the volume and the lattice form followed by the modification of the properties.

Magnetization is a consequence of the influence of the magnetic field on magnetically non-compensated constituent of a particle provided it is high enough to affect the structure significantly.

We should take into account that quantum mechanical forces forming the magnetism are of short range in fact, so deep understanding of the regularity if interaction is necessary for the estimation of this process.

The elastic energy is an immediate energy of long range. These are elastic stresses in the structure that form the linearity of the magnetization regardless of important details of microscopic interactions. By definition, atoms and molecules have small magnetic moments of non-compensation. The structure is the totality of molecules and atoms brought into the sites of the structure (several atoms and molecules) and bound in the lattice by the compatibility of valent and free electrons.

The state of the structure and its predisposition to paramagnetism is formed by high-temperature physical and chemical processes where the magnetic factor is absent by definition. In other words, the high-temperature area has no ability for magnetization.

The succeeding cooling and bulk compression result in the loss of heat energy transformed into the loss of the energy of the elastic stresses in the structure. This process is followed by the linear evolution of the parameter due to the mechanisms of bulk elasticity.

This process is the factor forming the spin non-compensation of sufficient intensity at the proper state of the structure that allows the structure to react on the magnetoelasticity and magnetization in the applied magnetic field. These are the approaches of the analysis that permit to define the causal role of the laws of bulk elasticity in the formation of the magnetism as well as their leading role in the first and second order structural phase transitions.

Chapter 10

Nature of bulk elasticity and its role in the formation of phase transition

The review of the numerous results taken in the previous chapters, was dedicated to the study of the properties of materials under influence of three thermodynamic parameters (temperature, magnetic field, pressure) and showed that the inclusion in the number of influencing parameters of high pressure significantly enlarges information base and it makes it possible in a new way to glance at nature of the observed phenomena.

10.1. The bulk elasticity of solid under the external influences

Study of conductivity in the simple and in the complex materials under the conditions for the joint action of three parameters: magnetic field, pressure and the temperature also in the sufficiently wide range of temperatures (to 350 K), pressures (to 1.8 GPa) and magnetic pour on (to 8 kOe) was determined the similar influence of these thermodynamic forces on the properties of materials (see chapter 8), which indicates the united mechanism of these influences. The analysis of experimental data showed that the action of temperature, magnetic field and pressure cause a linear change of the resistance properties for many materials. The influence of external actions, thanks to existence of cross effects (thermoelasticity, magnetic piezoelectric effect) leads to volume change too.

Changes in the properties and volume are linear and reversed behavior over a wide range acting parameters. So it can be the properties being investigated are depended by the bulk elasticity of solid? Which nature of this connection? What mechanism of the effect of temperature, magnetic field, pressure on the properties?

According to main principles of thermodynamics [222, 223] the state function of an arbitrary volume of a solid (free Gibbs energy) depends on the set of operating thermodynamics parameters.

$$\Phi = U - TS - HB - \sigma\varepsilon \tag{10.1}$$

For the selected operating forces, the complete differential of the state function is

$$d\Phi = -SdT - \varepsilon_\lambda d\sigma_\lambda - B_i dH_i \tag{10.2}$$

Or in the generalized form

$$d\Phi = -x_i dX_i \tag{10.3}$$

where x_i are the generalized co-ordinates (S is the entropy, ε is the deformation, B is the magnetic induction) and X_i are the generalized thermodynamics forces (T is the temperature, H is the magnetic field, σ is the mechanical stress).

Series expansion of the generalized coordinate $x_i = \frac{\partial \Phi}{\partial X_i}$ in the Tailor's series at the equilibrium point X_{0j} in absence of magnetic, thermal and mechanical fields and consideration of the first order terms only allowed us to define the change of any parameter under the action of all forces:

$$dx_i = -\left(\frac{\partial^2 \Phi}{\partial X_i \partial X_j} \right)_0 dX_j = M_{ij} dX_j \tag{10.4}$$

where M_{ij} is the matrix of thermodynamics coefficients. Its components are as follows: $q_i = -\frac{\partial^2 \Phi}{\partial T \partial H_i}$ is the pyromagnetic coefficient; $\alpha_\lambda = -\frac{\partial^2 \Phi}{\partial T \partial \sigma_\lambda}$ is the coefficient of thermal expansion; $\chi_{ij} = -\frac{\partial^2 \Phi}{\partial H_i \partial H_j}$ is the magnetic receptivity, $b_{i\mu} = -\frac{\partial^2 \Phi}{\partial H_i \partial \sigma_\lambda}$ is the magnetostriction (piezomagnetic) coefficient, $s_{\lambda\mu} = -\frac{\partial^2 \Phi}{\partial \sigma_\lambda \partial \sigma_\mu}$ are elastic coefficients. Thus, the influence of any thermodynamics force changes other parameters of the system, and the change of even one parameter entails appearance of all three forces.

Now we select one parameter, namely deformation ε describing the change of volume. The deformation can be carried out by three ways, videlicet heating, magnetization and deformation (the hydrostatic pressure is a special case of mechanical deformation $\sigma_\lambda = \sigma_{ij} = -\delta_{ij} P$). Consequently, the deformation (and as the consequence, stressed) state of system is formed under the effect of three thermodynamic forces, each of which gives the contribution to the general state of the body in accordance with the relationship:

$$d\varepsilon_\lambda = \alpha_\lambda dT + b_{k\lambda} dH_k + s_{\lambda\mu} d\sigma_\mu \tag{10.5}$$

The first component $\alpha_\lambda dT$ describes the change of volume with the heating (thermal expansion). The second component $b_{k\lambda}dH_k$ shows a change of volume under the action of magnetic field (magnetostriction phenomenon). The term $d\varepsilon_{\lambda 3} = s_{\lambda\mu}d\sigma_\mu$ describes the deformation of body under the mechanical deforming and it is Hooke's law.

If the solid is fixed and does not have a possibility to free change of volume $d\varepsilon = 0$ then the thermoelastic stresses appears at heating of the material in the absence of magnetic field $d\sigma_\lambda = -\frac{\alpha_\lambda}{s_{\lambda\mu}}dT$ (mechanocaloric effect). The magnetic field can lead to heating of material too (magnetocaloric effect).

As this follows from (10.5), $d\varepsilon_\lambda = 0$ at the absence possibility to the free expansion and action of one of the parameters will cause a change in two rests, which reflects proceeding into solid redistribution of energy. Hence it follows that there are the necessary to compulsorily control all three parameters during experiments, but not two, as this usually is done. Thus, if body is fixed, then the stress state of solids changes under heating or under magnetic field.

However, a change in the stressed state of solid occurs also in the presence of conditions for a free change of volume under the effect of heating, magnetic field and pressure. This is caused by the following reasons. The fact is that even in the absence any external actions, energy of body is not zero. In the material is a certain stored deformation energy and “zero” internal stresses even at absolute zero. These stresses are caused as reaction on the attracted forces between the atoms, which ensure the retention of the integrity of solid body.

The stresses, caused by the external action (pressure, temperature, magnetic field) allow to regulate the volume of solid and to change its stressed state, but they are only relative small addition to the already existing zero stresses. Summary stress field are determined by the sum of internal and external stresses.

10.2. Internal “zero” stresses in the solid

The volume of solid body is determined by the existing balance of forces of attraction and repulsion between the separate atoms, when they are united into single whole. In the quantum chemistry it is assumed that the atom is the positively charged nucleus, surrounded by the electrons rotating around [224-227]. An electron in the atom is considered as electron cloud with the nonhomogenous density in the radial direction (fig 10.1).

Sizes and form of atom are determined by its electron shell. The simplest cloud form have *S*- electron (sphere). *P*-, *d*-, *f*- electrons have a form of dumbbell, four-blade or even more complex (Fig. 10.2) [227].

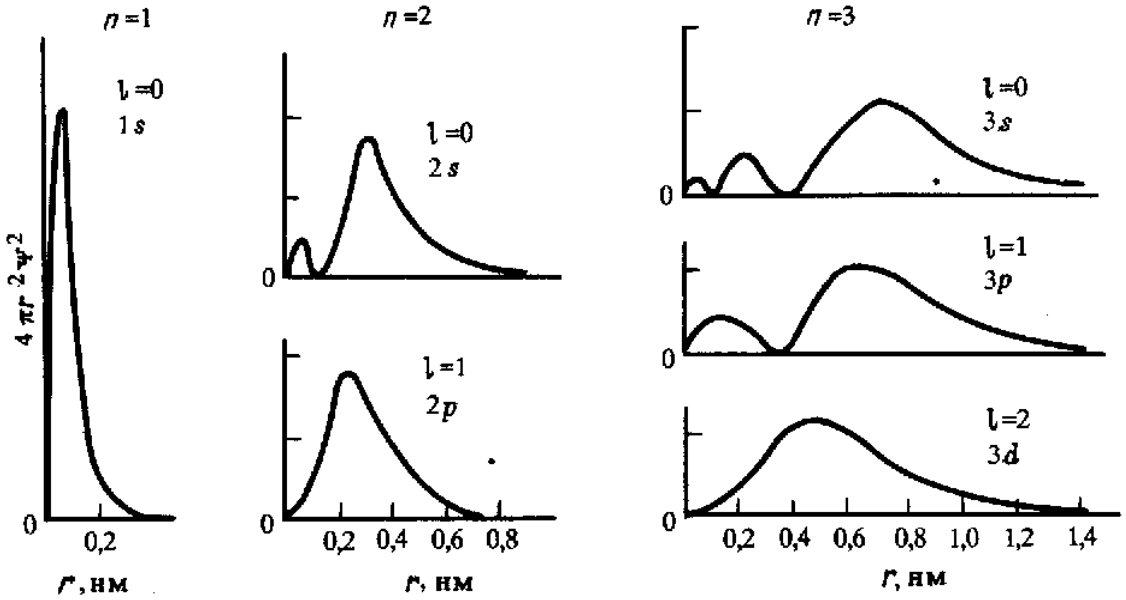

Figure 10.1. Radial distribution of density probability for electron (electron density) at a distance R from the nucleus [224].

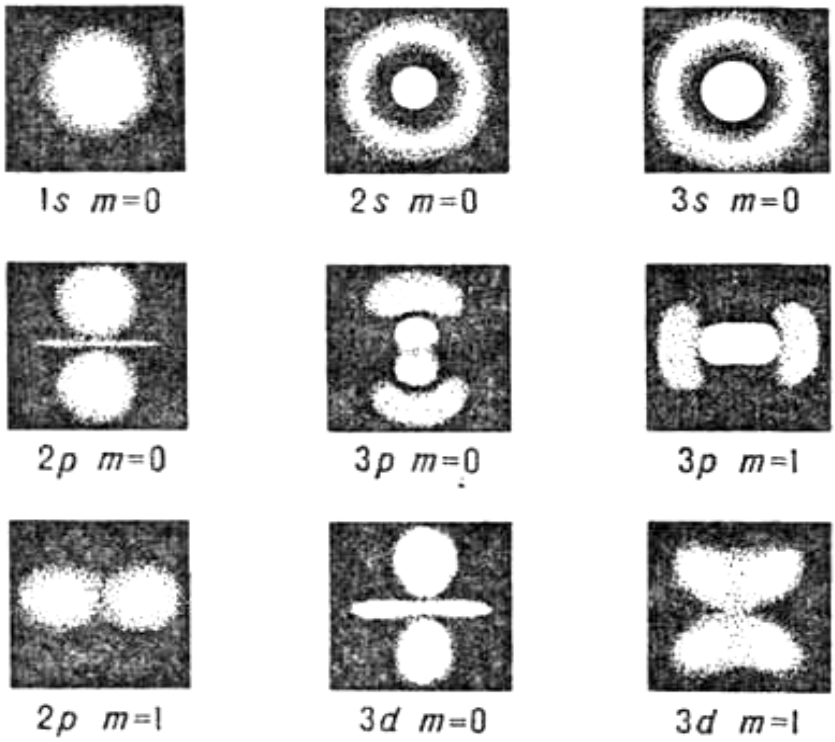

Figure 10.2. Form of electron clouds for different state of electron [227].

Free atom does not have clear boundaries; therefore there are several systems of the determination of the atomic radius, analysis and comparison of which is carried out in the work [228]. In some works [225, 232] the atomic radius includes 90% of electron density, while in others [229-231] it

corresponds to the maximum value of electron density (fig.10.1). The results of the quantum-mechanical calculations of the orbital radius of free atoms for some elements, made works [229-232] give to table.10.1. As we see that the results of calculations differ almost two times.

In the number of works the atomic radius are determined from the data of the measurement of interatomic distances in the crystalline bodies as half of the distance between the lattice site (effective radius). It is clear, that an effective radius is always less than the sizes of free atoms, since with the formation of solid bodies the overlapping of electron orbits unavoidably occurs.

Table 10.1.

	Z		Atom radius R_0, A^o					E_o
			[229]	[230]	[231]	[232]	[233]	[233]
2	3	Li	1,45	1,58	2,37	1,5	1,67	1,0
	4	Be	1,05	1,04	1,99	0,9	1,13	1,5
	5	B	0,85	0,77	1,76	1,2	0,91	
3	11	Na	1,80	1,71	2,5	1,5	1,89	0,9
	12	Mg	1,50	1,28	2,31	0,8	1,60	1,2
	13	Al	1,25	1,31	2,28	1,0	1,43	1,5
4	19	K	2,20	2,16	2,91	1,36	2,36	0,8
	20	Ca	1,80	1,68	2,79	1,54	1,97	1,0
	21	Cs	1,60	1,57	2,67	1,63	1,64	1,36
	22	Ti	1,40	1,48	2,57	1,66	1,46	1,54
	23	V	1,35	1,40	2,49	1,55	1,34	1,63
	24	Cr	1,40	1,45	2,42	1,83	1,27	1,66
	25	Mn	1,40	1,28	2,36	1,88	1,30	1,55
	26	Fe	1,40	1,23	2,29	1,91	1,26	1,83
	27	Co	1,35	1,18	2,24	1,9	1,25	1,88
	28	Ni	1,35	1,14	2,18	1,65	1,24	1,91
	29	Cu	1,35	1,19	2,10	1,81	1,28	1,90
	30	Zn	1,35	1,06	2,10	0,8	1,39	1,65
5	37	Rb	2,35	2,29	3,04	1,3	2,48	0,8
	38	Sr	2,00	1,84	2,99	1,6	2,15	1,0
	39	Y	1,80	1,69	2,83	1,6	1,81	1,3
	40	Zr	1,55	1,59	2,72	2,16	1,60	1,6
	41	Nb	1,45	1,58	2,63	2,28	1,45	1,6
	42	Mo	1,45	1,52	2,56	2,2	1,39	2,2
	43	Tc	1,35	1,39	2,50	1,93	1,36	1,9
	44	Ru	1,30	1,41	2,44	1,69	1,34	2,2
	45	Rh	1,35	1,36	2,39	1,78	1,34	2,3
	46	Pd	1,40	0,57	2,34	1,7	1,37	2,2
	47	Ag	1,60	1,29	2,30	2,05	1,44	1,9

Free atoms enter into interaction and form the solid body at a certain distance with the rapprochement to each other. As a rule, at the atmospheric pressure and room temperatures, the simple solid are formed by the atoms of the uniform elements, which have the nonpolarized electrons. Here we are limited only of metallic materials.

The attracting forces between the atoms are included at the close distances, and the overlapping of electron clouds occurs. The covalent bond appears in the direction of the maximum overlap of electron clouds, which depends on the type of the interacting electrons and number of atoms. As a result the ordering of atoms into the crystal structure take place under the action of chemical forces and solid body is formed.

Chemical forces of interaction (attracting forces) between the neutral atoms are described by the ionization potential E_i, which characterizes energy of the electron detachment from the atom, and also the electronegativity E_o, which characterizes the capability of atom to attract electrons for itself. The increase of electronegativity E_o the element corresponds to increase the attraction force of electrons to atom. Values E_o for the row of metals are given in table. 10.1.

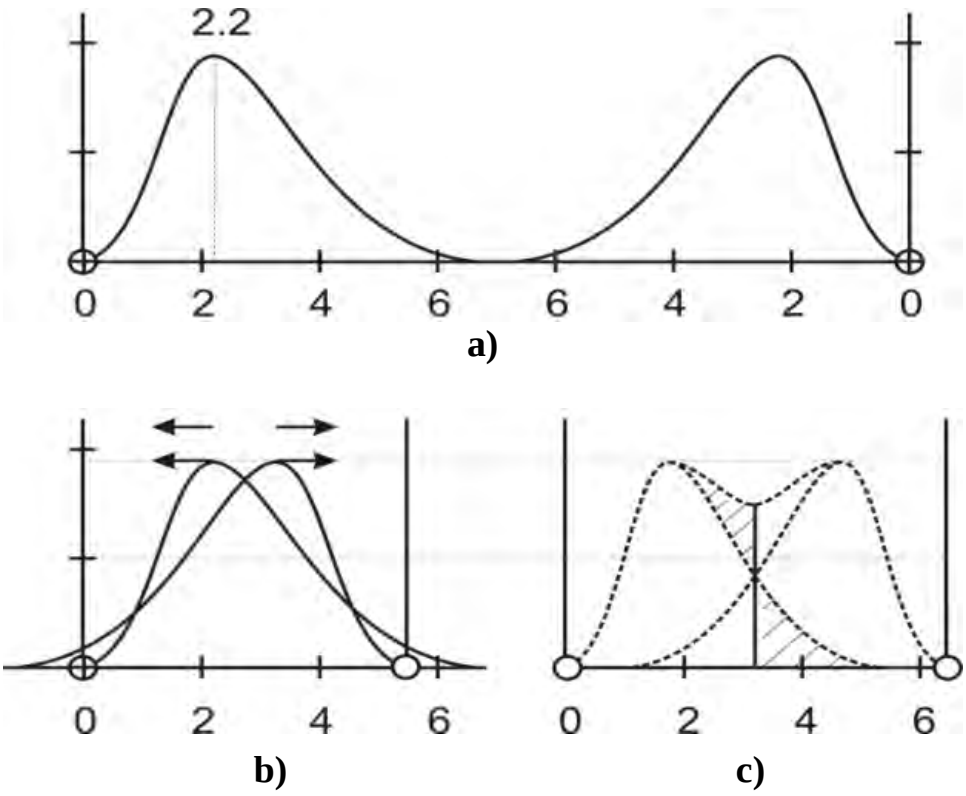

Figure 10.3. Diagram of the appearance of internal stresses. Overlap and the deformation of electron clouds with the rapprochement of the atoms of K a) the density of the electron cloud of free atoms; b) the overlap of orbitals in the solid; c) the addition of orbitals in the solid.

Since the atoms are not solid spheres, the deformation of the electron clouds of atoms occurs with the packing of atoms into crystal lattice; therefore the sizes of atoms in the solid are substantially less than the dimensions of free neutral atom. In Fig. 10.3 is schematically shown the distribution of the density of the electron cloud of two free atoms of potassium (fig.10.3a) and the overlap of these clouds with the rapprochement of atoms.

A probability of the detection of electrons grows in the regions of overlap. The simplest case of summary density distribution function is the addition of the functions of free atoms, whose result is shown in fig.10.3b. The general electron cloud is symmetrical because the polarization is absent for the identical atoms. As can be seen from figure 10.3, the volume of atom decreased, but the density of electron cloud increase. The stored deformation energy of atom increases also.

We see that each atom in the solid is in the compressed state, but it attempts to restore own volume. Why? Most likely because that each particle, each atom has specific volume, which, just as mass and particle charge, is a certain constant. However, in contrast to the mass and the charge, volume is not hard constant, because depends on ambient conditions, i.e., one is capable to react to the external actions, to decrease with the compression, to increase with the heating, to change its form in the magnetic field.

Obviously that the dimensions of crystal lattice and the volume of body will be determined by the balance of forces of attraction, determined by the chemical atomic bond and repulsive forces. Although, as it is assumed in chemistry, the nature of repulsive forces has electrical nature, undoubtedly, the elastic forces of electron shells have contribution to repulsion forces. The inclusion of the elastic forces of in the force balance which form solid, makes it possible to connect the together electrical, chemical and mechanical properties of solid. Nature of all properties is united and now we can find the place of mechanical properties in connection with other properties of solids.

Thus, the deformation of electron shells leads to the appearance internal stresses in the solid, which exist also at absolute zero. These “zero” stresses are the measure of the forces of chemical attraction and compensate them, determining the value of interatomic distances in crystal lattice of body. Such internal stresses are the new collective property of material, found during the association of atoms into new system as solid. Note that because orbitals often have the complex anisotropic form (fig.10.2), the amount of deformation of electron shells when the atoms pack into the lattice is different will be in the different directions. It is determines the anisotropic tensor nature of elastic properties.

Existence of correlation between the chemical bond and the elastic properties of elements could confirm the presence of internal stresses. Data of bulk modulus for the metals of 2 - 6 periods of the periodic table in accordance with the electronegativity to Pauling are given in fig. 10.4. The graph show the

actually linear correlation between the attracting forces in atoms and the strength of material which, as we assume, is caused by the deformation of electron shells. The obtained dependence indicates existence of the regular connection between the chemical and elastic properties of solid bodies.

Very good correlation between the density of electron shells and the elasticity of material is observed. In Fig. 5 and 6 are shown the values of the bulk modulus and density of the electron shells $\boldsymbol{\rho_d}$ for a number of chemical elements. An estimate of the average density of electron shells is given in Table 2. The density $\boldsymbol{\rho_d}$ are executed according to formula $\rho_d = \frac{Zm_e}{V_d}$, where Z - the atomic number of element, m_e - the mass of electron, V_d - volume of the deformed atom in the lattice.

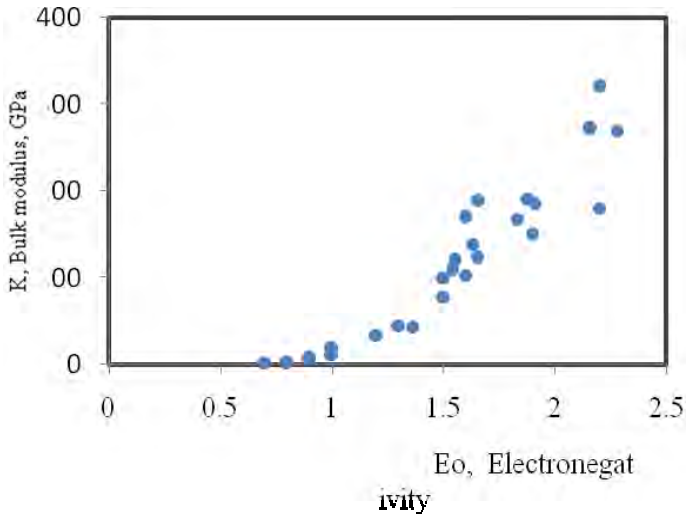

Figure 10.4. Correlation of the bulk modulus and electronegativity.

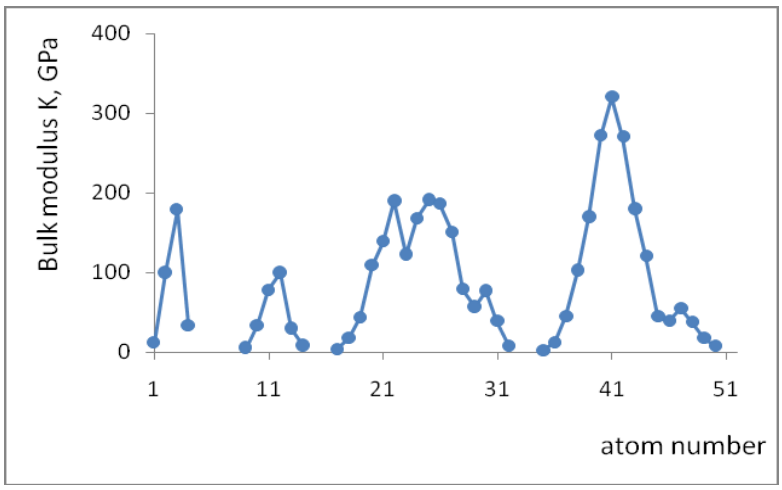

Figure 10.5. Influence of atomic number on the elastic properties of the elements.

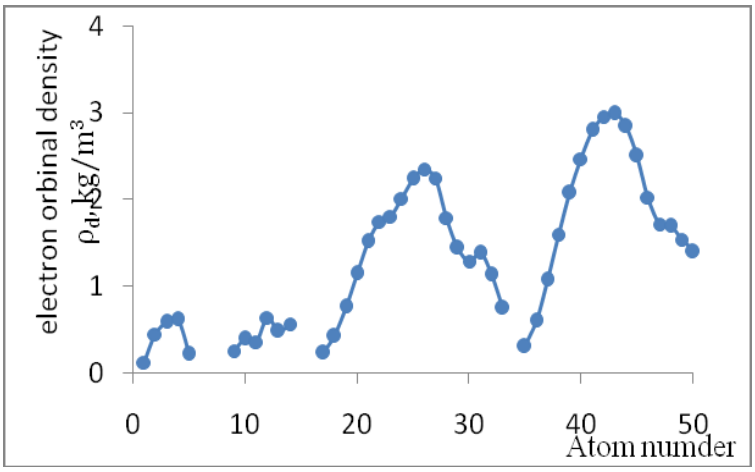

Figure 10.6. Influence of the atomic number on the density of the electron shells.

The surprising agreement of the behavior for dependences confirms the hypothesis that the density of electron shells determines the strength of the material.

10.3. Estimation of internal stresses

The values of internal stresses are sufficiently high and attain several GPa.

1. The estimation of internal stresses within the linear theory of elasticity is made on the assumption that the deformability of electron cloud correlates with the elastic properties of the material:

$$\sigma_{lm} = c_{lmik}\varepsilon_{ik} \tag{10.6}$$

where C_{lmik} are elastic modules of material. For isotropic materials we can use the simplified equation

$$\sigma_i = K\varepsilon_i \quad \text{or} \qquad \sigma = K \cdot \frac{\Delta V}{V_0} \tag{10.7}$$

where K is bulk modulus (compression modulus) [234-235], $\Delta V = V_0 - V_d$ is the change of volume of free atom V_o at packing the free atom to crystal lattice (the simplest case of the spherical form of the atom is examined $V_o = \frac{4\pi}{3} R_o^3$), V_d is the volume of the deformed atom in the lattice, calculated from the data of element density $V_d = \frac{m_a}{\rho}$ (m_a is atom mass, ρ is density) .

Table 10.2.

period	Z	element	R_a, A° [3]	V_0 $10^{-30}m^3$	m_a, a.m.u.	ρ, 10^3 kg/m^3	V_d, $10^{-30}m^3$	ΔV, $10^{-30}m^3$	K, GPa	ρ_e, kg/m^3	σ, GPa	U_d, eV
2	3	Li	2,37	55,64	6,94	0,534	21,57	34,07	12	0,125	**7,7**	0,7
	4	Be	1,99	33,44	9,01	1,848	8,07	25,37	100	0,446	**76**	6,0
	5	B	1,76	22,76	10,81	2,34	7,67		179	0,586		5,5
	6	C				2,25	8,85		34	0,616		
	7	N				0,80	29,05			0,219		
	8	O										
	9	F										
	10	Ne										
3	11	Na	2,5	65,31	23,0	0,97	39,36	25,95	6	0,254	**2,3**	0,2
	12	Mg	2,31	50,85	24,3	1,74	23,19	27,66	34	0,394	**18,4**	1,6
	13	Al	2,28	49,54	27,0	2,69	16,66	32,88	78	0,360	**51,5**	5,1
	14	Si				2,33	20,00		100	0,637		
	15	P				1,82	28,24		30	0,484		
	16	S				2,07	25,71		9	0,566		
	17	Cl										
	18	Ar										
4	19	K	2,91	101,9	39,1	0,86	75,47	26,47	3,4	0,229	**0,9**	0,07
	20	Ca	2,79	90,77	40,1	1,55	42,92	47,85	18	0,424	**9,5**	1,4
	21	Cs	2,67	79,56	44,9	2,99	24,95	54,82	44	0,765	**30,4**	5,1
	22	Ti	2,57	70,95	47,8	4,54	17,51	53,44	109	1,144	**81,7**	13,5
	23	V	2,49	64,53	50,9	6,11	13,84	52,69	139	1,512	**112,6**	18,2
	24	Cr	2,42	59,24	52,0	7,18	12,02	47,22	190	1,744	**150,1**	18,8
	25	Mn	2,36	54,94	54,9	7,21	12,65	42,29	123	1,798	**93,5**	12,7
	26	Fe	2,29	50,19	55,8	7,87	11,77	38,42	168	2,010	**127,7**	15,1
	27	Co	2,24	46,98	58,9	8,9	10,99	35,99	191	2,235	**145,1**	17,0
	28	Ni	2,18	43,30	58,7	8,9	10,85	32,45	186	2,348	**139,0**	13,8
	29	Cu	2,10	38.71	63,5	8,96	11,77	26,94	151	2,242	**104,2**	8,7
	30	Zn	2,10	38,71	65,4	7,13	15,29	23,42	79	1,785	**47,8**	3,4
	31	Ga	2,24	46,98	69,7	5,91	19,58	30,4	57	1,440	**36,8**	3,4
	32	Ge				5,32	22,65		77	1,285		
	33	As				5,73	21,70		39	1,383		
	34	Se				4,79	27,36		8	1,129		
	35	Br				3,12	42,51			0,749		
	36	Kr										
5	37	Rb	3,04	117,4	85,5	1,53	92,73	24,70	2,6	0,303	**0,55**	0,04
	38	Sr	2,99	111,7	87,6	2,54	57,26	54,47	12	0,603	**5,76**	0,9
	39	Y	2,83	94,74	88,9	4,47	33,01	61,73	45	1,075	**29,25**	5,5
	40	Zr	2,72	84,12	91,2	6,65	22,77	61,33	103	1,598	**75,2**	14,3
	41	Nb	2,63	76,04	92,9	8,57	17,99	58,05	170	2,072	**129,2**	23,3
	42	Mo	2,56	70,13	95,9	10,28	15,49	54,64	272	2,466	**209**	35,2
	43	Tc	2,50	65,31	98.	11,50	14,00	51,31	320	2,795	**249,6**	39,0
	44	Ru	2,44		101,1	12,37	13,56		270	2,952		
	45	Rh	2,39	57,06	102,9	12,45	13,72	43,34	180	2,989	**136,8**	18,1
	46	Pd	2,34	53,55	106,4	12,02	14,69	38,86	121	2,84	**88,3**	10,4
	47	Ag	2,30	50,85	107,8	10,49	17,07	33,78	45	2,50	**29,7**	3,1
	48	Cd	2,27	48,89	112,4	8,65	21.57	27,32	39	2,022	**21,5**	1,8
	49	In	2,41	58,50	114,8	7,31	26,07	32,43	55	1,71	**30,2**	3,3
	50	Sn	2,31	51,55	118,7	7,31	26,95	24,60	38	1,69	**17,8**	1,,2
	51	Sb	2,17	43,30	121,7	6,69	30,21	13,09	18	1,539	**5,4**	0,2
	52	Te				6,24	33,94		8	1,394		

The results of calculations are given in Table 10.2. For the calculations are used the maximum values R_0, given in the work [231]. The densities of elements, atomic mass are taken from [233, 236,237], the values of the elastic bulk modulus are taken from [234-235], stresses are calculated by formula (10.7).

The elastic deformation energy of atom is shown in tabl.10.2 too. Approximate estimations of this energy were made by formula $U_d = \int \sigma \cdot dV \approx \frac{1}{2}\sigma \Delta V$.

Estimations show that the stored energy of elastic deformation in the atom is very great and must be considered with a study of effects in solids.

2. Estimations of stresses from the data of volume change during the melting

Internal stresses can be also estimated, using data [234, 233] with respect to a change in the volume of material during the melting (see table 10.3). Latent heat of melting λ can be considered as energy of deformation (energy of increase of lattice parameters) per unit mass, i.e., as the energy, spent on an increase in the volume of the body at constant temperature of melting. Hence it is possible to find the stress

$$\sigma = \frac{\Delta E}{\Delta V} = \frac{m\lambda}{\Delta V} = \frac{\rho V \lambda}{\Delta V}, GPa \qquad (10.8)$$

Estimation according to (10.8) shows that inner stress reach to 4 – 22 GPa subject to element.

Table 10.3.

Period	Z	element	$\Delta V/V_t$ %	λ, кj/кg	ρ, 10^3 kg/m^3	σ, GPa	K, GPa
3	11	Na	2,2	115	0,96	4,1	6
	12	Mg	4,2	344	1,74	14,2	34
	13	Al	6,6	400	2,7	16,4	78
4	19	K	2,4	59,7	0,86	2,2	3,4
	30	Zn	6,9	102	6,9	10,2	70
5	47	Ag	5,0	105	10,5	22,0	45
	50	Sn	2,6	60	7,3	16,8	55
6	79	Au	5,2	60	19,3	22,3	170
	82	Pb	3,6	25	11,3	7,8	42

3. Estimations of stresses according to the data of the work [181]

For the results shown on fig.8.7, the identical value of conductivity testifies about the identical structure of material determined by internal stresses. Pressure of 0.1 GPa gives the same contribution to the solid's stress state as the temperature rise of 6,3 K, or the magnetic field H = 2.3 kΘ. So heating by Δ T ~ 300 K correspond to stresses Δσ ~ 4 GPa.

We see that different ways of estimation gives the same order of values. The greatest stresses 1- of 150 GPa are obtained during the estimation by Hooke's law, but this connected with the fact that we used data for the maximum values of the orbital radius of free atom.

So, **the total inner stress** consists of two components: the ‘zero’ stress already presented in solid before external influences and the stress created by the external influence. The second component can be managed in various ways: by the change of pressure, temperature, magnetic field in compliance with the eq. (10.5).

10.4. Nature of structural phase transformations

Phase transitions, observed in many materials, are fixed with respect to an abrupt change in their properties and are connected first of all with reconstruction of the structure of crystals. In accordance with the general principles of physics of crystals [238], reconstruction of structure occurs, when in the specific systems of deformation (slip, chipping, twinning, martensite transformation and others) are attained the critical values of the shear stresses of τ_c, which are the constant of material, which depends on the symmetry of lattice and elastic properties.

The concept of existence of the spectrum of the critical stresses (and, correspondingly, the spectrum of the critical or quantum values of energies) represents on the macrolevel the existence of the quantum energy states of the deformed atom in the solid. The specific critical form and volume of atom corresponds to each such quantum state of energy on the microlevel.

On the macrolevel the external influence (pressure, temperature and magnetic field) causes a linear change of the properties between the critical points, and the jump of properties upon transfer through these critical points. On the microlevel there is the linear (elastic) change for volume and form of atom under P, T and H impact between the critical points and the jump of the form and the size of atom upon transfer of the critical values of energy. The new adjustment of atoms to each other leads to a change in the symmetry of the crystal.

Note that for s- and p- elements, for which the distance between energy levels is sufficiently great, the significant energies are necessary for achievement critical volume; therefore the linear laws of volume elasticity and other properties acts over a wide range temperatures, pressures, magnetic field. For 3d, 4d- elements, in which the overlap of electron levels is observed, the several sequential structural transformations can be observed already in the small interval of the values of temperature, pressure, and field.

As it was said above, the tensor of the total internal stresses of σ_{ij} is a sum of the external stresses, caused by the action of temperature, pressure, magnetic field, and the internal “zero” stresses, relative to the deformation of electron shells at aggregation of atoms into solid. This stress tensor contains

the diagonal components corresponded to volume change and the deviator part corresponded to shape part.

The main contribution to the tensor of total stresses give internal stresses, but with the aid of the action of one or several external factors (temperature, pressure, magnetic field) it is possible to substantially change the form of the tensor of total stresses in such a way that the critical value of stress will be achieved in the operational deformation systems and the structure of material will be reconstructed.

Shear stress is located as the convolution of the tensor of total stresses in the weakest and vulnerable direction in the anisotropic crystal:

$$\tau = \sigma_{ij} p_i q_j \tag{10.9}$$

where p_i, q_j are vector components that determine the surface and direction of the deformation systems, and σ_{ij} is tensor of total stresses.

Each of the parameters P, T, H gives the own contribution to value τ, as a result of cross effects (eq. 10.5). Because of the linearity (elasticity) of the contribution of thermo-, baro- and magnetoelastic components to the total stress the critical stress can be presented in the form to two-dimensional surface (3-axed ellipsoid) in 3-diomentions phase space, where along the axes are plotted the thermo-, baro- and magnet elastic components of stress (fig.10.7a). Actually this indicating surface of critical stresses is the phase diagram of the structural state of crystal.

Fig.10.7b shows the lines of level (isobar) which corresponds to section of surfaces of critical stresses at constant pressures when $P_3 > P_2 > P_1$. It should be noted that T - H - P diagram for the phase transitions in the ferroelectrics [1] and in perovskites [177] take the similar form, which testifies in favor proposed model.

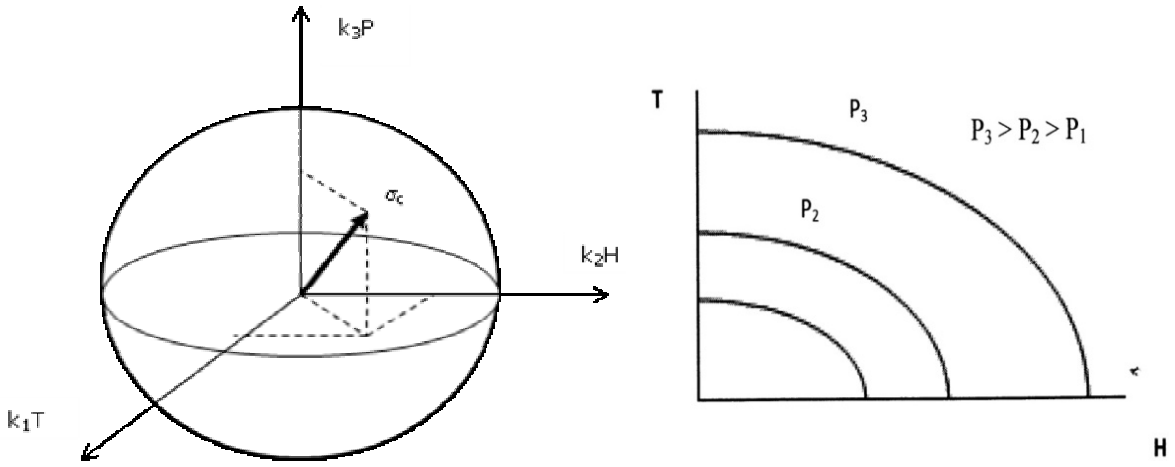

Figure 10.7. Surface of critical stresses (a) and level line (b) in the phase space (P, H, T).

The analysis of numerous studies of other materials (see previous chapters) shows that many anomalies and peculiarities of properties find the explanation within the frame of the suggested hypothesis. Internal stresses always be present in the material and indicate united nature of phase transitions as the consequence of a change in the structural symmetry of the crystals

Conclusions

1. Experiments under high pressure have shown the importance and the necessity of consideration of mechanical stresses in solids. Internal stresses are inalienable descriptions of new co-operative property of material found at the union of single atoms to a solid. Among other thermodynamic factors, stress can be considered as important integrating characteristics of a solid, as it is the most sensible to the material structure.
2. The appearance of internal stresses is conditioned by deformation of electron orbitals at the formation of a solid and depends on the nature of bonds between atoms. The anisotropic character of stresses is related to the anisotropic form and size of orbitals.
3. The value of stresses in solid is high (few GPa) and corresponded energy of elastic deformation of the atom too (few eV) therefore this stored elastic energy must be taken into account while considering many different effects.
4. Phase transitions are consequences of structural reconstructions of crystal at some critical stresses.
5. Influence of different external forces (temperature, magnetic field, pressures and oth.) causes change of internal stresses, because of cross effects. Therefore achievement of critical stresses in a crystal (and subsequent phase transition) can be achieved by different ways.

References

1. Bruce A.D., Cowley R.A *Structural Phase Transitions. //* London: Taylor and Francis Ltd, 326 p. (1981).
2. Van Santen J.H., Jonker G.H. *Electrical Conductivity of Ferromagnetic Compounds of Manganese with Perovskite Structure //* Physica 16, pp.599–600 (1950).
3. Kusters R. M., Singleton J., Keen D. A., McGreevy R., Hayes W. *Magnetoresistance measurements on the magnetic semiconductor* $Nd_{0.5}Pb_{0.5}MnO_3$*//* Physica B155, pp.362-365 (1989).
4. Von Helmolt R., Wecker J., Holzapfel B., Schultz L., Samwer K. *Giant negative magnetoresistance in perovskitelike* $La_{2/3}Ba_{1/3}MnO_x$ *ferromagnetic films //* Phys. Rev. Lett. 71, pp.2331 - 2333 (1993).
5. Kadomtceva A.M., Popov Y.F., Vorobiev G.P. and all. Anomalies of thermal expansion and magnetostriction with the phase transitions in the single crystals $La_{1-x}Sr_xMnO_3$ // Fizika Nverdogo tela, V.42(6), 1077-1082 (2000).

6. Polyakov P. I., Kucherenko S. S. Dynamics of structural phase transition and changes in properties under the influence of elastically anisotropic deforming stresses, regularities of critical lines and points in magnetic semiconductors and magnetic dielectrics // Journal of Magnetism and Magnetic Materials 278, 138-155 (2004).
7. van den Handel J., Gijsman H. M., Poulis N. J. *The magnetic susceptibilities of an anti-ferromagnetic single crystal of $CuCl_2 \cdot 2H_2O$//* Physica 18, 862 (1952).
8. Landau L.D., Lifshitc E.M. Theoretical physics. Electrodynamics of continuous media. Moscow, 532 p. (1973).
9. Kapitca P.L. Scientific proceeding. V.1. *The strong magnetic fields*. Moscow, Science, 461 p. (1988).
10. Lazarev B.G. *Life in the science. Selected preoceeding. Memory*. Kharkov, 704 p. (2003).
11. Mattis D. *The Theory of Magnetism* (Harper, New York, 1965).
12. P.Bridgmen. Physics of high pressure. Moscow (1935).
13. P.Bridgmen. Newest works in the high-pressure area. Moscow (1948).
14. D.S.Tsiklis. Rechnology for physical chemistry studies at high pressures. Moscow (1951).
15. K. Bradley, Using of high pressures technique for studies of solid. Mir, Moscow (1972).
16. Ch. Pool. Technology of EPR spectroscopy, Moscow (1970).
17. E.S.Itskevich. PRIB TEKH EKSP (Priboru I thechnika experiment) № 3, 6 (1999).
18. A.A.Galkin, V.A.Popov, P.I.Poljakov, V.G.Sunkov. FNT (Fizika nizkich temperatur), V. 2, 49 (1976).
19. P.I.Poljakov, V.G.Sunkov. Prib Tekh Eksp, № 1, 223 (1977).
20. V.G.Sunkov E.I.Osuka. Technology of light alloys, Institute of the light alloys, Moscow, № 5 (1974).
21. E.S.Itskevich, A.N.Voronovski, A.F.Gavrilov. Prib Tekh Eksp (Priboru I thechnika experiment) № 6, 161 (1966).
22. P.I.Poljakov, V.V.Permjakov, V.G.Sunkov, I.G.Gavrish. Prib Tekh Eksp (Priboru I thechnika experiment) № 1, 201 (1982).
23. D.V. Montgomery, Creation of strong magnetic field by the use of solenoids, Mir, Moscow (1971).
24. V.V.Permjakov, I.G.Gavrish, N.V.Tarjanik, N,G Usov. ЖТФ (Journal of technical physics), V.49, 427 (1979).
25. A.V.Oleinik, P.I.Poljakov, V.G.Sunkov. High Pres Phys Tech V.4, № 1, 88 (1994).
26. V.P.Djakonov, V.I.Markovich, P.I.Poljakov. FTT, V. 30, 1878 (1988).
27. V.P.Djakonov, V.I.Markovich, P.I.Poljakov and all. FNT V.16, 1424 (1990).
28. I.S.Maksimov, N.I.Mesin, Y.M.Nilolaenko, P.I.Poljakov, V.A.Shtaba. (*Fizika I technika vusokich davlenij*) V.10, № 1, 28 (2000).
29. P.I.Paschenko, P.I.Poljakov, S.S.Kucherenko, V.A.Shtaba. (*Fizika I technika vusokich davlenij*) V.11, № 1, (2001).
30. S.S.Kucherenko, P.I.Paschenko, P.I.Poljakov, V.A.Shtaba. *Pisma v J. Tecn. Experim. Physics*. N 11, 24 (2001).
31. S.S.Kucherenko, V.I.Michajlov, P.I.Paschenko, P.I.Poljakov, V.A.Shtaba, V.I.Djakonov. *Pisma v J. Tecn. Physics*. N 27, вып. 15, 38 (2001).

32. S.S.Kucherenko, P.I.Paschenko, P.I.Poljakov, V.A.Shtaba, A.A.Shemjakov. *Fizika nizkich temperature*, V.27, 761 (2001).
33. P.I.Polyakov, V.V.Sljusarev, V.A.Shtaba. FTVD (*Fizika I technika vusokich davlenij*. V.10, № 1, 94 (2000).
34. S.Svenson. Physics of high pressure. Moscow, 367 p. (1963).
35. S.S.Kabalkina. X-ray studies at the high pressures. Moscow, Science. 174p. (1979).
36. Marchal W. *The antiferromagneticism of $CuCl_2 \cdot 2H_2O$ //* Journal of Physics and Chemistry of Solids V.7, 159-164 (1958).
37. Nagamiya T. *Antiferromagnetism* // Proc. Internat. Conf. Theor. Phys.- Tokyo, P. 742-749 (1953).
38. Nagamiya T. *Theory antiferromagnetic resonance absorption in $CuCl_2*2H_2O$* // Progr. Theoret. Phys. V. 11, N3.- P. 309. (1954).
39. Fisher. *Nature of critical states*. Moscow, 220 p. (1968).
40. Rundle R.E. *Antiferromagnetic Ordering and Electronic Structure of $CuCl_2*2H_2O$ as Determined from Nuclear Magnetic Resonance//* J. Am. Chem. Soc79. P. 3372. (1957).
41. V.G.Bar'jachtar, V.A.Popov. Theory of the intermediate state AFM at first-order phase transition in magnetic field. // Pisma v JFEPh. V.9, N11. p. 634. (1969).
42. E.V.Zarotchentsev, V.A.Popov. Energy spectra and resonance frequencies of the biaxial antiferromagnet. // FTT. N8. P. 2489. (1964).
43. V.A.Popov, V.I.Skidanenko. Nonlinear effects in the antiferromagnets // Proc. IPNT Ac.sci. USSR. V. 18. p.17. (1972).
44. Umebayashi H., Shikane G., Frazer B.C., Cox D.E. *Canted Antiferromagnetism of $CuCl_2*2D_2O$ //* Jour. of Applied Physics.- 1967.- 38, N3.- P. 1461.
45. Date N., Nagata K. *Antiferromagnetic Resonance in Hydrated Copper Salts* // Jorn. Appl. Phys.- 1963.- 34, N4.-P. 1038.
46. Harding G.L., Lanchester P.C., Street R. *The low temperature magnetic thermal expansion of $CuCl_2*2H_2O$* // J.Phys. C- 1971.- 4, N 11-12.- P. 2923.
47. Harker D. *The Crystal Structure of Cupric Chlorid Dehydrate* // Z. Krist.- V.93, N10. P.136-145. (1936).
48. Peterson S.W., Levy H.A. *Proton Positions in $CuCl_2 \cdot 2H_2O$ by Neutron Diffraction* // Jorn. Chem. Phys. V.26, N1.- P. 220-221 (1957).
49. Poulis N.J., Harderaan G.E.G. *Position des Proton Dans $CuCl_2 \cdot 2H_2O$ Determince par la Metode de la Resonance Magnetique Nucleaire*// Journ. Chem. Phys. 50. P. 110-113. (1953).
50. S.V.Ivanova, S.I.Lukin, V.T.Telepa. *The temperature dependence of the elastic parameters of antiferromagnetic single crystal* $CuCl_2 \cdot 2H_2O$ и $CrCuCl_3$// FTT. V.23, N4, p.1173 (1981).
51. Lecuyer B., Revard J.P. *Susceptibilites magnetiques de monocristaux de $CoCl_2 \cdot 6H_2O$ ed $CoCl_2 \cdot 6H_2O$ a basse temperature* // C P.acad. Sc, Paris. 269 (B). P. 78. (1969).
52. Umebayashi H., Frazer B.C., Cox D.E., Shirane G. *Spin-Density Distribution in $CuCl_2 \cdot 2D_2O$* // Phys. Rev. 1968.- 167 N2..- P- 519-524.
53. Shirane G., Frazer B. C., Friedberg S. A. *Magnetic structure of $CuCl_2 \cdot 2H_2O$* // Physics Letters, Volume 17, Issue 2, 1 July 1965, Pages 95-96.

54. Yong W.M., Verstelle J.S. *Antisimmetric exchanging interaction and spin-spin relaxation in $CuCl_2 \cdot 2H_2O$*// Phys. Lett.- 1972.- A40, N 5.- P. 403.
55. Yung-Li W., Herbert Callen *Spin-wave in the antiferromagnetic under spin-flop and metastability of spin-flop phase*// J. Phys. and Chem. Solids.- 1964.- 25, N12.- P. 1459.
56. Naiman C., Lawrence T. *Time relaxation spin-flop phase in $CuCl_2 \cdot 2H_2O$* // J. Appl. Phys.- 1965.- 36, N 3.- P. 1161.
57. N.K.Danshin. A.C.Zelter, V.A.Popov. *Four-sublattice model of biaxial antiferromagnet and its comparison with the experiment* // FNF, V.11, N7, p. 755-768. (1985).
58. Maxwell L.R., Mcqwire T.R. *Antiferromagnetic Resonance*// Reviews of modern physics.- 1953.- 25, N 1.- P. 279.
59. Van der Sluijs, Zweers B.A., De Klerk D. *The Upper Transition Field of $CuCl_2 \cdot 2H_2O$ from 1 to 4°K*// Phys. Lett.-1967.- 24A, N 12.- P. 637-638.
60. Taeko N. *Dynamic behavior of the magnetization vectors at the sublattices in antiferromagnetics*// J. Phys. Soc. Japan.- 1969.- 27, N 2.- P. 343.
61. Forstat H., Bailey P., Ricks J.P. Spin-flop phenomenon in $LiCuCl_2.2H_2O$// J. Appl. Phys.- 1971.- 42, N 4.- P. 1559-1560.
62. Terrell J., Lawrence T. *Influence of demagnetizing field on behavior of $CuCl_2 \cdot 2H_2O$ near of the sublattice reorientation field*// J. Appl. Phys.- 1967.- 39, N 3.- P. 1464.
63. Poulis N.J., Hardeman G.E.G. *The Threshold Field Phenomenon in an Antiferromagnetic Single Crystal* // Physica.-1954.- 20, N 1.- P. 7-12.
64. V.G.Barjachtar, A.A.Galkin, S.V.Ivanova, P.I.Poljakov, V.I.Kamenev. Magnetoelastic properties of the dihydrate of copper chloride under the pressure. FTT. V.21, N 5, P.1517-1522. (1979).
65. A.A.Galkin, S.V.Ivanova, P.I.Poljakov, V.I.Kamenev. *Structural, magnetic and resonance properties $CuCl_2 \cdot 2D_2O$*// FTT. V. 21, N9, p.2580-2583. (1979).
66. S.M.Rjabchenko, L.A.Shulman. *On the influence of exchange mutually- action in the crystal $CuCl_2 \cdot 2H_2O$ on wideline EPR.* // FTT, V.8, N7, p.2213-2217 (1966).
67. Iton J., Fujimoto M., Ibamoto H. *Paramagnetic Resonance Absorption in Three Chlorides of Copper*// Letters to the Editor. N 2. P. 852. (1952).
68. C.J.Gorter Observations on antiferromagnetic crystals $CuCl_2.2H_2O$// Rev. Mod. Phys. V.25, N 2.- P. 332-343 (1953).
69. Renard J.P. *Resonance magnetique des deutons en champ nul dans $CuCl_2 \cdot 2D_2O$*// Le Journ. de Physique. V.33, N 11-12.- P. 1059-1066. (1972).
70. Zimmerman N.J., Bastmeijer J.D., Handel J. AFMR *and critical width of the paramagnetic resonance line in $LiCuCl_2 \cdot 2H_2O$*// Phys. Lett. A40, N 3. P. 259. (1972).
71. V.G.Barjachtar, A.A.Galkin, V.G.Telepa. *Intermediate state in the zone of the tilting of sublattices in the antiferromagnetic single crystal $CuCl_2 \cdot 2H_2O$* // FNT. V.1, N. 4. P.483-487 (1975).
72. Date M. *Antiferromagnetic Resonance in $CuCl_2 \cdot 2D_2O$* // Journ Phys. Soc. Japan. V.12, N 11. P.1168 (1957).
73. Nagamiya T. *Theory of Antiferromagnetism and Antiferromagnetic Resonance Absorption, II* // Progress of Theoretical Physics 6, pp.350-355 (1951).
74. Kittel C. *Theory of Antiferromagnetic Resonance* // Phys. Rev. 82, 565 - 565 (1951).

75. Gorter C.J., Haantjes J. *Anti-ferromagnetism at the absolute zero of temperature in the case of rhombic symmetry* // Physica, Volume 18, Issue 5, May 1952, Pages 285-294.
76. Yosida K. *On the Antiferromagnetism of $CuCl_2 2H_2O$ Single Crystal* // Progress of Theoretical Physics 7, pp. 25-38 (1952).
77. Nagamiya T. *Theory of Antiferromagnetic Resonance in $CuCl_2 \cdot 2H_2O$* // Progress of Theoretical Physics 11, pp. 309-327 (1954).
78. Gorter C. J. *Observations on Antiferromagnetic $CuCl_2 \cdot 2H_2O$ Crystals* // Rev. Mod. Phys. 25, 332 - 337 (1953).
79. Date M., Nagata K. *Antiferromagnetic Resonance in Hydrated Copper Salts* // J. Appl. Phys. 34, pp. 1038-1044 (1963).
80. V.G.Barjachtar, A.E.Borovik, V.A.Popov, E.P.Stefanovskij. V.G.Barjachtar *Fluctuations of domain walls in the antiferromagnet* // FTT, 12, 3289-3297 (1970).
81. V.G.Barjachtar, A.A.Galkin, S.N.Kovner, V.A.Popov. *Antiferromagnetic resonance in the dihydrate of copper chloride at the low frequencies with the tilting of the magnetic moments of the sublattices* //Pisma v JETF, V.10, p.292-296 (1969).
82. V.G.Barjachtar, A.N.Bogdanov, V.A.Popov. *Antiferromagnetic resonance in the intermediate state with spin-flop transition.* // Inst. Tech. Phys. AcSc USSR, Kiev, preprint, (1985).
83. A.A.Galkin, A.V.Vetchinov, N.K.Danshin, A.A.Popov. *Excitation of the connected branches of the uniform AFM $CuCl_2 \cdot 2H_2O$ in inclined magnetic field* // FNT, V.3, 185-193 (1977).
84. V.G.Barjachtar, A.A.Galkin, S.N.Kovner, V.A.Popov. *Resonance absorption in the dihydrate of copper chloride in the inclined magnetic field* // Dokl.AcSc USSR, Phys., V.190, p.1056-1058 (1970).
85. Ubbink J. Theoretical interpretation of the antiferromagnetic resonance in copper chloride // Physica, Volume 19, Issues 1-12, P.919-927. (1953)
86. Gerritsen H.J. On the interpretation of some data obtained with antiferromagnetic resonance in hydrated copper chloride // Physica, Volume 21, Issues 6-10, Pages 639-650. (1955).
87. Ubbink J. Theory of anti-ferromagnetic resonance in a crystal of rhombic symmetry at the absolute zero // Physica, Volume 19, Issues 1-12, 1953, Pages 9-25.
88. E.V.Zarotchentsev, V.A.Popov. The ground states of the biaxial antiferromagnet //FTT, V. 6, 1579-1588 (1964).
89. Poulis N. J., van den Handel J., Ubbink J., Poulis J. A., Gorter C. J. On Antiferromagnetism in a Single Crystal // Phys. Rev. 82, 552 - 552 (1951).
90. Ubbink J., Poulis J.A., Gerritsen H.J., Gorter C.J. Anti-ferromagnetic resonance in copper chloride // Physica, Volume 18, Issues 6-7, June-July Pages 361-368. (1952).
91. Gerritsen H.J., Okkes R., Bölger B., Gorter C.J. Antiferromagnetic resonance in hydrated copper chloride at 32000 MHz // Physica, Volume 21, Issues 6-10, P.629-638. (1955).
92. Hardeman G.E.G., Poulis N.J. Antiferromagnetic resonance at low frequency // Physica, V.21, Issues 6-10, Pages 728-736. (1955).

93. Yamazaki H., Date M. New Antiferromagnetic Resonance Lines in $CuCl_2 \cdot 2H_2O$ // Journal of the Physical Society of Japan Vol.21, No.8, August, pp. 1615-1615. (1966).
94. Yosida K. Theory of the Antiferromagnetic Resonance Absorption in $CuCl_2 2H_2O$ // Progress of Theoretical Physics 7, pp. 425-432 (1952).
95. V.G.Barjachnar, A.A.Galkin, V.T.Telepa. *Intermediate state in the zone of the tilting of sublattices in the antiferromagnetic single crystal* $CuCl_2 \cdot 2H_2O$ // FNT 1, 483-487 (1975).
96. A.A.Galkin, N.K.Danshin, A.V.Vetchinov. *Dependence on the pressure of the antiferromagnetic resonance* $CuCl_2 \cdot 2H_2O$ // FNT 2, 1311-1319 (1976).
97. V.G.Barjachnar, A.A.Galkin, E.P.Stefanovsij, V.G.Telepa. *Dependence of the width of the domain of existence of intermediate state in an antiferromagnetic single crystal of the dihydrate of copper chloride on the temperature* // FTT, V. 18, 3047-3049 (1976).
98. V.V.Eremenko, A.V.Klochko, V.M.Naumenko. *Antiferromagnetic resonance in intermediate state* $CuCl_2 \cdot 2H_2O$ // Pisma v JETP, V.40, 219-221 (1984).
99. V.V.Eremenko, A.V.Klochko, V.M.Naumenko, V.Pishko. *Antiferromagnetic resonance in intermediate state* $CuCl_2 \cdot 2H_2O$ // FNT, V.11, 327-331 (1985).
100. A.A.Galkin, S.N.Kovner. *Antiferromagnetic resonance* $CuCl_2 \cdot 2H_2O$ *at low frequency* //Pisma v JETF, V. 9, 456-459 (1969).
101. A.V.Oleinik, P.I.Poljakov, V.A.Popov. *Relaxation satellites of the resonance absorption of HF Field in* $CuCl_2 \cdot 2H_2O$ in inclined magnetic field // FNT, V. 13, 155-164 (1987).
102. A.A.Galkin, S.N.Kovner, P.I.Poljakov. *Resonance properties of the antiferromagnetic dihydrate of copper chloride under the pressure* // Dokl. Ac.Sc. USSR, phys., V.208, p. 811-813. (1973).
103. A.V.Oleinik, P.I.Poljakov. *On existence in the intermediate state in* $CuCl_2 \cdot 2D_2O$ *in ac-surface* // FTT, V. 24, p.3190-3192 (1982).
104. A.V.Oleinik, P.I.Poljakov, V.A.Popov. *Antiferromagnetic resonance in the heterogeneous intermediate state ac- plate*.// FTT, V. 30, 283-285 (1988).
105. A.S.Borovik-romanov, L.A.Prozorova. Study of the antiferromagnetic resonance $MnCO_3$ in strong magnetic field // abstract, X int. conf. Phys Low temper. Moskow, V. 4, p. 201-205. (1966).
106. K. Svenson. Phisics of high-pressure // Moscow, -299p., (1963).
107. Influence of high pressures on the substance. V.1, Kiev, 321p. (1987).
108. I.V.Lebedev. Technology and the instruments of SHF// Moscow, 428 p (1970).
109. K.Bradley. Application high pressures technique to study of solid // Moscow, Mir, 284 p. (1972).
110. Benedek G.B. Magnetic Resonance at Pressure // New-York: Intersience. (1963).
111. Bradley B.S. High Pressure Physics and Chemistry. // New-York, Vol. 1 & 2. (1963).
112. D.S.Tsiklis. Technology of physical chemistry of experiments with the high and ultrahigh pressures. Moscow, Ed. “Chemistry”. 246 p. (1976).
113. K.S.Alexandrov. Structural phase transitions into crystals under high pressure // Novosibirsk, Nauka, 141 p. (1982).
114. Benedek G.B., Kushida T. Nuclear magnetic resonance in antiferromagnetic MnF_2 under hydrostatic pressure // Phys Rev. 118, 46-57 (1960).

115. Worlton T., Brugger R.M., Bennion R.B. Discovery of phase diagram Cr_2O_3 under pressure// J Phys Chem Solids 29, 435-438 (1968).
116. Lemis G., Drickamer H. Measurment dependence high-pressure for X-ray in Cr_2O_3 // J Chem Physics. - 1966.-45. - P. 224.
117. K.Johnson, A.Sievers. Hydrostatic-Pressure Study of Antiferromagnetic Resonance in $FeCl_2$ // Phys. Rev. B 7, 1081 - 1083 (1973).
118. V.A.Popov. V.S. Kuleshov. *Influence of high pressure on AFMR* // FTT. N 16. p. 612. (1974).
119. A.A.Galkin, N.K.Danshin, A.V.Vetchinov. AFVR depended of high pressure in $CuCl_2 \cdot 2H_2O$ // FNT 2(10) 1311-1319 (1976).
120. V.I.Makarov, G.V.Suchina. *The study of NMR in. $CuCl_2 \cdot 2H_2O$ near Neel's temperature* // abstract МКМ, Moscow, p. 209. (1973).
121. V.G.Baryakhtar, A.A.Galkin, S.V.Ivanova, V.I.Kamenev, P.I.Poljakov. Influence of magnetostriction on the resonance properties of $CuCl_2 \cdot 2H_2O$ under pressure // XX-th Congress AMPERE "Magnetic Resonance and Related Phenomena" Tallin, August 21-26? 1987, p. 212.
122. S.I.Ivanova, P.I.Poljakov. *Study of AFMR in$CuCl_2 \cdot 2D_2O$ under high pressure* // FNT. 1981. V. 7, N8.-C. 1029-1036.
123. Poulis N.J. *Spin dinamic of low. dimensional magnetic system* // *Abstracts XX^{th}* congreess AMPERE.- Tallinn, 1978.- V.1.- P. 45.
124. Kotthaus J.P., Jaccarino V. *Antiferromagnetic Resonance Linewidths in MnF* // Phys. Rev. Lett. 28, 1649 - 1652 (1972).
125. L.A.Prozorova, A.S.Borovik-Romanov. *Study of antiferromagnetic resonance in manganese carbonate in the strong magnetic fields* // LETPh. V. 55, N5. p. 1727-1736. (1968).
126. E.A.Turov. Physical properties of the magnetically ordered crystals// Moscow, 225 p. (1963).
127. E.V.Zarichenysev, V.A.Popov. The ground states of the biaxial antiferromagnet // FTT, V.6, №6, c.1579-1588. (1964).
128. L.D.Landau, E.M.Lifshits. Elastic theory // Moscow, 202 p. (1965)
129. Blazey K.W., Rohrer H., Webster R. Magnetocaloric Effects and the Angular Variation of the Magnetic Phase Diagram of Antiferromagnetic $GdAlO_3$ // Phys. Rev. B 4, 2287 - 2302 (1971).
130. Galkin A. A., Kovner S. N., Popov V. A. Antiferromagnetic Resonance in CuCl2 · 2 H2O in Inclined Magnetic Field near Intermediate State // Physica Status Solidi (b) Volume 57, Issue 2, Date: 1 June 1973, Pages: 485-495.
131. Urushibara, Y. Moritomo, A. Asamitsu, G. Kido, and Y. Tokura, Phys. Rev. B 51, 14103 (1995).
132. H. Y. Hwang, S. W. Cheong, P. G. Radaelli, M. Marezio, and B. Batlogg, Phys. Rev. Lett. 75, 914 (1995).
133. Y. Tokura, Y. Tomioka, and H. Kuwahara, J. Appl. Phys. 79, 5288 (1996).
134. A. P. Ramirez, J. Phys.: Condens. Matter 9, 871 (1997).
135. V. M. Loktev and Yu. G. Pogorelov, Fiz. Nizk. Temp. 26, 231 (2000) [Low Temp. Phys. 26, 171 (2000)].
136. J.-S. Zhou and J. B. Goodenough, Phys. Rev. B 62, 3834 (2000). 136a. Paschenko at al., Neorg. Mater. 35, 1294 (1999).

137. V. V. Runov, D. Yu. Chernyshov, A. I. Kurbakov, M. K. Runova, V. A. Trunov, and A. I. Okorokov, Zh. Eksp. Teor. Fiz. 118, 1174 (2000) [JETP Lett. 91, 1017 (2000)].
138. M.B. Salamon, M. Jaime, Rev. Mod. Phys. 73 (2001) 583.
139. F. Mascarenhas, K. Falk, P. Klavins, J.S. Schilling, Z. Tomkowicz, W. Haase, J. Magn. Magn. Mater. 231 (2001) 172.
140. N. Fujii, R. Zach, M. Ishizuka, F. Ono, T. Kanomata, S. Endo, J. Magn. Magn. Mater. 224 (2001) 12.
141. V. Moshnyaga, S. Klimm, E. Gommert, R. Tidecks, S. Horn, K. Samwer, J. Appl. Phys. 88 (2000) 5305.
142. V.P. Pashchenko, S.S. Kucherenko, P.I. Polyakov, Fiz. Nizk. Temp. 27 (2001) 1370.
143. V.P. Pashchenko, S.I. Kharsev, O.P. Cherenkov, Inorgan. Matter. 35 (1999) 1294.
144. I.V. Medvedeva, K. Barner, G.H. Rao, N. Hamad, Yu.S. Bersnev, J.R. Sun, Physica B 292 (2000) 250.
145. G.H. Jonker and J.H. Van Santen, Physica 16 (1950) 337.
146. R.N. Van Santen and G.H. Jonker, Physica 16 (1950) 599.
147. P.I. Polyakov, S.S. Kucherenko, JMMM 248, 396 (2002).
148. S.S. Kucherenko, V.I. Mikhaylov, V.P. Pashchenko, P.I. Polyakov, V.A. Shtaba, V.P. Dyakonov, Pisma v Zhourn. Tech. Phys. 27 (2001) 38.
149. P.I. Polyakov, S.S. Kucherenko, Pisma v Zhurn. Teh. Fiz. 28, 8, (2002).
150. P.I. Polyakov, S.S. Kucherenko Fiz. Nizk. Temp. 28, (2002), 1041.
151. P.I. Polyakov, V.P. Pashchenko, S.S. Kucherenko, Defect and Diffusion Forum, 208-209 (2002) 307.
152. N.J. Poulis, G.E. Hardeman, B. Bolyer, N. Commun Physica 18 (1952) 429.
153. G.J. Butterworth and V.S. Zidell, J. Appl. Phys. 40 (1969) 1033.
154. N.J. Poulis, J. Van der Handle, J.A. Poulis, C.J. Gorter, Phys. Rev. 82 (1951) 552.
155. J. Ubbink, J.A. Poulis, H.J. Gerritsen Physica 18 (1952) 361; Physica 19 (1953) 928.
156. J.N. Poulis, N.J. Gerritsen, C.J. Gorter, Physica 19 (1953) 928.
157. Cf. J. Phys. Radium 12 (1951) 149.
158. V.V. Eremenko, V.M. Naumenko, Yu.G. Pashkevich, V.V. Pshiko, Pisma v Jurnal Exper. Theor. Fiz. 38, (1983), 97.
159. V.G. Baryakhtar, V.V. Eremenko, V.M. Naumenko, Jurnal Exper. Theor. Fiz. 88, (1985), 1382.
160. T. Nagamiya, K. Yosida, R. Kubo, Antiferromagnetism and Phys. 4, (1955), 1.
161. E.V. Zarochencev, V.A. Popov, Fiz. Tverd. Tela 6, (1964), 1579.
162. A.C. Borovik-Romanov, Antiferromagnetism, Itogi Nauki, Moscow, 1972.
163. E.A. Turov, Physical properties of magnetic ordered crystalls, Academy of Sciences of the USSR, Moscow, 1963.
164. K.P. Belov, A.K. Zvezdin, A.M. Kadomtseva, R.Z. Letvin, Orientational transitions in rare-earth magnetics, Moscow: Science, (1979), 320pp.
165. P.I. Polyakov, Abstract of doctoral thesis, Donetsk, 1996.
166. A.A. Galkin, V.A. Popov, P.I. Polyakov, Fiz. Tverd. Tela 17, (1975) 2123
167. P.I. Polyakov, S.S. Kucherenko, Proceeding of New Magnetic Materials in Microelectronics – 18, Mosc. State Univer., Moscow, (2002), 714.
168. S.A. Friedberg, N. Commun, Physica 18 (1952) 714.

169. P.I.Polyakov, V.A.Turchenko FTT-2007, Minsk October 26-29, 2007, pp. 184-185.
170. R.F.C. Marques, M. Jafelicci Jr., C.O.Paiva-Santos, L.C. Paiva-Satos, L.C. Varanda, R.H.M. Godoi, JMMM, 226-230, p.812-814, (2001).
171. C.N.R Rao, A.K. Chectham and R. Mahesh, Chem Mater 8 (1996), 2421
172. L.P. Gorkov. Usp. Fiz. Nauk. v. 168. № 6 (1998), p. 665 - 671.
173. A. Urushibara, Y. Moritomo, T. Arima, A. Asamitisu Phys. Rev. B., 51. (1995), p.14103.
174. Y. Tokura, A. Urushibara, Y. Moritomo, T. Arima, J. Phys. Soc. Jpn., 63 (1994), 3931.
175. L.I. Abramovich, L.I. Karaeva, A.V. Michurin, Zh. Exper. Theor. Phys., V. 122. № 5 (11) (2002), p. 1063 - 1073.
176. A.I. Abramovich, O.Yu. Gorbenko, A.R. Kaul, L.I. Koroleva, A.A. Michurin, Phys. Tverd. Tela. 46. № 9 (2004), p. 1657-1662.
177. N.A. Babushkina, E.A. Chistotina, O. Yu. Gorbenko, A.R. Kaul et.al., Phys. Tverd. Tela. 46. № 10 (2004), p. 1821-1827.
178. P.Kapitza, Proc. Royal Society of London A, vol.123 (1928), p.292-372.
179. A.V. Lazuta, V.A. Ryzhov, A.I. Kubakov, V.A. Trounov, JMMM. 258-259 (2003), p. 315.
180. Yu.F. Popov, A.M. Kadomtseva, G.P. Vorob'ev, K.I. Kamilov, A.A. Muhin et al. Phys. Tverd. Tela. V. 46. № 12 (2004), p. 2148-2150.
181. P.I. Polyakov, S.S. Kucherenko. Technical Physics Lethievs. 28. № 4 (2002), p. 311-314.
182. P.I. Polyakov, S.S. Kucherenko, O.V. Budko. JCFM 2005. Ukraine, Crimea, Partenit. October 3-8. pp. 80, 122; FTT - 2005, Bielorus, Minsk, October 26 - 29 (2005) Collected Papers, V. 1, p. 29 - 31.
183. P.I.Polykov, V.A. Ryumshina // NMRCM-2007, St. Petersburg, Russia, 9-13 Juli, p.105-160, p.114.
184. P.I. Polyakov, NMRCM-2006, St. Petersburg, Russia, 9-13 Juli, p.22; NMMM-20, Moscow-2006, 12-16 June, pp.768-769, pp. 832-833.
185. E. Dagotto, Takashi Hotta, Adriana Moveo, Physics Reports 344 (2001), p. 1-153.
186. Y. Tomioka, A.Asamitsu, Y. Moritomo, et.al., Phys. Rev. Lett. V.74, 25 (1995), p.5108-5111.
187. A.V. Oleinik, P.I. Polyakov, V.A. Popov, Fiz. Tverd. Tela. V. 34. № 9. (1992), p. 2850-2851; Fiz. Tverd. Tela. V. 34. № 2 (1992), p. 678-681.
188. V.V.Eremenko, V.A.Sirenko. *Magnetic and magnetoelastic properties of antiferromagnets and superconductors* // Kiev, (2004).
189. J. W. Stout, Stanley A. Reed The Crystal Structure of MnF_2, FeF_2, CoF_2, NiF_2 and ZnF_2 // J Am Chem Soc Vol. 76, No. 21: November 5, pp 5279 – 5281 (1954).
190. K.L.Dudko, V.V.Eremenko, V.M.Fridman. // JTEPh, V. 61, 678-688 (1971).
191. A. R. King, D. Paquette Spin-Flop Domains in MnF_2 // Phys. Rev. Lett. 30, 662 - 666 (1973).
192. R. L. Melcher Elastic Properties of MnF_2 // Phys. Rev. B 2, 733 - 739 (1970)
193. Glen A. Slack Thermal Conductivity of CaF2, MnF2, CoF2, and ZnF2 Crystals // Phys. Rev. 122, 1451 - 1464 (1961).

194. J. W. Stout, H. E. Adams Magnetism and the Third Law of Thermodynamics. The Heat Capacity of Manganous Fluoride from 13 to 320°K. // J Am Chem Soc 64, pp 1535-1538 (1942).
195. D. F. Gibbons Thermal Expansion Coefficients of Manganese Fluoride // Phys. Rev. 115, 1194 - 1195 (1959).
196. D.N.Astrov, C.I.Novikova. // JETP, v.37, 1197-1201 (1959).
197. J. W. Stout, Maurice Griffel Paramagnetic Anisotropy of Manganous Fluoride // Phys. Rev. 76, 144 - 145 (1949).
198. Charles Trapp, J. W. Stout Magnetic Susceptibility of MnF_2 // Phys. Rev. Lett. 10, 157 - 159 (1963).
199. S. Jacobs Spin-Flopping in MnF_2 by High Magnetic Fields // J. Appl. Phys. 32, 615-625 (1961).
200. A.S.Borovik-Romanov. Sums of the science // Moscow, AcSc URSS, 320 p. (1962).
201. Y. Shapira, S. Foner and A. Misetich Magnetic-Phase Diagram of MnF_2 from Ultrasonic and Differential Magnetization Measurements // Phys. Rev. Lett. 23, 98 - 101 (1969).
202. V.V.Eremenko A.A. Klochko V.M.Naumenko // JETPh, V. 89, 1002-1017 (1985).
203. K.L.Dudko, V.V.Eremenko, V.M.Fridman. // (JETPh), V. 61, 1553-1559 (1971).
204. J.J.Thomson. “Indications relatives à la constitution de la matiere” *Congres International de Physique*; Gauthier–Villars: Paris; Vol. 3, p. 138 (1908).
205. P. Kapitza *The Change of Electrical Conductivity in Strong Magnetic Fields. Part II. The Analysis and the Interpretation of the Experimental Results* // Proceedings of the Royal Society of London. Series A 123, 342-372 (1929).
206. A. Sommerfeld *Zur Elektronentheorie der Metalle auf Grund der Fermischen Statistik* // Zeitschrift für Physik A Hadrons and Nuclei 47, 1-32 (1928).
207. P. Kapitza *The Change of Electrical Conductivity in Strong Magnetic Fields. Part III. Magnetostriction* // Proceedings of the Royal Society of London. Series A 135, 537-554 (1932).
208. B.G.Lazarev, N.M.Nachimovich, E.A.Parfenova// JETP (JETPh) V. 9, 1182 (1939).
209. E.S.Borovik. // JETP, V. 25, 91 (1952).
210. N.N.Bogoljubov, // JETP, V. 34, 58 (1952).
211. N.B.Brandt, N.I.Ginsburg. *Influence of high pressure on the superconductive properties of the metals* // Uspechi fisicheskich nauk, v. 85, 485-519 (1965).
212. L.S.Kap, B.G.Lazarev, L.I.Sudovtsev // Dokl.AcSc.URSS, v. 69, 173 (1949).
213. B.G.Lazarev, V.I.Makarov. // JETP, v. 50, 546 (1966).
214. V.G.Barjachnar, B.G.Lazarev, V.I.Makarov, I.V.Ignatieva.//Fozoka metallov I metallovedenie, v. 65, 829-842 (1967).
215. David R. Nelson, Michael E. Fisher *Soluble renormalization groups and scaling fields for low-dimensional Ising systems* // Annals of Physics 91, 226-274 (1975).
216. K. -H. Höck, H. *Thomas Statics and dynamics of “soft” impurities in a crystal* // Zeitschrift für Physik B Condensed Matter [On 1998 – The European Physical Journal B - Condensed Matter and Complex Systems] 27, 267-271 (1977).
217. K. B. Lyons, P. A. Fleury *Light-scattering investigation of the ferroelectric transition in lead germinate* // Phys. Rev. B 17, 2403 - 2419 (1978).

218. E. Pytte *Dynamics of Jahn-Teller Phase Transitions* // Phys. Rev. B 8, 3954 - 3959 (1973).
219. Feynman R.P. Statistical Mechanics. Massachusetts: W.A. Benjamin Inc. 1972.
220. R. A. Cowley: J. Phys. Soc. Jpn. 28 (1970) Suppl., p. 239.
221. Göran Niklasson *Theory of transport properties of an anharmonic crystal* // Annals of Physics 59, 263-322 (1970).
222. R.Holyst, A.Ponrewierski, A.Ciach. Thermodynamica, Warshawa (2005).
223. P.Buhler. Thermodynamics of matter at high pressure. St.Peterburg, Yanus (2002).
224. N.S.Achmetov. General and inorganic chemistry. Moscow (2001).
225. L.Poling. General Chemistry. Moscow (1974).
226. W.H.Flygare. Molecular structure and dynamics. Prentice-Hall, Inc., New Jersey (1978).
227. M.Kurt, R.Wicks, Chemistry lecture. Westtown School, (2004).
228. S.S.Batsanov. Systematic of atom radius. J. structural chemistry, Moscow, V.3, N5, p.616-627 (1962).
229. J.Sleter. J.Chem.-Phys., V.41, p.3199 (1964).
230. J.Waber, D.Cromer. J.Chem.Phys. V.42, p.4116 (1965).
231. R.Boyd. J.Phys. V.B1), p.2283 (1977).
232. G.B.Bokij. Cristal chemistry. Moscow (1971).
233. http://www.iem.ac.ru/web-elements
234. Table of Physical quantities. Ed. N.K.Kikoin, Moscow, Atomizdat (1976).
235. I.N.Francevich, F.F.Voronov, S.A.Bakuta. Elastic constants and elasticity modules of metals and nonmetals. Kiev, (1982).
236. G.W.C. Kaye and T.H. Laby in Tables of physical and chemical constants, Longman, London, UK, 15th ed., (1993).
237. A.M. James and M.P. Lord in Macmillan's Chemical and Physical Data, Macmillan, London, UK, 1992.
238. Contemporary crystallography. Ed. L. A.Shuvalov, A.A.Urusovskaja and all. V.4. Physical properties of crystal. Moscow, “Nauka” (1981).